

Book of Abstracts

**Joint Fifth International Conference on Solid State
Crystals and Eighth Polish Conference on Crystal
Growth**

Book of Abstracts: Joint Fifth International Conference on Solid State Crystals and Eighth Polish Conference on Crystal Growth

Published May 2007, ISBN 83-89585-14-6

Copyright © 2007 pielaszek research

Disclaimer

The Organisers and the Publisher have made every effort to provide accurate and complete information in this Addendum. However, further changes or corrections may still be necessary and may be made without notice after the date of publication. To ensure that you receive the most up-to-date information, please check the Corrigenda, if issued.

Revision: 12.1.30, 2007-05-10 18:11 GMT

Table of Contents

Foreword	1
Organisers	1
Sponsors	2
Programme	3
Sunday, 20 May	3
Monday, 21 May	3
Tuesday, 22 May	40
Wednesday, 23 May	75
Thursday, 24 May	83
Abstracts	87
Satellite events	89
The 2nd Polish - Japanese - German Crystal Growth Meeting	91
Index	99

Foreword

The Fifth International Conference on Solid State Crystal and Eighth Polish Conference on Crystal Growth (ICSSC-5 & PCCG-8 Conference) is held at Zakopane-Koscielisko WDW mountain resort center on May 20-24th 2007. The Conference is organized for the second time as joint conference linking efforts of Poland's crystal growth and the optoelectronic communities. The ICSSC-5 & PCCG-8 Conference continues earlier efforts to contact these communities with the world latest achievements in these areas in hospitable Polish mountain environment.

The ICSSC-5 & PCCG-8 Conference is organized by Polish Society for Crystal Growth (PSCG- PTWK) in cooperation with the members of the Scientific and Advisory Committees. The organizers of the Conference support young scientist to participate in the Conference following the general policy of encouraging young people to enter this difficult yet fascinating field. The Conference was financially supported by Ministry of Science and Higher Education (Poland) and International Union for Crystallography (IUCr). The organizers express their gratitude for this valuable financial help.

The ICSSC-5 & PCCG-8 Conference is followed by the Second Polish-Japanese-German Crystal Growth Meeting (PJG-CGM2), held at the same location on May 24-25th 2007. The PJG-CGM2 Workshop, organized commonly with Japanese and German crystal growth communities is devoted for discussion of development of growth of crystals of wide bandgap semiconductors in these three countries. The organizers would like to thank Prof. Tsuguo Fukuda and Prof. Jochen Friedrich for invaluable help in organization of the Workshop.

The aim of both events is to provide interdisciplinary forum for exchange of novel ideas and discussion of latest achievements in crystal growth, optoelectronics and related areas. The following topics are covered: crystal growth fundamentals and dynamics, material and structural properties related to crystal growth and the characterization under immensely different length scales. The optoelectronics chapter is devoted to active and passive devices, their manufacturing and applications.

Reflecting the wide spectrum of the discussed problems at the Conference and CG Meeting, the Scientific Committee decided to publish the proceedings of the Conference in two international journals: Crystal Research and Technology (Wiley Interscience) and Opto-Electronics Review (Versita, co-published with Springer-Verlag GmbH). The Organizers would like to thank the Editors for their kind agreement to publish the proceedings.

The Conference Chairman wish to express thanks to all who helped to organize ICSSC-5 & PCCG-8 Conference and PJG-CGM2 Workshop.

The Conference Chairmen

Stanislaw Krukowski & Wojciech Sadowski

Organisers

The Fifth International Conference on Solid State Crystals & Eight Polish Conference on Crystal Growth (ICSSC-5 & PCCG-8 Confer-

ence) is organized by Polish Society for Crystal Growth (PSCG - PTWK). The Second Polish-Japanese-German Crystal Growth Meeting (PJG CGM2) is organized by Polish, Japanese and German Crystal Growth Communities.

Polskie Towarzystwo Wzrostu Kryształów
Polish Society for Crystal Growth
ul Wólczynska 133,01-919 Warszawa
Tel: 48 22 8880244, fax: 48 22 632 42 18
e-mail: stach@unipress.waw.pl
NIP: 118-14-85-963
URL: <http://www.ptwk.org.pl>

Bank Account: Bank Millennium S.A., no: 23 1160 2202 0000 0000
1235 1497

Scientific Committee

- Stanisław Krukowski, *Institute of High Pressure Physics PAS, Warsaw, Poland - Chairman*
- Wojciech Sadowski, *Gdańsk University of Technology, Gdańsk, Poland - Co-Chair*
- Maciej Bugajski, *Institute of Electron Technology, Warsaw, Poland*
- Mirosław Drozdowski, *Poznań University of Technology, Poznań, Poland*
- Michał Leszczyński, *Institute of High Pressure Physics PAS, Warsaw, Poland*
- Anna Pajączkowska, *Institute of Electronic Materials Technology, Warsaw, Poland*
- Antoni Rogalski, *Military Academy of Technology, Warsaw, Poland*
- Keshra Sangwal, *Lublin University of Technology, Lublin, Poland*
- Ewa Talik, *University of Silesia, Katowice, Poland*

International Advisory Committee

- Robert F. Sekerka - President IOCG
- Roberto Fornari
- Jacek Kossut
- Zygmunt Luczynski
- Włodzimierz Nakwaski
- Wolfgang Neumann
- Sylwester Porowski
- Gerald B. Stringfellow
- Marek Szymonski
- Marek Tlaczala
- Jacques Villain

Organizing Committee

- Stanisław Krukowski, IHPP PAS, Warsaw, Poland – Chairman
stach@unipress.waw.pl
- Dorota Pawlak, IEMT, Warsaw, Poland – Secretary
dorotkapawlak@hotmail.com
- Bolesław Łuczniak, IHPP PAS, Warsaw, Poland – Treasurer
bolo@unipress.waw.pl
- Michał Leszczyński, IHPP PAS, Warsaw, Poland - Exhibition
mike@unipress.waw.pl

- Paweł Strak, IHPP PAS, Warsaw, Poland - Home Page & Publications
strak@unipress.waw.pl
- Paweł Kempisty, IHPP PAS, Warsaw, Poland – Home Page & Publications
kempes@unipress.waw.pl

Proceedings - Guest Editors

- Crystal Research & Technology - Keshra Sangwal
- Jacques Villain - Antoni Rogalski

Time and place

- ICSSC-5 & PCCG-8 Conference: 20-24 May 2007
- PJG CGM2 Workshop: 24-25 May 2007

WOJSKOWY DOM WYPOCZYNKOWY - WDW
"KOŚCIELISKO"

ul. St. Nędzy - Kubińca 101

34 - 511 Kościelisko k/Zakopanego

Tel/fax: + 18 - 207 93 00 (all the day)

Tel.: +18 - 207 93 14

e-mail: wzw@wzw.zakopane.pl

web site: <http://www.wzw.zakopane.pl/>

Sponsors

Ministry of Science and Higher Education (Poland)

International Union for Crystallography (IUCr)

Institute of Electronic Materials Technology

Institute of High Pressure Physics Polish Academy of Sciences

Labsoft - Biuro Techniczno-Handlowe

Programme

Sunday, 20 May

Reception

Sunday afternoon, 20 May, 16:00

Welcome Party

Sunday evening, 20 May, 20:00

Monday, 21 May

Breakfast

Monday morning, 21 May, 7:00

Opening Ceremony

Monday morning, 21 May, 8:45

Chair: Stanisław Krukowski

Czochralski Lecture

The Czochralski-Method - where are we 90 years after Jan Czochralski's invention

Monday morning, 21 May, 9:00

9:00

Invited oral

The Czochralski -Method - where are we 90 years after Jan Czochralski's invention

Georg Mueller

E-mail: georg.mueller@ww.uni-erlangen.de

Jan Czochralski invented his method of pulling a crystal from the melt 90 years ago. In the meantime the “Czochralski method (Cz)” became the most important technique for growing semiconductor and optical crystals from the melt on an industrial scale.

Although, the principle of the Czochralski method looks quite simple, it needs an immense number of sophisticated technical details and process know how to come to the present stage of development for the growth of large size and low defect single crystals – which will be briefly illustrated by some examples of Czochralski-grown semiconductor and optical crystals from industrial production.

Nevertheless, further improvements and developments are necessary to fulfill the future requirements of up-scaling and improvement of crystal quality. Such kind of improvements beyond the present status of the Czochralski technique require a profound analysis of the mechanisms of heat and species transport which are relevant for the stability of the growth process and the performance of the growing crystal. It was clearly demonstrated in the last few years, that modeling by numerical simulation is an indispensable tool to analyze the

Czochralski process and help to understand the governing mechanisms.

The contribution will present examples of this kind of modeling the Czochralski technique in correlation with experimental investigations in order to illustrate the present status of understanding relevant processing phenomena. Furthermore, it will be shown what problems need still to be solved in the future in order to further improve the yield and quality of Czochralski -grown crystals.

The presentation is based on results obtained in the author's laboratory and on actual literature data.

Coffee Break

Monday morning, 21 May, 9:45

Session I: Theory and modeling

Monday morning, 21 May, 10:15

Chair: Georg Mueller

10:15

Invited oral

Ab initio based growth simulations of group-III-nitrides

Joerg Neugebauer

Max-Planck-Institut für Eisenforschung, Department of Computational Materials Design, Max-Planck-Str. 1, Düsseldorf D-40237, Germany

E-mail: j.neugebauer@mpie.de

A challenge in performing crystal growth simulations is the large range of relevant length and time scales. While eventually being interested in a description on a mesoscopic/macroscale (the size of typical defect or surface features is in the order of 10..100 nm and the growth time is in the order of seconds up to hours) the mechanisms leading to these structures (adatom adsorption, diffusion, desorption, island nucleation) require a resolution in the length scale of atomic bonds (10^{-1} nm) and in the time scale of atomic vibrations (10^{-13} s). Therefore, common approaches to simulate growth have been restricted on specific properties (on the mesoscopic/macroscale) and included microscopic information only indirectly by empirical/adjustable parameters. Examples are rate equations or continuum models. While these approaches give valuable insight into qualitative aspects of growth a quantitative analysis requires to include the microscopic mechanisms directly.

A rather new approach to describe microscopic growth mechanisms is the application of *ab initio* methods such as density-functional theory (DFT). The key idea of these methods is to describe nature on the most fundamental level: The growing crystal and its structural elements are decomposed into the most elementary building blocks such as atomic nuclei and electrons and the interaction between them is described by the fundamental laws of electrodynamics and quantum mechanics. In the present talk I will discuss how by combining density-functional theory with concepts of thermodynamics, continuum theory and/or statistical physics simulations can be performed which allow to bridge between microscopic and mesoscopic/macroscale scales. Such multiscale simulations which combine methods developed for various length and time scale provide the

unique opportunity to combine the advantages of *ab initio* methods (universality and predictive power) with the efficiency of mesoscopic/macroscale models to describe system sizes relevant for crystal growth. To discuss the application but also the present limitations of *ab initio* based multiscale simulations the focus will be on various issues regarding crystal growth, defect formation and doping of wide bandgap semiconductors such as group-III nitrides (GaN, AlN, InN and their alloys).

In the first part of the talk the focus will be on equilibrium properties and structures. Specifically, it will be discussed how *ab initio* methods can be employed to predict bulk crystal properties such as thermal expansion coefficients, elastic constants, thermodynamic constants, formation energies of compounds, defects and impurities. Based on these results the presently achievable accuracy of these methods will be discussed [1-3].

A generalization of these concepts to surfaces allows to calculate the stability and electronic properties of surfaces/interfaces as function of the growth conditions (chemical potentials). Based on these results it became possible to identify conditions where e.g. surface reconstructions are stable or when the surface becomes unstable against step formation (surface roughening), faceting or the formation of nanostructures [4]. The same approach allowed also to identify the effect impurities/dopants have on these properties. An interesting result which emerged from these studies was that for certain growth conditions the dopant/impurity concentration on the surface can be orders of magnitude larger than in bulk. This has been shown to largely effect the growth morphology and can be even used to grow metastable phases which are otherwise not found in nature [5]. Also, this effect can be used to control the formation of nanostructures such as quantum dots, the formation of alloy fluctuations [6] or to achieve chemical ordering in semiconductors [4]. The effect dopants have on the surface morphology will be shown to also affect the doping efficiency. For example, the surface can enhance/reduce the formation of parasitic phases and thus the bulk solubility [7].

Finally, it will be discussed how the *ab initio* calculated barriers [8] can be used to perform growth simulations on a mesoscopic length and time scale. A direct approach would be to use the barriers to calculate the transition rates, construct a master equation and solve it by kinetic Monte Carlo (kMC). While this approach works well to study growth at low temperatures it becomes exceedingly expensive at high temperatures which are needed to achieve smooth surfaces. We have therefore developed a new method which is called adatom density Monte Carlo [9]. Using this method it will be shown how mechanisms controlling self-organization in V-grooves or lateral epitaxial overgrowth (which is used to reduce the dislocation density in group-III nitrides) can be identified.

In conclusion, the combination of density functional theory (giving an accurate description of the atomistic and electronic structure) with concepts of thermodynamics, statistical physics or continuum theory allows to address a wide range of crystal growth and doping problems which are not feasible by any of the methods alone due to the large range of relevant length and time scales. While this approach is still in its infancy first results are very promising and future improvements in the methods and in computers will allow to perform these types of studies routinely.

[1] C.G. Van de Walle, J. Neugebauer, J. Appl. Phys. **95**, 3851-3879 (2004).

[2] J. Neugebauer, phys. stat. sol. (c) **6**, 1651-1667 (2003).

[3] C.G. Van de Walle and J. Neugebauer, Nature **423**, 626 (2003).

[4] J.E. Northrup, L.T. Romano, and J. Neugebauer, Appl. Phys. Lett. **74**, 2319 (1999).

[5] J. Neugebauer, T. Zywietz, M. Scheffler, J.E. Northrup, and C. G. Van de Walle, Phys. Rev. Lett. **80**, 3097 (1998).

[6] H. Chen, R.M. Feenstra, J.E. Northrup, T. Zywietz, J. Neugebauer, and D.W. Greve, Phys. Rev. Lett. **85**, 1902 (2000).

[7] J. Neugebauer, phys. stat. sol. (b) **227**, 93 (2001).

[8] J. Neugebauer, T.K. Zywietz, M. Scheffler, J.E. Northrup, H. Chen, and R.M. Feenstra, Phys. Rev. Lett. **90**, 056101 (2003).

[9] L. Mandreoli, J. Neugebauer, R. Kunert, and E. Schöll, Phys. Rev. B **68**, 155429 (2003).

10:45

Invited oral

Numerical investigation of crystal growth process of bulk Si, SiC and nitrides

Koichi Kakimoto

Kyushu University, Fukuoka, Japan

E-mail: kakimoto@riam.kyushu-u.ac.jp

This paper introduces the potential regarding numerical analysis of crystal growth process of bulk Si, SiC and nitrides by using a global model. A three-dimensional analysis of temperature distribution in a TMCZ furnace of Si single crystals was studied by using an originally developed algorithm. Temperature distribution in a furnace for SiC by using sublimation method was also investigated. Moreover, thermal conductivity of four different poly-type of SiC was studied by using molecular dynamics method. The growth rate of GaN was numerically investigated by using a global model in a system of solution growth. We considered the local equilibrium condition of nitrogen at a free surface of gallium and lithium mixed melt in this calculation. Thermal conductivity of nitrides was investigated by molecular dynamics from the point of view of defects such as vacancies and dislocations.

11:15

Oral

Preference for fcc atom stacking observed during growth of defect-free LJ₃₂₈₁ cluster

Wiesław Polak

Lublin University of Technology, Institute of Physics, Nadbystrzycka 38, Lublin 20-618, Poland

E-mail: w.polak@pollub.pl

Growth simulations of 3-dimensional Lennard-Jones (LJ) clusters/nuclei from the vapour phase were carried out in order to estimate the role of kinetic and energetic effects in determining the internal structure of the clusters. The kinetic effects have been clearly observed recently [1] in case of defected clusters LJ₃₂₈₁ with internal structure proposed by van de Waal [2], where they lead to overgrowth of fcc structure instead of more energetically preferred hcp structure. The 3281-atom LJ cluster of ideal octahedral shape determined by eight dense-packed planes {111} and of the fcc internal

structure, analysed here, is free from growth stimulating surface defects and therefore is an ideal candidates for comparison.

Growth simulations of LJ clusters were realised using the two-temperature-region model [3] based on Monte Carlo method. The initial ideal cluster LJ_{3281} was thermally equilibrated at a selected growth temperature and put into supersaturated vapour. The used value of the vapour atom concentration $n_v = 0.002$ (in reduced units of LJ system) was selected since it proved to be optimal to form well-arranged cluster structure in a reasonable simulation time [3]. The simulated growth was realised from $N = 3281$ up to 6000 atoms at two reduced growth temperatures $T^* = 0.30$ and 0.50 corresponding to 36 K and 60 K for argon clusters. The internal structure in final clusters was precisely analysed by determining the number of fcc and hcp units and their location in the cluster. For this purpose, the structural analysis based on the Coordination Polyhedron Method [4] and visualisation using the PovRay program were used.

Growth of the ideal fcc clusters is strongly temperature-dependent: at low temperature clusters evolve from octahedral to an irregular shape, while at the higher one they are close to spherical. The internal structure in new cluster regions built at the low temperature is characterised by many stacking-fault layers of fcc and hcp character. This is caused by approximately the same binding energies for fcc and hcp structure and a low adatom movement on the cluster surface. The temperature increase up to $T^* = 0.50$ removes partly this ambiguity in cluster structure formation showing preference for the fcc structure. This is evident from statistics of newly created structural units, where the fcc units are approximately four times more numerous than those of the hcp character.

The possible explanation of this preference is in energetic effects caused by different interaction energy of two fcc or two hcp layers located on the neighbouring (111) planes of the initial fcc cluster. Such layers should contact at the edge of octahedral cluster where they are inclined one to another at the obtuse angle of about 109° . Two neighbouring hcp planes avoid such contacts at this position, while this angle is ideal to make contact of two fcc layers. This means that the fcc layer, when initiated on one surface, can easily propagate to the neighbouring planes. The higher temperature facilitates this kinetic process of the fcc layer propagation by higher surface diffusion of adatoms. The second mechanism, which helps to form fcc surface layer from adatoms, involves structural rearrangement of hcp islands [5] before they are able to originate stacking-faults hcp layer.

Literature

- [1] W. Polak, Europhys. Lett., accepted for publication.
- [2] B. W. van de Waal, J. Chem. Phys. 98 (1993) 4909.
- [3] W. Polak, Phys. Rev. B 71 (2005) 235413.
- [4] W. Polak, Phys. Rev. B 67 (2003) 115402.
- [5] S. Somasi, B. Khomami R., and Lovett, J. Chem. Phys. 114 (2001) 6315.

Coffee Break

Monday morning, 21 May, 11:30

Session II:Nitrides: bulk

Monday afternoon, 21 May, 12:00

Chair: Mike Leszczynski

12:00

Invited oral

Bulk growth of gallium nitride. Challenges and difficulties

Michał Boćkowski

Polish Academy of Sciences, Institute of High Pressure Physics (UNIPRESS), Sokolowska 29/37, Warszawa 01-142, Poland

E-mail: bocian@unipress.waw.pl

The progress in blue laser diodes is still limited by the lack of high quality, large and cheap gallium nitride wafers. One of the main goal of nitride community is to have GaN single crystals in shape of real ingots, ready to slice them to form of two or three inches substrates about 300 mm thick. However due to extreme melting conditions of GaN (6 GPa of N_2 and 2497 K [1]), this nitride cannot be grown from its stoichiometric melt by the Czochralski or Bridgman methods commonly used for semiconductors "cousins" as Si or GaAs. Therefore, the GaN crystals have to be grown by ways allowing lower pressures and temperatures.

There are some promising methods to obtain GaN substrates. First of them is Hydride Vapor Phase Epitaxy (HVPE) where GaN is deposited on foreign substrates (sapphire, GaAs, SiC) at temperatures about 1323 K and at ambient pressure. The foreign substrate is removed from the sample by etching or other lift off technique and then a large diameter free-standing GaN wafer may be obtained. The big advantage of this method is relatively fast growth rate in c-direction, exceeding 100 mm/h. The best quality free standing GaN crystals have been grown in Sumitomo Electric Industries Ltd. using A-DEEP technology (Advanced Dislocation Elimination by the Epitaxial growth with inverse pyramidal Pits) by deposition of GaN on stripe or round shape patterned GaAs wafers [2]. High quality laser structures have been grown on these substrates by MOCVD and MBE methods at Sony, NEC and Sharp Corporations. The present Nichia's lasers structures are grown exclusively on their HVPE free-standing substrates.

Gallium nitride can be also grown using the Na flux method at temperatures from 973 K to 1273 K and nitrogen pressure up to 5 MPa. This method is being developed in Tohoku University [3] and Osaka University [4] and yields bulk GaN single crystals with a size of few millimeters and defect density of order of 10^4 cm^{-2} . Various flux composition like Ca-Na and Li-Na have been also studied. Recently, the liquid phase epitaxy (LPE) technique applied to the Ca-Na flux system has been reported. 1 mm GaN thick layer with the dislocation density of order of 10^4 cm^{-2} has been deposited on MOCVD sapphire/GaN template [5]. None device or other epitaxial structure grown on the crystals has been ever reported in the literature.

In this paper the present status of the GaN growth by High Pressure Solution (HPS) method and the combination of HPS and HVPE methods will be presented. The challenges and difficulties on the road to obtain 2 inch low defect density GaN substrates will be discussed. Up to now the spontaneous high pressure solution growth of GaN results only in crystals having habit of hexagonal platelets of surface area of 3 cm^2 or needles with length up to 1 cm. The platelets with dislocation density 10^2 cm^{-2} have been used with success as substrates for lasers diodes. Recently, the platelets and needles have

been used also as seeds for the HVPE growth. On the other hand the LPE technique under pressure with GaN/sapphire templates, patterned GaN/sapphire templates and free standing HVPE as seeds has been examined and developed. These results will be described in this paper in details.

- [1] W. Utsumi et al., Nature Materials, Vol. 2, November (2003), 735
- [2] K. Motoki, reported on 4th International Workshop on Bulk Nitride Semiconductors, Makino, Japan, 2006
- [3] T. Yamada et al., J. Cryst. Growth 286 (2006) 494
- [4] F. Kawamura et al., Jpn. J. Appl. Phys. 42 (2003) L729
- [5] Y. Mori, reported on 4th International Workshop on Bulk Nitride Semiconductors, Makino, Japan, 2006

12:30 Invited oral

2D and 3D growth mode of nitride layers

Krzysztof Pakuła, Jacek Baranowski

*Warsaw University, Institute of Experimental Physics (IEP UW),
Hoża 69, Warszawa 00-681, Poland*

E-mail: Krzysztof.Pakula@fuw.edu.pl

Heteroepitaxial three dimensional (3D) and two dimensional (2D) growth mode of nitride layers on sapphire substrates are discussed. It is shown that the 3D or 2D growth mode of AlGaIn layers depends predominantly on the growth conditions of the underneath grown low temperature (LT) nucleation layer.

Commonly described in literature 3D growth mode is obtained on LT GaN or AlN nucleation layer grown relatively fast. Successive growth of secondary layer at high temperature begins from separated sites, where individual 3D crystallites are formed. Threading dislocations present in crystallites are bending on their facets, which reduces the quantity of dislocations. However, from the other hand, slight crystallographic misorientations between crystallites leads to creation of new dislocations which are generated during coalescence of the crystallites. As result edge and mix dislocations appearing are at similar density of about 10^9 cm^{-2} .

Modification of growth conditions of LT AlN nucleation layer, especially reduction of their growth rate leads to drastic changes in properties of the layer. Successive growth of secondary AlGaIn layer at high temperature starts evenly on whole surface retaining atomic flatness. Thus, the growth at high temperature occurs only at 2D mode. Therefore, it is possible to grow a very thin AlGaIn layers directly on top of LT AlN nucleation layer. Such layers contain large number (10^{10} cm^{-2}) of edge dislocations, and relatively small number (less than 10^8 cm^{-2}) of mix dislocations.

It is also shown, that decisive factors which determine the growth mode of AlN nucleation layer is a growth of the first few atomic layers on substrate surface. The slow growth of this few first atomic layers decide about the 2D growth mode, and the fast one about the 3D one.

13:00

Oral

Ammonothermal Growth of Bulk GaN for Extended Time

Tadao Hashimoto^{1,2}, Feng Wu^{1,2}, Makoto Saito^{2,3}, Kenji Fujito³, J. S. Speck^{1,2}, Shuji Nakamura^{1,2}

1. University of California, College of Engineering, -, Santa Barbara, CA 93106-5130, United States **2.** ERATO, JST, UCSB group, Materials Department, Santa Barbara, CA 93106, United States **3.** Mitsubishi Chemical Corp., Ibaraki 300-1295, Japan

E-mail: tadao@engineering.ucsb.edu

Recently, growth of bulk GaN crystals has been intensively researched because GaN wafers sliced from bulk crystals will solve all fundamental growth problems arising from heteroepitaxy. However, the extremely high price of state-of-the-art GaN wafers does not meet the cost requirement of LEDs for solid-state lighting. Among several bulk growth methods, the ammonothermal growth, which is the solvothermal growth using supercritical ammonia, has a high potential of realizing low-cost, high-quality GaN substrates due to its excellent scalability. In the early stage of our research, we demonstrated single-phase synthesis of wurtzite GaN powders with basic mineralizers and retrograde solubility of GaN in supercritical ammonobasic solutions. Through these experiments, we have achieved uniform growth of GaN films on an over-1-inch oval shaped seed crystal through fluid transport of Ga nutrient. However, it turned out that Ga nutrient was transformed to GaN in the nutrient crucible resulting in abrupt drop of the growth rate in about a day.

In this presentation, we report on consistent growth of GaN for extended time in the ammonothermal method with polycrystalline GaN nutrient and higher mineralizer concentration. GaN was grown in a cylindrical high-pressure autoclave having its internal diameter of 40 mm. Free-standing *c*-plane GaN grown by HVPE was used as seed crystals. The estimated defect density of the seeds was at the order of 10^8 cm^{-2} . The reactor was divided into an upper region and a lower region with a baffle to set a temperature difference in the dissolving region and the crystallization region. Since GaN has retrograde solubility in supercritical ammonobasic solution, the nutrient was placed in the colder region (upper region) and the seed crystals were placed in the hotter region (lower region). The temperature of the external heaters was maintained at about 507°C and 700°C for upper and lower region, respectively. Due to thick wall of the autoclave, the temperature difference between upper and lower region is estimated to be less than 50°C. The resulting ammonia pressure was about 180-190 MPa.

Single crystalline growth of GaN on both sides of seeds was confirmed with XRD and TEM. GaN also grew on the sidewalls (i.e. *m*-plane and *a*-plane) of the seeds. Unlike the Ga nutrient, which causes growth saturation problem, GaN nutrient with higher concentration of a mineralizer allowed continuous growth over extended time. Continuous growth was confirmed up to 50 days with growth rates of 0.8, 3.6, and 6 $\mu\text{m/day}$ along *+c*, *-c* and *m* direction, respectively. Growth on Ga-face (*+c*) has stronger tendency to form (10-11) facet at the edge of the seeds compared to N-face (*-c*). The FWHM of X-ray rocking curve obtained from N-polar side was 843 arcsec for 002 reflections and 489 arcsec for 201 reflections. Since the film on Ga-face was not thick enough, X-ray rocking curve was affected

by a signal from the seed, thus did not represent the structural quality of the grown layer.

Lunch

Monday afternoon, 21 May, 13:15

Session III:Nitrides - epitaxy

Monday afternoon, 21 May, 15:00

Chair: Unil Perera

15:00

Invited oral

Low temperature plasma assisted MBE growth for nitride optoelectronic devices

Czesław Skierbiszewski

Polish Academy of Sciences, Institute of High Pressure Physics (UNIPRESS), Sokolowska 29/37, Warszawa 01-142, Poland

E-mail: czeslaw@unipress.waw.pl

During last decade in a field of the GaN based optoelectronic devices the main achievements were attained by ammonia based metalorganic vapor phase epitaxy (MOVPE) and until very recently molecular beam epitaxy (MBE) was not regarded as a technology of choice. It was believed, based on thermodynamic considerations, that only growth at temperatures close to those used in MOVPE (as high as 1050°C for GaN) will result in device quality structures. Unfortunately, GaN starts to decompose at 800°C at vacuum conditions and MBE growth at temperatures below 800°C for typical nitrogen rich conditions leads to the three-dimensional growth mode and low material quality.

We present recent progress in growth of nitride based semiconductor structures using Plasma Assisted MBE (PAMBE). This technology is ammonia free and nitrogen for growth is activated in RF plasma source from nitrogen molecules. We describe new approach for growth of nitrides by PAMBE at temperatures much below 800°C. The crucial for this technique is to use thin, dynamically stable, metal (In or Ga) layer on (0001) GaN surface during the growth - making PAMBE growth conditions similar to liquid phase epitaxy. This significantly reduces barriers for N adatom diffusion enabling high quality 2D step-flow growth mode at low temperatures. We discuss also in detail the role played by threading dislocations (TDs) on low temperature growth mechanism. The presence of TDs changes growth mechanism, leading to spiral growth and formation of pyramids. The spiral growth is one of the important factors which deteriorates efficiency of nitride optoelectronic devices, e.g. in InGaIn it can lead to fluctuation of In composition and quantum well thickness, as well as formation of "V" defects. We show that growth on low TDs density bulk GaN substrates results in high quality of (In, Al, Ga)N layers with parallel atomic steps morphology and flat interfaces required for optoelectronic devices.

The new perspective for PAMBE has been opened recently by a demonstration of continuous wave (cw) blue-violet laser diodes [1, 2], high electron mobility transistor structures [3], resonant tunneling diodes [4] and intersubband devices [5]. All these devices were grown on low TDs density high pressure grown GaN bulk substrates. We will discuss also potential of PAMBE for UV and green

emitters as well as for intersubband devices operating at 1.5 mm telecommunication wavelengths.

[1] C. Skierbiszewski, et. al. Appl. Phys. Lett. **88**, 221108 (2006)

[2] C. Skierbiszewski, et. al. Appl. Phys. Lett. **86**, 011114 (2005)

[3] C. Skierbiszewski, et.al, Appl. Phys. Lett. **86** 102106 (2005).

[4] S. Golka et.al., Appl. Phys. Lett. **88**, 172106 (2006)

[5] C. Skierbiszewski et.al., Proc. of SPIE Vol. **6121**, 612109, (2006)

15:30

Oral

Investigation of GaN crystal quality on silicon substrate using GaN/AlN superlattice structures

Gwomei Wu, Chenwen Tsai, Naichuan Chen, Penhsiu Chang

Chang Gung University, Kwei-Shan 3333, Taiwan

E-mail: wu@mail.cgu.edu.tw

Group III-nitride semiconductors based on GaN have received much attention as materials for the realization of blue and green light emitting diodes. These devices are usually grown by metalorganic chemical vapor deposition (MOCVD) on sapphire or SiC substrates. On the other hand, silicon has become a desirable substrate for heteroepitaxy because of its high crystalline quality, large wafer size, low cost, and easy integration with the well-established silicon device technology. However, it is difficult to grow high quality GaN on silicon due to the large difference in lattice constant (-16.9%), crystal structure and thermal expansion coefficient (about 57%) that can result in high dislocation density. Therefore, the purpose of this study has been to investigate the crystal quality of GaN thin film on silicon substrates using GaN/AlN superlattice structures. The growth was carried out in an MOVPE system with a horizontal reactor (Aixtron 200/4 RF-S). Si(111) was chosen due to its trigonal symmetry favoring epitaxial growth of the GaN(0001) plane. Trimethylaluminum (TMAI), trimethylgallium (TMGa), trimethylindium (TMIn) and ammonia (NH₃) were used as Al, Ga, In and N sources, respectively. Various GaN/AlN superlattice intermediate layer structures have been designed to decrease the threading dislocation density of GaN epilayers. The characterization techniques included TEM, SEM and double crystal X-ray diffraction. The results showed that the insertion of GaN/AlN superlattices with suitable thickness and pair combinations could be effective in reducing the etch pit density in GaN film by more than one order of magnitude. Cross-sectional transmission electron microscopy (XTEM) study confirmed the efficiency of GaN/AlN superlattice in blocking threading dislocation propagation in GaN crystal. The design of nine period GaN/AlN(20nm/2nm) superlattice has been shown to be effective in reducing the dislocation density and can improve the crystal quality. In addition, we would discuss the dislocation bending in GaN/AlN interface and dislocation merge that has become a new dislocation process.

Coffee Break

Monday afternoon, 21 May, 15:45

Session IV: Other semiconductors - bulk and epitaxy

Monday afternoon, 21 May, 16:15

Chair: Jacek Baranowski

16:15

Invited oral

Stability diagram for crystal growth from the vaporKrzysztof Graszka

Polish Academy of Sciences, Institute of Physics, al. Lotników 32/46, Warszawa 02-668, Poland Institute of Electronic Materials Technology (ITME), Wólczyńska 133, Warszawa 01-919, Poland

E-mail: graszka@ifpan.edu.pl

We present experimental results and discuss dependence of the shape and morphology of the solid-vapor interface on growth rate and temperature distribution in the directional "contactless" crystallization of semiconductor materials from group A_2B_6 and A_4B_6 , and in the conventional vapor growth of ZnO, SiC and iodine. The tendency to grain selection and growth of high quality single crystals was found to be dependent on constitutional supersaturation, gas dynamics and surface kinetics. The evidence of the three kinds of instability was observed on the surface of the crystallization front in various stages of crystal growth. Diagram based on experimental data, summarizing the dependence of the stability criterion on temperature gradient in the crystal and concentration gradient of crystal components in the vapor is presented and discussed. Surface roughening and evolution of flat faces at the growth interface is investigated. The way of optimization of the growth system by gradual elimination of the mechanisms deciding on the instability is shown. The novel aspect of this work is presentation of validity of the interaction between temperature field and vapor component concentration field, resulting in more general description of the growth system than simple relation between temperature and supersaturation, investigated in former papers.

16:45

Invited oral

Catalytic growth by molecular beam epitaxy and properties of ZnTe-based semiconductor nanowires

Tomasz Wojtowicz¹, Elżbieta Janik¹, Wojciech Zaleszczyk¹, Janusz Sadowski¹, Grzegorz Karczewski¹, Piotr Dłużewski¹, Sławomir Kret¹, Wojciech Szuszkiewicz¹, Elżbieta Dynowska¹, Jarosław Domagała¹, Marta Aleszkiewicz¹, Lech T. Baczewski¹, Alexei Petroutchik¹, Adam Presz², Wojciech Pacuski³, Andrzej Golnik³, Piotr Kossacki³, Holm Kirmse⁴, Jean F. Morhange⁵, Wolfgang Caliebe⁶

1. Polish Academy of Sciences, Institute of Physics, al. Lotników 32/46, Warszawa 02-668, Poland **2.** Polish Academy of Sciences, Institute of High Pressure Physics (UNIPRESS), Sokolowska 29/37, Warszawa 01-142, Poland **3.** Warsaw University, Faculty of Physics, Hoża 69, Warszawa 00-681, Poland **4.** Humboldt University of Berlin, Institute of Physics, Newton Street 15, Berlin 12489, Germany **5.** Universite Pierre et Marie Curie, Place Jussieu, Bat F Boite 39, Paris 75252, France **6.** Hamburger Synchrotronstrahlungslabor HASYLAB (HASYLAB), Notkestrasse 85, Hamburg D-22603, Germany

E-mail: wojto@ifpan.edu.pl

We review our results on the growth of ZnTe-based nanowires (NWs) and on their basic structural and optical properties. The nanowires were produced by molecular beam epitaxy (MBE) with the use of mechanism of catalytically enhanced growth. Semiconductor nanowires have attracted considerable attention recently as very versatile nanoscale building blocks for the assembly of electronic and optoelectronic devices. Nanowires based on ZnTe can play particularly important role in the bottom-up approach to nanoelectronics due to the ease of p-type nitrogen doping of this semiconductor. Additionally magnetic atoms (e.g. Mn) can also be easily incorporated into ZnTe host, the successful growth of ZnTe-based nanowires opens new perspectives for applications in prototype nanospintronic devices, that would take advantage of spin of carriers, in addition to or instead of their charge.

The growth of ZnTe, ZnMgTe and ZnMnTe nanowires was performed from elemental Zn, Mn, Mg and Te sources on the surface of (001), (110) and (111)B oriented GaAs substrates with Au nanocatalysers. Gold nanoparticles were formed by in-situ thermal reorganization of thin layers (from 0.3 to 2 nm) of gold deposited from electron gun source in a separate MBE chamber. The catalytic growth was optimised by varying the Zn/Te flux ratio, substrate temperature and annealing of Au-layers.

The growth of nanowires was observed in-situ by reflection high energy electron diffraction and their morphology and structural properties were assessed by field-emission scanning electron microscopy (FE-SEM), high resolution transmission electron microscopy (TEM), and atomic force microscopy (AFM). Additional studies of the composition of both nanowires and the Au-rich nanocatalysers were performed with the use of energy dispersive X-ray spectroscopy (EDX). Optical properties of NWs were assessed by photoluminescence and Raman scattering studies performed in both macro and micro regime.

Our studies revealed that nanowires with an average diameter of about 40 nm and length above 1 μm are mono-crystalline in their upper parts, their growth axis is $\langle 111 \rangle$, and they grow along $\langle 111 \rangle$ directions of the substrate, independent of the substrate orientation. Au-rich (with 20% of Ga) spherical nanocatalyser was always visible at the tip of a nanowire, thus indicating that vapour-liquid-solid mechanism is responsible for the growth of ZnTe-based nanowires. Analysis of the length vs. diameter of the NWs points to the large contribution of the addatoms diffusing along the NWs surface to the growth rate.

This research was partially supported by the Ministry of Science and Higher Education (Poland) through grant N507 030 31/0735 and by the Network "New materials and sensors for optoelectronics, information technology, energetics and medicine".

17:15

Oral

Combustion Synthesis of Crystalline SiC Nanofibres: Process Characterization

Andrzej Huczko¹, Magdalena Osica¹, Michał Bystrzejewski¹, Hubert Lange¹, Stanisław Cudziło²

1. Warsaw University, Faculty of Chemistry, Pasteura 1, Warszawa 02-093, Poland 2. Military University of Technology (WAT), Kaliskiego 2, Warszawa 00-908, Poland

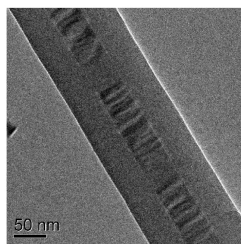
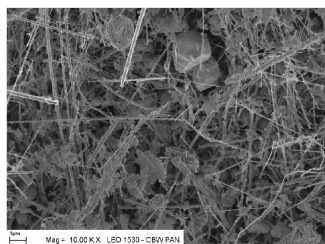
E-mail: ahuczko@chem.uw.edu.pl

SiC as an outstanding large-gap semiconductor exhibits a set of unique physical and chemical parameters, which makes it a promising candidate for numerous applications. If SiC were fabricated in the form of 1-D nanocrystallites, it would have new properties resulting from both its marked shape-specific and quantum-confinement effects. In this presentation, we describe the spontaneous formation of 1-D SiC nanostructures by silicon dehalogenation of poly(tetrafluoroethylene). The growth of nanofibres is initiated by the combustion synthesis in the Si-PTFE system. This process is based on the fact that the strong exothermic reaction propagates rapidly through the mixture of solid reactants. Rapid cooling of the products can lead to nucleation of 1-D nanocrystallites without any growth [1,2].

The synthesis process itself was monitored by emission spectroscopy measurements to evaluate reaction temperature and pressure control to calculate the pressure histories of combustion.

The effect of process variables, as reactants characteristics and ratio, initial pressure and combustion environment, reactor configuration, etc., on the reaction yield was studied.

The as obtained products were characterized by electron microscopy, Raman spectroscopy, XRD diffraction, and chemical analysis. The β -SiC nanofibres ca. 20-100 nm in diameter and up to 20 μ m in length (see the Figure) were the main component of solid reaction products. The conversion degree above 90% of starting elemental Si, was obtained. The technique to purify chemically (up to 98%) the SiC nanofibres was elaborated.



SEM images of SiC nano fibre TEM images of a SiC nanofibre

Acknowledgment

This work was supported by the Ministry of Science and Education through the Department of Chemistry, Warsaw University under Grant No. 4T08D 021 23.

References

- [1] A. Huczko et al., J. Phys. Chem., 2005, 109, 16244
- [2] S. Cudziło et al., Carbon, 2005, 43, 1778

Dinner

Monday evening, 21 May, 18:00

Poster Session 1

Monday evening, 21 May, 19:00

19:00

Poster

P101

Effect of impurities in supersaturated solutions and its effect on cluster growth by gravity driven concentration gradient studies

Govindan Anandha babu, Perumalsamy Ramasamy

E-mail: ganand_babu@yahoo.com

Previous measurements of concentration gradients formed in long columns of supersaturated glycine solutions indicate that small amounts of impurities, such as valine, can lead to increase in the magnitude of the gradient. This indicates that the impurity enhances cluster formation [1]. The concentration gradients were measured in two supersaturated systems- Potassium dihydrogen phosphate with potassium chloride as the impurity and Benzophenone with Urea as the impurity. Metastable zone widths of the supersaturated solutions were also measured in the presence of impurities. Weight average molecular weight, M_w , Degree of Association, p , Number average molecular weight, M_n , Average number of molecules per cluster, n , and weight average cluster diameter were calculated for Potassium dihydrogen phosphate and Benzophenone supersaturated solutions. The cluster sizes are estimated from the concentration gradient data in the presence and absence of impurities and also changes noted in metastable zone widths. The changes in concentration gradients of supersaturated solutions appear to be a reliable indicator of the effect of impurities on cluster growth and nucleation.

The presence of KCl in KDP caused an increase in the concentration gradient and cluster size compared to pure system. The presence of Urea in Benzophenone caused decrease in the concentration gradient and cluster size compared to pure system. Recently discovered Sankaranarayanan-Ramasamy method is used to grow long crystals of good optical quality [2-3]. Long columns of solution are used in this method. For larger particular column height cluster size may attain critical size. At a particular stage more number of embryos and critical nuclei present in solution may come to the bottom of the solution due to gravitational field. At this stage crystal growth process will be disturbed. Determination of critical height of Potassium dihydrogen phosphate and Benzophenone solutions is in progress.

References

- [1] R.M.Ginde, A.S.Myerson, J.Crystal Growth.116 (1992)41.
- [2] K. Sankaranarayanan, J.Crystal.Growth.284 (2005)203.
- [3] N.Balamurugan and P.Ramasamy, Crystal Growth and Design 6(2006)1642.
- [4] J.W.Mullin and C.L.Leci, Phil .Mag.19 (1969)1075.
- [5] M.A.Larson and J.Garside, Chem.Eng.Sci.41 (1986)1285.

19:00	Poster	P102
-------	--------	------

Stabilized nanoapatites doped with REE obtained from aqueous solution

Nataliya V. Babayevskaya, Alexandra S. Kryzhanovskaya, Yuriy N. Savin, Alexander V. Tolmachev

Institute for Single Crystals NAS of Ukraine (ISC), 60 Lenin Ave., Kharkov 61001, Ukraine

E-mail: Babayevskaya@isc.kharkov.ua

Nowadays apatite-like compounds and impurity-doped apatites ($\text{Me}_{10}(\text{Zr}_4\text{O}_{10})\text{X}_2$) have been studied extensively since they are widely used as luminescence materials for optical ceramics and light converting coatings. Technology trade development of luminescent nanoceramics requires the controllability of particle size and shape as well as phase composition of crystalline material. Properties of apatite nanocrystals are the subject of considerable controversy connected with nano-sized effects and site-selective emission spectra. Therefore the effect of synthesis conditions on physical and chemical properties of nanocrystalline phosphors is the topical problem.

Nano-crystalline polymer-stabilized fluorapatite doped with Eu^{3+} , Tb^{3+} , Ce^{3+} (hereafter FAP:REE³⁺) has been synthesized from aqueous solution. The samples were studied by XRD, SEM, TEM and XPS methods. It is shown that during the synthesis of nanocrystalline FAP from aqueous solution the contamination of CaF_2 phase (30-50 nm crystals) is difficult to avoid. Synthesis conditions were optimized for preparing monophase polycrystalline FAP:REE³⁺. Effective segregation coefficients of REE at various conditions were determined. Coherent length of the perfect crystalline domains along 002 direction is 15-50 nm. FAP:REE³⁺ nanocrystals (50-200 nm in length) have complex rod-like and plate-like structure. Cell parameters varying with dopant concentration and are $a = 9.376\text{-}9.450$, $c = 6.863\text{-}6.872$.

The influence of REE concentration, temperature and annealing duration on luminescence intensity was studied.

19:00	Poster	P104
-------	--------	------

Growth and characterization of YAG single crystals doped with large concentration of vanadium.

Andrzej L. Bajor¹, Jaroslaw Kisielewski¹, Krzysztof Kopczynski², Jadwiga Mierczyk², Dorota A. Pawlak¹, Marek A. Swirkowicz¹, Tadeusz Łukasiewicz¹

1. Institute of Electronic Materials Technology (ITME), Warszawa 01919, Poland **2.** Military University of Technology, Institute of Optoelectronics (IOE), Kaliskiego 2, Warszawa 00-908, Poland

E-mail: Andrzej.Bajor@itme.edu.pl

Yttrium Aluminium Garnet (YAG) doped with V ions is an interesting optical material, especially useful as non-linear absorber (Q-switch) working in the spectral range of approx. 1100 to 1400 nm (1300 nm being the optimal wavelength). Besides, it has a noticeable absorption band around 800 nm which makes it applicable in lasing applications (diode pumped lasers). YAG:V single crystals were grown by the Czochralski method using Cyberstar Oxypuller 05-03 equipment. Thermal system consisted of iridium crucible of

50 mm diameter, and a passive iridium afterheater of 60 mm diameter. Inductive heating with Hüttinger generator was used. It is very important that the vanadium ions are located in defined sites in the crystal structure (oxygen tetrahedrons). To obtain this, different growth atmospheres were applied (nitrogen without and with admixture of oxygen), and, besides, the as-grown boules were annealed in reducing atmospheres after the growth processes. Finally, good quality single crystals, [111]-oriented, with vanadium content of 0.6 to 3.5 at. % were obtained. They were up to 25 mm in diameter and up to 70mm in length.

The initial concentrations of vanadium (0.6 to 1.5 at. %) were found to be a little bit too small for optimal Q-switching operation. Therefore, we have also tried to grow crystals with larger concentrations, namely of 1.5 and 3.5 at. %. One needs to remember that the larger the doping is, the larger is also the potential concentration of V^{+3} ions. However, this process of vanadium reduction into V^{+3} ions doesn't seem to be linear. Besides, as a rule, the larger the doping is, the larger the crystal imperfections can become. So, a certain optimal value of vanadium doping should be expected.

We have used several techniques of vanadium reduction into V^{+3} ions, and the thermal reduction in vacuum was found to be optimal. By spectroscopic and polarimetric investigations we have also determined that the crystals with increased doping concentrations were optically homogeneous. The absorption coefficient at 1300 nm wavelength was found to be as large as 1.75 cm^{-1} in crystals doped with largest concentrations of vanadium, i.e. it was approx. 20 % larger than those reported elsewhere¹. This makes our crystals a better source for Q-switching operation.

References :

1. Z. Mierczyk, Z. Frukacz, "YAG:V³⁺ – new passive Q-switch for lasers generating radiation within near infrared range", Opto-Electronics Rev., 1 (2000) 67-74.

19:00	Poster	P105
-------	--------	------

Optical and electrical properties of ZnO:X (X=Al, Mg, In, Ce, Er) crystalline layers

Wacław Bala¹, Beata Derkowska¹, Michał Wojdyła¹, Bouchta Sahraoui², Marid Addou³, Zouhair Sofiani³, Mateusz Rębarz¹

1. Nicolaus Copernicus University, Institute of Physics, Grudziądzka 5/7, Toruń 87-100, Poland **2.** Université d'Angers, ERT N°15 Cellules Solaires Photovoltaïques Plastiques, Laboratoire POMA, UMR CNRS No 6136, Angers, France **3.** Laboratoire Optoelectronique et Physico-Chimie des Matériaux Université of Ibn Tofail, 14000 Kenitra, Kenitra 14000, Morocco

E-mail: wbala@fizyka.umk.pl

The transparent conductive oxide films have been attractive significant attention in optoelectronic devices such as organic and inorganic electroluminescence diodes (OLED, LED), and photovoltaic cells (PV). Impurity doped ZnO thin layers have been widely used in solar cells and electroluminescence devices because of their higher thermal stability, non-toxic nature, low price, easy fabrication and good electrical and optical behaviour, compared with other oxide materials such as ITO, SnO_2 and others.

In this paper, pure zinc oxide and X (X=Al, Mg, In, Ce, Er)-doped zinc oxide layers were deposited on glass and (111) Si substrates by reactive chemical pulverisation spray pyrolysis and dip coating (sol-gel) technique using zinc and X (X=Al, Mg, In, Ce, Er) chlorides as precursors. The effects of X concentration on the structural, electrical and optical properties of ZnO:X thin layers were investigated in detail. These films were characterized by X-ray (XRD) scanning electron microscopy (SEM), atomic force microscopy (AFM), photoluminescence, DC and AC electrical conductivity measurements.

All deposited ZnO and ZnO:X layers at 725 K are polycrystalline and indicate highly c-axis oriented structure. The dimension of crystallites depends on incorporation of dopant atoms (X) into the ZnO layers. The photoluminescence spectra of the layers have been studied as a function of the deposition parameters such as doping concentration, temperature of substrate and post grown annealing. The photoluminescence spectra were measured at the temperature range from 13 K to 320 K.

19:00	Poster	P106
-------	--------	------

The correlation between the crystal structure and magnetic ordering in ternary RT_2X_2 and RTX_3 compounds

Wiesława Bażela

Cracow University of Technology, Institute of Physics (PK),
Podchorążych 1, Kraków 30-084, Poland

E-mail: dyakon@ifpan.edu.pl

In this paper the influence of the crystal structure on the magnetic ordering in ternary RT_2X_2 and RTX_3 (R is the rare earth metal, T the 3d, 4d or 5d transition metal and $X = \text{Si or Ge}$) compounds is studied. These compounds crystallize in three types of crystal structure which have been derived from the tetragonal $BaAl_4$ structure: in a body-centered $ThCr_2Si_2$ type structure (space group $I4/mmm$), in a primitive $CaBe_2Ge_2$ -type (space group $P4/nmm$) and in a body-centered structure $BaNiSn_3$ (space group $I4mm$). The position of R atoms in these crystal structures causes the anisotropic character of magnetic interaction between the R ions, and the Ising-like model can be used to explain the stability of magnetic ordering. In the rare-earth sublattice the different magnetic structures, namely, collinear AFM and non-collinear AFM cosinusoidally modulated, are observed. The analysis of the magnetic structure of RT_2X_2 ($X = \text{Si, Ge}$) compounds reveals a strong dependence of magnetic ordering on the a/c ratio (a, c are the lattice constants). For $a/c < 0.415$, a simple collinear ordering is observed (for example, in $(Nd, Tb, Dy, Ho, Er)Rh_2X_2$, $PrCu_2X_2$, Rf_2Si_2 , RCo_2X_2 – AF I type; in $NdFe_2Si_2$ and $(Nd, Pr)Fe_2Ge_2$ – AF II type and in $(Gd, Tb, Dy, Ho, Er)Cu_2X_2$ – AF IV type), while the compounds with $a/c > 0.415$ exhibit oscillatory magnetic structure (for example, in $(Tb, Dy, Ho, Er)Os_2Si_2$; in RPd_2X_2 and $(Tb, Dy, Er)Pd_2Si_2$ – LSW IV; in RRu_2X_2 and $TbRu_2X_2$ – LSW II. These relations are performed for large numbers of RT_2X_2 compounds. Another types of magnetic structure than result from this relation are observed for compounds with T = Mn, Fe and Au (for example, in $TbFe_2X_2$ – LSWIV).

The various magnetic structures observed above can be interpreted by the RKKY model of interactions. Such conclusion is supported by the fact that the nearest R – R distance is equal to the lattice para-

meters a of ~ 0.4 nm (in plane) and ~ 0.6 nm (between plane) and that these compounds are good electrical conductors. In isotropic RKKY model, the Fermi vector is dependent strongly on both the a/c ratio and on the number of free electrons Z per magnetic ion. The analysis of modulated magnetic structures RRu_2Si_2 ($R = Tb - Er$) based on RKKY model indicates that the order is stable for $Z \approx 3$. This is in agreement with discussed covalent bonds in tetrahedron TX_4 in $ThCr_2Si_2$ -type crystal structure.

The Néel temperatures in the RPd_2Si_2 , RRu_2Si_2 and RRh_2Si_2 series depend randomly on the number of f -electrons. This fact suggests that the influence of crystalline electric field (CEF) should be also considered in explaining the magnetism in these compounds. The CEF at the R site can strongly affect the magnetic properties of the RT_2X_2 systems. The orientation of magnetic moment with respect to the fourfold axis is connected with the sign of the (CEF parameter). The positive sign at coefficient indicates that the magnetic moment is normal to the tetragonal axis or creates an angle ϕ with it. Its negative value indicates that the moment is aligned along the c -axis. As an example, the magnetic ordering in $TbIrSi_3$ and $TbIr_2Si_2$ will be discussed.

19:00	Poster	P107
-------	--------	------

Analysis of thermochromic effect in $[NH_4]_2CuCl_4$ crystal

Radosław Belka

Kielce University of Technology (KUT), Al.1000-lecia PP no 7,
Kielce PL-25-312, Poland

E-mail: r.belka@tu.kielce.pl

In this paper the thermochromic effect in $[NH_4]_2CuCl_4$ (A-CuCl) crystal is discussed. It belongs to a group of A_2MX_4 crystals (where A- ammonium group or organic cation, M – metal ion, X – halogen ion) [1]. It is known, that for some of them in case when $M = Cu^{2+}$ the thermochromic effect has been observed, which is demonstrated primarily by the change a color from green to yellow [2]. For A-CuCl crystal author observed the change of color from blue to green at 345K.

The A-CuCl crystal has been grown from water solution of 0.1 moles of $CuCl_2$ and 0.2 moles of NH_4Cl using slow evaporation method at the room temperature. The sample was split and polished to obtain the plate with 1mm thickness. The transmission spectra were measured using AVS-S2000 fiber optics spectrometer in wavelength range of 250 – 850nm and in temperature from room temperature to 350K. The results are presented in fig.1.

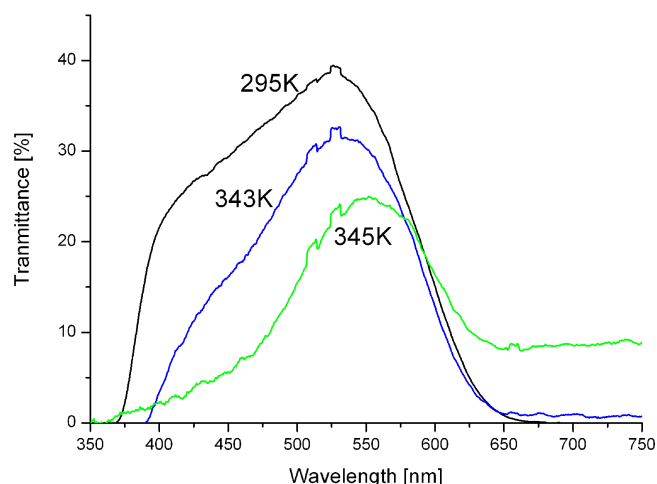


Fig.1. Transmittance spectra of A-CuCl crystal in different temperatures.

Spectral properties of A_2MX_4 ($M = Cu, Co, Mn$) crystals are correlated to the electronic transitions in metal ions [3]. In crystals with Cu^{2+} ion an electrostatic influence of ligands leads to splitting of 2D term. Additionally, due to Jahn-Teller phenomenon the $CuCl_4$ tetrahedra are strongly deformed.

Theoretical model of interaction of ligands with 3d orbitals based on crystal field theory [4] was elaborated. It allows to estimate the influence of molecule deformation on splitting of energy level. Simulations show that the value of the splitting can be clearly different from that for the case of perfect tetrahedron. Transmission spectra for the investigated crystal are limited by absorption bands connected with electronic transitions in Cu^{2+} ion and also probably by ligand-metal charge transfer. With increase of the temperature a shift the absorption edge is observed. Simulations show that it may be connected with reduction of deformation of the polyhedra. The appearance of transparency in the region above 650nm has been observed at 343K. It may be connected with a change of symmetry of the polyhedra and in consequence with a change of selection rules.

[1] Kałuza S., Suchańska M., Belka R., Leśniewski S.: *The phase transitions in ferroelectric crystals of A_2MX_4 and AMX_3 type*, Ferroelectrics, 2002, vol. 273, pp.143-148.

[2] Polovinko I., Kałuza S., Korczak Yu., Kapustianik V.: *Thermochromic properties of the A_2CuCl_4 crystals*, Molecular Physics Reports 18/19, 67, 1997

[3] Kałuza S., Suchańska M., Polovinko I.: *Studies of absorption spectra of A_2BCl_4 ($B=Cu, Co$) crystals with organic cations*, Ferroelectrics, vol. 239, 2000, pp. 189-196.

[4] Ballhausen C.: *Introduction to Ligand Field Theory*, McGraw-Hill, New York, 1962

19:00

Poster

P108

Structure and magnetic properties of carbon encapsulated Fe nanoparticles obtained by arc plasma synthesis

Jolanta Borysiuk¹, Agnieszka Grabias¹, Jacek Szcztyko², Andrzej Twardowski², Michał Bystrzejewski³, Hubert Lange³

1. Institute of Electronic Materials Technology (ITME), Wólczyńska 133, Warszawa 01-919, Poland 2. Warsaw University, Faculty of Physics, Hoża 69, Warszawa 00-681, Poland 3. Warsaw University, Faculty of Chemistry, Pasteura 1, Warszawa 02-093, Poland

E-mail: jolanta.borysiuk@itme.edu.pl

Carbon encapsulated Fe nanoparticles were obtained using arc plasma synthesis. TEM (transmission electron microscopy) and Mössbauer spectroscopy showed that Fe particles consist of metallic and carbide phases encapsulated by graphitic carbon. The particles were of 10–100 nm in diameter, and were covered by carbon layers 5–15 nm thick. The transmission Mössbauer spectra revealed two magnetic and two paramagnetic components, related to iron containing phases. It was shown that about 47% of iron atoms are located in the Fe₃C phase. The remaining iron belongs to the bcc Fe and fcc Fe(C) phases. Magnetic measurements showed that saturation magnetization M_s was equal to 53 emu/g, which is about 25% of the saturation magnetization of bulk iron. The remnant to saturation magnetizations ratio was $M_r/M_s \sim 0.15$, showing that the carbon coated Fe nanoparticles are ferromagnetic.

19:00

Poster

P109

Impulsive excitation of mechanoluminescence in gamma irradiated Er doped calcium fluoride single crystals

Nameeta Brahme, Vidya Sahu, Durga P. Bisen, Rajeev S. Kher

Pt. Ravi Shankar Shukla University (RSSU), N.H.6, Raipur 492010, India

E-mail: namita_brahme@rediffmail.com

Impulsive technique has been used for Mechanoluminescence (ML) measurements in γ -irradiated Er doped CaF_2 crystals. The crystals of $CaF_2:Er$ were grown by Bridgman technique at BARC Mumbai. The cleaved crystals were annealed at 450 °C for about two hours and cooled very slowly and then irradiated for different time from ^{60}Co source having an exposure rate of 2.8×10^3 Gy/hr. ML is excited impulsively by the impact of moving piston onto γ -irradiated $CaF_2:Er$ crystals. Two peaks are observed in ML intensity V_s time curve and it is seen that the peak intensity of first and second peak (I_{m1} and I_{m2}) increases with increasing impact velocity. However the time corresponding to first and second peak (t_{m1} and t_{m2}) shift towards shorter time values with increasing impact velocity. It is also seen that the total ML intensity I_T initially increases with the impact velocity and then it attains a saturation value for higher values of the impact velocity. Theoretical model is proposed which explains the experimental results satisfactorily.

19:00 Poster P110

Secondary Ion Mass Spectroscopic Study of Mn-Implanted Silicon after Thermal Annealing

Guangyu Chai¹, Lee Chow¹, Andrzej Misiuk², Adam Barcz³, Arun Shunmugavelu¹, Eun S. Choi⁴, Richard Vanfleet⁵, M. Pruszczyk²

1. University of Central Florida, Orlando, FL, United States **2.** Institute of Electron Technology (ITE), al. Lotników 32/46, Warszawa 02-668, Poland **3.** Polish Academy of Sciences, Institute of Physics, al. Lotników 32/46, Warszawa 02-668, Poland **4.** National High Magnetic Field Laboratory (NHMFL), Tallahassee, FL 32310-3706, United States **5.** Brigham Young University, Provo, UT 84602, United States

E-mail: chow@ucf.edu

Re-distribution of Mn⁺ implanted Czochralski silicon (CzSi:Mn) and floating zone silicon (FzSi:Mn) after thermal annealing between 300°C and 1000°C has been studied using secondary ion mass spectrometry (SIMS). The silicon substrates were implanted with 160 keV Mn⁺ ion to a dose of $1 \times 10^{16} \text{ cm}^{-2}$ at room temperature and at 310°C. The Mn profiles after annealing above 900°C showed multiple concentration peaks for the samples implanted at room temperature, indicating the influence of defect structures on the diffusion behavior. For the Si sample that was implanted at 310°C, only one concentration peak was observed. The SIMS depth profiles were compared with recent reports [1,2] of depth profiles of Mn implanted silicon. We also carried out cross sectional TEM and magnetization measurements to correlate the micro-structural and magnetization data with depth profile obtained by SIMS.

[1] M. Bolduc, C. Awo-Affouda, F. Ramos, and V. P. LaBella, J. Vac. Sci. Technol. A **24**(4), 1648 (2006).

[2] A. Misiuk, J. Bak-Misiuk, B. Surma, W. Osinniy, M. Szot, T. Story, J. Jagielski, J. Alloys Comp., **423**, 201 (2006).

19:00 Poster P111

Spectroscopic Properties of Tm³⁺:Bi₂TeO₅ Single Crystal

Grażyna Dominiak-Dzik¹, Witold Ryba-Romanowski¹, Radosław Lisiecki¹, Istvan Foldvari²

1. Polish Academy of Sciences, Institute of Low Temperature and Structure Research (INTiBS), Okólna 2, Wrocław 50-422, Poland **2.** Hungarian Academy of Sciences, Research Institute for Solid State Physics and Optics (SZFKI), Konkoly Thege M. út 29-33, Budapest H-1121, Hungary

E-mail: dzik@int.pan.wroc.pl

Single crystal of bismuth tellurite Bi₂TeO₅ (BTO) doped with trivalent thulium (Tm³⁺) was grown by the Czochralski method and investigated by spectroscopic techniques (absorption, emission). The Bi₂TeO₅ structure is orthorhombic with the space group *Abm2*. Tm³⁺ ions, introduced as an optical impurity into BTO, substitute Bi³⁺ ions located in sites with C₁ and C_s point symmetry.

Polarised absorption and emission measurements, carried out at 5 and 300 K are presented. Results obtained were used to determine

the energetic structure of thulium levels within the 4f^N ground electronic configuration.

Emission located in the visible and near infrared (650 and 790 nm) characterises the system under study. The attention was put on luminescence dynamics. The time evolution of the emission intensity from the ³H₄ and ¹G₄ thulium luminescent states was investigated at low and room temperature. Luminescence decay curves are presented. Experimental lifetimes of thulium luminescent levels are compared with those in other Tm³⁺-doped systems.

19:00 Poster P112

Mechanisms of heterogenous growth of calcium fluorapatite coatings from strongly supersaturated aqueous solutions

Andrey G. Doroshenko, Yuriy N. Savin, Alexander V. Tolmachev

E-mail: doroshenko@isc.kharkov.ua

Fluorapatite (Fap, Ca₁₀(PO₄)₆F₂) and hydroxyapatite (HAp Ca₁₀(PO₄)₆OH₂) use as the bioactive coatings of implants [1]. Fap is relevant precursors in production of optical and laser materials, templates of a burial of radioactive materials, mineral fertilizers, is of interest, as idealizing composite and structural mother of marine deposits in the form of marine sedimental apatite [2].

In this study the kinetics and mechanisms of Fap coatings growth and effect of the degree of a supersaturation on a phase composition, structure and morphology of coatings are studied.

Growing of Fap coatings carried on by mixing the aqueous solutions in system CaCl₂ – KH₂PO₄ – NaOH – NaF–NaCl–H₂O in a temperature-controlled quartz reactor (200ml) using the constant composition method, at fixed pH=6,5 and temperature 37±0.5 °C.

It is found, that coatings are textured - plains (002), and oriented predominantly parallelly the surfaces of an emulsion carrier. The size of coherent scattering fields of sample studied is 39 nanometers. The calculated radius of an extreme nucleus has compounded 0,9 nanometers. The kinetics of fluorapatite coatings showed, that at supersaturation $s < 4$, the coatings grow on the dislocation dode, and when the supersaturation $s > 4$ - three-dimensional nucleuses mechanism. It is shown, that at growth on the dislocation dode, the growth rate is checked by diffusion of ions on surfaces of crystalline nucleuses, and processes of mass transfer do not influence on growth rate.

[1] Eun-Jung Lee, Su-Yeon Chae, and Hyoun-Ee Kim. Improvement in biocompatibility of fluoridated apatite with addition of resorbable glass. J. Am. Ceram. Soc., 89 [5] (2006) 1748–1751

[2] A. Aklil, M. Mouflih, S. Sebti. Removal of heavy metal ions from water by using calcined phosphate as a new adsorbent. Journal of Hazardous Materials. 2004, V. A112, P. 183–190

19:00 Poster P113

Layered cobaltites: single crystal growth, structure, transport and magnetic propertiesKazimierz Conder¹, Marian Stingaciu¹, Ekaterina Pomjakushina¹, Andrew Podlesnyak²**1.** Paul Scherrer Institut (PSI), WLG, Villigen PSI 5232, Switzerland **2.** Hahn-Meitner-Institute (HMI), Glienicker Str. 100, Berlin D-14109, Germany

E-mail: kazimierz.conder@psi.ch

Complex cobalt oxide perovskites with general formula $\text{RBaCo}_2\text{O}_{5+x}$ (R=rare earth) have been attracted considerable interests because of their interesting properties: magnetic and metal-insulator transitions, giant magnetoresistance, ionic conductivity and a structural similarity to high temperature superconductors. All the compounds are oxygen non-stoichiometric ($0 < x < 1$) and the cobalt cations can adopt different oxidation and spin states. Growing of single crystals of these materials is very difficult. Preliminary studies of pseudobinary phase diagrams $\text{RCoO}_3\text{-BaCoO}_3$ (R=Pr, Ho and Tb) have been shown that the compounds melt incongruently and the primary crystallization fields are very narrow. Crystal growth experiments have been performed using Traveling Solvent Floating Zone method using a mirror furnace. Generally, during the crystal growth experiments it has been difficult to stabilize the floating zone, especially for very low growing rates (below 0.5 mm/h). The resulting materials were often polycrystalline with many cracks. From many experiments performed, the best results have been obtained in the case of R=Tb and Nd. For these two systems good quality single crystals in size of several mm³ could be obtained. For these crystals measurements of magnetization, resistivity, specific heat, thermopower, neutron diffraction and muon spin rotation have been performed.

19:00 Poster P114

Physico-chemical properties of borate single crystals of different structural typesElena Dolzhenkova, Vyacheslav N. Baumer, Alexander V. Tolmachev*Institute for Single Crystals NAS of Ukraine (ISC), 60 Lenin Ave., Kharkov 61001, Ukraine*

E-mail: dol@isc.kharkov.ua

Borate single crystals are promising materials for non-linear optics, acoustoelectronics, piezotechnology, dosimetry and scintillation materials for detection of thermal neutrons.

The main structural units in borate single crystals are boron-oxygen complexes (B_nO_m) with direct covalent bonds shared by common oxygen atom in different ways. Cations of metals are linked with oxygen atoms by ionic bonding. Crystallochemical peculiarities of borate single crystals allow to realize all four structural types known for compounds with different types of bonds (islet, chain, layer, skeleton) in these crystals. Therefore, in this borate system we can observe the role of crystal structure peculiarities in the formation

of their physico-chemical properties.

The perspective of the practical use of borate crystals require the study of their physico-mechanical properties. In this study we investigated the peculiarities of the deformation and fracture of borate crystals of different structural types under mechanical stresses.

It is found that all the types of borate crystals are characterized by a strong temperature dependence of dislocation motion. Slipping in this crystals starts at the temperature $T \sim 0.9T_{\text{melt}}$. It is established that slip in islet type $\text{Li}_6\text{REB}_3\text{O}_9$ (RE=Gd, Eu, Y) borate single crystals occurs in the planes most closely packed with respect to oxygen ions. The system of cleavage plane in these single crystals is associated with the break of RE-O bridging bonds and the longest Li-O bonds in five-vertex polyhedra of Li. Slipping in $\text{Li}_2\text{B}_4\text{O}_7$ single crystals of skeleton type takes place along the cavities of the boron-oxygen skeleton. And it is found that crack propagation in this crystal occurs in each case along the atomic layers linked by bridging oxygen atoms between the main structural units (B_4O_9). It is shown that chain- and layer-type borate single crystals LaB_3O_6 and beta- BaB_2O_4 are damaged practically without deformation.

19:00 Poster P115

Growth and Magnetic properties of rubidium rare earth double tungstates single crystals.Mieczysław T. Borowiec¹, Vladimir P. Dyakonov^{1,2}, Tetyana Zayarnyuk¹, Marek Berkowski¹, Andrzej Szewczyk¹, Maria Gutowska¹, Eduard E. Zubov^{1,2}, Wiktor Domuchowski¹, Marek Barański¹, Henryk Szymczak¹**1.** Polish Academy of Sciences, Institute of Physics, al. Lotników 32/46, Warszawa 02-668, Poland **2.** National Academy of Sciences of Ukraine, Donetsk Technical-Physical Institute, R. Luxemburg 72, Donetsk 83114, Ukraine

E-mail: dyakon@ifpan.edu.pl

Magnetic and thermal investigations of the rubidium rare earth double tungstates $\text{RbRE}(\text{WO}_4)_2$ (RE= Dy, Nd, Sm) have been performed and compared with some potassium rare earth double tungstates.. Rubidium rare earth double tungstate single crystals have been grown by the top-seeded solution growth method (TSSG). They crystallize in the monoclinic crystal structure, with the C2/c space group. Using the X-ray diffraction measurements the unit cell parameters have been determined.

The magnetic properties as a function of both temperature and magnetic field intensity have been studied. The magnetization has been measured in the temperature region from 4.2 K to 100 K and in magnetic field up to 1.45 T. A strong anisotropy of magnetic properties was found. The data on temperature and field dependencies of magnetization was used to determinate the exchange interaction parameters. Results of study of magnetic properties of the rubidium rare earth double tungstates have been compared with result obtained for potassium rare earth double tungstates.

The specific heat measurements in these single crystals are also presented. The specific heat $C(T)$ of the $\text{RbDy}(\text{WO}_4)_2$, $\text{RbNd}(\text{WO}_4)_2$ and $\text{RbSm}(\text{WO}_4)_2$ crystals have been measured over a temperature range of 1.6–300 K in magnetic field up to 10 T.

These crystals are established to be new perspective materials for an

adiabatic demagnetization.

This work was supported by EU project DT-CRYS, NMP3-CT-2003-505580, by Polish State Committee on Science (KBN) (decision of project No. 72/E-67/SPB/6. PR/DIE 430/2004-2006).

19:00 Poster P116

Growth kinetics and crystallization front shape in Cz-process of Nd: YAG, Cr,Ca : YAG and Cr,Ca,Nd : YAG crystals

Reza Faiez

E-mail: rfaiez@gmail.com

In Cz-process, the crystallization front shape is a strong indicator of the crystal thermal history. The radial non-uniformity of thermal history, associated with the curved ($\kappa \neq 0$) front shape, affects the crystal structure and properties. The ideal flat ($\kappa = 0$) interface is not generally stable during the growth of high-melting point oxides typically exhibit convex ($\kappa > 0$) to melt front shapes. The crystal rotation rate, ω generates a forced upward flow in the melt central column and affects the boundary layer thickness in BPS model. Experimentally, the abrupt interface inversion in Cz-growth Nd:YAG and Yb:YAG crystals with $A = (r/R) \sim 0.4$, could be observed only at the final stages in which both the melt depth, h and the fluid flow Ra-number has significantly decreased. From simulations of the melt parabolic temperature, T_w - dependence on h along the crucible wall, some critical positions, $h^* \leq A h_0$ are found for which the buoyancy forces should change the sign. However, at the same positions in the melt central column, the forced upward flow ($Re \sim r^2 \omega$) is relatively strong. Around such positions the S/L interface inversion would suddenly occur. In Cz-growth of Nd,Cr,Ca:YAG crystal ($V \sim 1$ mm/hr; $\omega = 24$ rpm) and after a well-shoulder ($\Phi \sim 38.5$ mm) stage, some strong tendency to decrease ($\sim 24\%$) in diameter was observed without any measurable external perturbation. So a critical cross section (CCS) of ~ 8.5 mm in thickness was formed. This was almost the same as experienced in the case of Cr,Ca:YAG growth leading to abrupt separation of the flat-interface shoulder from the melt. A sharp decrease in rotation rate was needed to regain the Nd,Cr,Ca:YAG growth stability. The process continued safely under the new growth conditions (NGC: $\Phi = 29.5$ mm, $\omega = 12$ rpm). However, the detailed spectral study of the crystal ($L = 176$ mm) revealed that Cr^{4+}/Al^{3+} tetrahedral site occupation is limited to the initial part ($L = 48.5$ mm) including the up-cone and CCS-region. The rest of the body ($L = 128$ mm), grown under the new growth conditions (NGC) and clear green in color, is evidently dominated by Cr^{3+} ions. The shoulder-stage instability might be described as a perturbation developed near by the tri-junction point affecting the fluid flow and heat transfer in a region just close to the S/L interface. However, the observed sharp decrease in diameter, associated with $\kappa \rightarrow 0$, is mainly attributed to the internal radiation heat transfer which fails for the body of highly coated surface. In fact, the brown/red color of the initial part appeared only after polishing the surface being completely coated with impurities deposited by vapor-phase transport. As well, the applied NGC obviously prevented the charge compensation mechanism (CCM) so that Ca^{2+}/Y^{3+} octahedral site occupation couldn't be realized. In BPS model δ_D/Φ represents the aspect ratio

of the boundary layer and the higher δ_D/Φ , the lower is k_{eff} as the segregation coefficient of the solute. This was the outcome of the applied NGC leading to a sharp decrease in Re-number of the flow field. The layer thickness δ_D should be increased about 42% while the diameter Φ has effectively (24%) decreased. Thus, NGC has resulted in a higher ($\sim 87\%$) δ_D/Φ affecting k_{eff} of Ca^{2+} ions of $k < 1$ and stopped CCM as the prime condition for Cr^{eff+}/Al^{3+} site substitution.

19:00 Poster P117

Crystallization of $(Co/Ni/Mg)_3V_2O_8$ mixed orthovanadates by the floating zone method

Jan Fink-Finowicki

Polish Academy of Sciences, Institute of Physics, al. Lotników 32/46, Warszawa 02-668, Poland

E-mail: finow@ifpan.edu.pl

$Co_3V_3O_8$ and $Ni_3V_3O_8$ crystals with the so called staircase Kagomè structure exhibit unusual magnetic properties due to a partial magnetic frustration, therefore these materials have recently attracted much interest [1-3]. In the last years Mg, Co, Ni and orthovanadates were obtained by the floating zone [4,5].

The orthorhombic crystal structure of Co, Ni and Mg orthovanadates is based on slightly deformed cubic close packing of oxygen ions. $3/8$ of existing octahedral positions are occupied by Co^{2+} , Ni^{2+} or Mg^{2+} ions and $1/8$ of tetrahedral positions by V^{5+} ions. Similarity both in the lattice parameters (determined mainly by the ionic radius of oxygen ions) and in chemical properties of these compound cause the possibility of formation their solid solutions in the whole composition range. Therefore it is possible to modify the magnetic properties by putting magnetic Co^{2+} (with $S=3/2$), Ni^{2+} ($S=1$) or non-magnetic Mg^{2+} ions in the staircase Kagomè structure. Single crystals of mixed orthovanadates were grown from polycrystalline feed rods by floating zone technique using a double ellipsoidal optical image furnace. Crystallization processes were carried out in 0.1 MPa oxygen atmosphere at growth rate of 2 mm/h. Due to the noncongruent crystal melting a special attention was paid to finding the proper starting composition.

- [1]. R. Szymczak, M. Baran, R. Diduszko, J. Fink-Finowicki, M. Gutowska, A. Szewczyk, and H. Szymczak. *Phys. Rev. B* **73**, 094425 (2006).
- [2]. Y. Chen, J. W. Lynn, Q. Huang, F. M. Woodward, T. Yildirim, G. Lawes, A. P. Ramirez, N. Rogado, R. J. Cava, A. Aharony and O. Entin-Wohlman, A. B. Harris, *Phys. Rev. B* **74**, 014430 (2006)
- [3]. M. Kenzelmann, A. B. Harris, A. Aharony, O. Entin-Wohlman, T. Yildirim, Q. Huang, S. Park, G. Lawes, C. Broholm, N. Rogado, R. J. Cava, K. H. Kim, G. Jorge, and A. P. Ramirez, *Phys. Rev. B* **74**, 014429 (2006)
- [4]. J. D. Pless, N. Erdman, D. Ko, L.D. Marks, P. C. Stair, and K. R. Poeppelmeier, *Crystal growth & Design* **3**, 613 (2003)
- [5]. G. Balakrishnan, O. A. Petrenko, M. R. Lees, and D. M. K. Paul, *J. Phys.: Condens. Matter* **16**, L347 (2004).

19:00 Poster P118

Study of the third order nonlinear optical properties of $\text{Zn}_{1-x}\text{Mg}_x\text{Se}$ and $\text{Cd}_{1-x}\text{Mg}_x\text{Se}$ crystals

Beata Derkowska¹, Franciszek S. Firszt¹, Bouchta Sahraoui², Agnieszka Marasek¹, Magdalena Kujawa¹

1. Nicolaus Copernicus University, Institute of Physics, Grudziądzka 5/7, Toruń 87-100, Poland 2. Laboratory POMA, UMR CNRS, University of Angers, 2 Boulevard Lavoisier, Angers 49045, France

E-mail: ffirszt@fizyka.umk.pl

Third order nonlinear optical susceptibilities ($c^{(3)}$) of ternary $\text{Zn}_{1-x}\text{Mg}_x\text{Se}$ and $\text{Cd}_{1-x}\text{Mg}_x\text{Se}$ crystals have been measured using standard degenerate four wave mixing (DFWM) method at 532nm. The nonlinear transmission technique have been applied to check if our crystals exhibit two-photon absorption. The two-photon absorption coefficients (b), is directly related to the imaginary part of the third order nonlinear optical susceptibility at the excitation wavelength. The studied $\text{Zn}_{1-x}\text{Mg}_x\text{Se}$ and $\text{Cd}_{1-x}\text{Mg}_x\text{Se}$ solid solutions were grown from the melt by the modified high-pressure Bridgman method. For both crystals the energy gap increases with increasing Mg content.

In the case of $\text{Zn}_{1-x}\text{Mg}_x\text{Se}$, we have found that the value of third order nonlinear optical susceptibility ($c^{(3)}$) decreases with increasing of Mg content. An explanation of this behavior results from the dependence of optical nonlinearities on the energy band gap (E_g) of the studied crystals.

We have also found that the value of third order nonlinear optical susceptibility ($c^{(3)}$) for $\text{Cd}_{0.64}\text{Mg}_{0.36}\text{Se}$ is higher than for $\text{Zn}_{0.65}\text{Mg}_{0.35}\text{Se}$. This behavior can be understand if one take into consideration that the free carrier concentration in $\text{Cd}_{1-x}\text{Mg}_x\text{Se}$ samples is about four orders of magnitude higher than that in $\text{Zn}_{1-x}\text{Mg}_x\text{Se}$ ones with comparable Mg content respectively. It is commonly known that when the electric conductivity increases the values of nonlinear optical properties increase.

In the case of $\text{Cd}_{1-x}\text{Mg}_x\text{Se}$ with low content of Mg, no response was observed for the studied wavelength since the energy gap in such crystals is smaller than the photon energy of laser radiation.

From the performed measurements one can conclude that the incorporation of Mg as constituent into ZnSe and CdSe crystals leads to change the third order nonlinear optical susceptibilities.

19:00 Poster P119

Photoelectric and Photothermal Investigations of $\text{Zn}_{1-x-y}\text{Be}_x\text{Mn}_y\text{Se}$ Solid Solutions

Franciszek S. Firszt, Karol Strzałkowski, Jacek Zakrzewski, Stanisław Łęgowski, Hanna Męczyńska, Agnieszka Marasek

Nicolaus Copernicus University, Institute of Physics, Grudziądzka 5/7, Toruń 87-100, Poland

E-mail: ffirszt@fizyka.umk.pl

$\text{Zn}_{1-x-y}\text{Be}_x\text{Mn}_y\text{Se}$ semiconductor is an interesting material for spintronics as a spin filter layer with possible applications in memory

technology. Changing of the content of beryllium allows obtaining materials with different energy gap and lattice constant, matched to different substrates. For application in multilayer technology, knowing of optical and thermal properties of such material is very important. Up to date there are only a few papers concerning $\text{Zn}_{1-x-y}\text{Be}_x\text{Mn}_y\text{Se}$ material. This work deals with photoconductivity, luminescence and photoacoustic investigations of bulk $\text{Zn}_{1-x-y}\text{Be}_x\text{Mn}_y\text{Se}$ mixed crystals.

$\text{Zn}_{1-x-y}\text{Be}_x\text{Mn}_y\text{Se}$ solid solutions were grown from the melt by the modified Bridgman method. Photoluminescence and photoluminescence-excitation spectra were measured in the temperature range from 30K to room temperature. Photoacoustic spectra were measured applying the mechanically chopped radiation from the xenon lamp after passing through monochromator. The PA signal was detected using an open photoacoustic cell with PZT transducer and lock-in technique. Photoconductivity and transmission spectra were carried out at room temperature.

Photoluminescence spectra at low temperatures of $\text{Zn}_{1-x-y}\text{Be}_x\text{Mn}_y\text{Se}$ samples with Mn content not exceed 5% consist of relatively weak exciton line, shallow donor-acceptor band (edge emission) and the main yellow luminescence band positioned at the energy about 2.05 eV associated with Mn ions. The exciton line was observed in samples with Mn content up to 0.2. For larger concentration of manganese only yellow emission is observed at temperatures from 35K to room temperature. The photoluminescence-excitation spectra, when the emission is detected at 2.05 eV, consist of four clearly resolved components, interpreted as due to transitions from the ground $6A_1(^6S)$ state of Mn to different excited states associated with crystal field splitting.

The piezoelectrically detected photoacoustic spectra were interpreted using Jackson and Amer theory. From the spectral dependence of the amplitude and phase of photoacoustic signal the variation of energy gap with composition was determined. It was found that the influence of Mn on the value of energy gap is much lower than Be. Very important parameter characterizing semiconductors is the thermal diffusivity, which describes the process of thermal transport in semiconductors and characterizes the time required to establish the thermal equilibrium in the investigated material. In this work thermal diffusivity was determined from the dependence of photoacoustic signal on modulation frequency of radiation illuminating the sample. It was calculated with the method of fitting of experimental data to theoretical model developed by Blonskij et al.

The excitation spectra of photoconductivity were measured in the energy range from 0.8 eV to 3.6 eV and compared with PA and PLE spectra.

The photoluminescence-excitation spectra provide information concerning radiative recombination processes in semiconducting materials, while photoacoustic spectral characteristics are directly related to the nonradiative transition paths. Photoconductivity measurements can provide information on both, radiative and nonradiative recombination processes of excited carriers. Some fundamental parameters characterizing semiconducting materials obtained for $\text{Zn}_{1-x-y}\text{Be}_x\text{Mn}_y\text{Se}$ with the mentioned above different methods were compared and discussed.

19:00	Poster	P120
-------	--------	------

Aspects of Wüstite Crystal Growth

Steffen Ganschow, Detlef Klimm, Dirk Maier

Institute for Crystal Growth (IKZ), Max-born Str. 2, Berlin 12489, Germany

E-mail: ganschow@ikz-berlin.de

Wüstite (FeO) constitutes one end member of magnesiowüstite, the fundamental phase in the Earth's lower mantle. In the 1970s Ringwood proposed a model for the Earth's core with wüstite being the major light component. Accordingly, wüstite is presumably the only component occurring in both, the core and in the mantle. Studies of its phase transformations, redox equilibria etc. are fundamental for understanding the core formation and its interaction with the mantle. Although the existence field of wüstite is extraordinarily wide, it does not include stoichiometric wüstite, "FeO". The (non)stoichiometry of wüstite is more correctly expressed by the formula Fe_xO with $x = 0.83 \dots 0.96$ being dependent on the oxygen fugacity. Moreover, wüstite is not stable at room temperature. It rather decomposes in a eutectoid reaction to magnetite Fe_3O_4 and metallic iron Fe around 560°C.

In this work, the growth of wüstite single crystals by the micro-pulling-down technique is described. Crystals grown at different pulling rates are characterized by X-ray and microscope techniques. The room temperature lattice constant determined by X-ray diffraction at single crystal accounts for 4.312 Å. This value corresponds to a composition $\text{Fe}_{0.956}\text{O}$ near the solubility limit on the iron rich side of the existence field.

19:00	Poster	P121
-------	--------	------

Temperature dependence of the linear electrooptic coefficients r_{113} and r_{333} in lithium niobate

Piotr T. Gorski, Rafał Ledzion, Włodzimierz W. Kucharczyk, Krzysztof Bondarczuk

Technical University of Łódź, Institute of Physics, Wólczajska 219, Łódź 93005, Poland

E-mail: piotr.gorski@p.lodz.pl

A new method for measurements of values of individual linear electrooptic coefficients and their temperature dependencies is proposed. In the approach, both the electric-field-induced changes with temperature in the crystal birefringence and the temperature dependence of the ordinary and extraordinary indices are taken into consideration. To measure the changes in the electric-field-induced birefringence the dynamic polarimetric technique was employed (see, e.g. Ref. [1]). The method was applied for linear electrooptic coefficients r_{113} and r_{333} and their intrinsic counterparts. Our measurements were performed within the temperature range 25°C - 200 °C for samples of stoichiometry approximately 49.3%. Contrary to the results obtained for the coefficient r_{222} [2], we found r_{113} and r_{333} to be significantly temperature dependent. The changes in r_{113} and r_{333} are stronger than those obtained by interferometric means and reported for the same coefficients in Ref. [3], however, in Ref. [3] the stoichiometry of samples has not been indicated.

This work has been supported by Polish Ministry of Science and Information Society Technologies, grant no. 1 P03B 102 29.

[1] R. Ledzion, K. Bondarczuk, P. Górski and W. Kucharczyk, Cryst. Res. Technol. 34, 745, (1999).

[2] P. Górski, K. Bondarczuk and W. Kucharczyk, Opto-Electron. Rev.12, 459 (2004).

[3] J. D. Zook, D. Chen, G. N. Otto, Appl. Phys. Lett. 11, 159 (1967).

19:00	Poster	P122
-------	--------	------

Characterization of Pr, Yb, and Ce doped InP layers by PL and SIMS

Jan Grym, Olga Procházková, Jan Lörinčík, Jiří Zavadil, Karel Žd'ánský

Czech Academy of Sciences, Institute of Photonics and Electronics, Chaberská 57, Prague 18251, Czech Republic

E-mail: grym@ure.cas.cz

InP-based semiconductor materials belong to promising candidates for wider use in optoelectronic devices. Parameters of the devices are determined to a large degree by properties of component materials and by technology employed in the fabrication process. Contemporary science offers an extended array of procedures designed to achieve excellent quality of bulk and layer materials. We exploit specific properties of some rare earth elements (REE) in the preparation of InP layers by liquid phase epitaxy (LPE). Dealing with REE in III-V semiconductors, two approaches are usually used. The first approach takes advantage of the gettering properties of REE. The extraordinarily high chemical reactivity of REE can be used for the removal of unwanted impurities from semiconductor compounds. Combined with appropriate technology, additions of REE have been shown to lead to pure semiconductor materials of both conductivity types [1]. We proposed the application of InP-based structures in the fabrication of radiation detectors [2]. The second approach exploits specific luminescence properties of REE when incorporated into the lattice of the crystalline semiconductor material. REE doped semiconductors show sharp luminescence due to the intra-4f-shell transitions. Focusing on InP layers prepared by LPE, the incorporation of REE was confirmed in the case of Yb doping [3]. Photoluminescence (PL) and electrical measurements indicated successful incorporation on Ce doped layers [4]. In most cases, however, REE do not enter the InP lattice.

InP single crystal layers were grown by LPE on (100) oriented InP:Sn and InP:Fe substrates with Pr, Ce, and Yb addition to the melt. The growth process was commenced under flowing high-purity hydrogen at a temperature of 660 °C with a cooling rate of 0.7 °Cmin⁻¹. The metallic REE was mechanically embedded into the melt to prevent its contact with the surrounding ambient at the stage before the growth process to reduce the high affinity of REE especially towards oxygen and hydrogen.

We focused on the characterization of InP epitaxial layers by photoluminescence (PL) and secondary ion mass spectroscopy (SIMS) in order to explain: (i) the gettering effect and conductivity crossover for Pr treated samples, (ii) the incorporation of REE into the InP lattice for Yb and Ce treated samples. Information about chemical ho-

mogeneity of the layers was provided by the measurement of the depth concentration profile by SIMS. The concentration profile was determined for the applied REE and typical electrically active impurities. We analyzed and distinguished native and impurity-related defects from those introduced by REE admixture.

We conclude that a significant improvement of the InP layer purity with addition of Pr into the growth melt was observed. PL spectra were markedly narrowed and fine spectral features were resolved. The incorporation of Yb and Ce into the InP lattice was confirmed by PL and SIMS.

The work has been supported by the grant of the Academy of Sciences of the Czech Republic AV0Z 20670512-1054 and by the Czech Science Foundation grant 102/06/0153.

[1] Zakharenkov, L.; Kozlovskii, V.; Gorelenok, A.; Shmidt, N.: Rare-earth elements in the technology of III-V compounds **1997**, 91-130

[2] Procházková, O.; Grym, J.; Zavadil, J.; Zdánský, K.: *Journal of Crystal Growth*, **2005**, 275, e959

[3] Korber, W. et al.: *Journal of Crystal Growth*, **1986**, 79, 741

[4] Zavadil, J.; Procházková, O.; Gladkov, P.: *Crystal Research & Technology*, **2005**, 40, 498

19:00	Poster	P123
-------	--------	------

Characterization of Ir and IrO₂ Schottky contacts on n-type 4H-SiC under high temperature stress

Norbert Kwietniewski, Marek Guzewicz, Anna Piotrowska, Eliana Kaminska, Krystyna Golaszewska

Institute of Electron Technology (ITE), al. Lotników 32/46, Warszawa 02-668, Poland

E-mail: margu@ite.waw.pl

The unique properties of SiC, such as high thermal conductivity, thermal stability and chemical inertness combined with high concentration, wide bandgap, and high mobility, make them materials of choice for high-frequency/high power/high temperature applications. To take the full advantage of this material, high quality thermally stable Schottky contacts to SiC are required. Up to now, Ti, Al, and Ni were tried as the most widely used n-type Schottky contacts in SiC-based devices. While successfully used in standard conditions, in high temperature and harsh environment they survive rather low time because of their degradation. Therefore, it was necessary to seek other materials for high quality thermally stable Schottky contacts.

In this work we report on optimisation of Ir and IrO₂ Schottky contacts to n-type 4H-SiC and their performance under high temperature stress. Ir and IrO₂ contact metallization was deposited by magnetron sputtering from metallic Ir target. Ir films were dc sputtered in Ar, IrO₂ films were formed by reactive rf process in Ar-O mixture. The deposition parameters (the ratio of Ar/O₂ flow, power, oxygen partial pressure) were adjusted with the goal to obtain film conductivity as high as possible. Schottky contacts were heat treated in Ar atmosphere up to 900°C to evaluate thermal stability of the contact. Thermal tests of the contacts were conducted in air and Ar at 600°C for time up to 100 hours. Surface morphology of Ir and IrO₂ films was characterized by optical and atomic force microscopies, crystal

structure was examined using x-ray diffraction. Sheet resistance of metallization was measured by four-point-probe. The Schottky barrier heights of iridium and iridium oxide on 4H-SiC were investigated as a function of annealing temperature and ageing time by current-voltage (I-V) and capacitance-voltage (C-V) techniques.

The Schottky barriers of the as-deposited Ir/n-SiC and IrO₂/n-SiC are 1.40 eV and 1.53 eV, respectively. Annealing at 600°C for 10 min. increases slightly the barrier height but the subsequent annealing does not influence on that barrier height. The long-term stability of Ir/SiC and IrO₂/SiC Schottky barrier heights will be discussed.

The research is partially supported by the Ministry of Science and Information Society Technologies, Poland, under the grant 3T11B 042 30.

19:00	Poster	P124
-------	--------	------

Optical images of real structure for oxide crystals grown from the melt

Liudmila I. Ivleva, Nikolai V. Bogodaev, Irina S. Voronina, Pavel A. Lykov, Liudmila Y. Berezovskaya, Vjatcheslav V. Osiko

A.M. Prokhorov General Physics Institute of Russian Academy of Sciences (GPI), Vavilov Str. 38, Moscow 119991, Russian Federation

E-mail: ivleva@ran.gpi.ru

Real structure of growing crystal is strongly defined by growth conditions. We suggest new method of investigation of optical homogeneity of oxide crystals. The method is based on observation of optical images of the samples formed in two-wave mixing scheme under holographic amplification in photorefractive crystals.

At present work real structure of crystals grown by Czochralski method and modified Stepanov technique was studied. The peculiarities of micro- and macromorphology and their dependence on the growth conditions were investigated for crystals with scheelite structure (calcium, strontium, barium tungstates and molybdates) and tetragonal tungsten bronze structure (strontium-barium niobate solid solutions).

The method of non-destructive control of optical quality for the transparent materials provides the observation of very thin structure inhomogeneities which could not be observed by conventional methods.

19:00	Poster	P125
-------	--------	------

Analysis of the quadratic electrooptic response of BaTiO₃ crystal in the ferroelectric phase

Marek Izdebski, Włodzimierz W. Kucharczyk

Technical University of Łódź, Institute of Physics, Wólczańska 219, Łódź 93005, Poland

E-mail: marek.izdebski@p.lodz.pl

The quadratic electrooptic response of a noncentrosymmetric uniaxial crystal may origin either from the real quadratic electrooptic effect or a complex indirect contributions, that despite the fact that are related to the linear electrooptic effect, are proportional to the square of the applied electric field. Within indirect contributions, those due

to the linear electrooptic modulation of the light intensity and the modulation of the distance between axes of two partially interfering refracted light beams are of greatest importance [1]. Although the latter effect is usually unintended, it is often unavoidable in real electrooptic devices. Considering the low-temperature ferroelectric phase of BaTiO_3 , one can observe relatively large difference between individual linear electrooptic coefficients [2]. Therefore, the indirect quadratic effect in the crystal depends strongly on the direction of the modulating electric field and the direction of the light beam.

In our work we analyse different configurations and show that the effective coefficient of the indirect quadratic electrooptic effect may be comparable or even higher than the experimental values of quadratic coefficients reported in Ref. [3]. Our analysis is based on the extended Jones matrix calculus, where the partial interference of shifted refracted beams is allowed for [4]. A Gaussian distribution of the light intensity within its cross-sections is considered [5].

This work has been supported by Polish Ministry of Science and Information Society Technologies, grant no. 1 P03B 102 29.

[1] M. Izdebski and W. Kucharczyk, J. Opt. A: Pure Appl. Opt **7**, 204 (2005).

[2] R. L. Sutherland, *Handbook of Nonlinear Optics*, Marcel Dekker Inc., New York - Basel, 2003.

[3] M. Melnichuk and L. T. Wood, J. Opt. Soc. Am. A **22**, 337 (2005).

[4] M. Izdebski and W. Kucharczyk, J. Opt. Soc. Am. A **21**, 132 (2004).

[5] M. Izdebski and W. Kucharczyk, J. Opt. Soc. Am. A **23**, 1746 (2006).

19:00	Poster	P126
-------	--------	------

Investigations on the nucleation kinetics, growth and thermal properties of the organometallic nonlinear optical crystal: $\text{Hg}(\text{N}_2\text{H}_4\text{CS})_4\text{Zn}(\text{SCN})_4$

Rajarajan Kaliamoorthy, Sagayaraj Popu, Sankar Ra, Vetha Potheher

R.V.Government Arts College, Chengalpattu, Tamil Nadu State, Chennai 603001, India

E-mail: krarajan_k2002@yahoo.co.in

Investigations on the nucleation kinetics, growth and thermal properties of the organometallic nonlinear optical crystal: $\text{Hg}(\text{N}_2\text{H}_4\text{CS})_4\text{Zn}(\text{SCN})_4$

K.Rajarajan^{*}, P.Sagayaraj^{#@}, R.Sankar⁺, and Vetha Potheher[#]

^{*}Department of Physics, R.V.Government Arts College, Chengalpattu-603 001, India

⁺Crystal Growth Centre, Anna University, Chennai-600 025, India

[#]Department of Physics, Loyola College, Chennai-600 034, India

Abstract: Single crystals of Tetrathiourea mercury(II) tetrathiocyanato Zinc(II) $\text{Hg}(\text{N}_2\text{H}_4\text{CS})_4\text{Zn}(\text{SCN})_4$; (TMTZ) were grown by slow evaporation technique. The solubility of TMTZ was estimated at different temperatures in a mixture solvent of ethanol and water.

The induction period was measured for the different supersaturation ratios ($S=1.1, 1.2, 1.3$ and 1.4). The study reveals that the induction period of TMTZ decreases with increase in supersaturation. The metastable zone width of TMTZ was measured by polythermal method and thereby the zone width suitable for growing bulk size single crystal of TMTZ was estimated to be $35-45^\circ\text{C}$. The grown crystals have also been subjected to structural, optical and thermal studies. The TG-DTA and DSC studies show that the sample is stable up to 185.3°C and there is no water of crystallization below 179°C , which indicates that the sample can be effectively utilized for various device fabrications below 179°C .

@Corresponding author: Dr.P.Sagayaraj, Reader in Physics, Loyola College, Chennai – 600 034, India Phone: 044-22490490 Fax: 91-44-28231684 Email: psagayaraj@hotmail.com; psraj@loyolacollege.edu

19:00	Poster	P127
-------	--------	------

Elastic properties of $\text{KGd}(\text{WO}_4)_2 : \text{Ho}^{3+}$ single crystals studied by Brillouin spectroscopy

Dobrosława Kasprowicz¹, Sławomir Mielcarek², Aleksandra Trzaskowska², Andrzej Majchrowski³, Edward Michalski³, Mirosław Drozdowski¹

1. Poznań University of Technology (PUT), Nieszawska 13A, Poznań 60-965, Poland 2. Adam Mickiewicz University, Faculty of Physics (AMU), Umultowska 85, Poznań 61-614, Poland 3. Military University of Technology (WAT), Kaliskiego 2, Warszawa 00-908, Poland

E-mail: dobkas@phys.put.poznan.pl

Potassium gadolinium tungstate crystals $\text{KGd}(\text{WO}_4)_2$ doped with rare earth ions are very attractive solid-state laser materials [1]. It was found that $\text{KGd}(\text{WO}_4)_2$ crystals activated with trivalent lanthanide Ln^{3+} ions show high efficiency for stimulated emission at low pumping energies under laser diode excitation [2]. The crystal structure, optical and spectroscopic properties of pure and many Ln^{3+} ions doped $\text{KGd}(\text{WO}_4)_2$ crystals have been already described [3]. However, it is still a little known on their elastic properties at hypersonic frequencies.

Investigated pure and holmium doped $\text{KGd}(\text{WO}_4)_2$ single crystals were obtained by means of the Top Seeded Solution Growth method from $\text{K}_2\text{W}_2\text{O}_7$ solvent [4].

The Brillouin spectra of $\text{KGd}(\text{WO}_4)_2 : \text{Ho}^{3+}$ crystals were collected at room temperature for the $[100]$, $[010]$, $[001]$, $[110]$, $[-110]$, $[011]$, $[0-11]$, $[101]$ and $[-101]$ acoustic phonons in 90° and 180° scattering geometries. Some additional configurations of measurements have been applied for refractive indices determination. Using the measured frequencies of the acoustic phonons propagating in the main crystallographic directions the velocities of the proper elastic waves have been calculated. For investigated $\text{KGd}(\text{WO}_4)_2 : \text{Ho}^{3+}$ crystals the values of elastic constants C_{22} , C_{44} , C_{66} and C_{46} associated with the longitudinal and transverse acoustic phonons propagating along the a and b crystallographic axes and the direction perpendicular to ab plane have been calculated. We compared the obtained values of the elastic constants with the proper values of the elastic constants determined for $\text{KGd}(\text{WO}_4)_2$ crystals [5]. The obtained results show that the elastic properties of $\text{KGd}(\text{WO}_4)_2 : \text{Ho}^{3+}$ crystals are affected

by the doping by Ho^{3+} ions.

Acknowledgement

This work was financed by the Research Project: MNiI 1 PO3B 058 27.

[1] A. A. Kaminskii, A. F. Konstantinova, V. P. Orekhova, A. V. Burtashin, R. F. Klevtsova, A. A. Pavlyuk, *Crystallography Reports*, 46 (2001) 665 – 672.

[2] M. C. Pujol, M. Aguiló, F. Díaz, C. Zaldo, *Optical Mater.*, 13 (1999) 33.

[3] M. C. Pujol, M. Rico, C. Zaldo, R. Sole, V. Nikolov, X. Solans, M. Aguiló, F. Díaz, *Appl. Phys. B*, 68 (1999) 187 – 197.

[4] A. Majchrowski, M. T. Borowiec, E. Michalski, *J. Cryst. Growth*, 264 (2004) 201.

[5] D. Kasprończ, S. Mielcarek, A. Majchrowski, E. Michalski, M. Drozdowski, *Cryst. Res. Technol.*, 41(2006)541.

19:00	Poster	P128
-------	--------	------

Investigation of optical homogeneity in and around the core region in $\text{GdCa}_4\text{O}(\text{BO}_3)_3$ single crystals.

Andrzej Kłos¹, Edyta Wierzbicka^{1,2}, Andrzej L. Bajor¹, Barbara Kaczmarek¹

1. *Institute of Electronic Materials Technology (ITME), Wólczyńska 133, Warszawa 01-919, Poland* 2. *Warsaw University, Institute of Experimental Physics (IEP UW), Hoża 69, Warszawa 00-681, Poland*

E-mail: Andrzej.Klos@itme.edu.pl

Gadolinium calcium oxide borate $\text{GdCa}_4\text{O}(\text{BO}_3)_3$ (GdCOB) crystals have monoclinic, noncentrosymmetric symmetry, and, therefore, exhibit nonlinear effects. Especially they are potential effective generator of the 2nd and higher harmonics of electromagnetic radiation. However, we have discovered that many crystals owe a core region situated in their central parts. In contrary to e.g. YAG crystals, when the core can be seen with a naked eye, the core in GdCOB is visible only in polarized radiation (this can be also evidenced by the X-ray techniques).

A question arises on the nature of the core and its potential use (or disuse) in optics and optoelectronics. In this work we report our primary results concerning the optical homogeneity around the core and in the core region itself. The core in many cases can consume up to 20 – 25% of the crystal diameter.

The GdCOB melts congruently and can be grown by the Czochralski method. Single crystals with diameters up to 35 mm and lengths up to 50 mm were grown from the stoichiometric ratio of Gd_2O_3 , CaCO_3 and B_2O_3 . The powders were prepared by solid - state reaction. The crystals were grown in nitrogen atmosphere from a 100 mm dia. iridium crucible using the [010]-oriented seed. The pulling rate was in the range of 0,8 – 1 mm/h, and the rotation speed was adjusted to 20 rpm.

The as-grown crystals were colourless and their good optical homogeneity was evidenced by optical (spectroscopic, polariscopic) and X-ray techniques (X-ray Lang projection topography in transmission and back reflection geometry).

We have observed two types of the core, namely the one with large gradients of birefringence, and the other one when the birefringence was fairly constant, compared with the neighbouring regions in the crystals. However, the latter case was found to be predominant. It is worth noting that this phenomenon, i.e. that the core was found to be the most homogeneous part of the crystals, was evidenced accordingly by the optical and X-ray techniques. Therefore, we can conclude that the core in GdCOB might be also of a potential use in optical applications.

19:00	Poster	P129
-------	--------	------

Structural inhomogeneities in $\text{GdCa}_4\text{O}(\text{BO}_3)_3$ single crystals

Andrzej Kłos¹, Jarosław Domagała²

1. *Institute of Electronic Materials Technology (ITME), Wólczyńska 133, Warszawa 01-919, Poland* 2. *Polish Academy of Sciences, Institute of Physics, al. Lotników 32/46, Warszawa 02-668, Poland*

E-mail: Andrzej.Klos@itme.edu.pl

Gadolinium calcium oxide borate $\text{GdCa}_4\text{O}(\text{BO}_3)_3$ (GdCOB) crystals have monoclinic, noncentrosymmetric symmetry, and, therefore, exhibit nonlinear effects.

The GdCOB melts congruently and can be grown by the Czochralski method. Single crystals with diameters up to 35 mm and lengths up to 50 mm were grown, from the stoichiometric ratio of Gd_2O_3 , CaCO_3 and B_2O_3 . The powders were prepared by solid - state reaction. The crystals were grown in nitrogen atmosphere from a 100 mm dia. iridium crucible using the [010] -oriented seed. The pulling rate was in the range of 0,8 – 1 mm/h, and the rotation speed was adjusted to 20 rpm.

Recently by X-ray Lang projection topography in transmission and back reflection geometry we have revealed some structural defects in GdCOB. Density of these defects change along the sample and a core, which is situated in the central part of the sample. In the core density was found to be the lowest [1].

In order to find the nature of this core we used Rocking Curve Imaging (RCI) techniques based on high-resolution diffraction method [2]. That allows us to obtain quantitative information on crystallographic misorientations and lattice quality of large sample area with high spatial resolution.

The sample was cut perpendicularly to the crystal growth direction. We discovered a certain inhomogeneity of lattice constants. 2D strain maps were analyzed, and the excess strains in out of the core region respect to the central part of the sample were evaluated to be of the order 5×10^{-5} . These strains generate spatial deformations in the crystal in lattice in the core region. Fluctuations in spatial distributions of Bragg angle out of the core region were also discovered. This can be attributed to the segregation of crystal components during the growth process.

1. E.Wierzbicka, A.Kłos, M.Lefeld-Sosnowska and A.Pajęczkowska, *Phys. Stat. Sol. (a)* 203 (2) (2006) 220-226

2. J.Z.Domagała, Z.R. Zytkeiwicz, I. Grzegory, M. Leszczynski, J.M Yi., J.H. Je, XTOP 2006, 8th Biennial Conference on High Res-

olution X-Ray Diffraction and Imaging, Baden-Baden, Germany, 18-09-2006, Abstract book p. 111

19:00 Poster P130

The investigation of structural perfection and faceting in highly Er - doped $\text{Yb}_3\text{Al}_5\text{O}_{12}$ crystals

Katarzyna B. Kołodziejak¹, Wojciech Wierzchowski¹, Tadeusz Łukasiewicz¹, Michał Malinowski, Krzysztof Wieteska², Walter Graeff³

1. Institute of Electronic Materials Technology (ITME), Wólczyńska 133, Warszawa 01-919, Poland **2.** Institute of Atomic Energy (IEA), Otwock-Świerk 05-400, Poland **3.** Hamburger Synchrotronstrahlungslabor HASYLAB (HASYLAB), Notkestrasse 85, Hamburg D-22603, Germany

E-mail: katarzyna.kolodziejak@itme.edu.pl

The $\text{Yb}_3\text{Al}_5\text{O}_{12}:\text{Er}$ crystals are interesting as promising material for lasers generating efficient emission in the near infrared range, working due to the upconversion mechanism. The trivalent erbium ion provide 2.94 μm line very useful for medical application and 1.55 μm for light guide communication. Due to the presence Yb^{3+} the metastable levels of Er^{3+} can be very effectively excited even by the radiation of much longer wavelengths. $\text{Yb}_3\text{Al}_5\text{O}_{12}$ (YbAG) is of cubic symmetry and belongs to the space group $\text{Ia}\bar{3}\text{d}$. It is isostructural with frequently used yttrium aluminum garnet with a lattice parameter 1% greater. In the laser applications a structural quality of the crystal is of great importance.

The presently investigated crystal with 0%, 1.5 at.%, 10 at.% and 30 at.% of erbium were grown by Czochralski method from iridium crucible. In order to obtain a good homogeneity of chemical composition and distribution of erbium, a relatively large rotation rate of the crystals was applied in the growth process, resulting in the convex growth surface. The structural perfection investigated by means of various synchrotron X-ray diffraction methods including monochromatic beam topography, observation of the rocking curves and topographic methods using white synchrotron white beam. The experiments were performed at E2 and F1 experimental stations in HASYLAB.

The most important observed defects were segregation fringes and growth facets. The monochromatic beam topographs confirmed low level of lattice parameter changes connected with the segregation of the erbium and low level of strains in the crystals. The segregation fringes were, however, more distinct in crystals with higher erbium concentration. Only in one sample the monochromatic beam topography revealed some "rosettes", which may be attributed to the dislocation outcrops.

The observed facets formed a characteristic patterns, dependent on the rotation rate of the crystals. The observed facets may be identified as corresponding to $\{221\}$, $\{211\}$ and $\{301\}$ planes. The first of them are usually forming a core, observed in the most of the crystals, sometimes neighbouring with $\{211\}$. The third type of crystals correspond to the planes inclined at 43 and occurs at highest rotation rate. The investigation of the facets was confirmed by the transmission section topographs, which allowed the location growth bands in

the intersection of the sample with the synchrotron beam.

19:00 Poster P131

Growth and microstructures of $\text{ZnO} - \text{WO}_3$ and $\text{TiO}_2 - \text{WO}_3$ eutectic crystals

Katarzyna B. Kołodziejak¹, Dorota A. Pawlak¹, Krzysztof Rozniatowski², Barbara Kaczmarek¹, Ewa Starnawska³, Darek Artel¹, Włodzimierz Szyrski¹, Tadeusz Łukasiewicz¹

1. Institute of Electronic Materials Technology (ITME), Wólczyńska 133, Warszawa 01-919, Poland **2.** Warsaw University of Technology, Faculty of Materials Science and Engineering (InMat), Wołoska 141, Warszawa 02-507, Poland **3.** Polish Geological Institute (PGI), Rakowiecka 4, Warszawa 00-975, Poland

E-mail: katarzyna.kolodziejak@itme.edu.pl

The self – organized micro – structures of $\text{ZnO} - \text{WO}_3$ and $\text{TiO}_2 - \text{WO}_3$ will be presented. Their growth is based on directional solidification of binary eutectics by the micro-pulling down method. In the case of $\text{ZnO} - \text{WO}_3$ eutectic, the pattern phase is formed by ZnO and the matrix phase is formed by ZnWO_4 . Recently it has been discovered that $\text{ZnO} - \text{WO}_3$ eutectic is a blue phosphor material with the prospective use in advanced flat panel display and lighting applications (a micro/ nanostructured light source). [1] This property could be used as an advantage in looking for metamaterials applications. The qualitative and quantitative analysis of the microstructures obtained with different pulling rate, and cathodoluminescence of the eutectics will be presented.

[1] H. Hayashi, A. Ishizaka, M. Haemori, H. Koinuma, Appl. Phys. Lett., 82, 1365 (2003).

19:00 Poster P132

Growth and microstructure of $\text{ZnO} - \text{Bi}_2\text{O}_3$ eutectic

Katarzyna B. Kołodziejak¹, Dorota A. Pawlak², Krzysztof Rozniatowski⁵, Ryszard Diduszek¹, Michał Malinowski^{1,3}, Marcin Kaczkan³, Ewa Starnawska⁴

1. Institute of Electronic Materials Technology (ITME), Wólczyńska 133, Warszawa 01-919, Poland **2.** Institute of Electronic Materials Technology (ITME), Warszawa 01919, Poland **3.** Warsaw University of Technology, Institute of Microelectronics & Optoelectronics (imio), Koszykowa 75, Warszawa 00-662, Poland **4.** Polish Geological Institute (PGI), Rakowiecka 4, Warszawa 00-975, Poland **5.** Warsaw University of Technology, Faculty of Materials Science and Engineering (InMat), Wołoska 141, Warszawa 02-507, Poland

E-mail: katarzyna.kolodziejak@itme.edu.pl

Eutectics are special materials which are both a MONOLITH and a MULTIPHASE MATERIAL [1]. Thanks to this and their product properties they might behave as metamaterials. In this work a new binary eutectic of $\text{ZnO}-\text{Bi}_2\text{O}_3$ system will be presented. Two types of microstructures has been obtained in this eutectic: globular and fibrous. The pattern phase is formed by ZnBi_2O_6 . The quantitative analysis of the microstructure, luminescence and cathodoluminescence of the eutectic will be presented.

[1] J. Llorca, V. M. Orera, *Progress in Mat. Sci.*, 51, 711 (2006)

19:00 Poster P133

ZnMnO Films grown by Atomic Layer Deposition with uniform Mn distribution

Krzysztof Kopalko¹, Aleksandra Wójcik¹, Marek Godlewski^{1,2}, Elzbieta Guzewicz¹, Rafał Jakiela¹, Matti Putkonen^{3,4}, Lauri Niinistö³

1. Polish Academy of Sciences, Institute of Physics, al. Lotników 32/46, Warszawa 02-668, Poland **2.** Cardinal Stefan Wyszyński University, College of Science, Warszawa, Poland **3.** Laboratory of Inorganic and Analytical Chemistry, Helsinki University of Technology, P.O. Box 6100, FIN-02015 Espoo, Helsinki, Finland **4.** Benq Oy, Ensimmäinen savu, Vantaa FIN-01510, Finland

E-mail: kopalk@ifpan.edu.pl

Atomic layer deposition (ALD) method enables a low temperature (LT) growth, using reactive organic precursors. This is possible, since reaction precursors are sequentially introduced to a growth chamber. Thus, they meet only at a surface of a growing film. Our recent investigations indicated that LT growth is the most promising way to avoid formation of foreign phase inclusions of MnO in ZnMnO material and to block spinodal decomposition [1-3]. These are crucial steps for obtaining material with controlled magnetic properties. ZnMnO is intensively studied for spintronics applications at present. It was clearly shown that inclusions of various Mn oxides, which are present in most of films grown with high temperature methods, give dominating magnetic response of the ZnMnO samples.

In this presentation we discuss growth conditions of LT ZnMnO with the ALD method optimized to get the required structural and magnetic properties. We show that LT ALD films of ZnMnO, those obtained with either zinc acetate or DEZn and Mn(acac)₃ or Mn(thd)₃ as zinc and manganese precursors, are practically inclusions free. The so-obtained material is promising for spintronics applications under the condition that p-type doping will be improved.

1. A. Wójcik, K. Kopalko, M. Godlewski, E. Guzewicz, R. Jakiela, R. Minikayev, W. Paszkowicz

Appl. Phys. Lett. **89**, 051907 (2006).

2. A. Tomaszewska – Grzęda, A. Opalińska, E. Grzanka, W. Łojkowski A. Gedanken, M. Godlewski, S. Yatsunenkov, V. Osinniy, and T. Story

Appl. Phys. Lett. **89**, 242102 (2006)

3. A. Wójcik, M. Godlewski, E. Guzewicz, R. Jakiela, M. Kiecana, M. Sawicki, M. Guzewicz, M. Putkonen, L. Niinistö, Y. Dumont, and N. Keller

Appl. Phys. Lett. (in press)

19:00 Poster P134

Effect of annealing on electrical properties of low temperature ZnO films

Iwona A. Kowalik¹, Elzbieta Guzewicz¹, Krzysztof Kopalko¹, Marek Godlewski^{1,2}, Aleksandra Wójcik¹, Victor Osinniy¹, Tomasz Krajewski¹, Tomasz Story¹, Marek Guzewicz³

1. Polish Academy of Sciences, Institute of Physics, al. Lotników 32/46, Warszawa 02-668, Poland **2.** Cardinal Stefan Wyszyński University, College of Science, Warszawa, Poland **3.** Instytut Technologii Elektronowej (ITE), al. Lotników 32/46, Warszawa 02-668, Poland

E-mail: ikowalik@ifpan.edu.pl

Last years zinc oxide is extensively studied as prospective materials for electronics (sensors) and optoelectronics. Most of electronic applications like sensors require suitable and controllable electric parameters of ZnO films, like high mobility and low doping concentration. We present results of Hall measurements on zinc oxide thin films grown at low temperature (LT) by Atomic Layer Deposition (ALD) method. In this method reagents (precursors) are introduced sequentially into the growth chamber and cycles when precursors reach the substrate are interspersed by cycles of purging with nitrogen. Because precursors meet only at a surface of the substrate we may use very reactive precursors and may apply different type of chemical reactions (synthesis, single or double exchange).

In the recent study we used double exchange reaction between metal organic diethylzinc and water vapor precursors and applied very low deposition temperature of 100-200°C. Hall coefficient measurements were done on ZnO thin films grown in this way show carrier mobility between 10 and 50 depending on deposition temperature and growth parameters (precursor's time and purging time). Carrier concentration was at the level of 10¹⁹ cm⁻³, which is about two orders of magnitude higher than expected for good quality Schottky contacts. We show that post-grown annealing can considerably improve electrical parameters of LT ZnO films. By low temperature post-growth annealing we managed to reduce free carrier concentration to below 10¹⁷ cm⁻³.

19:00 Poster P135

Complex intermetallics in Al-Ni-Cr and Al-Pd-Cr alloys

Wojciech Kowalski¹, Benjamin Brushko², Marian Surowiec¹, Dmytro Pavlyuchkov^{2,3}

1. University of Silesia, Institute of Materials Science, 12, Bankowa Str., Katowice 40-007, Poland **2.** Research Centre Jülich, Institute of Solid State Research (IFF), Jülich, Germany **3.** Institute for Problems in Materials Science (IPMS), 3, Krzhizhanskyy Str., Kiev 03680, Ukraine

E-mail: wko24@interia.pl

Quasiperiodic phases with symmetries forbidden by classic crystallography have been observed in systems of aluminum with transition metals. The paper presents investigations of the Al-Ni-Cr and Al-Pd-Cr phase diagrams by scanning and transmission electron microscopy, differential thermal analysis and X-ray powder diffractometry.

metry. In the Al-Ni-Cr four ternary crystalline phases were formed close to the compositions of binary m-Al Cr and h- Al Cr. One of them, designated as z with hexagonal structure, was formed in a wide range of composition between $\text{Al}_{82}\text{Ni}_{16}\text{Cr}_2$ and $\text{Al}_{71}\text{Ni}_{11}\text{Cr}_{18}$. The second phase z_1 , was found in samples containing slightly more aluminum. Electron diffraction patterns shows that the c parameter was the same as in z, but the a parameter was $\sqrt{3}$ larger. Another phase, designated as f, was found around $\text{Al}_{79}\text{Ni}_9\text{Cr}_{12}$. It exhibits a monoclinic structure and it incongruently melts at 835°C. The fourth ternary phase was found in $\text{Al}_{76}\text{Ni}_{22}\text{Cr}_{2}$ alloy annealed at 1000°C. We designate it as e. It was found to be only stable at elevated temperatures and not observed in the same sample at 900°C. The structure of the e phase was found to be orthorhombic.

In Al-Pd-Cr was found similar hexagonal phase also designated z, but its range was not so wide. Besides z-phase another phase designated as O was found. It was formed in a range between about $\text{Al}_{76}\text{Pd}_{19}\text{Cr}_{5}$ and $\text{Al}_{81}\text{Pd}_{4}\text{Cr}_{15}$ in 780°C, but in higher temperatures this range goes smaller. The TEM examinations shows an orthorhombic structure. This phase has space group *Pmmn* and a local atomic arrangement is similar to those in Al-Pd-Cr decagonal quasicrystals.

19:00 Poster P136

Near-electrode surface processes in langatate in connection with growth conditions

Nina S. Kozlova¹, Oleg A. Buzanov², Evgeniya V. Zabelina¹

1. Moscow State Steel & Alloys Institute, Moscow 117936, Russian Federation **2.** Fomos-Materials, 16 Buzheninova street, Moscow 107023, Russian Federation

E-mail: kozlova_nina@mail.ru

The aim of this scientific research is determination of the peculiarities of electrochemical process and their influence on electrophysical parameters of the langatate.

We have shown the strong influence of the material of current conducting coats on electrophysical parameters of langatate ($\text{La}_{0.5}\text{Ga}_{0.5}\text{Ta}_{0.5}\text{O}_{1.4}$) samples in wide range of temperatures.

We detected short circuit current in the langatate samples without preliminary polarization. We interpreted these results according to the scientific discovery "Phenomenon of electrochemical decomposition of polar dielectric crystals" diploma № 216, priority - 18 may 1991 by Blistanov A.A., Kozlova N.S., Geras'kin V.V. registered by International Association of Authors of Scientific Discoveries. In this scientific discovery author experimentally determined new earlier unknown phenomenon of electrochemical decomposition of polar dielectric crystals – the spontaneous appearance of emf and short circuit current caused by different chemical activity of surfaces perpendicular to the polar axe.

We show that near-electrode surface processes in LGT are caused by electrochemical decomposition of polar cuts and the intension of these processes depends on growth conditions and the material of current conducting coats.

The observed phenomenon of electrochemical decomposition in langatate is supposed to be the main reason of surfaces' degradation observed on the devices on the basis of these crystals.

19:00 Poster P137

Investigation of growth kinetics and crystal morphology of sodium fluorosilicate ice-analogue crystals in solution and in gel

Mariusz J. Krasinski^{1,3}, Krystyna R. Krasinska¹, Zbigniew Ulanowski²

1. Technical University of Łódź, Center of Mathematics and Physics (CNMF), Wólczajska 219, Łódź 93005, Poland **2.** Science and Technology Research Institute, University of Hertfordshire, Hatfield, Herts AL10-9AB, United Kingdom **3.** Technical University of Łódź, Institute of Physics, Wólczajska 219, Łódź 93005, Poland

E-mail: mariusz.krasinski@p.lodz.pl

Sodium fluorosilicate is an interesting material because its crystals show morphologies very similar to those of ice crystallizing in the atmosphere and its refractive index is very close to that of ice. Therefore it is possible to study the optical properties of cold clouds using these ice-analogues instead of real ice crystals [1-4]. Such experiments, important particularly for improving our understanding of climate change, have been conducted at University of Hertfordshire for some years [2-4] and they confirmed the usefulness of fluorosilicates as a cheaper and easier alternative to experiments involving direct use of ice crystals.

In this work we present results of an investigation of growth kinetics and morphology of sodium fluorosilicate crystals. The aim of this research is to understand the relation between growth conditions and crystal morphology and kinetics, which should provide indications on how to obtain a broad range of analogue crystal habits typical of ice crystals on the one hand, while maintaining uniform crystal size and shape populations on the other hand.

Three methods were used to grow sodium fluorosilicate crystals. In the first one supersaturation was obtained by controlled evaporation of the solute. Evaporation rates from 1 to 10 % of solute per minute were used. The sizes of most of the fluorosilicate crystals grown by this method were from 100 to 250 µm and the morphology was strongly dependent on the supersaturation (Fig. 1). At low supersaturations hexagonal columns, hexagonal plates and a variety of twins were the most frequently observed habits. At higher supersaturations stars, sector stars and dendrites were observed. During the experiments the growth rate as a function of the evaporation rate and time was measured. In most of the experiments the growth rate was in the range of 10-40 nm/s. The experiments allowed us to construct a map (with the quantitative data) indicating which growth conditions are most appropriate for obtaining different morphologies

In the second method supersaturation was obtained by solution cooling. In these experiments the growth rate and supersaturation were precisely measured for hexagonal prisms and plates. These experiments allowed us to estimate the kinetics coefficient for the solution growth of sodium fluorosilicate.

Sodium fluorosilicate crystals were also grown in tetramethoxysilane (TMS) gel. In this case the crystals obtained were greater than those grown in solution - up to 1 mm in size. Two types of morphology were observed during gel growth: very well formed hexagonal crystals with additional high index faces and aggregates of small crystals

During the experiments we obtained many habits typical of ice crystals

tals growing in the atmosphere (hexagonal columns, plates, stars or dendrites) and also some habits not common for ice crystals, such as “dog bones”. Unfortunately, some important morphologies existing for ice crystals are still absent. Thus the deeper understanding of mechanisms leading to obtaining different habits is still required. In the other work [5] we present results of theoretical analysis of growth habits for hexagonal plates and columns.

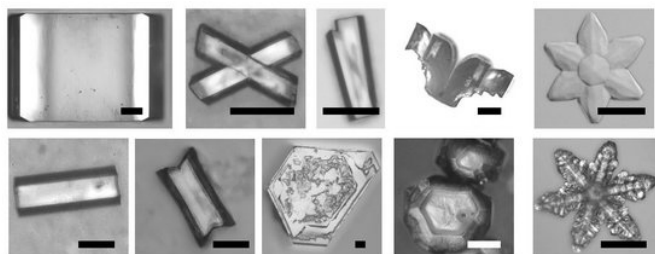


Fig. 1. Examples from the gallery of sodium fluorosilicate crystals habits obtained during the experiments. Scale bare is 100 μm .

1. A.J. Baran, *On the scattering and absorption properties of cirrus cloud*, J. Quantit. Spectr. Rad. Transf. 89 (2004) 17
2. Z. Ulanowski, E. Hesse, P. H. Kaye, A. J. Baran, R. Chandrasekhar *Scattering of light from atmospheric ice analogues*. J. Quantit. Spectr. Rad. Transf. 79-80C (2003) 1091
3. Z. Ulanowski, P. Connolly, M. Flynn, M. Gallagher, A.J.M. Clarke, E. Hesse, *Using ice crystal analogues to validate cloud ice parameter retrievals from the CPI ice spectrometer data*. 14th Int. Conf. Clouds Precipit., Bologna, pp.1175-1178 (2004)
4. Z. Ulanowski, E. Hesse, P.H. Kaye, A.J. Baran, *Light scattering by complex ice-analogue crystals*. J. Quantit. Spectr. Rad. Transf. 100 (2006) 382
5. J. Prywer, M.J. Krasinski, *The analysis of growth habits of sodium fluorosilicate ice-analogues crystals grown from solution and gel*. This conference

19:00

Poster

P138

The theoretical analysis of growth habits of sodium fluorosilicate ice-analogues crystals grown from solution and gel

Mariusz J. Krasinski¹, Jolanta Prywer²

1. Technical University of Łódź, Center of Mathematics and Physics (CNMF), Wólczńska 219, Łódź 93005, Poland 2. Technical University of Łódź, Institute of Physics, Wólczńska 219, Łódź 93005, Poland

E-mail: mariusz.krasinski@p.lodz.pl

The sodium fluorosilicate (Na_2SiF_6) crystals have recently received much attention because of their application as ice-analogues [1,2]. The refractive index of sodium fluorosilicate is very close to that of ice at visual wavelengths and its crystals replicate the variety of growth habits of atmospheric ice crystals. The shapes of ice crystals can significantly affect the radiative transfer in ice clouds and in this way influence the climate evolution. Hence, it is important to accurately represent cirrus cloud and their single-scattering properties in climate models and in remote sensing applications [3]. Proper interpretation of scattering data requires laboratory experiment with arti-

ficial clouds and ice-analogous crystals are cheaper alternative to difficult experiments on real ice. It is however vital for scattering experiments to obtain all typical for atmospheric ice habits and to know relation between growth conditions of sodium fluorosilicate and final shape of its crystals.

In this work we present results of theoretical analysis of growth habits in base of relative growth rates of individual surfaces of sodium fluorosilicates growing in solution and gel. The theoretical considerations are compared with experimental data concerning growth rates of particular faces.

Experimental data were taken from two types of experiment. In the first one, the saturation was obtained by the controlled evaporation of solute from initially undersaturated solution. In the second method, the crystals were grown in tetramethoxysilane gel and supersaturation was obtained by temperature decrease. During experiments in solution the growth rates and evolution of aspect ratio were continuously measured (see [4] for more information). Among variety of habits obtained during experiments (hexagonal columns, plates, sector plates, simple or six-armed stars, stellar dendrites and radiating dendrites) it seems that only hexagonal columns and plates, grown as well from solution and gel, are single crystals. Additionally, these habits are most common for atmospheric ice crystals. Thus, the theoretical analysis was performed for these two kinds of habits.

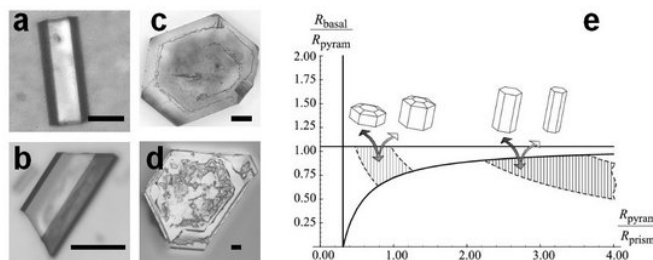


Fig. 1. Hexagonal columns (a,b) and plates (c,d), grown from solution and gel. Kinetic conditions corresponding to the growth of single crystals of these two characteristic habits of sodium fluorosilicate crystals (e). Scale bar is 100 μm .

These two kinds of habits which are under theoretical considerations are composed of basal and prism forms in the case of hexagonal columns (Fig. 1a, 1b) and, additionally of pyramidal form in the case of hexagonal plates (Fig. 1c, 1d). In order to explain these different habits, we use an idea of the critical growth rate R_{hkl}^{crit} which is defined as the normal growth rate of the (hkl) face at which a given size of this face is preserved. Taking into account the measured *in situ* growth rates and the analytical expression that relates the critical growth rate R_{hkl}^{crit} with the growth rates of each face, we obtained the kinetic conditions corresponding to growth of different habits of sodium fluorosilicate crystal, which are schematically presented in Fig. 1e. The experimental data and theoretical analysis demonstrates that the crystals of hexagonal columns and plates grow with appropriate relative growth rates within the dashed regions only. The theoretical approach in connection with experimental data allows us also to derive the kinetic conditions corresponding to the appearance of the pyramidal form, which is characteristic for hexagonal plates only.

1. Z. Ulanowski, E. Hesse, P.H. Kaye & A.J. Baran. *Light scattering by complex ice-analogue crystals*. J. Quantit. Spectr. Rad.

Transf. 100 (1-3), pp.382-392 (2006)

2. Z. Ulanowski, E. Hesse, P. H. Kaye, A. J. Baran, R. Chandrasekhar *Scattering of light from atmospheric ice analogues*. J. Quantit. Spectr. Rad. Transf. 79-80C (2003) 1091
3. A.J. Baran, *On the scattering and absorption properties of cirrus cloud*, J. Quantit. Spectr. Rad. Transf. 89 (2004) 17
4. M.J. Krasinski, K.R. Krasinska, Z. Ulanowski, *Investigation of growth kinetics and crystal morphology of sodium fluorosilicate ice-analogue crystals in solution and in gel*, This conference

19:00	Poster	P139
-------	--------	------

Morphology of front solidification of Al-Cu-Co single quasicrystals

Włodzimierz Bogdanowicz, Jacek Krawczyk

University of Silesia, Institute of Materials Science, 12, Bankowa Str., Katowice 40-007, Poland

E-mail: jackkk777@wp.pl

Materials with quasi-crystalline phases, including Al-Cu-Co single quasicrystals, belong to a modern generation of functional and constructional materials with unique physical properties. They can be used in automobile, aircraft and space industry. In this work the growth morphology of one- and two-subgrain Al-Cu-Co single quasicrystals was studied. The single quasicrystals were obtained by the modification of inclined front crystallisation (IFC) method, which enabled the determination of some morphological traits of solidification front and the relation between these traits and parameters of the growth process. This method was chosen because in the case of Bridgman or Czochralski methods, when the solidification front is perpendicular to the solidification direction, single quasi-crystals may be obtained at much lower solidification rates than for single crystals. At high solidification rates the diffusion cannot supply an appropriate quantity of cobalt necessary for single quasi-crystal growth along the entire solidification front. On the basis of relation between traits and parameters of the growth process the IFC method was suggested to determine thermal undercooling of the front solidification of quasicrystal growing from the molten phase and its dependence on the growth rate. The mechanism of growth of Al-Cu-Co single quasicrystals has been found to change at the growth rate of around 0.25 mm/min. Obtained samples have been subjected to metallography observation, X ray powder diffraction and Laue diffraction. The subgrain of the mosaic of the single quasi-crystals was examined by X-ray topography oscillation method (modification of the Auleytner method).

19:00	Poster	P140
-------	--------	------

Phasons and subgrain boundaries of Al-Cu-Co single quasicrystals

Włodzimierz Bogdanowicz, Jacek Krawczyk

University of Silesia, Institute of Materials Science, 12, Bankowa Str., Katowice 40-007, Poland

E-mail: jackkk777@wp.pl

Since the quasicrystals became ones of the constructional materials, science concentrated on their mechanical properties. Single-

quasicrystals are materials which useful properties are most needed in automobile, aircraft and space fields. They are good thermal conductors (in one direction), possess a high hardness and structure stability at high temperature. The microstructure and electron diffraction pattern of two-subgrain single quasicrystals of Al-Cu-Co alloys was studied. Two-subgrain single quasi-crystals of Al-Cu-Co alloy were obtained using a modification of the IFC method. All the single quasi crystals obtained through solidification on substrate were examined by Laue diffraction. The subgrain of the mosaic of the single quasi-crystals was examined by X-ray topography oscillation method (modification of the Auleytner method). It has been determined that low angle boundaries generate phasonic defects, which may propagate along a tenfold symmetry axis. To confirm this, tenfold electron diffraction patterns (EPD) obtained for single quasi-crystals in the as-grown state were compared with those after annealing at 100°C. The presence of subgrain boundaries in single quasicrystals increases the concentration of phasonic defects in them. The assumption that the subgrains boundary generates phasons is also confirmed by the fact that FWHM of X-ray reflexes measured for as-grown single quasi crystals containing a low-angle boundary (two subgrain) were always larger than for single quasi crystals without such boundary (one subgrain).

19:00	Poster	P141
-------	--------	------

Growth and characterization of (Co,Fe)Si₂ solid solution crystals

Wojciech Gurdziel, Jacek Krawczyk, Zygmunt Wokulski

University of Silesia, Institute of Materials Science, 12, Bankowa Str., Katowice 40-007, Poland

E-mail: jackkk777@wp.pl

Metal disilicides are good thermal and electrical conductors, possess a high hardness and chemical stability. They have properties which are the most required in microelectronic fields. There are used in VLSI and ULSI circuits.

One of disilicides, which possesses above mentioned specificity is CoSi₂. It crystallizes in C1 (fluorite) type of crystal structure (space group). From the electrical properties CoSi₂ can be classified into metallic silicides. It can be doped with different elements for far possibility of changing their properties. In our work we chose iron as a dopant thanks to semiconducting character of β-FeSi₂ so the mean goal of this work was obtaining of (Co, Fe)Si₂ solid solution crystals.

Four melting processes were performed. Each of melts included different percent of iron contents, from 1 at.% to 50 at.% of Fe. Melting process was conducted by Bridgman method in the furnace with vertical temperature gradient under inert atmosphere. Raw materials: Co (99,8%), Fe (99,98%) and Si (99,999%) (weighed from 15g to 20g) were placed in alumina crucibles and melted at a temperature 1550°C. Next crucibles with melt were slowly pulled out from the high temperature zone.

Obtained samples of Co_{1-x}Fe_xSi₂ have been subjected to metallography observation, X-ray and mechanical properties research. Metallography observation shown three different separate phases which were confirmed by X-ray phase analysis. Laue patterns shown that Co_{1-x}Fe_xSi₂ for x > 1.0 at.% of Fe ingots were not monocrystalline. It was also shown that the growth of Co_{1-x}Fe_xSi₂ solid solution

crystals is possible only for $x = 1$ at. % of Fe.

19:00 Poster P142

Microstructural analysis by X-ray diffraction and influence of rare earth elements on magnetism in nanosize $\text{Fe}_{2.85}\text{RE}_{0.15}\text{O}_4$

Aleksandar Kremenovic^{1,2}, Bratislav Antic², Zeljka Cvejic³, Srdan Rakic³, Cedimir Jovalekic⁴

1. VINCA Institute, POB 522, Belgrade 11001, Serbia and Montenegro **2.** Faculty of Mining and Geology, Laboratory for Crystallography, University of Belgrade, Djusina 7, Belgrade, Belgrade 11000, Serbia and Montenegro **3.** Department of Physics, Faculty of Natural Sciences, University of Novi Sad (UNS), Novi Sad 21000, Serbia and Montenegro **4.** Center for Multidisciplinary Studies, University of Belgrade, Kneza Visaslava 1, Belgrade 11000, Serbia and Montenegro

E-mail: akremen@EUnet.yu

A series of the RE (RE = Gd, Dy, Ho, Tm and Yb) as well as Y and In substituted magnetites (Fe_3O_4): $\text{Fe}_{2.85}\text{RE}_{0.15}\text{O}_4$, $\text{Fe}_{2.85}\text{Y}_{0.15}\text{O}_4$ and $\text{Fe}_{2.85}\text{In}_{0.15}\text{O}_4$ were obtained by high energy ball milling. A mixture of crystalline powders of A_2O_3 (A = Y, In, Gd, Dy, Ho, Tm and Yb) and Fe_2O_3 were used as starting materials to produce $\text{Fe}_{2.85}\text{RE}_{0.15}\text{O}_4$, $\text{Fe}_{2.85}\text{Y}_{0.15}\text{O}_4$ and $\text{Fe}_{2.85}\text{In}_{0.15}\text{O}_4$ spinels. Mechanochemical treatment was performed in a planetary ball mill (Fritsch Pulverisette 5) for 20 hours.

To analyze magnetic behavior of the spinels studied, it is important to define, as precise as possible, the microstructure of the investigated samples. Therefore, we used transmission electron microscopy (TEM) image to investigate particle size and morphology. The crystallite size and strain and their anisotropy in samples were determined by refinements of the TCH-pV parameter and cubic harmonic function methods (incorporated in the Fullprof computer program). The microstructure of Fe_3O_4 , $\text{Fe}_{2.85}\text{Y}_{0.15}\text{O}_4$ and $\text{Fe}_{2.85}\text{In}_{0.15}\text{O}_4$ was obtained by the Rietveld crystal structure refinement. The RMSS increase in the following order: $\text{Fe}_3\text{O}_4 < \text{Fe}_{2.85}\text{Y}_{0.15}\text{O}_4 < \text{Fe}_{2.85}\text{In}_{0.15}\text{O}_4$. This fact could be explained by the influence of Y^{3+} ($\gg 5\%$) and In^{3+} ($\gg 15\%$) on the crystal lattice strain. Crystallite size dimensions increase in following order $\text{Fe}_{2.85}\text{Y}_{0.15}\text{O}_4 < \text{Fe}_3\text{O}_4 < \text{Fe}_{2.85}\text{In}_{0.15}\text{O}_4$ what can be explained thought the cation radii influence on the crystallite size. The X-ray line broadening anisotropy due to crystallite size effect is significant for $\text{Fe}_{2.85}\text{Y}_{0.15}\text{O}_4$ (65 ± 15 Å) and $\text{Fe}_{2.85}\text{In}_{0.15}\text{O}_4$ (176 ± 39 Å). The X-ray line broadening anisotropy due to strain effect is small in all investigated samples. TEM analysis revealed that the particles are isotropic, with a relatively uniform size distribution and mean particle size of ~ 20 nm. In addition, the particle size is bigger than the crystallite size obtained by Rietveld method. It can conclude that the particles are composed of one or two crystallite.

Changes in coercivity H_C and saturation magnetization M_S of magnetite with substitution, was studied by M(H) measurements at 2 K by a SQUID magnetometer. The Y substituted Fe_3O_4 has the largest H_C and the lowest M_S . The changes in magnetic parameter values are due to difference in magnetic anisotropy, microstructure and structure parameters. Observed high field irreversibility (at 20 kOe) in ZFC/FC magnetization vs temperature is a consequence of high

anisotropy.

19:00 Poster P143

Self-organized microstructure of TiO_2 -MnO

Pawel Zybert^{1,2}, Katarzyna B. Kołodziejak², Dorota A. Pawlak², Krzysztof Rozniatowski³, Ryszard Didusko², Marcin Kaczkan⁴, Michal Malinowski^{2,4}, Wojciech Gebicki¹, Tadeusz Łukasiewicz²

1. Warsaw University of Technology, Faculty of Physics, Koszykowa 75, Warszawa 00-662, Poland **2.** Institute of Electronic Materials Technology (ITME), Wólczyńska 133, Warszawa 01-919, Poland **3.** Warsaw University of Technology, Faculty of Materials Science and Engineering (InMat), Wołoska 141, Warszawa 02-507, Poland **4.** Warsaw University of Technology, Institute of Microelectronics & Optoelectronics (imio), Koszykowa 75, Warszawa 00-662, Poland

E-mail: pzybert@if.pw.edu.pl

An eutectic from a TiO_2 -MnO system has been grown by the micro-pulling down method. Five different pulling rates were applied: 0.15, 0.45, 1, 5, and 10 mm/min. Also an eutectic doped with praseodymium ions has been grown. The eutectic may find potential application in the area of photonics. The qualitative and quantitative analysis of the eutectic microstructure, the phase analysis, luminescent properties and Raman spectra will be presented.

19:00 Poster P144

Effect of Li-C and Li-Al codoping in MgB_2 single crystals

Nikolai D. Zhigadlo¹, Janusz Karpinski¹, Sergiy Katrych¹, Mauro Tortello^{1,2}, Bertram Batlogg¹, Roman Puzniak^{1,3}, K. Rogacki^{1,4}

1. Laboratory for Solid State Physics ETH (ETH), Schafmattstr. 16, Zürich 8093, Switzerland **2.** Dipartimento di Fisica, Politecnico di Torino, Italy, corso Duca degli Abruzzi, 24, Torino 10129, Italy **3.** Polish Academy of Sciences, Institute of Physics, al. Lotników 32/46, Warszawa 02-668, Poland **4.** Polish Academy of Sciences, Institute of Low Temperature and Structure Research (INTiBS), Okólna 2, Wrocław 50-422, Poland

E-mail: zhigadlo@phys.ethz.ch

Two nearly noninteracting π and σ bands of different dimensionality are key ingredients in MgB_2 . Critical temperature and other superconducting properties of two-band superconductor depend on the doping level and on the interband and intraband scattering and can be modified by chemical substitutions. Due to strongly anisotropic character of MgB_2 , single crystal studies of its anisotropic properties are very important. In the crystals codoped simultaneously with Li-C and Li-Al one can expect compensation of electron doping with C or Al and increase of T_c . Following this strategy, we synthesized a series of $\text{Mg}_{1-x}\text{Li}_x(\text{B}_{1-y}\text{C}_y)_2$ and $\text{Mg}_{1-x}(\text{Al,Li})_x\text{B}_2$ single crystals under high-pressure/high-temperature conditions. Our experimental results show that holes introduced with Li in Li-C codoped crystals cannot counterbalance electrons coming from C. The T_c reduction in Li-C codoped crystals is a sum of T_c reduction of separate Li and C doping. The possible reason of it can be that holes added by Li occupy π band and do not compensate the electrons from C, which fill the σ band. The comparison of the results on $\text{Mg}_{1-x}(\text{Al,Li})_x\text{B}_2$ with

previous experiments on $\text{Mg}_{1-x}\text{Al}_x\text{B}_2$ crystals shows that T_c reduction is a function of Al concentration alone. This finding suggests that effect of Li in MgB_2 is far from trivial and not yet understood. The total influence of codoping on T_c of MgB_2 should be understood as a result of the competition of two effects: the first one is a codoping effect related to the changes of the carrier concentration and the second one is related to the introduction of new scattering centers, leading to the modification of the interband and/or intraband scattering.

19:00 Poster P145

Investigations on crystal growth and characterization of $\text{K}[\text{CS}(\text{NH}_2)_2]_4\text{Br}$ - a semi organic non-linear optical crystal

Krishna Kumar¹, Nagalakshmi Ramamoorthy²

1. Periyar University, Salem 636011, India 2. Nehru Memorial College, Tiruchirappalli 621007, India

E-mail: vkrishna_kumar@yahoo.com

Recent advances in non-linear optical materials (NLO) have invoked a large revival of interest in this area of research on account of their widespread industrial requirements. Among them metal organic compounds are of particular interest for the design of new NLO chromophores with large NLO susceptibilities. Hyperpolarizability (P) value can be drastically varied with electronic configuration of metal ions. Thiourea itself is in a centrosymmetric Pbnm space group and SHG inactive. But the architecture of introducing an inorganic component into the organic crystal to break the centrosymmetry is noticeable and yields non-centrosymmetric complexes, which possess NLO properties. The role of bromine ion is to control the crystal structure by bringing an extensive bonding between amino hydrogen and bromine ion leading to the growth of three-dimensional crystals. The resonance hybrid of thiourea also leads to the formation of three-dimensional network. Bromine can also improve the thermal stability of the compound. Hence, Br in the title crystal is effectual for second order non-linearity and production of second harmonic generation. An attempt has been made to give a complete vibrational picture for the title compound based on group theory for the first time. Crystals of KTTB were grown in saturated aqueous solution by slow evaporation technique. The synthesized salt was dissolved in deionized water and a mixture of acetone and water (1:1) at an optimized pH condition of 4.25. Transparent, colorless, good quality single crystals of KTTB were harvested within 2 to 3 weeks. The compositional analysis has been carried out using EDAX technique and the results were found to be in good agreement with calculated values. From the X-ray diffraction analysis, it has been found that the title compound crystallizes in tetragonal system and belongs to non-centrosymmetric space group P41. The relatively low angular spread of around 300-arc sec of the diffraction curve in high resolution X-ray diffraction shows that the crystalline perfection is reasonably good. FTIR and polarized Raman measurements in different scattering geometries have been carried out and the results are discussed in detail. The absorption of the crystal is less than 1 unit and its lower cut off wavelength is 350 nm. This can be attributed to the metal to ligand charge transfer or metal mediated ligand p - p* transition. The relative efficiency of KTTB with that of KDP has been measured by Kurtz and Perry technique. It is found that the

efficiency of the title crystal is 60 percent to that of KDP. This proposes the title crystal for capable applications in opto-electronics technology. Group theoretical considerations show that the 204 optical modes can be divided into 144 internal modes and 60 external modes. Thiourea molecule has a sulphur atom and two nitrogen atoms capable of being coordinated to a metal atom. Coordination is expected to affect the vibrational frequencies of thiourea, especially those of NH_2 stretching and C=S stretching vibrations. This is due to the formation S-M (sulphur to metal bond) in $\text{K}(\text{Tu})_4\text{Br}$ and it is expected to increase the contribution of high polar structure of the thiourea molecules resulting in the increase of the double bond nature of the C-N bond and a greater single bond character for the carbon to sulphur bond. In the crystal structure, thiourea molecules are planar and there exist extensive intra/inter molecular hydrogen bonds. The role of hydrogen bonding in determining the non-linear optical property is discussed in detail. Frequencies and intensities of bands attributed to the different modes slightly change when polarization vary in Raman spectra, which supports that the title crystal is non-centrosymmetric, which arises essentially due to the anisotropic nature of polarizability with respect to the normal coordinates of the molecular vibrations and also due to the planar nature of thiourea molecules. Thus the title crystal has good propensity for second harmonic generation. Further studies on heavy ion irradiation are in progress.

19:00 Poster P146

X-ray topography of $\text{Ca}_{0.5}\text{Sr}_{0.5}\text{NdAlO}_4$ single crystal

Agnieszka Malinowska^{1,2}, Maria Lefeld-Sosnowska³, Krzysztof Wieteska⁴, Wojciech Wierchowski², Walter Graeff⁵, Anna Pajczkowska²

1. Warsaw University of Technology, Faculty of Physics, Koszykowa 75, Warszawa 00-662, Poland 2. Institute of Electronic Materials Technology (ITME), Wólczyńska 133, Warszawa 01-919, Poland 3. Warsaw University, Institute of Experimental Physics (IEP UW), Hoża 69, Warszawa 00-681, Poland 4. Institute of Atomic Energy, Otwock-Świerk 05-400, Poland 5. Hamburger Synchrotronstrahlungslabor HASYLAB (HASYLAB), Notkestrasse 85, Hamburg D-22603, Germany

E-mail: malinows@if.pw.edu.pl

Oxide materials of general composition ABCO_4 (where A = Ca, Sr, Ba, B = La, Nd, Pr and C = Al, Ga) with the tetragonal perovskite-related K_2NiF_4 - type structure are considered as promising substrate materials for high temperature superconducting (HTSc) thin films, elements of thermal radiation receivers and other electronic devices due to their electrochemical and thermal properties and good lattice matching as well.

Crystals of high structural quality are required for such applications and characterisation of crystal lattice defects is of great importance. The growth of solid solution in the systems $\text{A}_x\text{A}'_{1-x}\text{BCO}_4$ or $\text{ABC}'_{1-x}\text{O}_4$ gives the possibility of obtaining the proper lattice parameter by the selection of the A/A' or C/C' ratio [1]. The linearity of lattice parameters a and c for the whole concentration range x ($0 \leq x \leq 1$) in solid solutions of SrLaAlO_4 - CaLaAlO_4 , SrNdAlO_4 - CaNdAlO_4 , SrPrAlO_4 - CaPrAlO_4 , SrLaAlO_4 - SrLaGaO_4 and SrLaAlO_4 - SrLaFeO_4 was shown in [2].

In the present paper the $\text{Ca}_{0.5}\text{Sr}_{0.5}\text{NdAlO}_4$ single crystal grown by the Czochralski method in the [100] direction was investigated. The investigations were performed by conventional projection transmission x-ray topography and synchrotron radiation white beam topography in transmission and back reflection geometry.

The conventional projection x-ray topographs reveal growth striations with strong black or white diffraction contrasts distributed periodically in the form of concentric rings. The small spotty contrasts - probably associated with precipitates - can be recognised in the strips. Most of them are interconnected by linear contrasts, which could correspond to the dislocations.

In the white beam back reflection synchrotron radiation projection topographs the lines of stripes are well visible. Many spotty diffraction contrasts are seen. They probably correspond to the intersection of dislocations with the crystal surface or they are associated with the near surface precipitates.

Transmission synchrotron section topographs provided a good visibility of segregation fringes and other defects at the intersection of the sample by the incident beam. A characteristic observed effect was bending of the section image caused by strong lattice strains connected with segregations.

[1] A. Novoselov, G. Zimina, A. Filaretov, O. Shlyakhtin, L. Komissarova, A. Pajczkowska, *Mater. Res. Bull.* **36** (2001) 1789.

[2] A. Novoselov, G. Zimina, L. Komissarova, A. Pajczkowska, *J. Crystal Growth* **287** (2006) 305.

19:00	Poster	P147
-------	--------	------

Elastic properties of zinc tris(thiourea) sulphate in a wide temperature range studied by Brillouin spectroscopy

Slawomir Mielcarek, Aleksandra Trzaskowska, Boguslaw Mroz, Krzysztof Komorowski

Adam Mickiewicz University, Department of Physics, Umultowska 85, Poznań 61-614, Poland

E-mail: miel@amu.edu.pl

The zinc tris(thiourea) sulphate (ZTS) crystallise in the orthorhombic system, point group mm2 at room temperature [1]. The crystal is particularly interesting because of its excellent nonlinear optical properties [2]. In the range 300 – 350 K it does not show any anomalies in elastic properties [3]. In low temperatures the Raman spectroscopy data indicated anomalies at 60 and 122 K, and the phase transition was characterised as a second order one [4].

The main aim of the study was determination of the elastic properties of the ZTS crystal by Brillouin spectroscopy in the range 80 – 300 K. The measurements were made on the ZTS single crystals obtained by the isothermal methods, characterised by good optical quality.

The temperature dependencies of the Brillouin shift were determined for the ZTS crystal in the principal directions and in a few mixed directions. The measurements were performed on a tandem type spectrometer made by JR Sandercock. The measuring system was described in an earlier work [5]. The results revealed anomalies in the bulk wave propagation rate and certain elastic constants at about

138 K.

[1] J. Ramajothi, S. Dhanuskodi, K. Nagarajan, *Cryst. Res. Technol.* **39**(5) (2004) 414-420.

[2] H. O. Marcey, L. F. Warren, M. S. Webb, C. A. Ebberts, S. P. Velsko, G. C. Kennedy, G. C. Catella, *Appl. Opt.*, **31** (1992) 5051-5055.

[3] A. V. Alex, J. Philip, *J. Appl. Phys.*, **90**(2) (2001) 720-723.

[4] M. Oussaid, P. Becker, M. Kemiche, C. Carabatos-Nedelec, *phys. stat. sol.(b)* **207** (1998) 103-110.

[5] B. Mroz, S. Mielcarek, *J. Phys. D*, **34** (2001) 395-399.

*Corresponding author, e-mail: miel@amu.edu.pl

19:00	Poster	P148
-------	--------	------

Growth of hippuric acid single crystals by unidirectional solution growth method and its characterization for NLO applications

Vijayan Narayanasamy, Bhagavannarayana Godavarthi

National Physical Laboratory (NPL), Dr.K.S.Krishnan Road, Delhi 110012, India

E-mail: nvijayan@mail.nplindia.ernet.in

In the recent past organic nonlinear optical single crystals were found to be suitable material for NLO applications because of its large nonlinear optical coefficients and high laser damage threshold compared to those of inorganic materials. Among the many well known nonlinear optical (NLO) materials, the organic salt of hippuric acid was found to be potential material for NLO applications. Its crystal structure was determined by Ringertz [1], found that the crystal belongs to orthorhombic crystal system and noncentrosymmetric in nature. The growth of hippuric acid single crystal by conventional slow evaporation solution growth method has already been reported [2]. In the present report, we have grown the title compound of hippuric acid by recently invented Sanakaranarayanan-Ramasamy method [3] using glass as the crucible. It has the unique advantage of 100% solution-crystal conversion is possible by this method. To the best of our knowledge there is no report is available on the growth of hippuric acid by unidirectional solution growth and this is the first report to the literature. The seed crystal was carefully prepared and mounted in the bottom of the V shaped glass crucible. The concentrated solution was prepared using dimethyl formamide (DMF) as the solvent. The filtered solution was decanted into the crucible, and it was fully closed with thick perforated plastic cover with hole at the centre. The whole experimental setup was housed into the constant temperature bath (CTB). Then the experimental condition was carefully observed and found that the seed crystal was started growing after 15 days. After a period of 40-45 days a good quality single crystal of HA was harvested from the glass crucible. Then the harvested specimen was cut and polished for the characterization analysis. The lattice dimensions and crystalline perfection were evaluated from the single crystal XRD and HRXRD analyses. The presence of C,H and N were identified from the elemental analysis. The optical behavior was assessed by UV-Vis. Analysis. The results will be presented in detail.

[1]. H. Ringertz, *Acta Crystallogr. B* **27** (1971) 285.

[2]. N.Vijayan, R.Ramesh Babu, R.Gopalakrishnan, P.Ramasamy, M.Ichimura and

M.Palanichamy, J. Crystal Growth, 273 (2005) 564.

[3]. K.Sankaranarayanan and P.Ramasamy, J. Crystal Growth, 280 (2005) 467.

19:00 Poster P149

Some optical properties of Yb^{+2} ions in YbF_3 -doped CaF_2 crystals

Irina Nicoara

West University of Timisoara (UVT), Bd.V. Parvan nr.4, Timisoara 300223, Romania

E-mail: nicoara@physics.uvt.ro

Growth and characterization of new laser materials is a very important research field. In the last time an important effort has been devoted to research of new Yb-doped laser crystals. Although RE ions are most easily stabilized as trivalent ions in CaF_2 crystals, the divalent state has certain distinct advantages for laser applications [1,2]. The change of valence has been attained by baking the crystals in a suitable atmosphere [3], by electrolytic coloration or exposing them to ionizing radiation [3,4].

In this work we report the growth and some optical properties of YbF_3 -doped CaF_2 crystals with high divalent Yb ions concentration obtained without any other treatment. Pure and various concentration YbF_3 -doped calcium fluoride crystals have been grown by vertical Bridgman method [5] using a special procedure. Transparent colorless, 1cm in diameter, 7cm long crystals were obtained. The optical absorption spectra of the crystals exhibit intense UV absorption bands, characteristic for divalent Yb ions: 230, 263, 275 and 365nm [1,3] with absorption coefficient ten times higher than for the IR bands. The optical properties of the crystals depend on the Yb and F ions positions in the lattice. The trivalent Yb ions substitute for Ca ions in the lattice. The excess charge on the RE ion is compensated by an interstitial fluoride ion located in various positions giving rise to a rich multisite structure, which leads to broad absorption and emission bands. The divalent ions substitute for Ca ions, do not need charge compensation and posses cubic symmetry. The emission spectra of the $\text{CaF}_2\text{-Yb}^{+2}$ crystals have been investigated by other authors only by exciting by 365nm absorption band [1,2,3]. The influence of the excitation by UV bands on the IR emission bands has been investigated by [3]. We studied the emission spectra of the obtained crystals exciting by 230nm absorption band and we obtained, for the first time, a high intensity, broad emission bands with 313, 335, 380 and 395nm peaks. The emission intensity strongly depends on the YbF_3 concentration.

References

- [1] A. A. Kaplyanskii et al., Opt. Spectrosc. 41(1976)615,
- [2] S. Lizzo et al. J. Lumin. 63(1995)223,
- [3] S. M. Kaczmarek et al. J. Phys.: Condens. Mater. 17(2005)3771,
- [4] D. S. McClure and Z. Kiss, J. Chem. Phys. 39(1963)3251,
- [5] D. Nicoara and I. Nicoara, Mater. Science and Eng. A 102, L1 (1988).

19:00 Poster P150

Crystal growth and scintillating properties of (Pr, Si)-doped YAlO_3

Mariya Zhuravleva¹, Andrey Novoselov¹, Akira Yoshikawa¹, Jan Pejchal², Martin Nikl², Jiri A. Mares², Anna Vedda³, Tsuguo Fukuda¹

1. Tohoku University, Institute of Multidisciplinary Research for Advanced Materials, Katahira 2-1-1, Aoba-ku, Sendai 980-8577, Japan 2. Czech Academy of Sciences, Institute of Physics, Cukrovarnicka 10, Prague 16253, Czech Republic 3. University of Milano-Bicocca, Department of Materials Science, via Cozzi 53, Milano 20125, Italy

E-mail: anvn@tagen.tohoku.ac.jp

Fast scintillators such as Ce^{3+} -doped YAlO_3 , Gd_2SiO_5 and Lu_2SiO_5 have found numerous applications in industry, high-energy physics and medical imaging techniques. An analogous to the fast 5d - 4f luminescence of Ce^{3+} , high energy shifted and even faster emission can be obtained from the 5d - 4f transition of the Pr^{3+} in host matrices with the medium-strength crystal field. Trying to find an appropriate host, we have recently reported luminescence properties of Pr^{3+} -doped $\text{Lu}_2\text{Al}_2\text{O}_7$, $\text{Y}_2\text{Al}_2\text{O}_7$, Y_2SiO_5 and Lu_2SiO_5 [1]. The Pr-doped YAlO_3 has been reported as well [2]. However, light yield of the Ce-doped scintillating materials is often decreased by electron trapping at point defects, which results in delayed radiative recombination at Ce^{3+} . In order to decrease the concentration of oxygen vacancies, codoping by tetravalent ions such as Zr was successfully realized in YAP:Ce [3]. It was also theoretically predicted that an excessive charge introduced by Zr ions in YAP:Ce can reduce the concentration of oxygen vacancies [4].

To continue systematic research work towards obtaining new scintillator materials, we have grown Pr-doped YAlO_3 (0.1, 0.5, 1 and 5 mol%), and Pr (1 mol%), Si (0.02 and 0.1 mol%) codoped YAlO_3 single crystals by the micro-pulling-down method. Crystal growth results, photo-, radio- and thermo-luminescence, scintillation decay and light yield measurements will be demonstrated. The influence of codoping on scintillator performance of Pr-doped YAlO_3 will be presented and discussed.

- [1] M. Nikl et al., J. Cryst. Growth 292 (2006) 416-421.
- [2] E.G. Gumanskaya et al., Opt. Spectr. 72 (1992) 155-159 (in Russian).
- [3] M.Nikl et al., Nucl. Instr. Meth. Phys. Research A 486 (2002) 250-253.
- [4] C.R. Stanek et al., phys. stat. sol. (b) 242 (2005) R113-R115.

19:00 Poster P151

Preparation and characterization of superconducting MgB_2 rods

Natalia Orlńska¹, Andrzej Zaleski², Józef Paszula³, Zygmunt Wokulski¹

1. University of Silesia, Institute of Materials Science, 12, Bankowa Str., Katowice 40-007, Poland 2. Polish Academy of Sciences, Institute of Low Temperature and Structure Research (INTiBS), Okólna 2, Wrocław 50-422, Poland 3. Faculty of Armament and Aviation Technology, Military University of Technology, 2, Kaliskiego Str., Warszawa 00-908, Poland

E-mail: natalkao@poczta.onet.pl

Since 2001, MgB_2 samples both in mono- and polycrystalline states were prepared [1]. However, from the application point of view, one of the most promising method of obtaining MgB_2 superconducting tapes and wires is the Powder-In-Tube (PIT) technique [2].

In our work superconducting $\text{Cu}/\text{Fe}/\text{MgB}_2$ and $\text{Steel}/\text{Cu}/\text{MgB}_2$ rods have been prepared using the modified PIT technique with explosive consolidation method. In this experiment the ex-situ process was used. Initial MgB_2 powder in Fe and Cu tubes was placed. In the next steps the inner tubes with initial materials were placed in additional tubes. After packing process two double arrangements of tubes with initial material were consolidated using the explosive process.

Metallographic observations, X-ray phase analysis and superconducting properties were investigated. The metallographic observations disclosed rigid and well consolidated MgB_2 rods. X-ray phase analysis appeared that this type of consolidation permits to obtain MgB_2 cores free from any voids and new phases. The transition temperature (T_c) for a cores samples determined by the ac susceptibility measurements indicates that T_c (~39 K) is almost the same as that earlier reported. Measurements of the magnetization-magnetic field were also carried out. From these analyses we can conclude that this method permits to obtain good quality MgB_2 rods.

References:

- [1] Z. Wokulski and N. Orlńska, *Materiały ceramiczne*, LVIII, 1/(2006), p. 21.
[2] B. A. Glowacki, M. Majors, M. Vickers, J E. Evetts, Y. Shi, I. McDougall, *Supercond. Sci. Technol.*, 14, 193 (2001).

19:00 Poster P152

Crystal growth and physical-mechanical properties of $\text{SrB}_4\text{O}_7:\text{Eu}^{2+}$ single crystals

Sergey Parkhomenko, Roman P. Yavetskiy, Elena Dolzhenkova, Tatyana Korshikova, Alexander Tolmachev

Institute for Single Crystals NAS of Ukraine (ISC), 60 Lenin Ave., Kharkov 61001, Ukraine

E-mail: parkhomenko@isc.kharkov.ua

Strontium tetraborate SrB_4O_7 (SBO) is a promising nonlinear optical material. The merit of this crystal is high mechanical strength (9

Moos) and low hygroscopicity [1]. Nowadays SBO activated with rare earth ions has been intensively studied as a effective material for solid state dosimetry [2]. Recently we have reported photo- and thermoluminescent (TL) properties of polycrystalline powders of strontium tetraborate, activated with different concentration of europium ions ($\text{SBO}:\text{Eu}^{2+}$). The single crystal $\text{SBO}:\text{Eu}^{2+}$ is a subject of investigation in this work.

The $\text{SBO}:\text{Eu}^{2+}$ single crystals were grown by Czochralski method from platinum crucibles in air onto single crystal seed oriented along the [001] direction. The rotation and pulling rates were 20 rpm and 0.25 mm/h, respectively. The axial temperature gradient in the crystallization zone was 70 K/cm. The source charge of $\text{SBO}:\text{Eu}^{2+}$ was synthesized by solid state reaction [3]. Strontium carbonate SrCO_3 (special purity grade) and boric acid H_3BO_3 (chemical purity grade) in stoichiometric ratio were used as the starting materials. Europium was introduced as oxide Eu_2O_3 (special purity grade).

Macrodefects (inclusions, impurities, cracks) have been investigated by metallographic methods. The system of easy distribution of cracks in SrB_4O_7 single crystals has been determined. Quality of grown crystals was controlled by results of X-ray analysis. XPA does not reveal any additional phase in samples studied within the limits of experimental error. The grown single crystals had the following crystallographic parameters: rhombic system, space group $\text{Pnm}2_1$, $a=10.71171(7)$ Å, $b=4.42687(3)$ Å, $c=4.23481(2)$ Å, $V=200.812(2)$ Å³, $Z=2$.

The main optical and luminescence properties of $\text{SBO}:\text{Eu}^{2+}$ single crystals have been studied. It has been shown, that TSL of $\text{SBO}:\text{Eu}^{2+}$ crystals in the 300 to 500 K range is associated with decay of electron centers (F^+ centers) localized in non-equivalent positions.

- [1] Yu.S. Oseledchik, A.L. Prosvirnin, V.V. Starshenko et al. // *J. Cryst. Growth*.-1994.-V.135.-P.373-376.

- [2] M. Santiago, C. Grassely, E. Caselli et al. // *Phys. stat. sol. (a)*.-2001.-V.185, #2.-P.285-289.

- [3] S.V. Parkhomenko, A.V. Tolmachev, M.F. Dubovik, et al. // Abstracts book, International Conference "CRYSTAL MATERIALS'2005" (ICCM'2005), Kharkov, Ukraine, 2005.

19:00 Poster P153

Growth and characterization of $\text{Li}_2\text{B}_4\text{O}_7$ single crystals pure and doped with Co ions

Danuta Piwowarska¹, Sławomir Kaczmarek¹, Marek Berkowski², Ireneusz Stefaniuk³

1. Szczecin University of Technology, Institute of Physics, Al. Piastów 48/49, Szczecin 70-311, Poland 2. Polish Academy of Sciences, Institute of Physics, al. Lotników 32/46, Warszawa 02-668, Poland 3. University of Rzeszow, Rejtana 16 A, Rzeszów 35-310, Poland

E-mail: dana@ps.pl

The paper reports on the growth conditions of $\text{Li}_2\text{B}_4\text{O}_7$ single crystals in both pure and Co doped ions. The crystals were grown by the Czochralski method at a growth rate of 0.6 mm/h and rotation rate 5.0 rpm in the Institute of Physics, Szczecin University of Techno-

logy, Poland. Technological factors affecting the quality of the crystals, both pure and doped, have been discussed. As raw materials boric oxide (B_2O_3), lithium bicarbonate (Li_2CO_3) and dopant ions (Co) in the form of oxides of purity 4N and 5N were used. The growth processes were carried out without protective atmosphere (in the presence of oxygen), with the use of platinum crucible, 50 mm in diameter and height. The optimum initial composition of melt has been defined, which is dependent on the speed of boric oxide evaporation reaching 90 mg/h. A schematic phase diagram of this solution is proposed. Starting concentrations of Co in the melt were: 0.5, 0.85 and 1 mol. % with respect to Li_2CO_3 . Absorption and EPR spectra were analyzed with the aim of define of oxidation state and site of cobalt ions. Optical measurements show that Co-doped $Li_2B_4O_7$ exhibit distinct absorption bands near 500, 1100 and 1500 nm associated with electronic transitions characteristic of Co^{2+} ions at octahedral Li^+ site positions. Low-temperature EPR measurements show that in the $Li_2B_4O_7:Co$ crystal two types of Co^{2+} complexes can be distinguished. Obtained single crystals $Li_2B_4O_7$ has been used in the processing system on the second harmonic generation of laser YAG:Nd.

19:00	Poster	P154
-------	--------	------

Growth and characterization of electro-optic Glycine lithium sulfate single crystals

Mythili Prakasam, Kanagasekaran Thangavel, Gopalakrishnan Rengasamy

AnnaUniversity (AU), Sardar Patel Road, Guindy, Chennai 600025, India

E-mail: myt_lp@yahoo.co.in

GLS crystals were grown with the optimized growth parameters. The formation of GLS compounds was confirmed by powder X-ray diffraction studies. Metastable zone width and induction period values have been determined in order to optimize the growth parameters. The interfacial tension values estimated using the experimentally determined induction period are found to be comparable with theoretical values. The density measurements were carried out by both theoretical and experimental methods. The NLO property of GLS crystals has been inferred by Kurtz- Perry technique. The mechanical hardness was tested by Vickers Microhardness tester.

Introduction

Materials with non-linear electro-optic properties have wide applications in modern optical and optoelectronic devices. Organic crystals possess high efficiency of frequency conversion, moderately high damage threshold, wide range of transparency. GLS crystallizes in orthorhombic structure with space group of $Pna2_1$. The study of the growth defects includes the defects such as inclusions, step growth, mechanical stress etc., which are due to poor control of crystal growth parameters. In the present study investigations have been made to evaluate the interfacial tension (γ), between the GLS (solute) and water based solution by measuring the induction period (τ) and hence to calculate critical radius (r^*), number of molecules in the critical nucleus (i^*) and Gibb's free energy (ΔG^*) for the formation of GLS.

Growth of GLS

GLS has got good solubility in water; the crystals were grown by slow cooling method. Saturated solution of GLS was prepared and extreme care was taken towards maintenance of temperature; even minor fluctuations in temperature will lead to inclusions and defects in the growing crystals. The beaker containing solution was kept in the constant temperature bath controlled to an accuracy of $\pm 0.1^\circ C$. The temperature was lowered at the rate of $0.5^\circ C/day$ and the crystals of GLS have been obtained (Fig).

Powder X-ray diffraction analysis

The powder sample of GLS was subjected to powder XRD analysis and the recorded XRD pattern is shown in Fig. The obtained powder X-ray diffraction data were analyzed by using PROSZKI software package and the lattice parameters were calculated. It is confirmed that GLS belongs to orthorhombic crystal system with space group $Pna2_1$. The cell parameters were found to be $a=16.423\text{\AA}$, $b=5.005\text{\AA}$ and $c=7.654\text{\AA}$.

Nonlinear optical properties

The grown crystals were characterized for their nonlinear optical property. Nd-YAG laser emits fundamental wavelength $\lambda = 1064$ nm. For this purpose, the output from Nd: YAG laser (1064 nm) model GCR-2 (10) was used as source and it was focussed on the sample. Pulse energy was 5mJ/sec and pulse width was about 10 ns. The output from the Q switched laser was focussed on the crystal. The output could be seen as a bright green flash emission from the GLS crystals. Further it was inferred that the relative SHG efficiency of GLS crystals was 52 times greater than KDP.

19:00	Poster	P155
-------	--------	------

Swift heavy ion induced modification on the Optical, Mechanical and Dielectric behaviour of GLS single crystals

Mythili Prakasam¹, Kanagasekaran Thangavel¹, Sharma Shailesh², Bhagavannarayana Gg², Saif Ali³, Pawankumar Kuliya³, Kanjilal Dd³, Gopalakrishnan Rengasamy¹

1. AnnaUniversity (AU), Sardar Patel Road, Guindy, Chennai 600025, India 2. National Physical Laboratory (NPL), Dr.K.S.Krishnan Road, Delhi 110012, India 3. Inter University Accelerator Centre (IUAC), Aruna asaf ali marg, Delhi 110067, India

E-mail: myt_lp@yahoo.co.in

Swift heavy ion (SHI) beams have become an indispensable role in material processing and in the modification of the surface layer of solids. Recent advances in the region of very high-energy physics and progress in the experimental methods have produced some qualitative new results regarding modifications induced by high-energy ions. High-energy heavy ion irradiation is an age old field in materials science and technology. When a swift heavy ion irradiation passes through matter; it loses its energy mainly in two ways. The interaction of heavily charged ions with electrons of the target material through Coulomb forces, produce a track of ionization and highly kinetic electrons along the path of the primary ion due to inelastic collision. This is known as electronic energy loss or electronic stopping (S_e). Nuclear energy loss or nuclear stopping (S_n) dominates at low energies, which is caused by the elastic scattering from

the screened nuclear potential of the target. Both S_n and S_c give rise to various modifications of the solids. In the regime of ion energies where electronic energy loss is dominant, several interesting features of modifications of solids have been observed in recent years.

Pure single crystals of Glycine Lithium sulphate (GLS) were irradiated at room temperature with 50 MeV Silver ions at fluences varying from 10^{10} to 10^{12} ions/cm² from the 15 UD Pelletron facilities at Inter University Accelerator Centre (IUAC), New Delhi. The pristine as well as irradiated GLS crystals were characterized by photoluminescence at room temperature and UV-Vis absorption to study the radiation induced defects. Photoluminescence and UV-Vis absorption show the formation of defects due to heavy ion impact. The ion-induced changes in mechanical behaviour have also been studied using Vickers micro hardness technique. The effect of swift heavy ion beam on dielectric dispersion was studied in detail. The second harmonic generation efficiencies of the pure and irradiated crystals were presented in comparison with KDP, which shows a tripling increase in SHG efficiency upon irradiation. Surface morphology was analysed by scanning electron microscopy for pristine and irradiated GLS crystals. Fig.1 explains the hydrogen ion concentration Vs irradiation fluence. The results will be presented in detail.

19:00	Poster	P156
-------	--------	------

Studies on the first order hyperpolarizability and Terahertz generation in an organic non-linear optical crystal 3-nitroaniline

Krishna Kumar¹, Nagalakshmi Ramamoorthy²

1. Periyar University, Salem 636011, India 2. Nehru Memorial College, Tiruchirappalli 621007, India

E-mail: nagaphys@yahoo.com

ABSTRACT

The development of organic materials for use in non-linear optical devices is of interest because their optical non-linearities are orders of magnitude larger than those of conventional materials. Moreover organic materials offer flexibility of molecular design, virtually an unlimited number of crystalline structures and a high damage resistance to optical radiation. In these molecules, the non-linear optical properties are believed to arise from an optically intense electronic state, in which electron density is transferred from the electron donor to electron acceptor traditionally referred to as charge transfer state. The main interest in nitro anilines comes from their recognized second harmonic generation capability and their large microscopic hyperpolarizabilities. Intermolecular hydrogen bonds are an effective tool for organizing organic molecules, very well typified by nitro aniline compounds, which associate via intermolecular H-bonds between the amino and nitro groups.

Owing to the development of ultra short-pulsed laser techniques, one can readily generate and detect terahertz radiation if good non-linear optical crystals having enough macroscopic second order non-linearity are available. Coherent tunable terahertz waves have great potential for frequency domain spectroscopy and THz imaging applications. For efficient THz wave generation, the NLO crystal is required to have large non-linear and low absorption co-efficients. So, organic crystals with a large non-linearity are promising candidates for wideband THz generation.

The growth of single crystals of the title compound has been undertaken from methanol solution by the slow evaporation technique from aqueous solution at room temperature. Transparent optical quality yellow colored crystals were harvested after the growth period of a week.

The hyperpolarizability calculations were carried out for the investigated compound by the Density Functional triply parameter hybrid model DFT/B3LYP using GAUSSIAN 98W, The HF/3-21 G (d, p) basis set has been employed. The calculated first hyperpolarizability of m-NA is 1.347006×10^{-30} esu, which is nearly seven times that of Urea. The experimental relative SHG efficiency was found to be 2.5 times that of urea.

The vibrational spectral studies also provide evidence for the charge transfer interaction between the donor and acceptor groups through p- electron movement. This p- electron cloud makes the molecule highly polarized and the intermolecular charge transfer interaction is highly responsible for the NLO properties of the title compound.

Therefore, the presence of intermolecular hydrogen bonding is responsible for high b value and this mechanism plays an important role in NLO activity

Optical pulses with a time width of 200 fs, repetition rate of 42 MHz and centre of wavelength 800 nm from a mode locked Ti: Sapphire laser were used for Terahertz studies of the title crystal. According to the geometrical considerations for the molecular arrangements in the crystal, the b-tensor components can be explicitly described using the first-order molecular hyperpolarizabilities (β). The largest b tensor component is found for b_{xxx} (137.5), which is equal to b_{xxx} in the title crystal. This is the indication of the non-linear polarization induced by the component and this particular tensor is responsible for THz generation in the crystal. The presence of phonon modes is consistent with the THz radiation of these crystals. In this direction a strong phonon modes observed from 0.9 - 2.3 THz for the title NLO crystal is concurrent with the values obtained from the FFT amplitude spectrum. Thus the spread of terahertz bandwidth of the investigated compound is of moderate range. This material can be recommended for terahertz imaging or the other applications where a large bandwidth is not needed. Further studies are in progress.

19:00	Poster	P157
-------	--------	------

Growth And Characterization of Nonlinear Optical L-Asparaginium Picrate Single Crystals.

Srinivasan Padmanabhan, Kanagasekaran Thangavel, Gopalakrishnan Rengasamy

AnnaUniversity (AU), Sardar Patel Road, Guindy, Chennai 600025, India

E-mail: krkkrishnan@annauniv.edu

ABSTRACT

Significant betterments have been accounted recently in the field of nonlinear optics in the area of materials engineering and the associated optoelectronic device technologies which experiences a revival of both practical and conceptual nature. The requirements of nonlinear optical materials are primarily regularized by the nonlinear figure of merit, and by the equally relevant optical quality and robustness of the materials towards different applications. Recent advances

in non-linear optical materials (NLO) have invoked a large revival of interest in this area of research on account of their widespread industrial requirements. The noetic construction of structurally controlled supramolecular assemblies (e.g., acentric and chiral solids) remains a great challenge even though the art of chemical synthesis of discrete molecules has significantly advanced in recent years. The relevance of organic materials in this percolating context is due to the fact that the delocalized electronic structure of Π -bonded organic compound offers a number of tantalizing opportunities in applications as non-linear optical materials. Organic crystals in terms of non-linear optical property possess advantages, when compared to their inorganic counterparts. Acentric molecules consisting of highly delocalized Π electron systems interacting with suitably substituted electron donor and acceptor groups exhibit a high value second order polarizability (β). L- Asparaginium picrate (LASP) is one such p donor acceptor molecular compounds in which L- Asparagine acts as donor and the picric acid as electron acceptor.

LASP crystals were grown by slow evaporation solution growth technique. Picric acid is less soluble in water, whereas L-asparagine shows more affinity towards solubility in water only. Equimolar quantities of the parent compounds picric acid (Loba Chemie, 99%) and L-asparagine (Loba Chemie, 99%) were dissolved in a mixture of acetone and water (1:1). On cooling of the solution, the salt was obtained by crystallization at low temperature (25 °C). The material was purified over again from aqueous solution by the recrystallization process. Single crystals of LASP have been grown from saturated solution (pH = 2.01) of the synthesized salt of LASP by the slow evaporation solution growth technique at 30 °C using a constant-temperature bath having the control accuracy of +0.01 °C. Yellowish crystals of size 1.5 x 0.8 x 0.4 cm³ have been obtained.

X-ray diffraction data were collected at room temperature using a single crystal X-ray diffractometer (ENRAF NONIUS CAD4, MoK α , λ =0.71069). The high resolution X-ray diffraction analysis was carried out to study the structural perfection of LASP. A multicrystal X-ray diffractometer (MCD) developed at NPL(National Physical Laboratory, New Delhi), set in (+,-,-,+) configuration has been employed using MoK α_1 radiation originated from a fine focus sealed tube X-ray generator (Philips, 1743; 2 kW). The rocking curve of LASP crystal recorded for (101) bears two additional peaks, with adjacent angles 40 and 12 arc sec away from the main peak. From the HRXRD results we elucidate that the incorporation of solvent into the growing crystal which is common in solution grown crystal is responsible for the very low angle boundaries and we conclude that the quality of the crystal is good.

Carefully selected samples of LASP were cut and polished on a soft tissue paper with fine grade alumina powder (0.1mm) dispersed in a mixture of acetone, water and DMFO(1:1:4). Each sample was covered on both sides with silver paste (air drying) to make the sample to behave as a parallel plate capacitor. A HIOKI 3635 Model LCR meter was used to measure the capacitance, dielectric loss (tan δ) and resistance of the sample as a function of frequency (range 30 – 95°C). A small cylindrical furnace (20 cm x 20 cm x 20 cm), whose temperature was controlled by a Eurotherm temperature controller (+0.01 °C) was used to house the sample. The dielectric constant was calculated by using the relation

$$\epsilon' = C t / \epsilon_0 A$$

where ϵ_0 is the vacuum permittivity, t is the thickness of the sample,

C is the capacitance and A is the area of cross section. The conductivity of the crystal was calculated using the relation

$$\sigma_{ac} = 2 \pi f \epsilon_0 \epsilon' \tan \delta$$

The results of dielectric behaviour are show that the dielectric constant (ϵ') and dielectric loss ($\tan \delta$) decreases with increase of frequency. The large values of dielectric constant at low frequency suggest that there is a contribution from all four known sources of polarization namely, electronic, ionic, dipolar and space charge polarization. The dielectric constant and dielectric loss decrease with increasing frequencies. The low value of dielectric loss ($\tan \delta$) indicates that the grown crystals of LASP are of reasonably good quality. The high dielectric constant makes the title crystal a better newbie for electro- optic modulators.

Qualitative measurement of relative SHG efficiency of LASP with respect to well known SHG materials KDP and Urea was made by Kurtz and Perry powder technique. The relative SHG efficiency elicits that the material is 66.5 times greater than that of KDP and 10 times that of Urea.

The hardness measurements were made on the prominent (301) plane of the crystal of thickness of 0.3 cm using Leitz –Wetzler Vicker's hardness tester fitted with a Vicker's diamond pyramidal indenter and attached to an incident light microscope (Neophot-2 of Carl-Zeiss, Germany). Loads ranging from 0.5 g to 5 g were used for making indentations, keeping the time of indentation constant at 10 s for all the cases. The fracture toughness K_{IC} was calculated using the relation.

$$K_{IC} = k P / a l^{1/2}$$

where the constant $k=1/7$ for the Vickers indenter, $l=C-a$ is the mean palmquist crack length. The value of Brittleness index Bi was calculated using

$$Bi = H_v / K_{IC}$$

The hardness study projects the crystal is moderately hard. The fracture toughness, brittleness index and the yield strength of LASP have been enunciated. The results will be presented in detail.

19:00	Poster	P158
-------	--------	------

Temperature Raman scattering study of $\text{CaAl}_{0.5}\text{Ta}_{0.5}\text{O}_3$ crystal

Tomasz Runka¹, Marek Berkowski², Mirosław Drozdowski¹

1. Poznań University of Technology (PUT), Nieszawska 13A, Poznań 60-965, Poland **2.** Polish Academy of Sciences, Institute of Physics, al. Lotników 32/46, Warszawa 02-668, Poland

E-mail: tomrun@phys.put.poznan.pl

The temperature Raman scattering study of $\text{CaAl}_{0.5}\text{Ta}_{0.5}\text{O}_3$ (abbreviated as CAT) perovskite crystal grown by the Czochralski method was carried out. The CAT crystal belongs to family of ordered perovskites with general formula. At room temperature, the crystal possesses orthorhombic $Pbnm$ structure with small deviation to monoclinic $P2_1/n$ structure, which results from octahedral distortions of simple cubic perovskite structure ($b^-b^+c^+$ tilt system in Glazer notation) and B-site cation ordering. [1-2].

The Raman spectra were recorded in spectral range 70 – 1000 cm⁻¹ for $Z(XX)Y$ and $Z(XZ)Y$ scattering geometry. The number of ob-

served Raman modes for investigated crystal is lower than theoretically predicted for monoclinic $P2_1/n$ structure. The site symmetry group analysis predicts 24 Raman-active modes ($12A_g + 12B_g$) associated with octahedral tilting and cation ordering. In room temperature Raman spectrum, we observe characteristic features (internal vibrations of F_{2g} , E_g and A_g symmetry) for cubic perovskite crystals with 1:1 B-site cations ordering [3]. It suggests the existence of regions with 1:1 B-site order in crystal structure. However, triply degenerate cubic-like mode $F_{2g}(2)$ splits into three nondegenerate modes $F_{2g}(2) \rightarrow 2A_g + B_g$ in monoclinic $P2_1/n$ structure. What is interesting, no splitting of doubly degenerate cubic-like mode E_g is observed. The numerous Raman bands observed below 300 cm^{-1} can be attributed to lattice vibrations. They can be assigned to translational vibrations of Ca^{2+} and $\text{B}'/\text{B}''\text{O}_6$ ions and tilt modes of $\text{B}'/\text{B}''\text{O}_6$ ions. The triply degenerate cubic-like mode $F_{2g}(1)$ attributed to translational motions of Ca^{2+} cations splits into three nondegenerate, distinctly separated modes $F_{2g}(1) \rightarrow 2A_g + B_g$ appearing in spectral range $180 - 240\text{ cm}^{-1}$.

The temperature investigations were carried out in wide temperature range from 77 K to 630 K. All bands recorded in spectra were fitted considering Bose-Einstein occupation factor. Significant temperature changes in spectral parameters of Raman bands, especially in the lattice modes region have been revealed. Some changes are connected with temperature induced distortions of oxygen octahedra, and on the other hand, with lattice parameter changes.

[1]. M. Berkowski, R. Aleksiyo, J. Fink-Finowicki, R. Diduszko, P. Byszewski, R. Kikalejshvili- Domukhowska, J. Cryst. Growth **269** (2004) 512.

[2]. I. Levin, J.Y. Chan, J.E. Maslar, T.A. Vanderah, S.M. Bell, J. Apply Phys. **90** (2001) 904.

[3]. T. Runka, R. Aleksiyo, M. Berkowski, M. Drozdowski, Cryst. Res. Technol. **40** (2005) 453.

19:00 Poster P159

Growth and characterization of Nd, Yb – Yttrium oxide nanopowders obtained by sol-gel method.

Agnieszka Rzepka¹, Witold Ryba-Romanowski², Ryszard Diduszko¹, Ludwika Lipińska¹, Anna Pajczkowska¹

1. Institute of Electronic Materials Technology (ITME), Wólczyńska 133, Warszawa 01-919, Poland **2.** Polish Academy of Sciences, Institute of Low Temperature and Structure Research (INTiBS), Okólna 2, Wrocław 50-422, Poland

E-mail: Agnieszka.Rzepka@itme.edu.pl

Yttrium oxide (Y_2O_3) is interesting host material for high power laser applications. Y_2O_3 belongs to group oxides with very high melting point. For yttria this is 2430°C . At about 2280°C its structural phase transition is observed. Furthermore its thermal conductivity is higher than well-known yttrium aluminum garnet (YAG) crystals and their thermal expansion coefficient is very similar. Moreover sesquioxide Y_2O_3 can be doped by rare earth ions and it is a good phosphor used in optical displays and light emitting devices.

In this work the nanosized powders of the following systems: Y_2O_3 ; $\text{Y}_2\text{O}_3:\text{Nd}^{3+}$; $\text{Y}_2\text{O}_3:\text{Yb}^{3+}$; $\text{Y}_2\text{O}_3:\text{Nd}^{3+}, \text{Yb}^{3+}$ were prepared by sol-gel method using EDTA, 1,2-Ethanediol and citric acid. Finally the one

phase compounds of Y_2O_3 doped 0,5 % Nd and 1, 2 or 4 % Yb were obtained.

The influence of thermal treatment on nanopowders properties were investigated. The gels were dried at 120°C for 12 h and then grinded in an agate mortar to obtain fine powder. The xerogel powders were heat treated at various temperatures from 600 to 1200°C in air. The calcining time was changed from 1 to 10 h. The crystal structures of samples were characterized by X-ray diffraction (XRD) using a Siemens D-500 diffractometer with $\text{CuK}\alpha$ radiation at 1.548 \AA . The size and morphology of nanopowders were analyzed by scanning electron microscopy (SEM) and were performed with DSM-950 microscope.

Average size of crystallites was evaluated using Scherrer formula and the sizes were increased with the calcining temperature ($600 \div 1200^\circ\text{C}$) from 10 to 75 nm. Also morphology of crystallites was changed with the temperature of calcination. The calcining time was changed from 1 to 10 h and it did not influence on the crystallite sizes. There were not (evident) relationships between the crystallite sizes and the time of calcination ($1 \div 10\text{ h}$), the concentration of doping elements (Nd, Yb) and the used complexing chemical compounds.

Spectroscopic investigation of nanopowders revealed occurrence of intense emission in near infrared region. Three emission bands characteristic of Nd^{3+} and one emission band characteristic of Yb^{3+} were recorded for $\text{Y}_2\text{O}_3:\text{Nd}^{3+}$ and $\text{Y}_2\text{O}_3:\text{Yb}^{3+}$ samples respectively. For $\text{Y}_2\text{O}_3:\text{Nd}^{3+}, \text{Yb}^{3+}$ samples the emission consists essentially of one band related to partially overlapping transitions of Yb^{3+} and Nd^{3+} . Analysis of luminescence decay curves indicates that metastable states of the two ions are linked by fast nonradiative energy transfer processes.

This work was supported by Ministry of Education and Science under the research project no.3T11B00430.

19:00 Poster P160

Pulsed laser deposition of CdTe, ZnTe and CdSe

Janusz Rzeszutek¹, Maciej Oszwaldowski¹, Piotr Kuświk¹, Viktor K. Savchuk²

1. Poznań Technical University, Institute of Physics (PUT), Nieszawska 13a, Poznań 60-965, Poland **2.** Institute of Applied Problems of Mechanics and Mathematics (IAPMM), 3B Naukova Str., Lviv 79060, Ukraine

E-mail: rzeszut@phys.put.poznan.pl

The goal of the work is the pulsed laser deposition (PLD) of CdTe, CdSe and ZnTe thin films with low-power laser pulses, as well as the investigation of the structural properties of thus obtained films. The PLD apparatus used in our experiments is described in detail elsewhere [1]. For the present purpose, it was supplied with a quadrupole mass spectrometer (QMS, HALO 301, Hiden Analytical) equipped with a pulse ion counter. The action of QMS has been synchronized with the laser action by a specially designed electronic device. With this improvement, the vapour cloud ejected from the target by a laser pulse, arrives at the spectrometer head in a right time to be analysed on chemical composition. This improvement enables also performing time-of-flight (TOF) experiments, from which the velocity distribution of the laser emitted particles is de-

terminated.

In our experiments we used a YAG:Nd laser operating with a 25 Hz pulse frequency. The pulse energy density on the target surface was 1.9 J/cm^2 or 2.3 J/cm^2 and the pulse duration was 100 ms. The targets were CdTe, CdSe, or ZnTe tablets of diameter of 2 cm made of the corresponding powdered materials pressed at the pressure of 700 atm. The films were deposited onto glass and GaAs(001) substrates held at 200°C . The film thickness ranged from $0.17 \mu\text{m}$ (CdTe) to $0.55 \mu\text{m}$ (CdSe).

The film surface appearance was studied with optic and atomic force microscopy. These investigation showed that at the low energy pulses used, the number of particularities incorporated into the films, which usually deteriorate the film quality, is very small. Otherwise, the film surfaces were very smooth and consisted of flat crystallites. However, the films on the GaAs substrates showed a more crystalline (better developed) form. The X-ray investigations revealed that all films were strongly textured in the (111) or (001) planes. Therefore, these preliminary results show that the preparation method adopted is very promising in preparing thin films of $A^{II}B^{VI}$ compounds and their composed structures.

The TOF measurements performed for all kinds of the emitted particles (atomic A^{II} and B^{VI} and diatomic B_2^{VI} species) showed that their velocity distributions are those of the Maxwellian-on-stream distribution, i. e. the distributions are considerably narrower than the classic Maxwellian distribution. Moreover, all the species for a given compound had roughly the same velocity distribution, i. e. they arrived to the substrate roughly at the same time. The average velocity was of the order 800 m/s . These properties are beneficial for the preparation of high quality stoichiometric thin films. It is worthy to note that the TOF measurements for CdTe, CdSe and ZnTe were performed for the first time.

1. M. Oszwaldowski, T. Berus, P. Sydorchuk, J. Rzesutek, Rev. Sci. Instrum., 74 (2003) 3160.

19:00	Poster	P161
-------	--------	------

Introduction to Quasicrystals

Feridoun Samavat

Physics Department, Bu-Ali sina university, Mahdیه St., Hamedan Hamedan, Iran

E-mail: fsamavat@yahoo.com

Introduction to Quasicrystals

Feridoun Samavat ^{1,*}, M. Hossein Tavakkoli ¹, Vahid Fayaz ²

^{1*} Department of Physics, Bu-Ali Sina University, Hamedan, Iran

² Islamic Azad university, Hamedan, Iran

Abstract

Quasicrystals are material with perfect long-range order, but with no three-dimensional translation periodicity. They are typically binary and ternary metallic alloys. Quasicrystals have characteristic physical properties. Some resemble those of periodic crystals while others have similar properties to amorphous alloys. Many of their mechanical physical properties are quite unusual by the standards of com-

mon metals. The peculiar physical properties of quasicrystals certainly give rise to the hope that they may become of some practical importance in the future. Some of these properties are surface related. This provides the main motivation for surface scientists to study this material. In this paper; quasicrystals, types of them, physical properties, surface science and potential applications of them have been discussed.

Keywords: Quasicrystals, Icosahedral quasicrystals, Polygonal quasicrystals, Aperiodic intermetallics.

* Corresponding author: Tel: +98 (0811) 8280440, Fax: +98 (0811) 8272404, E-mail address: FSamavat@basu.ac.ir & FSamavat@yahoo.com

19:00	Poster	P162
-------	--------	------

Observation of induced birefringence in crystals with scheelite structure

Liudmila I. Ivleva, Nikolai V. Bogodaev, Irina S. Voronina, Pavel A. Lykov, Liudmila Y. Berezovskaya, Vjatcheslav V. Osiko

A.M. Prokhorov General Physics Institute of Russian Academy of Sciences (GPI), Vavilov Str. 38, Moscow 119991, Russian Federation

E-mail: irinavoronina@list.ru

The crystals with scheelite structure such as BaWO_4 , SrMoO_4 are well-known Raman crystals, which are widely used in experimental studies and practical applications. Such non-linear optical materials with cubic nonlinearity and high SRS gain coefficient when being doped with Nd^{3+} ions can be also used as active medium and self-SRS shifter, simultaneously.

At present work the optical homogeneity of the crystals grown by Czochralski method and modified Stepanov technique was investigated. The values of anomalous birefringence were calculated and dependence of the thermal stresses on growth conditions was studied. The pictures of thermal stresses distribution along crystal boule were drawn and correlation with the crystal-melt interface form was shown. The photoelastic constants for the materials were experimentally estimated and the values of thermal stresses were obtained for different crystallization conditions.

19:00	Poster	P163
-------	--------	------

Self diffusion of Al and Mn in icosahedral Al-Pd-Mn quasicrystal

Feridoun Samavat

Physics Department, Bu-Ali sina university, Mahdیه St., Hamedan Hamedan, Iran

E-mail: fsamavat@yahoo.com

Self diffusion of Al and Mn in icosahedral Al-Pd-Mn quasicrystal

Feridoun Samavat ^{a,b}, Bruce V. King ^a, D. John O'Connor ^a

^a*School of Mathematical and Physical Sciences, University of Newcastle, Callaghan, New South Wales, 2308, Australia*

^b*Department of Physics, Bu-Ali Sina University, Hamedan, Iran*
Abstract

The self diffusion of Al and Mn in a single grain icosahedral $\text{Al}_{69.9}\text{Pd}_{20.5}\text{Mn}_{9.6}$ quasicrystal has been determined by a Low Energy Ions Scattering (LEIS) technique. LEIS technique has been able us to focus on the dynamics of concentration profiles at the surface and between the surface layers. The diffusion was determined by depositing the different elements (Al, Mn) on the surface and measuring the rate of change in surface composition as a function of temperature by LEIS, followed an arrhenius relation from which an activation energy for diffusion could be derived. The surface composition was monitored over the temperature range of 355K to 675K for Al and 355K to 575K for Mn. Activation energies of 0.17 ± 0.02 eV and 0.20 ± 0.01 eV have been measured for self diffusion of Al and Mn in i-Al-Pd-Mn respectively. No deviation from Arrhenius behavior was detected in the temperature range covered by the present experiments. From the low values of activation energy we propose that this range of diffusion is phason related, reflecting the specific nature of the icosahedral structure.

Keywords: Diffusion; Aluminum; Palladium; Manganese; Quasicrystals; Low Energy Ion Scattering

(LEIS); Al-Pd-Mn; Metallic surfaces.

19:00	Poster	P165
-------	--------	------

Kinetic studies of oxygen related defects in neutron irradiated silicon doped with carbon

Hańcza Barbara Surma

Institute of Electronic Materials Technology (ITME), Wólczyńska 133, Warszawa 01-919, Poland

E-mail: barbara.surma@itme.edu.pl

Oxygen is the most important residual impurity in Czochralski grown silicon (CZ-Si). Substituting an interstitial position in silicon lattice is electrically inactive but it play an important role in the creation of electrically active defects in irradiated silicon. The VO defect known as an A centre is one of the most important one. Its structure and properties has been intensively studied. It is well established that an energy level at $E - 0.16\text{eV}$ and a local vibrational mode (LVM) band at 830 cm^{-1} are associated with this defect. It is also known that interaction between carbon and oxygen atoms leads to appearance another defects among which CiOi is one of the most important one. The creation of electrically active oxygen-related defects during irradiation is highly undesired process in silicon detectors. In the recent years a silicon with an increased resistance for radiation is of a great demand. In this paper the kinetic studies of the three main defects VO, C_iO_i and VO_2 in neutron irradiated silicon doped with carbon during annealing between 300°C and 350°C were performed.

Samples from 6 different p or n type CZ-Si crystals with initial carbon concentration $0.8\text{--}5 \cdot 10^{16}\text{ at/cm}^{-3}$ and oxygen concentration $9.5\text{--}12 \cdot 10^{17}\text{ at/cm}^{-3}$ were irradiated with 2 MeV neutrons with dose $1 \cdot 10^{17}\text{ n/cm}^2$. After irradiation the samples were subjected to isothermal annealing at 300°C , 312°C , 325°C , 335°C and 350°C for 5' to 2000'. Intensity of the LVM absorption bands at 830 cm^{-1} , 889 cm^{-1} and 862 cm^{-1} related with VO, VO_2 and C_iO_i defects was controlled after each annealing process. The experimental results of defects annihilation/creation were compared with the theoretical curves obtained by simulation process taking into consideration all main de-

fect reactions and the physical interpretation of the simulation parameters is discussed.

19:00	Poster	P166
-------	--------	------

Growth, Spectroscopic, Optical, and Thermal Studies of catena – Poly[[cadmium (II)] – μ – β – alanine – di – μ – chloro] crystal, a semiorganic Nonlinear Optical Material

Ponnusamy S., Suruttaiya Udayar¹, Anbuezhian M., Maruthamuthu², Muthamizhchelvan C., Chellamuthu¹, Gunasekaran S., Sethu³

1. SRM Institute of Science and Technology (SRM), SRM Nagar, Kattankulathur, Chennai 603203, India **2.** Valliammai Engineering College (VEC), Kattankulathur, Chennai 603203, India **3.** Pachaiyappas College, Chennai, Chennai 600030, India

E-mail: suruponnus@gmail.com

A potential, semiorganic nonlinear optical (NLO) crystal, catena – Poly [[cadmium (II)] – μ – β – alanine – di – μ – chloro], has been grown by slow evaporation technique at 35°C . The Powder X – Ray Diffractogram of the crystal has been recorded and the various planes of reflection are identified. The compound crystallizes under orthorhombic system with space group Pna2, and the lattice parameters are: $a = 6.9664\text{ \AA}$, $b = 12.9222\text{ \AA}$, $c = 7.9546\text{ \AA}$ and $\alpha = \beta = \gamma = 90^\circ$. The qualitative analysis on the crystal has been carried by using Fourier Transform Infrared (FTIR) and Fourier Transform Raman spectral measurements. The coordination between cadmium chloride and amino acid is confirmed by the FTRaman spectrum. Optical behaviour such as UV – visible – NIR absorption spectra and second harmonic generation (SHG) for the crystal were investigated. The UV – Visible – NIR absorption spectrum establishes that the crystal acts as a good transmittance window and its lower cutoff is found to be as low as 200 nm, allowing for frequency conversion down to UV region. The SHG conversion efficiency is nearly equal to that of KDP crystal. The thermal stability of the crystal was analyzed with the aid of Thermogravimetric analysis (TGA) and Differential Scanning Calorimetry (DSC).

19:00	Poster	P167
-------	--------	------

Growth and investigation of optical properties of YVO_4 : Nd single crystals

Andrzej L. Bajor¹, Krzysztof Kopczynski², Jadwiga Mierczyk², Jaroslav Mlynczak², Marek A. Swirkowicz¹, Włodzimierz Szyski¹

1. Institute of Electronic Materials Technology (ITME), Wólczyńska 133, Warszawa 01-919, Poland **2.** Military University of Technology, Institute of Optoelectronics (IOE), Kaliskiego 2, Warszawa 00-908, Poland

E-mail: Marek.Swirkowicz@itme.edu.pl

Yttrium orthovanadate (YVO_4) crystals have magnificent optical, thermal and physical properties. For example, it has more than three times larger birefringence compared to that of lithium niobate, and this makes it especially useful in fiber optics, polarizers, optical isolators, and beam displacers. As a host material it is potential for

many lasing applications. However, to be used as optical material it needs to be optically homogeneous.

In this work we report on growth and investigation of optical homogeneity of Nd-doped YVO₄. The single crystals were grown in the nitrogen atmosphere by the Czochralski method with the use of Cyberstar Oxypuller 20-04 equipment. Thermal system consisted of iridium crucible of 50 mm dia. and passive iridium afterheater of 60 mm dia. Inductive heating was used. To suppress "tail" formation, changes of temperature distribution at the interface during the growth process were decreased by lifting the crucible to compensate lowering of the melt level. As a result, good quality, [100]-oriented single crystals with Nd content from 0.3 to 3 at.% were obtained. Their diameters and lengths were up to 25 mm and 50mm, respectively.

Optical homogeneity of these crystals was determined by means of space-variational optical spectroscopy, conoscopy and plane spectropolarimetry. In many cases we used samples in shapes of rectangular prisms oriented along the major X, Y and Z, crystallographic directions. Although a certain anisotropy could be evidenced depending on direction of observations, as might be anticipated from optical anisotropy of the crystals themselves, in general the crystals were found to be optically homogeneous and free from macroscopic defects. Sometimes, a certain optical inhomogeneity could be seen with some crystals, however, in a limited volume only. One could always find larger crystalline areas, potentially suitable for optical applications.

Lifetime measurements were also carried out on crystals doped with 0.5 at. % of Nd. This evidenced their potential use in laser techniques.

19:00	Poster	P168
-------	--------	------

Preparation and characterization of CoSi₂-Si eutectic composite

Wojciech Gurdziel, Krzysztof Szostek, Zygmunt Wokulski

University of Silesia, Institute of Materials Science, 12, Bankowa Str., Katowice 40-007, Poland

E-mail: chrissz@interia.pl

Recently very interesting materials for microelectronic applications are semiconductor based composites. Semiconductor-metal eutectic composites are generally characterized by special physical properties. The example of such composite is InSb-NiSb eutectic which is applied in microelectronic. In a literature there are not much data concerning Si-CoSi₂ eutectic composite that belongs to mentioned type. Therefore the aim of the study was to establish the general technological parameters of obtaining the Si-CoSi₂ fibrous eutectic.

The composite was obtained by *in situ* longitudinal directional crystallization technique using Bridgman method. Three different pulling down speeds were applied in order to examine influence of applied speeds on microstructure of the obtained ingots.

The obtained ingots were investigated using light microscopy (Opton interference microscope, Nikon alphaphot 2) and scanning electron microscopy (SEM), X-ray microanalyser (JEOL JMS-6480). It was shown that the morphology of CoSi₂ metallic fibres strongly depends on the crucible pulling down speed.

19:00	Poster	P169
-------	--------	------

XPS characterization of YAlO₃:Co single crystals

Ewa Talik¹, Magdalena M. Kruczek^{1,2}, Halina Sakowska², Włodzimierz Szyrski²

1. University of Silesia, August Chelkowski Institute of Physics, Department of Solid State Physics, Uniwersytecka 4, Katowice 40-007, Poland 2. Institute of Electronic Materials Technology (ITME), Wólczyńska 133, Warszawa 01-919, Poland

E-mail: talik@us.edu.pl

The perovskite-like yttrium aluminate YAlO₃ (orthorhombic structure) reveals a polarized laser beam and because of it, is an excellent host for solid state lasers scintillators and acoustooptic materials as well as Q-switch.

Comparing with YAG, the single crystals of YAP can be grown faster, have a smaller core and more favorable distribution coefficient for rare-earth dopants; it seems to be useful for laser host.

The YAP:Co single crystals were grown by the Czochralski method using iridium crucibles (54 mm in diameter and 52 mm in height) and iridium afterheater. Oxypuller 05-03 equipment made by Cyberstar (France) was used. As raw materials: Y₂O₃ (5N), Al₂O₃ (5N) and CoO + Co₂O₃ (4.85N) were used. The concentration of Co²⁺ ions was 0.22 at. %, 0.30 at. %, and 0.40 at. %. The crystals were grown under N₂ atmosphere with a gas flow rate of 0.4 l/min. The pulling rate was between 1 - 2 mm/h and the rotation rate was between 10 rpm and 20 rpm. An automatic diameter control was carried out using Cyberstar programme, in which weight differential was maintained constant. Sartorius balance was used to control the weight of the growing crystal.

The obtained single crystals up to 25 mm in diameter and 60 mm in length were free of macroscopic defects and inclusions of other phases.

The samples for measurements were taken from each crystal by slicing for a wafer ~1mm thickness, and double sides polishing. A part of this wafers were annealed in reduction atmospheres:

- 1) in hydrogen, at 1200⁰ C for 10 min,
- 2) in vacuum, at 1750⁰ C for 5 hour,
- 3) first in hydrogen at 1200⁰ C for 10 min and next in vacuum, at 1750⁰ C for 5 hour.

After annealing the wafers were slowly cooled down to room temperature.

The electron spectroscopy XPS shows the chemical composition is in agreement with a nominal composition of compound. A very low contamination of carbon was detected. The narrowest core level lines were observed for the sample annealed in hydrogen which was colourless.

References

1. S.Baccaro, K. Blažek, F.de Notaristefani, P. Maly, J.A. Mares, R. Pani "Scintillation properties of YAP:Ce", Nuclear Instruments and Methods in Physics Research A 361 (1995) 209-215,
2. G. Neuroth, F. Wallrafen, "Czochralski growth and characterisation of pure and doped YAlO₃ single crystals", Journal of Crystal

Growth 198/199 (1999) 435-439,

3.J.B. Shima, A. Yoshikawa, M. Nikl, N. Soloviev, J. Pejchal, D.H. Yoon, T. Fukuda, "Growth and characterization of Yb^{3+} -doped YAlO_3 fiber single crystals grown by the modified micro-pulling-down method", *Journal of Crystal Growth* 256 (2003) 298-304,

4. A.J. Wojtowicza, P. Bruyndonckx, W. Drozdowski, Z. Gałazka, J. Głodo, T. Łukasiewicz, P. Szupryczyński, S. Tavernierc, M. Wiśniewska, D. Wiśniewski, "Traps and recombination centers in $\text{YAlO}_3:\text{Ce}, \text{Co}$ ", *Nuclear Instruments and Methods in Physics Research A* 486 (2002) 482-485,

5. Andrzej J. Wojtowicz, "Rare-earth-activated wide bandgap materials for scintillators", *Nuclear Instruments and Methods in Physics Research A* 486 (2002) 201-207,

19:00	Poster	P170
-------	--------	------

Magnetic properties of CeNi_4Mn single crystal

Monika Klimczak¹, Ewa Talik^{1,4}, Andrzej Kowalczyk², Tomasz Toliński²

1. University of Silesia, August Chelkowski Institute of Physics, Department of Solid State Physics, Uniwersytecka 4, Katowice 40-007, Poland 2. Institute of Molecular Physics, Polish Academy of Sciences, Smoluchowskiego 17, Poznań 60-179, Poland

E-mail: talik@us.edu.pl

The development of one of the branches of modern electronics i.e. the spintronics is based on the spin polarization effects. It has been recently found that CeNi_4Mn exhibits exceptional and promising properties [1-3]. It is a soft ferromagnet with the coercive field below 5 Oe at 5 K. The saturation field is about 1.5 kOe. Simultaneously, the Andreev reflection measurements have shown that this compound can reach a spin polarization of the order of 66% [3]. The Curie temperature of CeNi_4Mn is equal to 140 K and, as was recently observed, by neutron diffraction - the magnetic ordering is of the ferromagnetic type with the magnetic moment of $4.6\mu_B$ at 17 K [1, 2]. The saturation magnetic moment at 2 K is $4.6\mu_B/\text{f.u.}$, which is nearly equal to $5\mu_B$ for the spin moment of the Mn^{2+} ion. This implies that both Ce and Ni do not carry any significant magnetic moment [1, 2].

CeNi_4Mn belongs to a widely studied series of compounds of the composition RNi_4X , where $\text{X} = \text{B}, \text{Al}, \text{Cu}, \text{Ga}, \text{Si}$ and Mn . It appeared that the substitution by various X leads to modification of the crystallographic structure. The parent compound CeNi_5 crystallizes in the hexagonal CaCu_5 -type of structure, space group $\text{P6}/\text{mmm}$ with Ce occupying the $1a$ site (0,0,0), Ni(1) in the $2c$ site (1/3,2/3,0) and Ni(2) in the $3g$ sites (1/2,0,1/2). This same structure is realized for $\text{X} = \text{Al}, \text{Cu}, \text{Ga}$ and Si with X and Ni(2) atoms statistically distributed over the $3g$ site [4]. For $\text{X} = \text{Mn}$ the hexagonal structure observed for all the previous substitutions switches to a cubic MgCu_4Sn -type of structure, which is a variant of the cubic AuBe_5 structure [1, 5].

The aim of this work was obtaining of the CeNi_4Mn single crystal and examination of its structural, magnetic, transport and electronic structure properties. The single crystal was obtained by the Czochralski method. CeNi_4Mn has grown in the hexagonal CaCu_5 -type

of crystal structure. From the ac magnetic susceptibility a transition to the ferromagnetic state has been found at about 140 K.

[1] Indu Dhiman, A. Das, S.K. Dhar, P. Raychaudhuri, Surjeet Singh, P. Manfrinetti, *Solid State Comm.* **141** (2007) 160-163

[2] E.N. Voloshina, Y.S. Dedkov, M. Richter, P. Zahn, *Phys. Rev. B* **73** (2006) 144412.

[3] S. Singh, G. Sheet, P. Raychaudhuri, S.K. Dhar, *Appl. Phys. Lett.* **88** (2006) 022506.

[4] Y.B. Kuz'ma and N.S. Bilonizhenko, *Kristallografiya* **18** (1973) 710.

[5] Ya.M. Kalychak, O.I. Bodak, and E.I. Gladyshevskii, *Izv. Akad. Nauk, SSSR, Neorg. Mater.* **12** (1976) 961.

19:00	Poster	P173
-------	--------	------

Growth and characterization of NLO-N-Bromosuccinimide (NBS) single crystals

Kanagasekaran Thangavel, Mythili Prakasam, Srinivasan Padmanabhan, Gopalakrishnan Rengasamy

Anna university, chennai 600025, India

E-mail: kanagu_sekaran@yahoo.co.in

Organic single crystals possess unique opto-electronic properties because organic molecules have delocalized electrons, namely, conjugated electron systems exhibit various photoresponses such as photoconductive, photovoltaic, photo catalytic behaviour and so on. The organic materials with intramolecular charge transfer compounds having large second order nonlinear optical effects. The organic compounds with electron rich (donor) and deficient (acceptor) substituents, provide the asymmetric charge distribution in the p electron system, show large nonlinear optical responses. Nonlinear optical crystals should meet several requirements, such as large phase-matchable nonlinear optical coefficient, a wide optical window around the visible region, mechanical and chemical stability and a high damage threshold. Some of these requirements based on molecular properties can be satisfied with the assistance of molecular design. It is possible to control the absorption edges of intramolecular charge transfer compounds by selecting the combination of donor and acceptor. Many of organic crystals have absorption in the blue light region and some of them have a cut-off wavelength more than 450 nm. This indicates the possibility of reduced conversion efficiency of SHG due to self-absorption of materials when using a semiconductor laser with 800 nm band. Organic materials are perceived as being structurally more diverse and therefore are believed to have more long-term promise than inorganics. A wide variety of organic materials are being investigated for frequency doubling. We have been concentrating on the growth of organic and semi-organic crystals for nonlinear applications, using low temperature solution growth technique.

We have grown N-bromosuccinimide single crystals for NLO applications. The growth experiments were carried out in a constant temperature bath with a set temperature (accuracy $\pm 0.01^\circ\text{C}$). As the grown crystal has a wide transparency range, that is, the absence of absorption in the visible region is a necessity for NLO. High quality and transparent crystals were grown and the grown crystals were subjected to XRD, FTIR, UV-VIS, Photoluminescence, mechanical

and dielectric studies. The results will be presented in detail.

19:00 Poster P174

Neutron powder diffraction study of the anion-deficient

$\text{La}_{0.70}\text{Sr}_{0.30}\text{MnO}_{3.00-\gamma}$ manganites

Sergei Trukhanov¹, Aleksey Trukhanov², Svetlana Zemskova³, Anatoliy I. Beskrovniy³, Henryk Szymczak⁴

1. The Joint Institute of Solid State and Semiconductor Physics of NASB, P.Brovki str., 19, Minsk 220072, Belarus **2.** Vitebsk State University (VSU), av. Moskovskaya 33, Vitebsk 210036, Belarus **3.** Joint Institute for Nuclear Research, Dubna, Russian Federation **4.** Polish Academy of Sciences, Institute of Physics, al. Lotników 32/46, Warszawa 02-668, Poland

E-mail: truhanov@ifftp.bas-net.by

Using powder neutron diffraction method the magnetic structure of the anion-deficient solid solution $\text{La}_{0.70}\text{Sr}_{0.30}\text{MnO}_{3.00-\gamma}$ ($\gamma = 0.15; 0.20$) at different temperatures has been determined. It is established that the magnetic structure changes with oxygen vacancies concentration. For the investigated samples the structural phase transitions have not been detected. The oxygen stoichiometric $\text{La}_{0.70}\text{Sr}_{0.30}\text{MnO}_{3.00}$ sample is ferromagnet with $T_c \sim 360$ K. At the $T = 287$ K the spontaneous magnetic moment is $M_S^C = 2.92(5) \mu_B / \text{f. u.}$, whereas at the $T = 10$ K – $M_S = 3.53(6) \mu_B / \text{f. u.}$ The direction of the total magnetic moment is along to [110]. For the anion-deficient $\text{La}_{0.70}\text{Sr}_{0.30}\text{MnO}_{2.85}$ sample the long-range magnetic ordering is absent for all the investigated temperatures. This sample is spin glass with the freezing temperature $T_f \sim 45$ K. For the anion-deficient $\text{La}_{0.70}\text{Sr}_{0.30}\text{MnO}_{2.80}$ sample is detected partial long-range antiferromagnetic ordering at the ~ 10 and ~ 40 K. At the $T = 40$ K the spontaneous magnetic moment is $M_S = 0.83(3) \mu_B / \text{f. u.}$, whereas at the $T = 10$ K – $M_S = 0.88(1) \mu_B / \text{f. u.}$ The direction of the antiferromagnetic axis is along to [111]. The obtained data confirm the theory of the magnetic phase state forming for the Sr-doped anion-deficient manganites. In according to this theory in case of orbital ordering absence the lowering of the coordination of the magnetic ion results to change of the indirect superexchange interactions $\text{Mn}^{3+}\text{-O-Mn}^{3+}$ sign from positive to negative. This work was partly supported by Belarus Fund for Basic Research (Project F06R-078).

19:00 Poster P175

Crystallization of silicon thin film by current-induced joule heating using tungsten overcoat

Gwomei Wu, Chenyen Wu

Chang Gung University, Kwei-Shan 3333, Taiwan

E-mail: wu@mail.cgu.edu.tw

Higher quality polycrystalline silicon thin films exhibited higher electron mobility and were useful for transistors for active-matrix flat-panel displays. The better compatibility with the peripheral circuits in an additional advantage in an integrated system. Several techniques have been employed to enhance the crystal quality of low temperature grown amorphous silicon, such as solid phase crystallization, excimer laser annealing, and metal-induced lateral crystallization. In this paper, we present a modified crystallization process us-

ing current-induced joule heating under vacuum. A thin layer of high temperature resistant tungsten was sputtered on the amorphous silicon as the conducting medium and metal seed. The thin film thickness was measured by α -stepper. The high current density provided effective means in crystallizing the amorphous silicon layer. The crystalline morphology was studied by scanning electron microscopy (SEM) after seccco-etch, transmission electron microscopy (TEM) and x-ray diffraction (XRD), under different annealing conditions. The grain size has been in the range of 0.1-1 μm and could be increased with annealing time. No tungsten silicide was observed. Some defects were formed due to the electron-migration effect. In addition, a heating profile due to current distribution would be proposed.

19:00 Poster P176

Growth of $\text{Li}_{1-x}\text{Gd}_x\text{Y}(\text{BO}_3)_3:\text{Eu}^{3+}$ solid solution for solid state dosimetry

Roman P. Yavetskiy, Alexander Tolmachev, Mikhail F. Dubovik

Institute for Single Crystals NAS of Ukraine (ISC), 60 Lenin Ave., Kharkov 61001, Ukraine

E-mail: yavetskiy@isc.kharkov.ua

Nowadays $\text{Li}_6\text{RE}(\text{BO}_3)_3$ (RE=Y, Eu, Gd, Yb) single crystals are intensively studied for different applications due to their promising optical properties. They belong to the monoclinic system, space group $P2_1/c$. $\text{Li}_6\text{Y}(\text{BO}_3)_3$ and $\text{Li}_6\text{Gd}(\text{BO}_3)_3$ crystals activated with erbium or ytterbium are considered as laser materials [1, 2]. Cerium activated $\text{Li}_6\text{Y}(\text{BO}_3)_3$ and $\text{Li}_6\text{Gd}(\text{BO}_3)_3$ crystals are prospective scintillation detectors for thermal neutrons registration [3]. Recently we have shown that $\text{Li}_6\text{Gd}(\text{Y})(\text{BO}_3)_3:\text{Eu}^{3+}$ possesses intense thermally stimulated luminescence (TSL). High TSL yield combined with high temperature of the main TSL peak and non-hygroscopicity allows one to consider these crystals as promising storage phosphors [4]. This work is devoted to develop a dosimetric material with variable value of effective atomic number Z_{eff} on the basis of $\text{Li}_6\text{Gd}_{1-x}\text{Y}_x(\text{BO}_3)_3:\text{Eu}^{3+}$ solid solution and to determine their storage properties.

Peculiarities of phase formation in the $\text{Li}_6\text{O-B}_2\text{O}_3\text{-RE}_2\text{O}_3$ (RE=Gd, Y) systems have been studied by means of differential thermal analysis and X-ray phase analysis. The solubility in the binary system $\text{Li}_6\text{Gd}(\text{BO}_3)_3\text{-Li}_6\text{Y}(\text{BO}_3)_3$ has been determined. It has been shown that $\text{Li}_6\text{Gd}_{1-x}\text{Y}_x(\text{BO}_3)_3$ solid solutions exist in all the concentration range of x values (sugar-like phase diagram). Pure and europium activated $\text{Li}_6\text{Gd}_x\text{Y}_{1-x}(\text{BO}_3)_3$ single crystals up to 15 mm in diameter and up to 20 mm in length have been grown using Czochralski method in air atmosphere. The influence of the growth conditions and seed crystal orientation on the structural perfectness of obtained crystals has been analyzed. The main physico-mechanical properties of $\text{Li}_6\text{Gd}_{1-x}\text{Y}_x(\text{BO}_3)_3$ crystals have been determined.

The models of charge carrier traps in $\text{Li}_6\text{Gd}_{1-x}\text{Y}_x(\text{BO}_3)_3:\text{Eu}^{3+}$ crystals have been proposed basing on the analysis of TSL, photoluminescence, thermal decoloration, and peculiarities of crystal structure. The possibility of practical application of $\text{Li}_6\text{Gd}_{1-x}\text{Y}_x(\text{BO}_3)_3:\text{Eu}^{3+}$ solid solutions with variable value of Z_{eff} for solid state dosimetry have been discussed.

- [1] J. Sablayrolles, V. Jubera, J.-P. Chaminade et al., *Optical Materials* 27 (2005) 1681.
- [2] Y. Zhao, X. Gong, Y. Lin et al., *Materials Letters* 60 (2006) 418.
- [3] J.P. Chaminade, O. Viraphong, F. Guillen, C. Fouassier and B. Czirr, *IEEE Transactions on Nuclear Science* 48 (2001) 1158.
- [4] R.P. Yavetskiy, E.F. Dolzhenkova, M.F. Dubovik et al., *Journal of Crystal Growth* 276 (2005) 485.

PTWK General Meeting

Monday evening, 21 May, 20:30

Tuesday, 22 May

Excursion

Tuesday morning, 22 May, 8:30

Lunch

Tuesday afternoon, 22 May, 13:00

Session V: Optoelectronics - passive devices

Maciej Bugajski

Tuesday afternoon, 22 May, 14:30

14:30

Invited oral

Infrared sensors in spacecraft that monitor planet earth

Paul Norton

IR Vision, Santa Barbara, CA 93105, United States

E-mail: p.norton@verizon.net

Life on the Planet Earth for humans and many other species is in jeopardy in the near term by a variety of man's activities that threaten to upset the climate. In addition, depletion of resources, catastrophic storms, alteration of weather patterns, and pollution may seriously disrupt or end the life of many of Earth's inhabitants. In addition to monitoring conditions on earth with visible imaging from aircraft or spacecraft, infrared sensors provide a wide range of unique information on the status of conditions on earth. This talk will be based on the sensors used in NASA's earth monitoring spacecraft. Examples of the infrared detector arrays used in some of these missions will be described.

15:00

Invited oral

High Operation Temperature (HOT) photodetectors

Jozef Piotrowski

Vigo System S.A., Swietlikow 3, Warszawa 01-389, Poland

E-mail: jpiotr@vigo.com.pl

The common belief that IR photodetectors must be cooled to achieve a high sensitivity is substantiated by the huge and noisy thermal generation in their small threshold energy optical transitions. Cryogenic cooling of detectors has always been the burden of sensitive infrared

systems, particularly those operating in the middle-wavelength (MWIR) and long-wavelength (LWIR) range of the IR spectrum. In contrast, infrared detectors with limited cooling have obvious advantages, including the elimination of power-consuming cryogenics; a reduction in size, weight, and cost; and greater reliability. Despite numerous research initiatives and the attractions of ambient temperature operation and low-cost potential—room-temperature IR detector technology enjoyed only limited success in competition with cooled photon detectors. Recent considerations of the fundamental detector mechanisms suggest, however, that near-perfect detection can be achieved without the need for cryogenic cooling. The limitations to perfect detection without cooling are of technological rather than fundamental nature.

The importance of sensitive and fast detection of long wavelength IR radiation without cooling was recognized in Poland in early 60's and became the main subject of Polish scientists. They proposed numerous concepts and practical solutions related to uncooled detection. In early 80's Vigo System S.A. was founded to commercialize uncooled IR detectors.

In this paper recent progress in fast and sensitive detection of the middle and long wavelength infrared radiation using uncooled or minimally cooled photodetectors is discussed. Photoconductive and photoelectromagnetic detectors are still in production but they are gradually replaced with photovoltaic devices which offer inherent advantages of no need for electric or magnetic bias. Sophisticated device architectures based on Hg_{1-x}Cd_xTe multilayer heterostructures have been proposed and implemented. The heterostructures have been grown by low temperature metalorganic vapor phase deposition (MOCVD). Thermal generation of charge carriers is minimized by careful optimization of the device architecture and reduction of the volume of active regions by monolithic integration of the devices with suitable microoptics. Solutions to other specific problems of high-temperature detection, such as poor collection efficiency due to a short diffusion length, the Johnson-Nyquist noise of parasitic impedances, and interfacing of very low resistance devices to electronics have been found. The dynamic resistance of the devices is increased by the use of multiple photovoltaic cells connected in series.

The present research and fabrication program includes devices which are optimized for any wavelength within a wide 1-16 μm spectral range and 200-300 K operation temperatures. The gap between performance of practical uncooled devices and fundamental limits set by quantum noise of the signal or background radiation is steadily narrowing. Picosecond range response time has been obtained in high frequency optimized devices.

The uncooled or minimally cooled infrared devices have found numerous civilian and military applications in areas such as thermography, process control, sensitive heterodyne detection, fast pyrometry, Fourier and laser spectrophotometry, imaging interferometry, laser technology and metrology, long-wavelength optical communication, ultrasensitive (ppb and ppt range) gas analyzers, imaging spectrophotometers, thermal wave nondestructive material testing, and many others.

Key words: HgCdTe, heterostructures, MOCVD, infrared photodetectors, uncooled operation

Coffee Break

Tuesday afternoon, 22 May, 15:30

Session VI: Optoelectronics - active devices

Antoni Rogalski

Tuesday afternoon, 22 May, 16:00

16:00

Invited oral

Quantum Dot Sensors for Multi-Band and Terahertz Detection

Unil Perera

Georgia State University, Department of Physics and Astronomy,
Atlanta, GA 30303, United States

E-mail: uperera@gsu.edu

With the interest in the terahertz region of the spectrum (0.1-3.0 THz) for applications in imaging, communication, security and defense, there is an increasing need for terahertz detectors exhibiting low dark current and operating at high temperatures. One major challenge is the reduction of the dark current (due to thermal excitations) associated with the terahertz detection mechanisms. Since quantum dot (QD) based detectors inherently show low dark currents, a QD based structure is a suitable choice for terahertz detectors. The work described here demonstrates a terahertz tunneling quantum dot infrared photodetector (T-QDIP) operating up to 150 K. In the T-QDIP structure grown by molecular beam epitaxy (MBE), a QD (InGaAs or AlGaAs) is placed in a well (GaAs/AlGaAs) followed by a double barrier (AlGaAs/InGaAs/AlGaAs) next to the well. The photocurrent generated by a transition from the ground state in the QD to a state in the well coupled with the double barrier (resonant state) can be selectively collected by resonant tunneling, while the double-barrier blocks the majority of the carriers contributing to the dark current (carriers excited to any other state in the well). Two important properties of the T-QDIP detectors are the tunability of the operating wavelength and the multi-color (band) nature of the photoresponse based on different transitions in the structure. Successful results on a two-color T-QDIP with photoresponse peaks at $\sim 6 \mu\text{m}$ and $\sim 17 \mu\text{m}$ operating at room temperature, and a terahertz T-QDIP responding at 6 THz ($50 \mu\text{m}$) at 150 K is presented. Furthermore, the wavelength bands in a dual-band T-QDIP resulting in transitions from the QD ground state to two states in the well coupled with double-barrier states (i.e. two resonant states) can be tuned by the bias. This is due to the dependence of resonance conditions for each resonant state on the applied bias. This would allow the separation of photocurrent due to two response bands without using external filters. This multi-band nature of T-QDIP detectors would be useful for applications such as mine detection, where scanning in two different wavelength bands greatly enhances detection capabilities and reduces false positives.

This work is done jointly with Prof. P. Bhattacharya's group at University of Michigan, Ann Arbor, under NSF grants, ECCS: 0620688 and ECCS: 0553051.

16:30

Oral

X-ray Diffraction as a Tool of InGaN layer Characterization.

Mike Leszczynski¹, Marcin Krysko¹, Jaroslaw Domagala², Robert Czernecki¹, Pawel Prystawko¹, Grzegorz Targowski¹

1. Polish Academy of Sciences, Institute of High Pressure Physics (UNIPRESS), Sokolowska 29/37, Warszawa 01-142, Poland

2. Polish Academy of Sciences, Institute of Physics, al. Lotników 32/46, Warszawa 02-668, Poland

E-mail: mike@unipress.waw.pl

InGaN layers are the heart of green/blue/violet optoelectronic devices. They are not only used as light-emitting quantum wells but also as anti-stressor layers or electron-injecting layers.

The most significant feature of InGaN layers is their tendency to be segregated. The In-rich clusters are very efficient light emitters despite a high dislocation density in heteroepitaxial relaxed structures, but at the same time they are a serious problem in more sophisticated devices, as laser diodes.

This work shows how X-ray diffraction can be used to monitor the In-segregation in the layers. A new simulation program enables us to estimate the range of In-content in thick InGaN layers as well as in the thin quantum wells. The XRD results are well matched with those obtained using transmission electron microscopy, as well as photoluminescence techniques.

Coffee Break

Tuesday afternoon, 22 May, 16:45

Session VII: Optoelectronics - active devices II

Tuesday afternoon, 22 May, 17:15

Chair: Paul Norton

17:15

Invited oral

Group III-Antimonide based infrared semiconductor lasers

Joachim Wagner

Fraunhofer-Institute of Applied Solid State Physics, Tullastr. 72,
Freiburg 79108, Germany

E-mail: wagner@iaf.fraunhofer.de

In this talk the current status of group III-Antimonide based semiconductor lasers, emitting in the $2 \mu\text{m}$ to $2.5 \mu\text{m}$ infrared spectral range, will be reviewed. Such lasers are needed for materials processing and laser surgery as well as for spectroscopic sensing and medical diagnostics. To cover this wavelength range GaInAsSb/AlGaAsSb quantum well (QW) lasers grown on GaSb substrates are best suited. The growth of the epitaxial layer sequence is almost exclusively performed by solid-source molecular-beam epitaxy (MBE). Valved cracker effusion cells are employed as As and Sb sources for the reproducible growth of lattice-matched or deliberately strained GaInAsSb and AlGaAsSb quaternary layers of differ-

ent compositions.

For broad area lasers emitting at 2 μm , high power efficiencies ($\sim 25\%$) and output powers of 2 W in cw mode (>9 W in pulsed mode) have been achieved at room-temperature. Laser bars with 19 emitters show at the same wavelength and temperature a cw output power as high as 21 W. To serve applications which require a better slow-axis beam quality than that provided by broad area lasers, the tapered laser concept has been adopted. Such lasers yield at 1.9 μm a nearly diffraction limited output with a beam quality factor of $M^2 < 1.7$ up to an output power of 1.5 W, resulting in a brightness of 30 MW/cm².

Optically pumped Vertical-External-Cavity Surface-Emitting Lasers (VECSELs) are attracting considerable current interest as an alternative to edge-emitting semiconductor diode lasers. VECSELs combine a high quality circular output beam, which is a feature of classical solid state lasers, with the wavelength versatility of a gain medium composed of semiconductor quantum structures. Group III-Antimonide based VECSELs composed of a GaInAsSb/AlGaAsSb QW active region and a GaSb/AlAsSb distributed Bragg reflector (DBR) emitting at 2.3 μm have been demonstrated. With just thermoelectric cooling to -20°C a maximum cw output power of 1.5 W with $M^2 < 3$ has been achieved, with the VECSEL chip bonded to an intra-cavity diamond heat-spreader for efficient heat removal.

17:45

Oral

Modelling guidelines for VCSEL designing

Włodzimierz Nakwaski

Technical University of Łódź, Institute of Physics, Wólczańska 219, Łódź 93005, Poland

E-mail: nakwaski@p.lodz.pl

Computer simulations are currently the most efficient and cheap methods in designing and optimisation of device structures. The most exact theoretical approaches are usually also the most time-consuming ones and need powerful computers. In some cases, cheaper simplified modelling simulations are sufficiently accurate. Therefore, an appropriate modelling approach should be chosen taking into account a compromise between our needs and our possibilities.

Modelling of an operation and designing of structures of vertical-cavity surface-emitting diode lasers (VCSELs) requires appropriate mathematical description of physical processes crucial for devices operation, i.e. various optical, electrical, thermal and recombination phenomena taking place within their volumes. Equally important are mutual interactions between above individual processes, usually strongly non-linear and creating a real network of various inter-relations.

Chain is as strong as its weakest link. Analogously, model is as exact as its less exact part. Therefore it is useless to improve exactness of its more accurate parts. All model parts should exhibit similar accuracy.

In VCSEL modelling, it is necessary to choose:

- between exact but at the same time more involved and more time-consuming vectorial optical approaches and simplified scalar

ones,

- between exact drift-diffusion electrical model and the simplified approach based on the Laplace equation,
- between rigorous thermal model including electro-thermal phenomena and phonon scattering at layer boundaries and the simplified model based on the thermal conduction equation and a bulk thermal conductivity,
- between exact microscopic recombination approach including many-body inter-actions and different temperatures of electron, hole and phonon gases and the approach based on the Fermi's Golden Rule coupled with the carrier and photon phenomenological rate equations,
- between full optical-electrical-thermal-recombination self-consistency and the partially electrical-thermal self-consistent model coupled with the optical and recombination ones.

Sometimes very accurate theoretical approaches starting from the so called first principles need equally exact values of various model parameters which are very difficult to be determined theoretically and are practically impossible to be measured. Then their rough values are estimated which completely ruins an exactness of the approach. A more recommended method is to use a simpler approach with some parameters taken from experiments which, in a natural way, takes into account all special features of a phenomenon under consideration, even those which have not been included in this simplified approach.

In conclusion, in any individual case, **a reasonable compromise should be reached between high modelling fidelity and its practical convenience depending on a main modelling goal, importance of expected results, available equipment and also financial possibilities.**

Dinner

Tuesday evening, 22 May, 18:00

Poster Session 2

Tuesday evening, 22 May, 19:00

19:00

Poster

P201

Effect of stress on structural transformations in GaMnAs

Jadwiga Bak-Misiuk¹, Andrzej Misiuk², Przemysław Romanowski¹, Jarosław Domagała¹, Janusz Sadowski¹, Adam Barcz¹

1. *Polish Academy of Sciences, Institute of Physics, al. Lotników 32/46, Warszawa 02-668, Poland* **2.** *Institute of Electron Technology (ITE), al. Lotników 32/46, Warszawa 02-668, Poland*

E-mail: bakmi@ifpan.edu.pl

Ferromagnetic semiconductors have recently received much interest, since they hold out prospects for using electron spins in electronic devices. Particularity GaMnAs has become the focus of current investigation because of its high Curie temperature.

The aim of present paper is to determine an influence of annealing under enhanced stress on the defect structure of GaMnAs.

As ($0.05 < x < 0.1$) layers of 0.3-0.8 mm thickness were grown on GaAs (001) substrates by molecular beam epitaxy (MBE). Next the samples were treated at 700 K (HT) under enhanced Ar hydrostatic pressure (HP, equal to 1.1 GPa) for 1 h. Structural investigations were carried out using X-Ray MRD-PHILIPS diffractometer in the double (DAD) and triple (TAD) axis configurations as well as by Secondary Ions Mass Spectroscopy (SIMS). The rocking curves and reciprocal space maps were recorded. Lattice parameters of the layers were determined from the symmetrical and asymmetrical X-Ray reflection. The Mn concentration, the lattice parameters of the layer as well as the strain state before and after processing were calculated.

The total concentration of Mn measured by SIMS method remained unchanged after the treatment. However, drastic decrease of the out-of-plane lattice parameter was detected. These treatment - induced changes depend strongly on the Mn concentration. For Mn concentration about 10 %, the diffraction peak coming from the layers disappears, while the detectable interference fringes as well as the SIMS results show that the thickness of the thin layer as well as Mn concentration remain unchanged. It has been found that post - growth annealing of GaMnAs under high pressure leads to the lattice constant contraction, more pronounced than that caused by annealing under 10^5 Pa. The rocking curve width (FWHM), layer thickness and lattice constant of the GaAs substrate remained unchanged after the treatment. Contraction of the lattice parameter can be related to the decreased concentration of interstitial Mn atoms and/or of arsenic antisites. The contribution of arsenic antisites and of Mn atoms, both substitutional and interstitial, to the a_{GaMnAs} value is given by the formula (compare [1]).

$$a_{GaMnAs}(x,y,z) = a_0 + 0.02x + 0.69y + 1.05z$$

where: a_0 - lattice constant of defects - free GaAs, y - concentration of As antisites, z - concentration of Mn in the interstitial positions. Possible structure change of GaMnAs from the cubic to hexagonal one [2] was also accounted for. The reason for stress - induced effects in GaMnAs layers has been discussed.

References

1. J. Masek, J. Kurdnowsky, F. Maca, *Phys. Rev. B* **67**, 153203 (2003).
2. V. M. Kaganer, B. Jenichen, F. Schipan, W. Braun, L. Daweritz, K. H. Ploog, *Phys. Rev. B* **66**, 045305 (2002).

19:00	Poster	P202
-------	--------	------

Growth of GaN layers on silicon and sintered GaN nano-ceramic substrates – TEM investigations

Jolanta Borysiuk¹, Piotr Caban¹, Wlodek Strupinski¹, Stanisław Gierlotka², Svetlana Stelmakh², Jerzy F. Janik³

1. Institute of Electronic Materials Technology (ITME), Wólczyńska 133, Warszawa 01-919, Poland **2.** Polish Academy of Sciences, Institute of High Pressure Physics (UNIPRESS), Sokolowska 29/37, Warszawa 01-142, Poland **3.** AGH University of Science and Technology (AGH), al. Mickiewicza 30, Kraków 30-059, Poland

E-mail: jolanta.borysiuk@itme.edu.pl

Heteroepitaxial GaN layers have been grown on many foreign substrates such as sapphire, silicon carbide or silicon. Therein, a common feature is that the GaN epitaxy proceeds *via* several stages, *i.e.*, nitridation, growth of the low temperature buffer layer, annealing, and, finally, growth of the layer with the reduced density of dislocations.

The mechanism of the GaN growth has also been investigated. Despite many efforts, the microscopic mechanism of island creation, dominant growth of selected grains, their coalescence, and the strain reduction *via* creation of dislocations have been only partially elucidated.

Recently, alternative GaN nano-ceramic substrates were developed [1, 2]. They offer a unique possibility to investigate the growth of GaN layers originated on various crystallographic orientations in nano-scale which is the subject of the reported transmission electron microscopic (TEM) study. For comparison, GaN layers on silicon were also investigated by this technique.

It is shown that the MOCVD growth of GaN layers on the GaN nano-ceramic substrates is highly anisotropic. The disorientation of the grains in the layer is much higher causing larger strains as compared to the GaN layer on the silicon substrate. In consequence, the flat growth front can be attained with higher difficulty. However, an appropriately thick GaN layer can, eventually, develop flat surfaces suitable for construction of optoelectronic structures. This can be achieved at the cost of creation of the relatively large density of dislocations and stacking faults.

We want to acknowledge a generous support of the Polish Committee for Scientific Research KBN, Grant 3 T08D 043 26

[1] E. Grzanka, S. Stelmakh, S. Gierlotka, A. Swiderska-Sroda, G. Kalisz, B. Palosz, M. Drygas, J. F. Janik, R. T. Paine: "In situ X-ray diffraction studies of distribution of strain during simultaneous sintering of nanocrystalline GaN powders under high-pressure high-temperature conditions"; EPDIC-10, September 1-4, 2006; Geneve, Switzerland.

[2] S. Stelmakh, A. Swiderska-Sroda, G. Kalisz, S. Gierlotka, E. Grzanka, B. Palosz, M. Drygas, J. F. Janik, R. T. Paine: "Microstructure and mechanical properties of GaN nanoceramics sintered under high-pressure high-temperature conditions"; International Conference on Nanoscience and Technology 2006 (ICN+T 2006); July 30-August 4, 2006; Basel, Switzerland.

19:00	Poster	P203
-------	--------	------

Growth of high resistivity GaN layers by compensating defects generation

Piotr Caban¹, Wlodek Strupinski¹, Andrzej Turos^{1,2}, Jolanta Borysiuk¹, Ewa Dumiszewska¹, Karolina Pagowska²

1. Institute of Electronic Materials Technology (ITME), Wólczyńska 133, Warszawa 01-919, Poland **2.** Andrzej Sołtan Institute for Nuclear Studies (IPJ), Świerk, Otwock-Świerk 05-400, Poland

E-mail: piotr.caban@itme.edu.pl

AlGaIn/GaN high electron mobility transistors (HEMTs) are one of the most important applications of III-nitride semiconductors in

modern microelectronics. They are usually produced in a planar structure on top of a GaN epilayer. High resistivity of GaN layers are prerequisite to obtain good electrical characteristics of HEMTs, especially the pinch-off effect. This can be obtained by compensation of the conductivity of as-grown layers either by defect or chemical mechanism.

In this paper we report on an attempt to obtain the carrier compensation effect in GaN by introducing controlled density of defects. It is well known that high mismatch strain leads to the nucleation of threading dislocations, dislocation loops and other defects that are produced at the substrate-layer interface. In order to be able to control defect distributions the following structure was grown using the MOCVD technique: first the thin AlN nucleation layer was grown on the sapphire substrate followed by the special buffer layer (SBL) of $\text{Al}_{0.4}\text{Ga}_{0.6}\text{N}$ covered with high temperature GaN layer of 1 μm thickness. Since the large part of lattice strain was accommodated by the SBLs the majority of dislocations was grown at the substrate-SBL interface. Consequently, by changing the SBL thickness dislocation propagation into GaN layer can be controlled.

The produced structures were characterized by RBS/channeling and high resolution TEM and XRD techniques, which enabled the judicious choice of the SBL thickness. The ultimate proof was the properly working HEMT device produced on such a high resistivity GaN layer.

19:00	Poster	P204
-------	--------	------

Distribution of strain in laterally overgrown GaAs layers determined by x-ray diffraction

Jaroslav Domagala, Aleksandra Czyzak, Zbigniew R. Zytkeiwicz
*Polish Academy of Sciences, Institute of Physics, al. Lotników
 32/46, Warszawa 02-668, Poland*

E-mail: czyzak@ifpan.edu.pl

Continuous improvement in quality of semiconductor structures and miniaturization of electronic devices leads to an increasing demand for techniques that allow detection and visualization of crystalline lattice microdefects. From many techniques available the Rocking Curve Imaging (RCI) based on synchrotron x-ray diffraction has gained much attention recently as the useful method of wafer defect analysis and industrial wafer quality inspection [1]. Using it quantitative information on crystallographic misorientations and lattice quality can be obtained by direct imaging of large sample area with high spatial resolution. However, for most crystal growers an access to the synchrotron radiation sources is still difficult and laboratory techniques are preferred. Therefore, we have developed a simple RCI version that makes use of conventional high resolution x-ray diffractometer.

Briefly, by specially designed set of slits and masks the size of the incident x-ray beam of the diffractometer is reduced to 6 $\mu\text{m} \times 0.5$ mm. Then, this narrow beam is precisely scanned in small steps across the sample surface and x-ray diffraction area map is collected. Both the ω and $2\theta/\omega$ scans could be used, that allows mapping of crystallographic misorientation and lattice parameter distributions along the sample area. The technique was used in this work to study crystallographic perfection of epitaxial laterally overgrown (ELO)

GaAs layers grown by the liquid phase epitaxy on SiO_2 -masked GaAs substrates. Since ELO layer consists of monocrystalline stripes regularly arranged on a substrate such samples are the best to demonstrate potential of the technique.

We will show, in agreement with our previous report [2], that laterally parts of ELO layers (wings) are tilted downwards due to their interaction with underlying mask. By using x-ray mapping this phenomenon can be easily distinguished from macroscopic sample curvature. Direction of the tilt and distribution of tilt magnitude across width of each wing can also be readily determined. The later allows us to measure the shape of lattice planes in individual ELO stripe and to compare it with the shape of layer surface. If large area of the sample is mapped fluctuation of wing tilts of various ELO stripes are monitored. In fully overgrown GaAs samples additional strain field is found at the plane where ELO stripes grown from adjacent seeds merge. This strain is due to coalescence of two wings tilted in opposite direction.

It is mentioning worthy that a common procedure applied for structural analysis of ELO layers is to measure x-ray diffraction curves under standard conditions of a wide x-ray beam. Such measurements are quite easy since the diffracted x-ray beam is highly intensive. Then, however, diffracted signal is integrated over many ELO stripes. Our results indicate some fluctuation of local wing tilts across the sample surface. This phenomenon, as well as macroscopic curvature of the sample, lead to broadening of diffraction curves obtained in the standard procedure and consequently to overestimation of the tilt angle value. In this way we show that local x-ray diffraction, e.g. x-ray mapping, must be used if precise information on wing tilt and its spatial distribution is required.

Acknowledgements: This work was partially supported by the Polish Committee for Scientific Research under grant No. 3T08A 021 26.

[1] D. Lubbert, T. Baumbach, J. Hartwig, E. Boller, E. Pernot, Nucl. Instrum. Methods B 160 (2000) 521.

[2] Z.R. Zytkeiwicz, J. Domagala, D. Dobosz, J. Bak-Misiuk, J. Appl. Phys. 84 (1998) 6937.

19:00	Poster	P206
-------	--------	------

Effect of temperature and mineralizer on phase stability and solubility of GaN under acidic ammonothermal conditions

Dirk Ehrentraut¹, Yuji Kagamitani¹, Naruhiro Hoshino¹, Tsuguo Fukuda¹, Hirohisa Itoh²

1. Tohoku University, Sendai, Japan 2. Mitsubishi Chemical Corp., Ibaraki 300-1295, Japan

E-mail: dirk@tagen.tohoku.ac.jp

The temperature effect of ammonium halogenides NH_4X ($\text{X} = \text{Cl}, \text{Br}, \text{I}$) on the phase stability of GaN synthesized under supercritical ammonothermal conditions in the temperature range 400–550 °C has been investigated. Self-nucleated hexagonal GaN (*h*-GaN), cubic GaN (*c*-GaN), and gallium oxide (Ga_2O_3) has been crystallized. The latter was formed from mineralizers containing a relatively high amount of oxygen. The tendency to form *c*-GaN increases from $\text{X} = \text{Cl}$ over Br to I . Decreasing the temperature supports the formation of *c*-GaN. Single-phase *h*-GaN can be grown from $\text{X} = \text{Cl}, \text{Br}$ at 550

°C. Solubility of GaN is discussed. The use of *h*-GaN substrate has a phase-stabilizing effect and lowers the stability range for overgrown *h*-GaN films. We show how the choice of precursor will have an impact on *a* and *c* lattice parameter of self-nucleated *h*-GaN.

19:00 Poster P207

Effects of composition grading at the heterointerfaces and Layers Thickness Variations on Bragg Mirror Quality

Jarosław A. Gaca¹, Marek Wojcik¹, Andrzej Turoś¹, Agata Jasik², Kamil Pierściński², Michał Kosmala²

1. Institute of Electronic Materials Technology (ITME), Warszawa 01919, Poland 2. Institute of Electron Technology (ITE), al. Lotników 32/46, Warszawa 02-668, Poland

E-mail: gaca-j@itme.edu.pl

GaAs/AlAs Bragg mirrors on GaAs with varied number of pairs of layers, were grown by molecular beam epitaxy (MBE) to be applied for semiconductor saturable absorber mirrors (SESAMs) and intensity modulators. Due to the random variation of the growth rate, substrate surface roughness and interdiffusion at the interfaces it is difficult to control perfectly the growth conditions of deposited layers. Thickness variations around the expected values and composition grading at the heterointerfaces can be expected and consequently, variations of the mirror reflectivity. In this paper the X-ray diffraction, optical reflectance, Rutherford backscattering/channeling (RBS) supported by numerical methods were employed to determine both the exact thickness of each layer and the composition grading at the interface between succeeding layers of (Al)GaAs/AlAs-based mirrors. To speed up the process and to make the result more reliable, the diffraction curve, RBS and reflectivity spectra were simulated concurrently using results of one simulation to verify the others. This process was carried out until the best fit between experimental and calculated curves was achieved. It was shown that the X-ray diffraction method aided by numerical calculations is the most sensitive to the thickness variation of each layer and composition grading at the interfaces, but it was also shown that combining all the methods employed in this work significantly speed up the whole process of resolving Bragg mirror structure. And thanks to this sensitivity of X-ray diffraction it was possible to assess to what extent the thickness of each layer may be varied and composition grading at the interfaces modified so that only negligible modification of reflectivity spectrum would be observed.

19:00 Poster P208

Determination of stress in composite engineered substrates for GaN-based RF power devices

Marek Guzewicz¹, Eliana Kaminska¹, Anna Piotrowska¹, Krystyna Gołaszewska¹, Jarosław Domagała², Hacene Lahreche³, Robert Langer³, Marie-Antoinette Poisson⁴, Philippe Bove³

1. Instytut Technologii Elektronowej (ITE), al. Lotników 32/46, Warszawa 02-668, Poland 2. Polish Academy of Sciences, Institute of Physics, al. Lotników 32/46, Warszawa 02-668, Poland 3. Picogiga Int., Place Marcel Rebuffat, Parc de Villejust, Courtaboeuf 91960, France 4. Alcatel Thales Lab, Route de Nozay, Marcoussis 91461, France

E-mail: margu@ite.waw.pl

Residual stresses and their impact on the performance of semiconductor devices are of permanent interest for crystal growers and device manufacturers. This is especially true for GaN-based RF power devices fabricated on mismatched substrates such as Si and SiC. Moreover, aiming at bridging the gap between the low-performance, low-cost single crystal Si and the high-performance, high cost single crystal silicon SiC as the starting substrates for the growth of device structures, composite engineered substrates based on silicon and silicon carbide materials have been recently proposed [1]. These substrates, namely mono-Si on poly-crystalline SiC (SopSiC) and mono-SiC on polycrystalline SiC (SiCopSiC), are engineered using Smart Cut™ technology.

In this paper we show the results of stress measurements in the composite SopSiC and SiCopSiC substrates as well as AlGaN/GaN HEMT structures grown on them. These have been compared with standard AlGaN/GaN HEMTs grown on sapphire and bulk Si substrates.

Two methods have been applied to determine the stress: (a) high resolution X-ray diffraction technique, using PHILIPS X'Pert MRD diffractometer to evaluate the lattice strain and (b) wafer curvature-based techniques, using ADE Mapper Shape Metrology System and Tencor®FLX-2320 Stress Measurement System, enabling stress measurement in temperature range of room temperature – 500 °C.

We have found that the results of HRXRD measurements are similar to those obtained by curvature-based methods on SopSiC and SiCopSiC substrates. The average film stress of -390 MPa is here in the Si(445nm)/SiO₂(210nm) bilayer of the SopSiC substrate, and the stress of -290 MPa is in the Si(955nm)/SiO₂(270nm) bilayer.

Residual stresses in HEMT structure grown on the composite substrate is 200 MPa and 100 MPa for SopSiC and SiCopSiC substrates, respectively. The AlGaN/GaN structure grown on sapphire is compressively stressed up to -600 MPa, and the HEMT structure grown on the (111)Si substrate is under low compression. The measurements of temperature dependence of stress σ show that $\sigma = -225$ MPa @ 500 °C for the HEMT structure grown on SopSiC substrate.

[1] <http://www.hyphen-eu.com/>

Part of the research was supported by the grant from the EC HY-PHEN Contract Number: FP6-027455.

19:00 Poster P209

Sublimation growth of AlN crystals on {111} TaC seeds

Carsten Hartmann, Christoph Seitz, Jürgen Wollweber, Martin Albrecht, Roberto Fornari

Institute for Crystal Growth (IKZ), Max-born Str. 2, Berlin 12489, Germany

E-mail: hartmann@ikz-berlin.de

AlN is the most promising material for wide bandgap optoelectronics and high power electronic devices. An almost equal thermal expansion coefficient and a small lattice mismatch with GaN (2.4 % along the *a*-axis) favour AlN substrates over sapphire or even over SiC. Its use results in a reduced defect density in devices which drastically improves their performance and lifetime.

Due to the lack of high quality AlN wafers for homoepitaxially-

seeded sublimation growth of AlN bulk crystals, other lattice-matched materials have to be employed as seeds. SiC covered by an epitaxial AlN layer is the only foreign substrate reported so far. In the present work, we introduce {111} TaC as an alternative substrate material. The misfit between the {111} TaC and the {0001} AlN plane is only 1.2%. This value is comparable with the lattice mismatch of 1.0% between SiC and AlN. As advantage over SiC, TaC brings a nearly complete thermal and chemical stability at the normal growth conditions ($T > 2000$ °C).

Unfortunately, there are no TaC single crystals exceeding 4 mm commercially available. Therefore, we fabricated our {111} TaC substrates by carburization of {111} Ta wafers (12 mm in diameter, 1 mm thickness) at 1900 °C in pure graphite powder and in Ar atmosphere. A main challenge is to prevent small-angle grain boundaries that occur under non-optimized process conditions. These grain boundaries result from stress induced by the little lattice expansion during the carburization.

AlN growth on TaC seeds was carried out in a rf heated reactor. A TaC crucible containing purified AlN powder was placed in a graphite assembly and was enclosed in a porous graphite foam insulation. Successful epitaxial seeding on the {111} TaC substrates is demonstrated and proved by electron back scatter diffraction measurements (EBSD). The initial island growth mechanism is observed and analyzed by secondary electron microscopy (SEM).

19:00	Poster	P210
-------	--------	------

Ammonothermal growth of thick gallium nitride films

Yuji Kagamitani¹, Dirk Ehrentauf¹, Naruhiro Hoshino¹, Akira Yoshikawa¹, Tsuguo Fukuda¹, Hirohisa Itoh²

1. Institute of Multidisciplinary Research for Advanced Materials (IMRAM), Sendai 980-8577, Japan 2. Mitsubishi Chemical Corp., Ibaraki 300-1295, Japan

E-mail: kagami@tagen.tohoku.ac.jp

A major drawback in GaN technology is the lack of large-size, single-crystalline GaN substrates of high quality, i.e. less than the 10^7 dislocations per cm^{-2} at present, due to thermal-expansion and lattice-parameter mismatch between GaN-based film and foreign substrates like $\alpha\text{-Al}_2\text{O}_3$ (sapphire) or SiC. High-pressure (>100 MPa), solvothermal techniques are well established and currently providing the largest crystals of $\alpha\text{-SiO}_2$ and ZnO from supercritical (SC) aqueous solutions. In the case of GaN, SC ammonia (NH_3) is employed as solvent. We have produced single-crystalline GaN films of < 200 mm in thickness on 1 cm^2 large, HVPE-grown (0001) GaN substrates employing NH_4Cl as mineralizer for solubility enhancement. System pressures < 170 MPa were applied. The average growth speed ranging 5 to 30 mm/day over longer growth runs is observed for the film growth on the (000-1) face. The maximum growth speed was achieved for the film grown at a supersaturation from a combined Ga/GaN precursor. The surface morphology of the grown film is not affected by the nature of the precursor, i.e. Ga metal or GaN

19:00	Poster	P211
-------	--------	------

High-resolution photoinduced transient spectroscopy of defect centers in Mg-doped GaN

Paweł Kamiński¹, Roman Kozłowski¹, Marcin Miczuga², Paweł Prystawko³, Elżbieta Litwin-Staszewska³, Michał Kozubal¹, Jarosław Żelazko¹

1. Institute of Electronic Materials Technology (ITME), Wólczyńska 133, Warszawa 01-919, Poland 2. Military University of Technology (WAT), Kaliskiego 2, Warszawa 00-908, Poland 3. Polish Academy of Sciences, Institute of High Pressure Physics (UNIPRESS), Sokolowska 29/37, Warszawa 01-142, Poland

E-mail: Pawel.Kaminski@itme.edu.pl

Defect levels in Mg-doped GaN epitaxial layers, grown on sapphire substrates by metal organic chemical vapor deposition (MOCVD), were investigated using high-resolution photoinduced transient spectroscopy (HRPITS). A novel approach to extraction of trap parameters from the photocurrent relaxation waveforms recorded in a wide temperature range has been applied. It is based on the two-dimensional analysis of the waveforms as a function of time and temperature using the correlation procedure or inverse Laplace algorithm. The effect of annealing on the material electrical properties and defect structure has been studied. Before annealing, the layer resistivity at 300 K was $\sim 5 \times 10^5 \Omega\text{cm}$ and after a heat treatment at 780 °C it dramatically dropped to $\sim 2.5 \times 10^2 \Omega\text{cm}$. In the as-grown layer with the high-resistivity, six traps with activation energies of 0.12, 0.13, 0.66, 0.95, 1.32 and 1.52 eV were revealed. The 0.12-eV and 0.13-eV traps are tentatively attributed to the carbon atoms occupying Ga sites in the vicinity of dislocations and in the dislocation-free regions, respectively. The 0.66-eV trap can be assigned to the complex composed of a nitrogen vacancy and hydrogen atom (V_N-H). The 0.95-eV trap is likely to be attributed to the complex involving gallium vacancy and two hydrogen atoms ($V_{Ga}-2H$) and the 1.32-eV trap seems to be related to the carbon interstitial C_i . In the sample subjected to the heat treatment, twelve traps with activation energies ranging from 0.12 to 1.38 eV were detected. In particular, the 0.17-eV trap related to the Mg_{Ga} acceptor, as well as the traps with activation energies of 0.59 eV, 1.06 eV and 1.22 eV assigned to $Mg_{Ga}-V_N$, $V_{Ga}-O_N$ and C_i-C_s complexes, respectively, were found. The results indicate that the main mechanism leading to electrical activation of Mg atoms is the decomposition of neutral $MgGa-H$ complexes. On the other hand, the annealing results in a self-compensation through the formation of deep-level complex defects.

19:00	Poster	P212
-------	--------	------

Adsorption processes during growth of GaN by HVPE

Paweł Kempisty^{1,2}, Stanisław Krukowski^{2,3}, Paweł Strak^{1,2}

1. Warsaw University of Technology, Faculty of Physics, Koszykowa 75, Warszawa 00-662, Poland 2. Polish Academy of Sciences, Institute of High Pressure Physics (UNIPRESS), Sokolowska 29/37, Warszawa 01-142, Poland 3. Warsaw University, Interdisciplinary Centre for Materials Modelling (ICMM), Pawin-skiego 5a, Warszawa 02-106, Poland

E-mail: kempes@unipress.waw.pl

Ammonia is typically used as source of nitrogen in HVPE growth of GaN. The growth is routinely carried out on GaN (0001) or Ga-surface. In most cases the ammonia flux is at least two orders of magnitude higher than GaCl flux.

Ammonia based methods have not been analyzed using ab initio methods in much detail. Recently a number of investigations were carried out using Siesta DFT based methods. The obtained results included the equilibrium configuration of the surface in presence and absence of hydrogen and ammonia. It was shown that the micro-state state of the surface depends on the size of the supercell used for the simulations.

Adsorption of the active species: ammonia, gallium chloride and hydrogen was investigated. It was shown that the adsorption processes occur without any energy barrier for all the three compounds. This results indicate that the surface state is determined by the ration of the fluxes, i.e. GaN(0001) surface remains in nitrogen-rich state.

Desorption of the adatoms was also considered. It particular it was shown that the desorption of a single Ga adatom is energy costly process. This confirms that the surface diffusion length of Ga adatoms is large, even compared to large inter-step spacing of order of several hundreds of lattice constants. Therefore the growth of GaN by HVPE method is controlled by the magnitude of Ga flux at the surface, i.e. it is transport-controlled.

[1] Kempisty P., Krukowski S. *Journal of Crystal Growth* 303 (2007) 37

19:00	Poster	P213
-------	--------	------

Thick GaN layers on sapphire with various buffer layers

Ryszard Korbutowicz¹, Ewa Dumiszewska^{2,3}, Joanna Prażmowska¹

1. Wrocław University of Technology, Faculty of Microsystem Electronics and Photonics (WEMIF), Janiszewskiego 11/17, Wrocław 50-372, Poland **2.** Institute of Electronic Materials Technology (ITME), Wólczyńska 133, Warszawa 01-919, Poland **3.** Warsaw University of Technology, Faculty of Materials Science and Engineering (InMat), Wołoska 141, Warszawa 02-507, Poland

E-mail: ryszard.korbutowicz@pwr.wroc.pl

It is wide known that gallium nitride is a very attractive material for optoelectronic devices such as blue and ultraviolet light sources, UV detectors, for high temperature/power electronics and microwave devices. For these purpose one need suitable substrates for device structures epitaxy. In the nature there are no native crystals of the gallium nitride, synthesis is very difficult and it is hard to obtain single crystal with good properties. Crystallization of freestanding GaN substrates could be made by either high-pressure synthesis, by sublimation method or ammonothermal method. However, the size of GaN crystals obtained in these ways is still too small for practical use. The current largest freestanding GaN substrate was obtained by growth of a thick GaN layer on a sapphire substrate using Hydride Vapour Phase Epitaxy (HVPE) and separation of the grown layer from the sapphire substrate.

We have investigated thick GaN layers deposited in HVPE system on composite substrates which were made on sapphire in Metalor-

ganic Vapour Phase Epitaxy (MOVPE) system. The following substrates: (00.1) sapphire substrates with AlN, AlN/GaN and GaN thin layers were used.

Composite GaN on sapphire Al₂O₃ substrates with different nucleation layers (GaN or AlN) were grown using an AIX 200/4 RF-S low-pressure reactor. The source gases were trimethylgallium (TMGa), trimethylaluminium (TMAI) and ammonia (NH₃). The reactor pressure was 200 mbar, and the layers were grown at 1048°C.

Thick GaN layers were deposited in conventional, open HVPE system: three-temperature zone furnace and horizontal quartz reactor. Nitrogen (6N) was used as the carrier gas. GaCl was formed by the reaction of gaseous HCl (6N) and liquid Ga (6N) at 920°C. HCl was diluted by nitrogen. NH₃ (7N) was used as the source gas. Total gas flow was about 4500 ml/min. The temperature in main grown zone was kept at 1065°C.

In this HVPE system thick GaN layers (in the range of 50 up to 80 micrometers) were deposited on the top of GaN/sapphire, AlN/sapphire and GaN/AlN/sapphire structures.

We have determined the optical parameters, crystallographic structure and quality of epitaxial thick GaN layers and made comparison of these three types thick layers. We have observed significant differences.

19:00	Poster	P214
-------	--------	------

Fabrication and optical simulation of patterned sapphire substrates for optimal light extraction efficiency of LEDs

Yeeu-Chang Lee¹, Tsung-Xian Lee², Ko-Tao Lee², Ching-Cherng Sun², Jenq Yang Chang², Jyh-Chen Chen³

1. Chung Yuan Christian University, Department of Mechanical Engineering, Chung-Li 32023, Taiwan **2.** National Central University, Department of Optics and Photonics, Chung-Li 32001, Taiwan **3.** National Central University, Department of Mechanical Engineering, Chung-Li 32001, Taiwan

E-mail: ycleel2@ms49.hinet.net

Lateral epitaxy growth onto a patterned sapphire substrate (PSS) has been demonstrated effectively to reduce the threading dislocation densities in GaN layers grown by metal organic chemical vapor deposition (MOCVD) for the fabrication of high-efficiency light-emitting diodes (LEDs). Meanwhile, light extraction efficiency (LEE) is also enhanced due to the scattering effect of patterned structure. The conventional PSS is fabricated by the photolithography and dry etching techniques, however, ion bombardment from the plasma etching generate the damage on the substrate and dry etching is also a cost and time consuming solution. In this study, we adopt wet etching method mixed sulfuric acid and phosphoric acid at high temperature to form 1-D and 2-D patterns with various depths on the substrate. The etching shapes will be naturally determined from the crystallographic facets of sapphire. Based on these etching patterns, we use Monte Carlo ray tracing method to calculate the LEE and also predict the light distribution of PSS LEDs.

19:00

Poster

P215

3-D simulation of the anisotropic effects during growth of sapphire crystal using heat exchanger method

Chung-wei Lu, Pei-Hung Chi

Department of Information Management, Jen-Teh Junior College,
Hou-Lung,, Miao-Li 35664, Taiwan

E-mail: lucw1@ms5.hinet.net

3D Computer simulations using the commercial code FIDAP and CFDRC, which are based on finite element techniques, were performed to investigate the effects of the anisotropic conductivity in a heat-exchanger-method crystal growth system on the convexity of the melt-crystal interface and the hot spots of sapphire crystal. Both the energy input to the crucible by the radiation as well as convection inside the furnace and the energy output through the heat exchanger are modeled by the convection boundary conditions.

The cross section flow pattern and the melt-crystal interface shape of the 3-D modeling results are confirmed to comparing with the previous 2-D simulation results. For the 3-D model, "hot spots" on the corners of the crucible are present as a donut type, and the hot spot shapes are changed with the values of the anisotropic crystal's conductivities. The outline of crystal becomes more convex when the crystal's conductivity of the z direction (k_{sz}) increases. The outline of crystal-melt interface is ellipse for anisotropic conductivity in the radial direction (k_{sx} and k_{sy}). Outline touch the crucible bottom is smaller than the maximum outline of the crystal so that the "hot spot" shapes are changed with the values of the anisotropic crystal's conductivities.

Keyword: HEM, oxide, crystal growth, solidification, numerical

* Corresponding author. E-mail address: lucw1@ms5.hinet.net

References:

- [1] D. Viechnicki and F. Schmid, J. Crystal Growth **26**, 162 (1974)
- [2] F. Schmid and D. J. Viechnicki, U.S. Patent 3,653,432 (1972)
- [3] C. J. Jing, N. Imaishi, T. Sato, Y. Miyazawa, J. Crystal Growth **216**, 372 (2000)
- [4] C. W. Lu and J. C. Chen, J. Crystal Growth **225**, 274 (2001).
- [5] C. W. Lu and J. C. Chen, Modelling and Simulation in Materials Science and Engineering **10**, 147 (2002).
- [6] J. C. Chen and C. W. Lu, J. Crystal Growth **266**, 239 (2004).

The flow diagram of cross section is shown in Figure 1.

Figure 2 and 3 demonstrate the sapphire crystal shape with different T_{iref} for constant h_c

(h_c is the convection coefficient of the heat exchanger).

(T_{iref} is the environmental temperature outside the crucible)

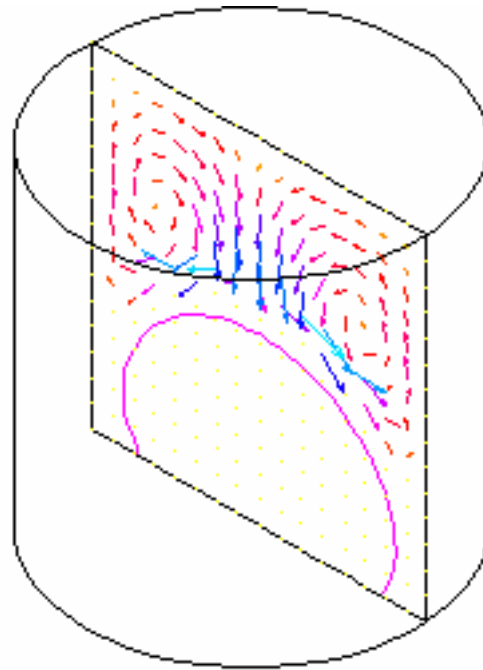


Figure 1

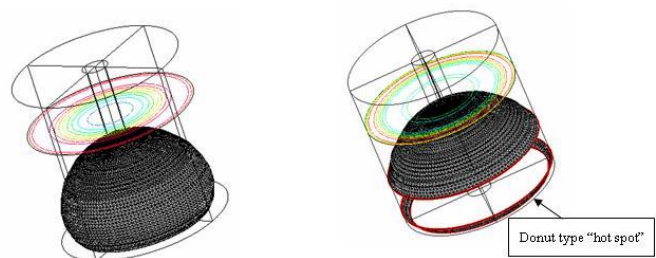


Figure 2 Figure 3

19:00

Poster

P216

Technological conditions to obtain high purity undoped GaP single crystals.

Aleksandra Mirowska, Waław Orłowski, Andrzej Hruban,
Stanisław Strzelecka, Andrzej Materna

Institute of Electronic Materials Technology (ITME), Warszawa
01919, Poland

E-mail: mirowska@itme.edu.pl

The aim of this work was to find out technological conditions which allow to obtain undoped GaP single crystals ("n" type) with carrier concentration below $5 \times 10^{16} \text{ cm}^{-3}$.

Synthesis by injection method and Czochralski crystal growth were used applying Liquid Encapsulation Technique. In this work the influence of water content in B_2O_3 encapsulant (applied during injection synthesis and LEC growth) on GaP crystals properties was in-

vestigated.

Two different thermal systems were applied: standard (2 heaters) and modified (with additional heater inside encapsulant layer). The reactions inside the crucible were investigated with the special focus on the role of carbon.

Undoped GaP single crystals with 2 inches diameter and carrier concentration below $5 \times 10^{16} \text{ cm}^{-3}$ and high mobility ($>130 \text{ cm}^2/\text{Vs}$) were grown.

19:00 Poster P217

Passivation of GaN surface by chemical bath deposition of thin CdS layers

Ewa Papis¹, Eliana Kaminska¹, Anna Piotrowska¹, Renata Kruska¹, Norbert Kwietniewski¹, Witold Rzodkiewicz¹, Andrzej Wawro²

1. Institute of Electron Technology (ITE), al. Lotników 32/46, Warszawa 02-668, Poland 2. Polish Academy of Sciences, Institute of Physics, al. Lotników 32/46, Warszawa 02-668, Poland

E-mail: papis@ite.waw.pl

GaN and related semiconductor compounds are important materials for optoelectronic and electronic applications, especially in high-temperature, high-power and high-efficiency systems. In order to exploit the full potential of these materials more effective methods of surface passivation are highly required. The standard methods of surface passivation of GaN-based devices rely on the use of silicon oxides or nitrides SiO_2 , Si_3N_4 and SiON . Several sulphur passivation processes including chemical treatments in $(\text{NH}_4)_2\text{S}$, Na_2S and CH_3CSNH_2 aqueous or alcoholic solutions have been proposed without definitive achievements. On the other hand, chemical bath deposited CdS films have been proven useful to passivation of III-V semiconductors surfaces [1].

In this paper we present the results on passivation of GaN surface using Chemical Bath Deposition (CBD) technique, forming CdS thin layers. $0.1 \text{ M } \text{SC}(\text{NH}_4)_2$ as sulphur source, $0.1 \text{ M } \text{CdSO}_4$ as source of Cd and $2.4 \text{ M } \text{NH}_4\text{OH}$ as solution for hydrolysis were used in the experiments. Variable Angle Spectroscopic Ellipsometry (VASE) was chosen to provide information of thickness, refractive index and dielectric function of passivating layers. Surface morphology was examined by optical microscopy with phase contrast and by Atomic Force Microscopy (AFM). To study the influence of CBD - CdS passivation on electronic properties on GaN surface, Ir/p GaN Schottky diodes were prepared on passivated and nonpassivated GaN samples. The results show, that Chemical Both Deposition from $0.1 \text{ M } \text{SC}(\text{NH}_4)_2$ - $0.1 \text{ M } \text{CdSO}_4$ ammonia solution enables to form thin ($d = 20 \text{ nm}$) CdS films, with good insulating properties ($\epsilon_2 = 0.0003$ at $E = 1.1 \text{ eV}$) and smooth surface ($\text{rms} = 1.2 \text{ nm}$). Increasing of height of Ir/p GaN barrier from 0.56 to 0.81 indicates that CdS layer deposited by Chemical Bath Deposition techniques enhanced performance of Schottky barrier.

Part of the research was supported by the grant from the EC HY-PHEN Contract Number: FP6-027455.

[1]. O. Vigil-Galan, J. Vidal Larramendi, I. Riech, G. Pena Rodriguez, A. Iribarren, J. Aguilar-Hernandez, G. Contreras-Puente, *Semicond. Sci. Technol.* 17, 1193, 2002.

19:00 Poster P218

Thermal properties of the 650-nm GaInP/AlGaInP quantum-well GaAs-based vertical-cavity surface-emitting diode lasers

Łukasz Piskorski, Robert P. Sarzała, Włodzimierz Nakwaski

Technical University of Łódź, Institute of Physics, Wólczańska 219, Łódź 93005, Poland

E-mail: lukasz.piskorski@p.lodz.pl

Short-wavelength lasing emission, especially that of 650 nm, may be applied in many various devices. Because of their wavelength much shorter than the wavelength of 850 nm of radiation emitted by standard arsenide diode lasers used in compact disks (CDs), they ensure much higher density of information in recording systems on digital versatile disks (DVDs). Analogously, the 650-nm radiation is widely used in laser printers. This radiation is also used in many branches of medicine, e.g. in photodynamic therapy. But the most important its application is associated with communication networks taking advantage of plastic (polymer) optical fibres (POFs) [1], for which the minimal optical attenuation corresponds to the 650-nm wavelength. Because of relatively great POF mechanical flexibility and additionally their much larger core For relatively short distances and moderate data rates, POFs are currently the lowest cost media to use for optical interconnect and the simplest to connectorize. There are still, however, some problems to produce proper high-performance sources of the carrier wave used in this communication networks.

Vertical-cavity surface-emission diode lasers (VCSELs) compose the most suited laser configuration for fibre application. Their 650-nm emitting active regions may be the GaInP/AlGaInP quantum wells (QWs). Hence the GaAs-based oxide-confined (OC) VCSELs with the above QWs [2] seem currently to be the best designs for the POF-based fibre optical communication.

POF optical communication may be used in cars, planes and ships. Therefore it should be resistant to some possible temperature increases. Accordingly, the main goal of this work is to examine thermal properties of the 650-nm AlGaInP VCSELs with the aid of a modified version of our comprehensive self-consistent model [3] simulating VCSEL operation. For increasing active-region temperatures, an increase in the VCSEL threshold current has happened to be mostly associated with the carrier leakage from the G valley of the $\text{Ga}_{0.43}\text{In}_{0.57}\text{P}$ quantum-well material to the X-valley of the $(\text{Al}_{0.67}\text{Ga}_{0.33})_{0.52}\text{In}_{0.48}\text{P}$ spacers. Nevertheless, the AlGaInP VCSELs have been found to exhibit splendid thermal behaviour with the characteristic temperature T_0 equal to 134 K for temperature increases up to 357 K. For 5-mm devices, maximal achievable output is decreased from 1.0 mW for 293 K to 0.6 mW for 320 K and to 0.33 mW for 340 K.

In conclusion, GaAs-based oxide-confined GaInP/AlGaInP VCSELs have been found to offer very promising performance at elevated temperatures as sources of the carrier 650-nm wave in the fibre communication using POFs.

The authors would like to acknowledge support from the Polish Ministry of Science and Higher Education (MNiSzW), grant No 3-T11B-073-29.

References

- [1] K. Ohdoko, T. Ishigure, and Y. Koike, *IEEE Photon. Techn. Lett.* **17** (2005) 79
 [2] A. Knigge et al., *IEE Proc.-Optoelectron.* **150** (2003) 110
 [3] R. P. Sarzała and W. Nakwaski, *J. Phys.: Condens. Matter* **16** (2004) S3121

19:00	Poster	P219
-------	--------	------

The influence of ridge sizes on room-temperature performance of the 405-nm InGaN/GaN RW diode laser

Piotr Karbownik, Robert P. Sarzała

Technical University of Łódź, Institute of Physics, Wólczńska 219, Łódź 93005, Poland

E-mail: rpsarzal@p.lodz.pl

Diode lasers emitting radiation of wavelengths shorter than 500 nm were practically initiated in 1996 by Nakamura et al.[1] who reported the first blue-emitting diode lasers based on $A^{III}B^V$ semiconductors. There have been, however, still some technological problems with manufacturing such nitride structures. The problems have been gradually overcome which has been strongly stimulated by extremely promising numerous application possibilities of blue and ultra-violet diode lasers in science, technology and various spheres of contemporary life. Hence a continuous progress in technology and optimisation of nitride devices is still accelerated by a strong demand for reliable, cheap, compact and high-performance lasing devices emitting radiation in this part of spectrum.

Structures of edge-emitting nitride diode lasers are usually equipped with electrodes placed on the same device side. It is a direct consequence of very high electrical resistivities of sapphire (Al_2O_3) used usually as a substrate material. Such structures require quite sophisticated and time-consuming processing which may additionally lead to a device damage and is definitely a reason of a considerable increase in a device cost. Besides, such a laser structure requires the p-side-up device configuration which is followed by heat-sinking problems deteriorating a device performance. The ridge-waveguide (RW) structure is usually used in these lasers creating an appropriate wave-guiding effect and, additionally, introducing better current-spreading confinement than the proton implantation, which is followed by lower lasing thresholds and much lower active-region temperature increases.

The main goal of the present work is to investigate an impact of diode-laser ridge sizes on its lasing performance with the aid of the comprehensive self-consistent optical-electrical-thermal-recombination model of nitride diode lasers [2]. The modern 405-nm InGaN/GaN RW laser structure reported by Kauer et al. [3] has been selected for this simulation. Contrary to usual structures of nitride diode lasers, the n-type GaN substrate material is used in this case instead of the sapphire one which enables application of the n-side bottom contact. This substrate is much more expensive than a sapphire one but it enables manufacturing nitride diode lasers of much better performance characteristics. Our simulation reveals that the lowest room-temperature lasing threshold may be expected for relatively narrow and deep ridges. For the structure under consideration, the lowest threshold current density of 5.75 kA/cm^2 has been determined for the 2.2-mm ridge width and the

400-nm etching depth. Then the active-region temperature increase was as low as only 24 K. For wider 5-mm ridge, this increase is twice higher. An impact of etching depth is more essential for narrower ridges. Quite a high values (between 120 and 140 K) of the characteristic parameter T_0 convince very good thermal properties of the above laser.

- [1] S.Nakamura et al., *J. Journal of Applied Physics*, 35 (1996) L74
 [2] R. P. Sarzała and W. Nakwaski, *J. Phys.: Condens. Matter* 16 (2004) S3121
 [3] M. Kauer et al., *Electronic Letters*, 41 (2005) 739

19:00	Poster	P220
-------	--------	------

Technology and characterisation of GaAsN/GaAs heterostructures for photodetector applications

Beata Ściana¹, Damian Radziejewicz¹, Damian Pucicki¹, M. Tlaczala¹, Jarosław Serafińczuk¹, Iwona Zborowska-Lindert¹, Przemysław Poloczek², Grzegorz Sęk²

1. Wrocław University of Technology, Faculty of Microsystem Electronics and Photonics (WEMIF), Janiszewskiego 11/17, Wrocław 50-372, Poland 2. Wrocław University of Technology, Institute of Physics, Wybrzeże Wyspiańskiego 27, Wrocław 50-370, Poland

E-mail: Beata.Sciana@pwr.wroc.pl

The nitrogen – containing conventional $A^{III}B^V$ semiconductor alloys, so called diluted nitrides ($A^{III}B^V-N$), have been extensively studied recently. Unusual properties of these materials such as a large band gap bowing coefficient b (40 eV for GaAs_{1-x}N_x with $x < 0.1\%$) and a large conduction band CB offset ($> 300 \text{ meV}$) come mainly from a large size difference between N (0.068 nm) and As (0.121 nm) and a large electronegativity of N (3.04) compared to Ga (1.81) and As (2.18). These features make $A^{III}B^V-N$ alloys very promising for applications in lasers and very efficient multijunction solar cells. There are not much papers devoted to applying these materials in photodetector device structures.

This work presents the technology and properties of undoped GaAs_{1-x}N / GaAs heterostructures used as active regions in the construction of MSM and PIN photodetectors. The atmospheric pressure metal organic vapour phase epitaxy (AP-MOVPE) was applied for growing MSM test structures with the nitrogen contents varied from 0.5 % to 1.74 %. The thickness of the absorption GaAs_{1-x}N_x layer was changed from 98 nm to 135 nm. The structural and optical properties of these structures were examined using high resolution X-Ray diffraction HRXRD, photoluminescence PL ($T = 80, 250 \text{ K}$) and photoreflectance spectroscopy PR ($T = 300 \text{ K}$). The DQW (double quantum well) PIN test structure was grown by radio-frequency molecular beam epitaxy RF MBE. The undoped active region consisted of two 10.5 nm thick GaAs_{0.99}N_{0.01} wells separated by 15.2 nm thick GaAs barrier layer was surrounded by undoped 200 nm thick GaAs and 100 nm thick p⁺-type GaAs from the top of the structure and by undoped 200 nm thick GaAs and 500 nm thick n⁺-type GaAs from the n-type GaAs substrate. The properties of the DQW active region were examined using PL measurements ($T = 300 \text{ K}$). Chemical wet etching was used for active region delineated to obtain the $80 \mu\text{m} \times 60 \mu\text{m}$ MSM and $\varnothing 125 \mu\text{m}$ PIN islands. The Ti/Pt/Au and Cu/Au metallization was applied for multifinger Schottky MSM

contacts with 1 μm / 2 μm and 1.5 μm / 3.5 μm finger width/ finger spacing. In the case of PIN device planar structure the Pt/Ti/Pt/Au and AuGe/Ni/Au metallization was used for the top ring contact to p⁺-GaAs and for the bottom contact to n⁺-GaAs, respectively. Dark and illuminated by different wavelength lasers ($\lambda = 650, 780, 850, 904, 980 \text{ nm}$; excitation power 20 and 40 μW) DC current-voltage characteristics were measured under the bias changed from -5 V to 5 V . Based on the obtained results the main device parameters as a dark current and a spectral response were estimated for both MSM and PIN structures.

19:00 Poster P221

Numerical Model of Electric Field in GaN/InGaN Light Emitting Diodes on Insulating Substrates

Jyh-Chen Chen¹, Gwo-Jiun Sheu¹, Farn-Shiun Hwu^{1,2}

1. National Central University, Department of Mechanical Engineering, Chung-Li 32001, Taiwan **2.** Department of Mechanical Engineering, Nanya Institute of Technology, Chung-Li 32091, Taiwan

E-mail: s1343015@cc.ncu.edu.tw

The current crowding effect in GaN-based light emitting diodes (LEDs) is essential in the design of highly efficient devices as well as the extraction of accurate diode quality factors from current-voltage data. In this regard, 3-D computational simulations using the commercial code FEMLAB, which are based on the finite element techniques, were performed to investigate the effects of the current distribution in GaN/InGaN light emitting diodes grown on sapphire substrates. The established 3D model of LED die can be used to show the real situations including plane effects and complex boundary conditions. In this study, the accuracy of numerical results is verified and discussed with previous literatures; a good correlation is obtained between the simulation and experimental result. The relations between current spreading with the geometries of LED structures are also simply discussed.

Keywords:Light emitting diodes (LEDs), Current spreading, Numerical simulation

References:

- [1] S. Nakamura in *High Brightness Light Emitting Diodes*, edited by G. B. Stringfellow and M. G. Craford (Academic, San Diego, 1998), p. 394.
- [2] I. Eliashevich, Y. Li, and A. Osinsky, *Proc. SPIE* vol. 3621, p. 28, 1999.
- [3] X. Guo, and E. F. Schubert, *Journal of Applied Physics*, vol. 90, pp. 4191-4195, 2001.
- [4] H. Kim, S. J. Park, and H. Hwang, *Applied Physics Letters*, vol. 81, No. 7, pp. 1326-1328, 2002.
- [5] X. Guo, and E. F. Schubert, *Applied Physics Letters*, vol. 78, No. 21, pp. 3337-3339, 2001.
- [6] Shatalov M et al., *Japanese Journal of Applied Physics*, vol. 41, No. 8, pp. 5083, 5087, (2002).

19:00 Poster P222

The influence of NH₃ gas flow on GaN nanowires synthesis by VPE method

Won young Song¹, Tongik Shin², Ho Jun Lee², Dae Ho Yoon^{1,2}

1. Sungkyunkwan University, Sungkyunkwan dvanced Institute of Nanotechnology, 300 Cheoncheon-dong, Jangan-gu, Suwon 440-746, Korea, South **2.** Sungkyunkwan University, Department of Advanced Materials Engineering, 300 Cheoncheon-dong, Jangan-gu, Suwon 440-746, Korea, South

E-mail: swylife@skku.edu

One-dimensional nanostructures such as nanowires, nanorods, nanotubes, and nanobelts have attracted much interest due to their application potentials as building blocks for assembling nanoelectronics and nanophotonics. Gallium nitride (GaN) has outstanding properties such as high thermal conductivity and direct wide bandgap of 3.39eV at room temperature. It was applied for a remarkably useful material in the field of optoelectronics and high power, high temperature electronics.

In this study, The GaN nanowires were synthesized by the vapor phase epitaxy (VPE) method. The phases of GaN nanowires were varied as a function of NH₃ gas flow. The alteration of NH₃ gas flow had essentially influence on GaN nanowires synthesis. Also it was important role of confirming characteristics of GaN nanowire. The shape of GaN nanowires was confirmed by using SEM. The EDX spectra was analyzed a chemical composition of GaN nanowires. The optical characteristics of the sample were investigated by photoluminescence. And we confirmed hexagonal GaN nanowires through TEM and XRD pattern

19:00 Poster P223

Recognition of chemical (electrically active) non-homogeneities in thick HVPE-grown GaN layers

Janusz Weyher^{1,4}, Renata Lewandowska^{1,2}, Carl Hemmingsson³, Hina Ashraf⁴, P.R. Hageman⁴, Boleslaw L. Lucznik¹, Izabella Grzegory¹

1. Polish Academy of Sciences, Institute of High Pressure Physics (UNIPRESS), Sokolowska 29/37, Warszawa 01-142, Poland **2.** Groupe d'Etude des Semiconducteurs, CNRS-UMR 5650, Université de Montpellier 2, cc074, 12 Place Eugene Bataillon, Montpellier 34095, France **3.** Linköping University, Department of Physics, Chemistry and Biology, Campus Valla, Linköping SE58183, Sweden **4.** University of Nijmegen, Fac. of Science, Dept. of Exp. Solid State Physics III, Toernooiveld, Nijmegen 6525 ED, Netherlands

E-mail: J.Weyher@science.ru.nl

Recently efforts are focused on growing by HVPE and by high pressure methods quasi-bulk thick epitaxial layers on GaN single crystals, MOCVD- and HVPE-grown templates. Using these technologies reduced dislocation density is achieved (as compared to that characteristic for standard hetero-epitaxial GaN layers) but still remarkable number of defects is present, including both dislocations and chemical non-homogeneities.

This communication will summarize the results of the study of chemical non-homogeneities which occur in thick homo- and hetero-epitaxial GaN layers. During the HVPE growth the macroscopic growth direction is changed at the edges of templates and inside the pinholes which results in higher carrier concentration. In the central part of the growing layers large area non-homogeneities also develop despite that the growth proceeds in the [0001] direction in macroscopic scale. Selective photo-etching is used for revealing these extended defects which show up as areas of different etch rate, i.e. different carrier concentration. The results were confirmed using cathodoluminescence and quantitative micro-Raman method [1]. The non-homogeneities were studied in GaN layers grown in different laboratories and they show markedly different morphological characteristics.

It will be shown that carrier concentration may vary up to two orders of magnitude across such material which considerably influences the structural quality of the subsequently grown homo-epitaxial layers and may have damaging impact to the device structures.

1. R. Lewandowska, J.L. Weyher, J.J. Kelly, L. Konczewicz, B. Lucznik, "Calibration of the PEC etching of GaN by Raman spectroscopy", (submitted to JCG).

19:00 Poster P224

MOCVD growth and characterization of ultrathin AlN/GaN superlattices on 0001 sapphire substrates

Marek Wojcik, Jarosław A. Gaca, Andrzej Turos, Wlodek Strupinski

Institute of Electronic Materials Technology (ITME), Wólczyńska 133, Warszawa 01-919, Poland

E-mail: Marek.Wojcik@itme.edu.pl

AlN/GaN superlattices (SLs) have been subject of intense investigation due to their potential applications for high power transistors and ultraviolet laser diodes. However, only a few reports are focused to their structural properties. In this work we report on the extended study of strained AlN/GaN SLs. Ultrathin (0.42/0.48 nm) AlN/GaN SLs were grown by the MOCVD technique on the top of a structure composed of thick 1000 nm Al Ga_x(1-x)N buffer layer, and AlN nucleation layer (≈20nm) on the x vicinal sapphire (0001) substrates. These samples were analyzed by means of high resolution x-ray diffraction (HRXRD) techniques, and cross-sectional transmission electron microscopy (TEM). It was found that for Al Ga_x(1-x)N layers with the same Al content as the average Al content in the whole volume of AlN/GaN SLs exhibit a good in-wafer composition uniformity. Moreover, no relaxation was observed i.e. both AlN and GaN layers have the same in-plane lattice parameter as the underlying buffer layer. The buffer layer is hence an effective substrate for the two-dimensional growth and ensures the proper the chemical and crystalline order of the AlN/GaN SLs. The strain evolution in the SLs structures is assessed by the high-resolution x-ray diffraction and reciprocal space mapping (RSM), using numerical simulation methods. It has also been shown that x-ray methods are sensitive enough to provide data necessary to determine chemical composition profile and crystallographic order even in the case of extremely thin AlN and GaN layers.

19:00 Poster P225

Optimisation of electrochemical sulphur treatment of GaSb and related semiconductors: application to surface passivation of GaSb/In(Al)GaAsSb TPV cells

Tadeusz T. Piotrowski¹, Krystyna Golaszewska¹, Ewa Papis¹, Jarosław Rutkowski², Renata Kruska¹, Jacek Szade³, Antoni Winiarski³, Anna Piotrowska¹

1. *Institute of Electron Technology (ITE), al. Lotników 32/46, Warszawa 02-668, Poland* **2.** *Military University of Technology, Institute of Applied Physics, ul. Kaliskiego 2, Warszawa 00-908, Poland* **3.** *University of Silesia, August Chelkowski Institute of Physics, Department of Solid State Physics, Uniwersytecka 4, Katowice 40-007, Poland*

E-mail: papis@ite.waw.pl

GaSb and related quaternary semiconductors offer a great potential for application in mid-infrared photovoltaics (PV) and thermophotovoltaics (TPV). The implementation of these materials, however, has been hampered by an inability to reproducible control of their surface properties. The surface treatment in sulphur containing solutions has received much attention and was applied to the improvement of the GaSb-based photodiodes electro-optical parameters. Little was reported about long-term stability of GaSb-based TPV cells.

In this work we have used heterojunction photodiodes grown by liquid phase epitaxy (LPE) on (100) n-GaSb:Te substrates. The mesa-type devices with mesa size of 500 μm × 500 μm were formed using photolithography and reactive ion etching in BCl₃ plasma. AgTe/Cr/Au and Au/Zn/Au metallizations were applied for backside n-type and front p-type ohmic contacts, respectively. The contacts were alloyed in H₂ at 250°C for 3 min. The processing of device structures was completed by surface passivation of mesa side-walls.

(NH₄)₂S, Na₂S, and (NH₄)₂CS have been chosen as sulphur sources in either aqueous or C₃H₇OH solutions. Electrochemical processing has been carried out at the current density of 0.4 – 4 mA/cm² for 15 – 30 min at room temperature. The parameters of electrochemical treatment – the current density and processing time – were optimised so as to fabricate the thickest possible overcoat with acceptable surface morphology (surface roughness below 10 nm). The passivating coatings obtained as a result of electrochemical sulphuration processes have been characterised by complementary use of Variable Angle Spectroscopic Ellipsometry (VASE), and X-ray Photoelectron Spectroscopy (XPS). The photodiode characterisation involved measurements of the current-voltage (I-V) characteristics, spectral response, and low frequency noise at 300 K. The I-V measurements were done using a computer controlled Keithley SourceMeter 2400 programmable meter. The relative photoresponse spectra were measured with a transimpedance amplifier coupled to a Fourier transform infrared (FTIR) spectrometer. Long-term performance under air exposure has been monitored within the time of 12 – 36 months, in 3-months intervals.

The results of VASE analyses have proven insulating character of passivating coatings (ε₂ = 0.014 and ε₂ = 0.029 at 1.1 eV). The spectroscopic dependence of ellipsometric functions ψ(λ) and Δ(λ) of n-GaSb surface passivated in 21%(NH₄)₂S-H₂O measured immedi-

ately after sulphur treatment and 3 years later were compared. No change of ellipsometric characteristics $\psi(\lambda)$ and $\Delta(\lambda)$, has been observed which indicates on good stability of the coating.

The key parameters of passivated GaSb/In(Al)GaAsSb photodiodes were monitored during 12 months. It has been found that after 12 months exposure of the photodiodes to ambient environment, the electrical and optical characteristics are unchanged. The above result confirms the chemical stability of applied passivating coatings.

Part of the research was supported by the grant no. 3T11B 00926 from the Ministry of Education and Science, Poland.

19:00	Poster	P226
-------	--------	------

Heterostructure Al_xGa_{1-x}As/GaAs solar cells

Joanna Prazmowska, Ryszard Korbutowicz, Beata Ściana, Bogdan Paszkiewicz, R. Paszkiewicz

Wrocław University of Technology, Faculty of Microsystem Electronics and Photonics (WEMIF), Janiszewskiego 11/17, Wrocław 50-372, Poland

E-mail: joanna.prazmowska@pwr.wroc.pl

In designing of solar cells structures the main emphasis is placed on improving the conversion efficiency. Various methods could be applied in order to enhance performance of device. Theoretical investigation and experimental examination of heterostructure Al_xGa_{1-x}As/GaAs solar cell were carried out. Modelling of consequences of GaAs quantum wells application in ordinary Al_xGa_{1-x}As/GaAs p-i-n solar cell device were determined. SimWindows version 1.5.0 made by David W. Winston was used to simulate devices under not concentrated AM 1.5 spectrum with P_{in} in average equal to 1000 W/m².

Heterostructures were placed within intrinsic region. Solar cell structure was optimized. Optimization of well and barrier width, well depth with constant value of intrinsic region width, number of wells in the intrinsic region, doping concentration of n region, width and doping concentration of p region was carried out. The depth of wells was altered by changing the fraction of Al in Al_xGa_{1-x}As barrier material. Results of modelling were compared with identical p-i-n solar cells without quantum wells.

AP-MOVPE technology was applied in order to fabricate solar cell device. Various measurements of structure as-growth were carried out. Electrical parameters and spectral characteristic of device were marked. I-V dark and illuminated solar cell plots were measured.

19:00	Poster	P227
-------	--------	------

Structure and Magnetization of Defect-Associated Sites in Silicon

Eun S. Choi¹, Lee Chow², Guangyu Chai², Andrzej Misiuk³, Adam Barcz^{3,4}, Richard Vanfleet⁵

1. National High Magnetic Field Laboratory (NHMFL), Tallahassee, FL 32310-3706, United States 2. University of Central Florida, Orlando, FL, United States 3. Institute of Electron Technology (ITE), al. Lotników 32/46, Warszawa 02-668, Poland 4. Polish Academy of Sciences, Institute of Physics, al. Lotników 32/46, Warszawa 02-668, Poland 5. Brigham Young University, Provo, UT 84602, United States

E-mail: chow@ucf.edu

Recently ferromagnetic hysteresis has been observed at room temperature in single crystalline silicon wafers implanted with Si or Ar ions, and also in silicon wafers irradiated with high flux of neutron beam [1]. The authors suggested that the paramagnetic defects created during implantation or irradiation maybe are among the factors responsible for the observed magnetic behavior. These results could also have important implications on the magnetic behaviors of metal implanted silicon wafers [2,3].

To better understand the mechanisms of the reported ferromagnetic hysteresis loop, we carry out high resolution transmission electron microscopic and magnetic study of Fz-Si and Cz-Si silicon wafers damaged, to produce different kinds of defects, by three different methods: (a) irradiation with 2.5 MeV electrons at a flux of 1×10^{17} cm⁻², (b) self-implantation with 150 keV Si⁺ ions at a flux of 2×10^{16} cm⁻², and (c) implantation with 20 keV He⁺ ions at an angle of 60° and at a flux of 1×10^{17} cm⁻². The results of these studies will be reported.

References

1. T. Dubruca, J. Hack, R.E. Hummel, and A. Angerhofer, Appl. Phys. Lett. 88, 182504 (2006).
2. M. Bolduc, C. Awo-Affouda, A. Stollenwerk, M.B. Huang, F. Ramos, G. Agnello, V. P. LaBella, Phys. Rev., B71, 033302 (2005).
3. P. R. Bandaru, J. Park, J. S. Lee, Y. J. Tang, L. H. Chen, S. Jin, S. A. Song, and J. R. O'Brien, Appl. Phys. Lett. 89, 112502 (2006).

19:00	Poster	P228
-------	--------	------

Comparison of various GaSb-based device structures for application in thermophotovoltaic cells

Krystyna Golaszewska¹, Tadeusz T. Piotrowski¹, Jarosław Rutkowski², Ewa Papis¹, Renata Kruszką¹, Elżbieta Dynowska³, Jacek Ratajczak¹, Anna Piotrowska¹

1. Institute of Electron Technology (ITE), al. Lotników 32/46, Warszawa 02-668, Poland 2. Military University of Technology, Institute of Applied Physics, ul. Kaliskiego 2, Warszawa 00-908, Poland 3. Polish Academy of Sciences, Institute of Physics, al. Lotników 32/46, Warszawa 02-668, Poland

E-mail: krystyg@ite.waw.pl

InGaAsSb compounds lattice-matched to GaSb substrate could potentially be used in a variety of optoelectronic devices operating in mid-infrared domain. Recently, thermophotovoltaic devices (TPV) based on InGaAsSb active layer attract increased attention. In this context, the optimisation of InGaAsSb/AlGaAsSb structures is of special concern.

The aim of this work is the optimisation of the designs to create the best structure for GaSb-based TPV cells, specifically with respect to comparison between p-n InGaAsSb homojunctions vs. p-n InGaAsSb/AlGaAsSb heterojunctions, and p-on-n vs. n-on-p cell configurations.

InGaAsSb/AlGaAsSb structures were grown by liquid phase epitaxy (LPE) technique in horizontal sliding boat system with Pd-diffused hydrogen atmosphere. The substrates for LPE growth were n- and p-type GaSb wafers, with the concentration of $n \sim 4 \cdot 10^{17} \text{ cm}^{-3}$ and $p \sim 5 \cdot 10^{18} \text{ cm}^{-3}$, respectively. 6N Ga, In, Sb and undoped GaAs were used as source materials and 6N Te as a dopant. The processes were performed at temperatures $T \sim 530^\circ\text{C}$ and $T \sim 593^\circ\text{C}$, at the cooling rate $R = 0.5^\circ\text{C/min}$. The post-growth characterisation included morphological and compositional analysis using AFM, TEM, EPXMA, and SIMS as well as transport measurement using van der Pauw and C-V methods.

The mesa-type devices with mesa size of $1\text{mm} \times 1\text{mm}$ were formed using photolithography and reactive ion etching in BCl_3 plasma. AgTe/Cr/Au and Au/Zn/Au metallizations were applied for backside n-type and front p-type ohmic contacts, respectively. The photodiode performance was established by measurements of the current-voltage characteristics, quantum efficiency, and spectral responsivity at 300 K. The relative photoresponse spectra were measured with a transimpedance amplifier coupled to a Fourier transform infrared (FTIR) spectrometer.

The most promising results have been obtained with 3-layer n-GaSb/n-GaInAsSb/p-GaAlAsSb heterostructure grown on n-GaSb substrate, characterized by quantum efficiency $\eta = 0,55$ and responsivity $R_1 = 0,85 \text{ A/W}$ @ $\lambda = 2,0 \mu\text{m}$.

Part of the research was supported by the grant no. 3 T11B 00926 from the Ministry of Education and Science.

19:00	Poster	P229
-------	--------	------

Photothermal investigations of SiC thermal properties

Krystyna Golaszewska¹, Eliana Kaminska¹, Anna Piotrowska¹, Jerzy Bodzenta², Anna Kazmierczak-Balata², Monika Pyka², Hacene Lahreche³, Robert Langer³, Philippe Bove³

1. Institute of Electron Technology (ITE), al. Lotników 32/46, Warszawa 02-668, Poland 2. Silesian University of Technology, Institute of Physics, Krzywoustego 2, Gliwice 44-100, Poland 3. Picogiga Int., Place Marcel Rebuffat, Parc de Villejust, Courtabouef 91960, France

E-mail: krystyg@ite.waw.pl

The thermal conductivity is a fundamental material property what is particular important in high-power/high-frequency microelectronic devices since the ability to dissipate heat is often the limiting factor that determines device performance. The new generation of microwave power devices will be with no doubt AlGaN/AlN high elec-

tron mobility transistors owing to their excellent high power handling capacity in high frequency operations. One of the major factors limiting the power performance and fabrication costs of these devices is the substrate material. Conventional sapphire and bulk silicon substrates come no longer into consideration because of low thermal conductivity. High-quality GaN-based epitaxial structures can only be grown on SiC or GaN substrates, which are expensive and limited in size. One possibility of reducing the wafer cost is the use of polycrystalline material. A novel approach recently proposed within the EC-funded HYPHEN Project (<http://www.hyphen-eu.com>) relies on the use of composite substrates made of thin single crystal "seed layer" transferred on the top of a thick semi-insulating polycrystalline material with efficient thermal dissipation.

SiC is a good thermal conductor, but thermal properties of SiC strongly depend on its crystal structure. Additionally, dopants cause decreasing of the thermal conductivity. Therefore, there is a need of having exact data on thermal diffusivity of various type of SiC (mono-, polycrystalline, doped), since the available literature and catalogue data present large discrepancy.

In this work we present the application of photothermal technique to determine thermal diffusivity α and thermal conductivity κ of polycrystalline 3C-SiC and, for comparison, monocrystalline 4H and 6H SiC. The applied method is based on generation of temperature field disturbance in the sample by modulated light beam and detection of harmonic component of the temperature over and under investigated sample. The probing beam from He-Ne laser is running parallel to the sample surface and is periodically deflected on the temperature field disturbance. This deflection is related to the thermal properties of the sample. The analysis consisting in fitting of theoretical curves which are the solution of the heat conduction equation to the dependences of the amplitude and the phase of the experimental signal on modulation frequency allows determination of the thermal diffusivity of the sample. The specific heat was determined using Differential Scanning Calorimeter DSC 1000.

We show, that thermal diffusivity of polycrystalline SiC wafers is on the level of $0.2 \text{ cm}^2 \text{ s}^{-1}$ and this result conforms to the thermal conductivity κ of $50 \text{ W m}^{-1} \text{ K}^{-1}$. For comparison, measured thermal diffusivity of monocrystalline 4H and 6H SiC were $0.6 - 0.9 \text{ cm}^2/\text{s}$ ($\kappa = 130 - 195 \text{ W m}^{-1} \text{ K}^{-1}$) and about $1.7 \text{ cm}^2 \text{ s}^{-1}$ ($\kappa = 373 \text{ W m}^{-1} \text{ K}^{-1}$), respectively.

Part of the research was supported by the grant from EC HYPHEN Contract Number: FP6-027455 and by the grant 3T11B 042 30 from Ministry of Science and Information Society Technologies, Poland.

19:00	Poster	P230
-------	--------	------

Liquid phase growth and characterization of laterally overgrown GaSb epitaxial layers

Danuta Dobosz¹, Aleksandra Czyzak¹, Jarosław Domagała¹, Zbigniew R. Zytkeiwicz¹, Krystyna Golaszewska², Magdalena Czapkiewicz¹, Tadeusz T. Piotrowski²

1. Polish Academy of Sciences, Institute of Physics, al. Lotników 32/46, Warszawa 02-668, Poland 2. Institute of Electron Technology (ITE), al. Lotników 32/46, Warszawa 02-668, Poland

E-mail: krystyg@ite.waw.pl

Epitaxy of GaSb based structures is of current scientific and technological interest due to their applications as optoelectronic materials in the mid-IR wavelength range, e.g. in photovoltaic and thermophotovoltaic devices. Some designs of such devices require monocrystalline epilayers grown over amorphous films that could further play a role of buried mirrors for photon recycling and/or be used as buried electrical contacts. Thus, there is a widespread interest in developing techniques which allow the growth of high quality semiconductor structures over insulating or electrically conductive films. Epitaxial lateral overgrowth (ELO) might be the technique of choice.

Epitaxial growth by ELO takes place on a substrate covered by a thin amorphous masking film in which a grating of narrow mask-free seeding windows is opened (see [1] for a review). The growth begins exclusively inside the windows, proceeds in a direction normal to the substrate and then continues in lateral direction over the mask. Finally, new epitaxial layer fully covers the masked substrate if growth is long enough for coalescence of adjacent ELO stripes.

In this report our recent results on ELO growth of GaSb layers on (100) GaSb substrates by the liquid phase epitaxy (LPE) are presented. We show that the aspect (width/thickness) ratio of the layers depends strongly on LPE growth conditions. In particular, silicon doping has been found crucial for successful lateral overgrowth of GaSb. The aspect ratio of the layers increases significantly with amount of silicon introduced to the melt up to the limit determined by silicon solubility in the Ga-Sb liquid solution. The results obtained allowed us to optimize the growth procedure, so the GaSb ELO layers with aspect ratio as large as 15 were obtained. Full coverage of the substrate with a new epitaxial layer is obtained when the spacing between the ELO seeding windows is reduced from 500 μm to 100 μm .

Substrates masked with a thin layer of electrically conductive ZrN or insulating SiO_2 were used. Perfect growth selectivity was obtained in both cases. Moreover, a high electrical conductivity of ZrN was preserved after LPE growth that is especially important if the ZrN mask is to be used as buried electrical contact in GaSb devices made of ELO structures.

Crystallographic perfection of the layers was studied by defect selective etching and high resolution x-ray diffraction. We show that substrate dislocations are efficiently blocked by the masking film and laterally overgrown parts of the layers (wings) are nearly dislocation-free despite a high density of dislocations in the substrates used. Also x-ray diffraction reciprocal space maps prove high crystallographic quality of laterally overgrown GaSb.

Downward tilt of ELO wings, the effect commonly observed in many other ELO structures was negligible in the GaSb layers grown on SiO_2 -masked substrates. This finding is explained as being due to low LPE growth temperature of GaSb. However, some residual wing tilt was found in the layers grown on ZrN-masked substrates.

Acknowledgements: This work was partially supported by the Polish Committee for Scientific Research under grants 3T08A 021 26 and 3T11B 00 926.

[1] Z.R. Zytkeiwicz, Thin Solid Films 412 (2002) 64.

19:00 Poster P231

Investigation of $\text{Ga}_{1-x}\text{In}_x\text{Sb}$ crystals growth by Czochralski method

Andrzej Hruban, Stanisława Strzelecka, Waław Orłowski, Andrzej Materna, Marta Pawłowska

Institute of Electronic Materials Technology (ITME), Warszawa 01919, Poland

E-mail: hruban_a@itme.edu.pl

$\text{Ga}_{1-x}\text{In}_x\text{Sb}$ bulk crystals are important material for thermo-photo-voltaic devices and sensors in the infrared region 1,7-6,8 microns. They can be also applied as high quality substrates for optoelectronic multicomponent and multilayer $\text{A}^{\text{III}}\text{B}^{\text{V}}$ epitaxial structures, allowing to overcome the lattice mismatch problems.

In this study the growth conditions of $\text{Ga}_{1-x}\text{In}_x\text{Sb}$ single crystals by Czochralski method were investigated. The big difficulties in crystallization of such $\text{A}^{\text{III}}\text{B}^{\text{V}}$ ternary compounds from the melt are connected with constitutional supercooling, wide separation between solidus and liquidus and differences of the distribution coefficient of components.

Crystal growth experiments were carried out from $\text{Ga}_{1-x}\text{In}_x\text{Sb}$ melt with increasing In contain up to 35at%. Especially, influence of pulling rate and liquid phase composition on monocrystalline growth was investigated. Crystals were grown in pure H_2 atmosphere in [111] direction, using GaSb and/or $\text{Ga}_{1-x}\text{In}_x\text{Sb}$ seeds. With increasing In contain in the melt, pulling rate was decreasing from 15mm/h up to 1mm/h. As result single crystals with dimensions length - (80-150)mm, diameter - (10-25)mm and In contain up to 6% were obtained.

The following methods were used for evaluation of obtained crystals properties:

- Wavelength Dispersion Spectroscopy and photoluminescence methods (indium contain and distribution).
- Hall measurements (electrical parameters).
- Chemical etching and Nomarski microscope observation and scanning microscopy (structure perfection).

19:00 Poster P232

CCVD Growth of 1-D Crystalline Carbon Nanostructures

Andrzej Huczko, Hubert Lange, Marta Domańska, Michał Bystrzejewski

Warsaw University, Faculty of Chemistry, Pasteura 1, Warszawa 02-093, Poland

E-mail: ahuczko@chem.uw.edu.pl

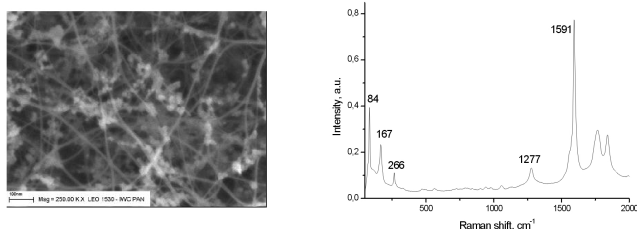
The carbon nanotubes (CNTs) can be classified as the 1-D crystals. The catalytic chemical vapor deposition (CCVD) and carbon arc plasma sublimation of graphite are at present the most explored ways of CNTs production on a large scale. Whether the products are single- or multi-walled carbon nanotubes (SWCNTs and MWCNTs, respectively) it depends on the selection of the catalyst and process

conditions. In the case of the CCVD method the starting carbon bearing materials also play a crucial role for the final product. In fact, there is a large variety of liquids and gaseous hydrocarbons that can be used for efficient CNTs synthesis.

The objective of this work was the synthesis of the SWCNTs from ferrocene aliphatic alcohol solutions by the CCVD method. The influence of alkyl chain length on the SWCNTs synthesis was investigated. The alcohols were injected to the reactor, a quartz tube placed in a furnace, in the liquid phase or as an aerosol. The carrier gas was Ar. The feeding rate, digitally controlled, was varied between 0.1 and 3 ml s⁻¹. Also the temperature distribution along the furnace was the variable parameter.

The morphology of the obtained products were investigated by scanning and transmission electron microscopy (SEM and TEM, respectively). The quality of the CNTs were also analyzed by using the Raman spectroscopy.

An example of SEM image and Raman spectrum of SWCNT product obtained from pentanol are shown in figure below, left and right respectively.



Acknowledgment

This work was supported by the Ministry of Science and Education through the Department of Chemistry, Warsaw University under Grant No. N204 096 31/2160.

19:00	Poster	P233
-------	--------	------

Compensating defect centers in semi-insulating 6H-SiC

Paweł Kamiński¹, Roman Kozłowski¹, Marcin Miczuga², Michał Pawłowski^{1,2}, Michał Kozubal¹, Jarosław Żelazko¹

1. Institute of Electronic Materials Technology (ITME), Wólczyńska 133, Warszawa 01-919, Poland 2. Military University of Technology (WAT), Kaliskiego 2, Warszawa 00-908, Poland

E-mail: Pawel.Kaminski@itme.edu.pl

High-resolution photoinduced transient spectroscopy (HRPITS) has been applied to studying electronic properties of point defects associated with the charge compensation in semi-insulating (SI) 6H-SiC substrates. The photocurrent relaxation waveforms were digitally recorded in a wide temperature range of 20 – 700 K and in order to extract the parameters of defect centers, a new computational procedure was implemented. It involves a two-dimensional analysis of the waveforms as a function of time and temperature using the correlation procedure or inverse Laplace algorithm. As a result, a set of waveforms is transformed into the spectral surface visualized in the three-dimensional space as a function of two variables: the temperature (T) and the emission rate (e_{γ}). Thus, the processes of thermal emission of charge carriers from defect centers are seen on the spec-

tral surface as the folds, the ridgelines of which give the temperature dependences of emission rate for detected defect centers. Each ridgeline is fitted with the Arrhenius equation and the activation energy E_a , as well as the pre-exponential factor A , related to the capture cross-section, are obtained. The fitting is carried out automatically by means of a neural network (NN) that creates the approximating surface and morphologically matches it to the shape of the fold corresponding to the defect center.

In this work, we have studied defect centers either in vanadium-doped or vanadium-free (undoped) SI 6H-SiC wafers. Vanadium atom ($3d^3 4s^2$) is an amphoteric impurity in SiC acting as a deep acceptor compensating shallow donors related to residual nitrogen atoms, as well as a deep donor compensating shallow acceptors associated with residual boron atoms. The resistivity of the V-doped wafer at 300 K was $\sim 1.0 \times 10^{10} \Omega \text{cm}$. In this material, five defect centers, labeled as TV1, TV2, TV3, TV4 and TV5, with activation energies of 0.08, 0.28, 0.43, 0.78 and 1.16 eV, respectively, were revealed. The centers TV1 (0.08 eV) and TV2 (0.28 eV) are likely to be attributed to the nitrogen donor and boron acceptor, respectively. On the other hand, the centers TV4 (0.78 eV) and TV5 (1.16 eV) are likely to be related to the vanadium acceptor (electron trap) $V^{3+/4+}$ and the vanadium donor (hole trap) $V^{5+/4+}$, respectively. The center TV3 (0.43 eV) can be assigned to a complex involving a vanadium atom and a native defect. The activation energy of dark conductivity equal to 1.26 eV indicates that the Fermi level in the V-doped 6H-SiC is located close to the deep level TV5 (1.16 eV). The resistivity of the undoped 6H-SiC wafer at 300 K was $\sim 3.0 \times 10^7 \Omega \text{cm}$. In this material, twelve defect centers, labeled as TU1-TU12, with activation energies ranging from 0.01 to 0.98 eV were detected. The activation energy of dark conductivity equal to 1.063 eV indicates that the Fermi level in the undoped 6H-SiC is located close to the deep level TU12 (0.98 eV). The origin of very shallow centers TU1 (0.01 eV), TU2 (0.02 eV) and TU3 (0.03 eV) is presently unclear. The experimental data reported so far on defect centers in 6H-SiC are also not sufficient for the identification of centers TU4 (0.09 eV), TU6 (0.11 eV) and TU10 (0.51 eV). However, the shallow centers TU5 (0.08 eV) and TU7 (0.130 eV) can be assigned to residual nitrogen atoms located in the hexagonal and cubic lattice sites, respectively. The center TU8 (0.53 eV) seems to be an electron trap related to the carbon vacancy and the center TU9 (0.63 eV) is presumably also an electron trap associated with the known defect center Z_1/Z_2 characteristic of both 4H- and 6H-SiC. The atomic configuration of the Z_1/Z_2 center, however, has not been established yet. On the other hand, the center TU11 (0.65 eV) can be identified with a hole trap assigned to a deep acceptor involving a boron atom and silicon antisite. The center TU12 (0.98 eV), responsible for the material high resistivity, is the predominant acceptor center compensating the shallow nitrogen donors. This center is likely to be attributed to a complex formed by intrinsic point defects including the isolated carbon and silicon vacancies, the Si antisite and the carbon vacancy-carbon antisite pairs.

19:00 Poster P234

Modeling of Silicon Carbide Semi-Insulating Properties

Oliwia M. Gąbka¹, Paweł Kamiński², Antoni Siennicki¹

1. *Warsaw University of Technology, Institute of Microelectronics & Optoelectronics (imio), Koszykowa 75, Warszawa 00-662, Poland* **2.** *Institute of Electronic Materials Technology (ITME), Wólczyńska 133, Warszawa 01-919, Poland*

E-mail: Pawel.Kaminski@itme.edu.pl

Silicon carbide is a wide bandgap semiconductor with the unique electrical and physical properties, including high breakdown voltage and excellent thermal conductivity. However, for the fabrication of a new generation of electronic devices operating at high power densities, high frequencies, and high temperatures, semi-insulating silicon carbide (SI SiC) wafers with a resistivity higher than $10^5 \Omega\text{cm}$ are necessary. These devices can be produced either by homoepitaxy (SiC MESFETs) or heteroepitaxy (GaN/GaAlN/GaN structures) on SI SiC substrates. The semi-insulating SiC crystals are obtained by compensating the residual shallow donors and acceptors with deep-level centers introduced either by vanadium doping or by controlled generation of native point defects. In such crystals, the Fermi level is pinned near the midgap to a partially ionized deep level. The former method is widely used for SiC bulk crystals grown by conventional physical vapor transport (PVT) technique. The latter one is more effective for the crystals of higher purity grown by high temperature chemical vapor deposition (HTCVD).

In this work, we show a very useful tool for simulating the electron and hole concentrations in 4H and 6H-SiC as a function of temperature, assuming the concentrations of the defects participating in the charge compensation, namely: the shallow donors, shallow acceptors and deep defect centers. The charge carrier concentrations, as well as the material resistivity are calculated in the temperature range between 50 and 800 K. The model is based on the numeric solution of the charge neutrality equation and determination of the Fermi level position for a given temperature. In the calculations, the temperature dependence of the bandgap energy is taken into account. On the grounds of the simulation results, the electrical properties of 4H and 6H-SiC correlated with the temperature changes in the Fermi level position for the nitrogen, boron and vanadium (or the native defect) concentrations in the range of 10^{15} - 10^{18} cm^{-3} are discussed. The modeling results are shown to be in a good agreement with the experimental data. The importance of the simulations for the optimization of the crystal growth processes aimed at obtaining the semi-insulating material is presented.

19:00 Poster P235

Crystallization of AgGaS_2 melts enriched with Ag_2S and Ga_2S_3

Konstantin A. Kokh¹, Elena F. Sinyakova¹, Anatoly A. Politov²

1. *Institute of Geology and Mineralogy SB RAS (IGM), Koptiyuga ave., 3, Novosibirsk 630090, Russian Federation* **2.** *Institute for Solid State and Mechanical Chemistry of RAS, Novosibirsk 630090, Russian Federation*

E-mail: k.a.kokh@gmail.com

Silver thiogallate (AgGaS_2) crystals have unique nonlinear optical properties. The crystals are usually grown from melts with starting composition lying on Ag_2S - Ga_2S_3 section since it is this part of Ag - Ga - S system which provides growth of high quality crystals [1]. It is accepted that there is a solid solution on the basis of AgGaS_2 with existence region ~ 1 -2 mol.% of Ga_2S_3 . In this work we consider experiments with directed crystallization of melts with slight deviation from stoichiometric composition of AgGaS_2 (in moles: 48% Ag_2S +52% Ga_2S_3 and 52% Ag_2S +48% Ga_2S_3). Two-zone synthesis procedure from Ag , Ga and S with nominal purity of 99.999% was the same as described in [2]. Synthesis and growth ampoules were sealed under 10^{-4} torr. Vertical Bridgman-Stockbarger technique was used for directed crystallization of the melts. Translation rate and axial temperature gradient at crystallization front was 2 mm/day and $\sim 3.5 \text{ deg C/mm}$, respectively. The change of melt composition was calculated for both experiments using measured chemical composition of the solid phase. Also the difference in unit cell parameters and luminescence spectra for AgGaS_2 grown from above described melts was found. We suppose these phenomena are due to different concentration of vacancies in grown crystals. Both mono-crystal samples and samples synthesized from elementary Ag , Ga and S were used for thermal analyses. Obtained data suggests that different ways of preparing the samples are responsible for defects concentration and thus for so wide range (70°C) of melting temperatures reported in scientific literature.

References:

1. Feigelson R. S., Route R. K., Recent developments in the growth of chalcopyrite crystals for nonlinear infrared applications, *Opt. Eng.*, 1987, v.26, N2, 113-119.
2. Zhao B., Zhu S., Li Z., Yu F., Zhu X., Gao D., Growth of AgGaS_2 single crystal by descending crucible with rotation method and observation of properties. - *Chi. Sci. Bull*, Vol. 46, No. 23, 2

19:00 Poster P236

Growth of $\beta\text{-Ga}_2\text{O}_3$ single crystal by μ -PD method and its characteristics

Ho Jun Lee¹, Tongik Shin¹, Joong Won Shur¹, Won young Song², Dae Ho Yoon^{1,2}

1. *Sungkyunkwan University, Department of Advanced Materials Engineering, 300 Cheoncheon-dong, Jangan-gu, Suwon 440-746, Korea, South* **2.** *Sungkyunkwan University, Sungkyunkwan Advanced Institute of Nanotechnology, 300 Cheoncheon-dong, Jangan-gu, Suwon 440-746, Korea, South*

E-mail: ejector@skku.edu

GaN has recently emerged as an important semiconductor for optoelectronic applications in light emitters and detectors. However, one of the serious problems impeding high quality GaN growth is the lack of a suitable lattice matched substrate. Sapphire is normally used as substrate to grow GaN, but lattice mismatch ($\text{GaN/Sapphire}=15\%$) and difference in the thermal expansion ($\text{GaN/Sapphire}=25.5\%$) between GaN and sapphire deteriorates the device performance and reduced its life-time. In order to provide an effective solution to this problem, the ideal situation would be the use of GaN substrate because of no difference in the lattice constant

and thermal expansion coefficient between GaN films and GaN substrate. Although there were several attempts to produce bulk GaN single crystal, it is very difficult to grow bulk GaN because of high temperature (1600°C) and gas pressure (10,000 atm) for GaN synthesis.

In present study, we grew β -Ga₂O₃ single crystal as a substrate by micro-pulling down (μ -PD) method for high quality GaN epitaxial growth. Even though β -Ga₂O₃ crystal does not have a hexagonal structure, hexagonal GaN can be fabricated on the surface of β -Ga₂O₃ single crystal using nitridation process. The chemical and structure characterization of β -Ga₂O₃ single crystal were confirmed by x-ray photoelectron spectroscopy (XPS) and high-resolution X-ray diffraction (HR-XRD).

19:00	Poster	P237
-------	--------	------

Comparison of gettering capability of various extrinsic techniques and enhancement of gettering ability of polycrystalline silicon layers

David Lysacek, Michal Lorenc, Lukas Valek

ON SEMICONDUCTOR Czech Republic, Roznov p.R. 75661, Czech Republic

E-mail: david.lysacek@onsemi.com

Treatments of semiconductor wafer backside such as deposition of polycrystalline silicon layers or quartz back side damage (BSD) have been used for removing unwanted impurities from the device area already for about 30 years. Solubility of heavy metals in the polycrystalline silicon or in the disturbed backside layer at a high temperature is generally more than an order of magnitude higher than in the silicon substrate. Polycrystalline layer and BSD region are preferably occupied by metals such as copper, nickel or iron and so enhance the gettering capability of the semiconductor wafer.

In this work, gettering capability of silicon wafers with various back side treatments was measured by the Method of Controlled Contamination (MCC) prior and after high temperature annealing. The principle of the method is comparison of haze formed by various metal concentrations. The measurements were carried out on (100) 4" polished silicon wafers heavily doped with antimony. Bare silicon wafers were compared with wafers with polycrystalline silicon layer, BSD, or both.

During the high temperature process the polycrystalline layer partially recrystallizes and thus loses a great part of its gettering capability. Using the MCC we found that its gettering ability after annealing at 1100°C decreased by about 1.5 orders of magnitude. The polycrystalline layer experiences several high temperature steps during the device fabrication process. After each annealing the grain size of polycrystalline silicon layer significantly increases and this results in the loss of gettering sites and consequently decrease in the gettering capability. The solubility of metals in the annealed layer is going to be close to their solubility in the crystalline substrate.

In order to solve this undesirable phenomenon we have developed a multilayer system consisting of a number of alternating polycrystalline silicon – silicon dioxide layers. Utilization of the multilayer system for backside gettering as well as the idea of its function is the subject of US Patent proceedings. Fig. 1 shows the comparison of

gettering capability of the common polycrystalline silicon layer and the multilayer system measured by MCC method before and after high temperature annealing (3 hours at 1100°C). The resistance of the multilayer system against the loss of its initial gettering capability due to high temperature annealing is demonstrated and discussed in the paper.

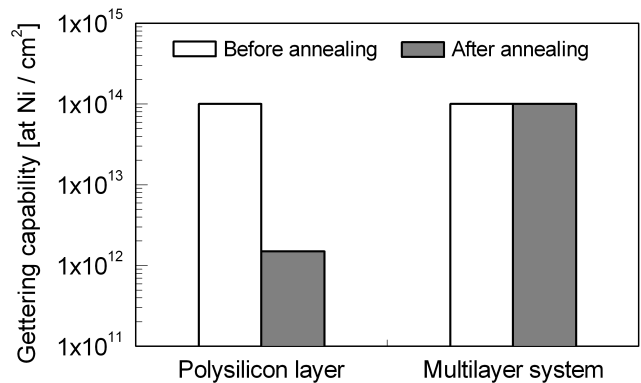


Fig. 1. Gettering capability measured by MCC before and after annealing at 1100°C for 3 hours.

19:00	Poster	P238
-------	--------	------

Pressure estimation in quartz ampoule in during InP synthesis by HGF method, on the base temperature distribution measurement.

Andrzej Materna¹, Zbigniew Rudolf², Marek Orzyłowski²

1. Institute of Electronic Materials Technology (ITME), Wólczyńska 133, Warszawa 01-919, Poland 2. Industrial Institute of Electronics (PIE), Długa, Warszawa 00-241, Poland

E-mail: amat@itme.edu.pl

The aim of this work was the estimation of P pressure during InP synthesis process, by HGF (Horizontal Gradient Freeze) method in quartz reactor. It was done in high pressure, multizone computer control furnace. Design of the furnace and P pressure control in quartz reactor by temperature profile control in furnace are described. Results of temperature measurements in phosphorus zone of reactor and their influence on evaporation dynamics are desired to obtain safety process of InP synthesis.

19:00	Poster	P239
-------	--------	------

Optimization of ultra-thin silicon wafers polishing process.

Artur Miros¹, Bronisław Piątkowski, Barbara Surma^{2,3}, Dariusz Litwin, Jacek Galas, Stefan Sitarek

1. Institute of Electronic Materials Technology, Silicon Department (ITME), Wólczyńska 133, Warszawa 01-919, Poland 2. Institute of Electronic Materials Technology (ITME), Wólczyńska 133, Warszawa 01-919, Poland 3. Institute of Electron Technology (ITE), al. Lotników 32/46, Warszawa 02-668, Poland

E-mail: artumik@poczta.onet.pl

The ultra – thin 2 inch diameter silicon wafer (111)-H(1x1) is necessary for a mirror focusing He-atom beam in a scanning atom micro-

scope. The purpose of this paper is elaboration of technology to obtain 2 inch ultra – thin silicon wafers (111) which have 50 mm thickness with thickness distribution ± 1.5 mm and miscut value below 0.05 deg. Optimization and improvement of our production technology enabled to make thin wafers which met these strict requirements. Due to the research and the implementation of these results we had got more yield from each work batch. The decisive and crucial factor in polishing process was getting of desirable shape of the wafers. Introduction of special tools to this process enabled to get much better geometry of this wafers. A satisfactory shape of both sides of these wafers, very good thickness distribution below 3 mm and very good quality of silicon surfaces have been obtained.

19:00	Poster	P240
-------	--------	------

Stress - mediated solid phase epitaxial re - growth of a-Si at annealing of Si:Mn

Andrzej Misiuk¹, Adam Barcz¹, Artur Wnuk², Jadwiga Bak-Misiuk³

1. Institute of Electron Technology (ITE), al. Lotników 32/46, Warszawa 02-668, Poland **2.** Institute of Electronic Materials Technology (ITME), Wólczyńska 133, Warszawa 01-919, Poland **3.** Polish Academy of Sciences, Institute of Physics, al. Lotników 32/46, Warszawa 02-668, Poland

E-mail: misiu@ite.waw.pl

Ion-beam-induced formation of amorphous silicon (a-Si) and its solid phase epitaxial re-growth (SPER) during annealing of implanted single crystalline silicon (c-Si) have attracted significant interest because of their importance for fabrication of Si devices [1]. SPER of a-Si depends, among others parameters, on processing temperature (HT) and pressure (HP) [2].

The structures prepared by implantation of Cz-Si with some metallic ions and annealed under HP have been reported to indicate interesting magnetic properties, of possible application in spintronics [3 - 5]. The HT - HP treatment of Si implanted with manganese (Si:Mn) affects its microstructure and magnetic ordering in a specific way [3, 5]. This motivated us to perform detailed investigation of the effect of HP applied at annealing of Si:Mn on its properties, related to SPER of a-Si.

Mn⁺ ions were implanted at room temperature with doses, $D = 2 \times 10^{15} - 1.2 \times 10^{16} \text{ cm}^{-2}$ and energy, $E = 160 \text{ keV}$, into (001) oriented p-type Czochralski grown silicon (Cz-Si). The Si:Mn samples were processed in Ar atmosphere for up to 10 h at up to 1400 K under HP up to 1.2 GPa. The depth distribution of Mn was investigated by Secondary Ions Mass Spectrometry (SIMS). Photoluminescence (PL) and X-Ray measurements were applied to determine the sample microstructure.

Mn⁺ implantation produces a-Si near the implanted ions range ($R = 140 \text{ nm}$), up to about 0.25 mm depth. The PL spectra of p⁺-implanted samples are featureless confirming complete amorphisation of the near – surface layer of Si:Mn.

SPER of a-Si is strongly dependent on implanted dose, on HT, processing time (t) and HP. Processing of the Si:Mn samples ($D = 2 \times 10^{15} \text{ cm}^{-2}$) for $t = 1 \text{ h}$ at 870 - 1000 K, both under 10^5 Pa and 1.2 GPa, results in the sharp minimum in Mn concentration at $\sim 150 \text{ nm}$

depth below the surface. SPER results in the movement of the a-c interface towards the surface. Since the solubility of Mn in c-Si is low, this re-crystallization expels Mn atoms from the re-growth region and the a-c interface moves toward the surface. The excess Mn atoms are accumulated at the a-c interface and so, depending also on the D value, the Mn concentration reach to a point, at which re-crystallization can not push longer excess Mn out of c-Si.

In the case of processing at 1070 – 1170 K, the a-Si is converted in part into polycrystalline material (as confirmed by X-Ray and PL measurements) while manganese silicides (such as Mn_4Si_7 [6]) are formed.

In Si:Mn prepared by high dose implantation ($D = 1 \times 10^{16} \text{ cm}^{-2}$) and processed at $\sim 1170 \text{ K}$, the effective out-diffusion of Mn to the Si:Mn surface increases with uniform stress applied; SPER and the Mn distribution are strongly dependent on p and t.

Our results help in understanding the mechanisms of SPER and, in the particular case of Si:Mn, suggest a new route to prepare, by the appropriate HT – HP treatment, the specific Si-Mn materials belonging to the Diluted Magnetic Semiconductor family.

[1] L. Pelaz, L.A. Marguez, J. Barbolla, J. Appl. Phys., 96 (2004) 5947.

[2] A. Misiuk, B. Surma, J. Bak-Misiuk, Solid State Phen., 108-109 (2005) 351.

[3] A. Misiuk, J. Bak-Misiuk, B. Surma, W. Osinniy, M. Szot, T. Story, J. Jagielski, J. Alloys Comp., 423 (2006) 201.

[4] A. Misiuk, L. Chow, A. Barcz, B. Surma, J. Bak-Misiuk, P. Romanowski, W. Osinniy, F. Salman, G. Chai, M. Pruszczyk, A. Trojan, in: High Purity Silicon 9, Eds: C.L. Claeys, R. Falster, M. Watanabe, P. Stallhofer, ISBN 1-56677-504-3, 2006, p. 481.

[5] A. Misiuk, B. Surma, J. Bak-Misiuk, A. Barcz, W. Jung, W. Osinniy, A. Shalimov, Mater. Sci. Semicond. Process., 9 (2006) 270.

[6] U. Gottlieb, A. Sulpice, B. Lambert-Andron, O. Laborde, J. Alloys Comp. 361 (2003) 13.

19:00	Poster	P241
-------	--------	------

Pulsed Laser Deposition of High Quality ZnTe Films Intended for Creating Low-Dimensional Semiconductor Heterostructures

Viktor K. Savchuk¹, Bohdan K. Kotlyarchuk¹, Rostyslav I. Lesyuk¹, Maciej Oszwaldowski²

1. Institute of Applied Problems of Mechanics and Mathematics (IAPMM), 3B Naukova Str., Lviv 79060, Ukraine **2.** Poznań Technical University, Institute of Physics (PUT), Nieszawska 13a, Poznań 60-965, Poland

E-mail: vikosav@iapmm.lviv.ua

Rapid progress in developing the producing technologies of semiconductor structures during the last years has enabled researchers to create structures with low-dimension scales (a few nanometers). In this case, the quantum properties of current carriers in such semiconductor structures play key role for determination of their main parameters. Such semiconductor heterostructures can be designed from semiconductor thin films with submicron thickness. However, the principal limitations of the traditional technologies do not enable the

growing of semiconductor heterostructures with: a detailed control of the stoichiometrical composition; high crystalline quality at a significantly lowered substrate temperature; narrow and well-defined profiles between separate films. Moreover, the ratio "cost/efficiency" is the main technological impediment to progress in the development of technological methods, in the creation of future generations of the elemental base for nanoelectronics, and in the production of atom/molecule scale components. One of the motivations of this research is the development of effective, low-cost and competitive growth technology on the basis of the Pulsed Laser Deposition (PLD) method. It enables to produce a low-dimensional semiconductor heterostructures with the arrays of quantum dots. Such heterostructures can be based on the II-VI semiconductor thin films, where the electron-phonon interaction in three- and two-dimensions is three orders of magnitude stronger than seen in III-V semiconductor heterostructures. Among heterostructures based on II-VI semiconductor compounds, ZnTe/CdTe heterostructure has great potential applications to the realization of efficient lightemitting diodes (LEDs) and photodetectors (PDs), which can operate at higher temperatures in the spectral regions from visible to far-infrared. The ZnTe/sapphire systems can be used in future as complicant substrates for the deposition of CdTe films with submonolayer thickness with the purpose of creating the arrays of quantum dots. Therefore, investigation of the PLD technological conditions with the purpose of growing the high quality ZnTe films on sapphire substrates were carried out. We established that in depending on deposition conditions, PLD method allows to grow the ZnTe films with the rate up to 103 Å/sec. Such high instantaneous deposition rates also create an "effective vacuum" of a few orders of magnitude lower. This effect assists in protection of the growing films from impurity by atoms of residual gas of vacuum chamber. We testified that deposition rate is important process parameter, which has great influence on the film properties through the nucleation growth stages. The films were characterized by X-Ray Diffraction (XRD) technique, optical absorption studies, Transmission Electron Diffraction (TEM), the surface morphology and roughness was analyzed by atomic force microscopy (AFM). The thickness of the films was in the range of 0.3-1.5 µm. These XRD analysis and TEM images confirm the decisive influence of the substrate temperature on the quality of crystalline structure of films deposited by PLD method. From XRD measurements was determined the optimal substrate temperature that allows to grown the textured ZnTe thin films. From the optical absorption measurements it was observed that the band gap increased from 2.30 eV – 2.70 eV as the grain size decreased from 100 nm – 20 nm. The surface morphology of ZnTe films deposited at different deposition conditions was examined by AFM.

19:00	Poster	P243
-------	--------	------

Investigations of the dynamic of crystallization of Si-ELO layers by LPE

Jan M. Olchowik¹, Iwona Jóźwik^{1,2}, Sławomir Gułkowski¹, Krystian Cieślak¹

1. Lublin University of Technology, Institute of Physics, Nadbystrzycka 38, Lublin 20-618, Poland **2.** Laboratoire de Physique de la matière (LPM), INSA, 7 avenue capelle, Lyon 69621, France

E-mail: j.olchowik@pollub.pl

ELO (Epitaxial Lateral Overgrowth) is a method of epitaxial crystallization on partially masked crystalline substrate by dielectric layers. Before the growth the substrate is covered with the thin dielectric film and patterned by means of photolithography technique in order to form silicon opened windows. In the next step the epilayers are deposited, growing laterally and vertically over the dielectric cover. The main advantage of such an approach is that the masking film prevents the defects propagation present in substrate into the ELO layer. Such a method of crystallization allows to use the poor quality substrate in application to many electronic devices, especially for solar cells [1], diminishing the costs of their production. The morphology of the grown ELO epilayers depends on various factors, such as: crystallographic orientation of the substrate, type of technology, atmosphere in which the growth occurs, pattern of the mask, etc. [2].

This work presents the new results of analysis of the dynamic of crystallization of Si-ELO layers, obtained by means of Liquid Phase Epitaxy (LPE). LPE is the most suitable method of epilayers crystallization for PV applications because of economical reasons.

The investigated Si-ELO layers were grown in various conditions: using standard horizontal LPE apparatus as well as vertical one with the temperature gradient, various solvents and various P-t regimes.

[1] – J.M. Olchowik, Polish Patent Nr P.339396 (2006).

[2]. I. Jozwik, J.M. Olchowik, *The epitaxial lateral overgrowth of silicon by two-step liquid phase epitaxy*, J. Cryst. Growth 294 (2006) 367-372.

19:00	Poster	P244
-------	--------	------

Polishing of InAs without the use of Bromine

Joanna Pawłowska, Anna Ostapska

Institute of Electronic Materials Technology (ITME), Warszawa 01919, Poland Institute of Electronic Materials Technology (ITME), Wólczyńska 133, Warszawa 01-919, Poland

E-mail: Joanna.Pawlowska@itme.edu.pl

The most common compounds user for polishing indium based, AIIIBV semiconductor (InAs, InP, InSb) are based on bromine with methanol. Measurements by Atomic Force Microscope (AFM) and X-ray Photoelectron Spectrometer (XPS) demonstrate negative influence of bromine on microgeometry and chemical purity of surface of standard InAs substrates (2" diameter; 400±25µm in thickness). As a superior alternative to bromine polishing we introduced two slurry system using acidic and alkaline reagents, simultaneously but separately applied on a polishing pad. With this method InAs substrates with Ra=0.1 nm of roughness and high chemical purity were obtained. The epi-layer test of such substrates, made by Hamamatsu-Japan, confirmed epi-ready status for wafers.

19:00 Poster P245

New mechanism of microcrystalline diamond formation through phase transition in spark discharge

Tetyana V. Semikina

Institute of Semiconductor Physics, NAS of Ukraine, Kiev, Ukraine (ISP), 45 pr. Nauki, Kyiv 03028, Ukraine

E-mail: tanyasemikina@rambler.ru

In this report the results of deposition of diamond particles with size 3-5 mm for 10 sec in spark discharge between two graphite rods of special shapes are presented. The process ran in hydrogen atmosphere (100 Torr) with different types of substrates: silicon, Al_2O_3 ceramics and non-alkaline glass under several variation of geometrical arrangement of substrates and graphite rods: distance between substrate and graphite rods was 5-10 mm with up and down position of substrates to graphite rods. The diamond nature of obtained particles was confirmed by sharp peak 1331 cm^{-1} in Raman spectrum and particles shape on scanning electron microscope images. Because the obtained growth rate of diamond particles in our process was higher than all known growth rates for process under low pressure we present our physical hypothesis of formation mechanism running in our experiment.

To elucidate the formation mechanisms our substrates were cut along in the place of diamond particles position by focused Ga ion beam. From the obtained scanning ion microscope (SIM) image it is evidence that diamond particle formation doesn't run on the substrate because the diamond particles are contiguous to surface of substrate only by corner. For comparison the SIM image of diamond particles formation running in chemical vapour deposition (CVD) process confirms that nucleation and follows growth occurs on the substrate surface. We suggest that in our process the diamond particles formation runs in the contact place of graphite rods where the high electric magnetic field and high temperature take place. The next suggestion is that diamond particles formation is not the result of chemical reaction between ionized carbon and hydrogen and their atoms because the reaction time (less than 10 sec) is evidently not enough for growing such big particles as we have (3-5 mm). That is why we decide that obtained diamond particles are the result of new phase transferring such as: solid state graphite rod @ melt carbon @ diamond particles. The hydrogen role in running process is analyzed. For this elucidating some experiments were carried out without hydrogen at pressure ~ 0 Torr. As a result was only graphite and diamond particles were not observed. Hydrogen plays some important role of energy transferring.

The next argument that diamond particles are not the result of chemical reaction is the fact that presence or absence of diamond particles on the substrate depends on graphite shape rods. We get diamond particles only in the case when graphite rods have sharper contact ends that consequently provided the biggest value of electromagnetic field in the contact place.

We conclude that diamond formation is the result of physical process under the conditions of high pressure and temperature that could be realised in local area of spark discharge.

Keywords: Spark Diamond, Spark Discharge, Hydrogen Atmosphere, Physical Formation

19:00 Poster P246

Nanostructural "cauliflower-like" diamond deposited in HFCVD closed system

Tetyana V. Semikina

Institute of Semiconductor Physics, NAS of Ukraine, Kiev, Ukraine (ISP), 45 pr. Nauki, Kyiv 03028, Ukraine

E-mail: tanyasemikina@rambler.ru

Nanostructural "cauliflower-like" diamond particles were obtained by hot filament chemical vapour deposition (HFCVD) methods from vapour of liquid carbon sources (acetone, butyl alcohol and ethanol) and hydrogen-rich atmosphere in closed system. The pressure of vapour of carbon liquid sources was changed from 3 to 10 Torr but the hydrogen pressure varied in wide range 294 – 600 Torr to investigate the influence of hydrogen and total pressure on running process. The process was carried out on two types of substrate: silicon and Al_2O_3 ceramics to determine the role of substrate on process of nanodiamond formation. Time of deposition included 5, 7, 10, 30 min.

Thus the novelty of our experiment based on the fact that nanostructural diamond was deposited in closed HFCVD system from vapour of liquid carbon sources in hydrogen atmosphere without argon on Si and Al_2O_3 ceramics substrates.

Cauliflower like diamond particles were obtained from all types of carbon liquid sources on Si substrate and from vapour of acetone on Al_2O_3 ceramics substrate. The diamond particles were characterized using field-emission scanning electron microscopy (SEM) and micro-Raman spectroscopy. Raman spectrum exhibits a first-order diamond peak centred at $1330\text{-}1332\text{ cm}^{-1}$. For all samples it was observed the wide signals in the range at $1400\text{-}1600\text{ cm}^{-1}$ that testify graphite presence during the deposition process. For example SEM image of obtained diamond particles deposited on Al_2O_3 substrates for 30 min demonstrates that size of second diamond particles forming cauliflower particles varies from 70 nm to 1.4 mm. In experiment under deposition time 10 min for this type of substrate the size of second diamond particles was lesser (50-70 nm). For deposition on Si substrate the clear dependence between process time and size of second diamond particles was not observed.

Because the total pressure was varied in wide range and we deposited the nanostructural diamond for all total pressure variation we assume that ability to get the nanodiamond is not very sensible to total pressure. The dependence between size of nanodiamond and total pressure should exist. We observed that decreasing of total pressure leads to reduction of cauliflower-like diamond size and consequently secondary diamond particles formed it. The detailed analysis of hydrogen and hydrogen pressure influence will be presented.

We consider that one from the main technological parameters leading to nanodiamond formation is temperature of space near substrate and on the substrate surface. The substrate in our experiment was heated gradually and the substrate temperature controlled from backside by thermocouple rose from 30 to $700\text{-}780\text{ }^\circ\text{C}$ rather fast. But the processing temperature near the surface substrate probably reached the value $1200\text{ }^\circ\text{C}$ that is the temperature for second diamond particles formation. The process temperature was observed with two-coloured pyrometer (CHINO, IR-AQ and IR-GAG) and consequently we could not determine accurately the temperature

close to the substrate surface.

Thus it was found technological conditions allowed to deposit nanostructural diamond from liquid carbon sources of different types on Si and Al_2O_3 substrates that is new result approaching us to nanodiamond deposition industrial application.

Keywords: Nanostructural Diamond, Liquid Carbon Source, Hot Filament CVD

19:00 Poster P247

Spectroscopy of Cz-Si samples subjected to implantation and thermal treatment under enhanced hydrostatic pressure.

Evgeny Shemchenko¹, Alexander Yakovec¹, Rostyslav V. Shalayev¹, Victor M. Varyukhin¹, Anatoly Prudnikov¹, Boris M. Efros¹, Andrzej Misiuk², M. Prujsczyk²

1. National Academy of Sciences of Ukraine, A.Galkin Donetsk Institute for Physics & Technology (DonPTI NASU), Roza Luxemburg 72, Donetsk 83114, Ukraine 2. Institute of Electron Technology (ITE), al. Lotników 32/46, Warszawa 02-668, Poland

E-mail: sharos@mail.ru

Recent developments in the fields of integrated circuits, CD technology, and of transmission of large volume information resulted in still growing interest in optical and spectral properties of silicon - related materials, in particular produced basing on single crystalline Czochralski grown silicon, Cz - Si. Electronic states related to the presence of structural defects and impurities in Cz-Si - related materials [1] are still intensively investigated.

In the presented work, Cz - Si samples prepared by implantation with hydrogen (Si:H) or oxygen (Si:O), and processed at up to 1400 K (HT) under enhanced hydrostatic pressure in argon atmosphere (HP, up to 1.2 GPa) have been investigated. It has been shown that the HT - HP treatment of implanted samples leads to the formation of nano - clusters. The nano - dimensional structure formation in the samples results in turn in essential changes of optical and spectral properties, being dependent on the HT - HP processing parameters.

The mechanism and nature of nano - dimensional structure formation in implanted single crystalline silicon, especially in Si:H, subjected to complex processing [2, 3], and the effects of HT - HP treatment on spectral characteristics of Si:H and Si:O are discussed. Usefulness of such materials for producing of sensors has been demonstrated.

1. A. Misiuk, B.M. Efros. Pressure-induced transformations during annealing of silicon implanted with oxygen: Physics and Technology High Pressure, 16 (2006) 49.
2. A.M. Prudnikov, A. Misiuk, I.E. Tyschenko, B.M. Efros. Solid state transitions investigations in DAC by spectroscopy methods: Defect and Diffusion Forum, 208-209 (2002) 315.
3. W. Wieteska, W. Wierzchowski, W. Graeff, A. Misiuk, A. Barcz, L. Bryja, V.P. Popov: Acta Phys. Polon. A, 102 (2002) 239.

19:00 Poster P248

Comparison of conduction of Sr and/or Mg doped LaGaO_3 by using of density of electrons' states' diagrams and searching which one is better for SOFC's electrolyte.

Leila Shekari¹, Esmail Saievar iranizad¹, MohamadReza Abolhasani¹, Mahdi Gholampoor²

1. Tarbiat modares university, Tehran 0098, Iran 2. Emam Ali university, Tehran 0098, Iran

E-mail: Leila.shekari@gmail.com

In this study, we compare density of states' diagrams from LaGaO_3 , $\text{LaGa}_{0.75}\text{Mg}_{0.25}\text{O}_3$, $\text{La}_{0.75}\text{Sr}_{0.25}\text{GaO}_3$ and $\text{LaO}_{0.75}\text{Sr}_{0.25}\text{Ga}_{0.75}\text{Mg}_{0.25}\text{O}_3$. With this comparison, we saw that the conduction of LG by adding Sr & Mg was increased. We realized that there are 3 bands of electrons in all this materials. And they all have 2 band gaps. The first one is between core & valence bands and the second is between valence & conduction bands. If doped the gaps are changed & the the valence bands are moved to the Fermi energy then the conductivity will be increased. In other cases the gaps width are the same and therefore the DOS of conduction bands would be important for comparison of their conductivities. We know that these provskite type of materials are ionic conductors. In this study we plot their electrons' states for the total energy. These plots show that the higher density of states increases the conductivity, which means that these electrons are useful for making ions & holes. And notice the diagrams show that LGM, LSG, LSGM & LG have higher conductivity, respectively. Kuan-Zong Fung have measured it experimentally. And these properties will be beneficial for solid oxide fuel cell's electrolyte; because not only they are better conductor but also making them, will be cheaper; because Ga_2O_3 is more expensive than MgO & SrO . We know from 496 to 729²³ Centigrades (intermediate temperature) this order is true but in higher temperature it means from 729 to 973 degree centigrade (high temperature) it will be different. Because the conductivity equation is liner ($\ln \sigma T \approx 1/T$), so we guess this order will be true from zero to 729 Centigrades. Then these diagrams are for the interval between zero and 729 Centigrades.

19:00 Poster P249

The influence of Al_2O_3 substrate annealing effect for ZnO nanowires synthesis using VPE method

Tongik Shin¹, Ho Jun Lee¹, Won young Song², Sang Woo Kim³, Dae Ho Yoon^{1,2}

1. Sungkyunkwan University, Department of Advanced Materials Engineering, 300 Cheoncheon-dong, Jagan-gu, Suwon 440-746, Korea, South 2. Sungkyunkwan University, Sungkyunkwan dvanced Institute of Nanotechnology, 300 Cheoncheon-dong, Jagan-gu, Suwon 440-746, Korea, South 3. Kumoh National Institute of Technology School of Advanced Materials and System Engineering, 1 Yangho-dong, Guumi, Gyeongbuk, GuMi 730-701, Korea, South

E-mail: tongik@skku.edu

Nanostructures semiconductors have been attracting increasing at-

tention due to their exceptional properties, which are different from those of bulk and thin film materials. Especially, a compound, wide direct band gap semiconductor with a large exciton binding energy has received much attention due to the potential applications for the opto-electronics field. A GaN is interesting material with excellent properties. In spite of GaN good properties, the synthesis of the compound is very difficult. On the other hand ZnO was easily synthesized. Most of groups investigated vertical ZnO nanowires synthesis, using MOCVD, chemical synthesis, and anodic aluminum oxide (AAO) template method.

In this study, we grew vertical ZnO nanowires by VPE method. ZnO nanowires were synthesized at about 800-1000°C, using ZnO and C powder source. We used Au catalyst as a seed. Especially we studied annealing effect of substrate. In case when the substrate was annealed, the ZnO nanowires were synthesized vertically on the substrate. We confirmed hexagonal ZnO nanowires using XRD pattern. The shape of nanowires was examined by SEM and TEM. The chemical composition of nanowires was analyzed by EDX with high resolution.

19:00	Poster	P250
-------	--------	------

Optical and electrical characterization of kdp doped PbI₂ single crystal

Mohd Shkir

Jamia Millia Islamia (JMI), Jamia Nagar, new delhi, Delhi 110025, India

E-mail: shkirphysics@gmail.com

The PbI₂ material was purified using the vacuum zone refining technique, this technique was fabricated in our crystal growth laboratory. This material was grown as single crystal by using this technique. The conductivity and band gap was measured by using UV/VIS spectrophotometer; the band gap was measured as 2.5eV of purified material. The KDP was doped as 1-4% w/w in PbI₂ purified material. After doping of the pure KDP in vacuum zone refining material, the conductivity was also measured. We found that the conductivity increased after doping. The band gap of doped material was also measured using UV/VIS spectrophotometer, which decrease. The Growth mechanism was also studied after doping, the dendritic behavior of crystal was observed with the doping of KDP. After 4% doping of KDP dendritic behavior of crystal is changed.

19:00	Poster	P251
-------	--------	------

Numerical study of crucible bottom shape on the heat transport and fluid flow during the seeding process of oxide Czochralski crystal

Mohammad Hossein Tavakoli¹, Hermann Wilke²

1. Physics Department, Bu-Ali Sina University, Mahdiah street, Hamedan 65174, Iran **2.** Institute for Crystal Growth (IKZ), Max-born Str. 2, Berlin 12489, Germany

E-mail: mhtavakkoli@yahoo.com

For the seeding process of oxide Czochralski crystal growth, the influence of the crucible bottom shape on the heat generation, temper-

ature and flow field of the system and the seed-melt interface shape have been studied numerically using the Finite Element Method. The configuration usually used in a real Czochralski crystal growth process consists of a crucible, active afterheater, induction coil with two parts, insulation, melt, gas and seed crystal. At first, the volumetric distribution of heat inside the metal crucible and afterheater induced by the RF-coil was calculated. Using this heat generation in the crucible wall as a source the fluid flow and temperature field in the entire system as well as the seed-melt interface shape were determined. We have considered the two cases flat and rounded crucible bottom shape. It was observed that using a crucible with a rounded bottom has several advantages such as:

- The position of the maximum of heat generation at the crucible side wall moves upwards, compared to the flat bottom shape.
- The location of the temperature maximum at the crucible side wall rises and as a result the temperature gradient along the melt surface is increased.
- The streamlines of melt flow are parallel to the crucible bottom and have a curved shape similar to the rounded bottom shape. This way we do not have secondary flow usually observed in the crucible wall/bottom corner.

These important features lead to increasing thermal convection in the system and influence the velocity field in the melt and gas domain which helps preventing some serious growth problems such as spiral growth.

19:00	Poster	P252
-------	--------	------

Characterization of swift heavy ion induced modification on the nonlinear optical Benzimidazole (BMZ) single crystals

Kanagasekaran Thangavel¹, Mythili Prakasam¹, Srinivasan Padmanabhan¹, Vijayan Nn², Sharma Shailesh², Bhagavannarayana Gg, Saif Ali³, Pawankumar Kulriya³, Kanjilal Dd³, Gopalakrishnan Rengasamy¹

1. Anna university, chennai 600025, India **2.** National Physical Laboratory (NPL), Dr.K.S.Krishnan Road, Delhi 110012, India **3.** Inter University Accelerator Centre (IUAC), Aruna asaf ali marg, Delhi 110067, India

E-mail: kanagu_sekaran@yahoo.co.in

The 50MeV Si ion irradiation induced modifications on structural, dielectric, optical and mechanical properties of Vertical Bridgman grown Benzimidazole (BMZ) crystals have been studied. The high resolution X-ray diffraction studies show that amorphization increase on increasing fluence of ion irradiation. The dielectric constant and dielectric loss as a function of frequency and temperature are studied. The hardness behaviour of both irradiated and unirradiated crystals has been explained with indentation effects. UV-VIS studies reveal decrease in bandgap values on irradiation, is explained. The scanning electron micrographs show the collapse of the grain boundaries on irradiation.

1.INTRODUCTION

Optoelectronics and nonlinear Optics are expected to play a major role in photonics, which is emerging as a multidisciplinary new frontier of science and technology, capturing the imagination of scient-

ists and engineers worldwide. High energy heavy ion irradiation produces electronic excitation/ionization in solids, which leads to many changes in their properties. It is known that when an ion beam passes through matter, it causes damage, which depends on the type and the energy of the ion and the properties of the medium. It is generally pictured that atomic displacements are primarily induced by the elastic collisions and not by electronic excitation or ionization. However, slowing down of energetic heavy ions in insulator targets is known to induce structural changes called latent tracks¹, which result from atomic displacements in the material along the path of the ion. These atomic displacements in narrow column along the incident ion path are explained by coulomb expansion² or thermal spike³. In the present case, single crystals of BMZ were irradiated with 50MeV Si ions, which are capable of generating the modifications in the crystals. BMZ has the molecular formula of $C_7H_6N_2$ and crystallizes in orthorhombic crystal system. The high degree of symmetry of this crystal makes it suitable for investigation of its optical, mechanical, structural and dielectric properties. BMZ crystal is a potential material for NLO and scintillation detector and other related applications.

2. CRYSTAL GROWTH

The bulk single crystals of BMZ have been successfully grown by Bridgman technique using glass ampoule of length 22cm with wall thickness 1.2mm and necked portion is less than 1.5mm in diameter. The growth was performed with different ampoule configuration and the growth experiment was not successful when the wall thickness is less than the above thickness. The single zone resistive heating quartz furnace was used for growth so that insitu growth observation was possible during growth. The translation speed was 1mm/hr with temperature gradient of 2°C/cm. The grown crystals were 18cm in length and 1.8cm in diameter and the cut and polished crystal of BMZ is of 3cm in length (Fig.1). The BMZ crystals have been irradiated by 50MeV Si ion beam delivered from 15MV pelletron accelerator at IUAC, Delhi.

3.UV-VIS SPECTRAL STUDIES

Optical absorption studies performed on 50MeV Si ion irradiated BMZ crystals gives the spectral intensity of light transmitted through the specimen that determines the absorption edge, which is a measure of the bandgap. The absorption of light energy by organic materials in the ultraviolet and visible region involves promotions of electrons in σ , Π and n-orbital from the ground state to higher energy state. The electronic transitions (\rightarrow) that are involved in the ultraviolet and visible region are of the following types $\sigma \rightarrow \sigma$, $n \rightarrow \sigma$, $n \rightarrow \Pi$, and $\Pi \rightarrow \Pi^*$. The unirradiated BMZ crystal shows its characteristic peak at around 308nm, which is a $\Pi \rightarrow \Pi^*$ transition of the heteroatomic benzene ring. The characteristics peaks at 312nm and 318nm it are observed for irradiated BMZ crystals at fluences of 5×10^{11} ions/cm² and 5×10^{12} ions/cm², respectively. Fig.1 shows the absorbance with fluence on a log-scale at three different characteristic wavelengths of 308, 312 and 318nm. It may be concluded from the plot that the optical absorption increases (wavelength also increases) with increase of irradiation dose delivered to the BMZ crystals, resulting in higher concentration of defects. The broadening of absorption peak may be occurring due to increase in defect sites on SHI irradiation. The increase in absorption towards high wave number is an indication of high dc conductivity of BMZ crystal.

From the wavelength corresponding to the bandgap of material in

the absorbance curve a sudden rise in the absorbance is expected after irradiation. The threshold at which the absorption data showing abrupt rise is determined (graphically), this can be an indicative of the bandgap of material. Working on this hypothesis and equation (1) and utilizing the absorbance data (Fig.2), the wavelength threshold was determined by plotting tangents as shown in Fig.2

The values of bandgap determined were 6.07, 3.98 and 3.90 eV for unirradiated, irradiated at fluence of 5×10^{11} ions/cm² and 5×10^{12} ions/cm², respectively. The decrease in bandgap energy upon irradiation may be attributed to the creation of some intermediate energy levels due to structural rearrangements⁷, this can be inferred from the dielectric constant. The increase in absorbance can be explained by decrease in absorption co-efficient (α) on increasing the radiation dose. The absorption coefficient (α) of virgin and irradiated BMZ crystals was calculated by Mclean's formula.

Reference:

- (1) Prasad, P.N. and David, J.W., *Introduction to nonlinear optical effects in Molecules and Polymers*, John Wiley, New York, 1991.
- (2) Metha, G.K., *Physics Education*, 1994, 11-3, 245.
- (3) Lesueur, D. and Dunlop, A., *Radiat. Eff. Defects in solids*, 1993, 126, 163.

19:00	Poster	P253
-------	--------	------

Obtaining of semiconductor nanocrystals and formation of ensembles on their basis.

Yulia V. Yermolayeva, Neonila A. Matveevskaya, Alexander V. Tolmachev

Institute for Single Crystals NAS of Ukraine (ISC), 60 Lenin Ave., Kharkov 61001, Ukraine

E-mail: yermolayeva@isc.kharkov.ua

Semiconductor nanocrystals (NC) are intensively investigated as perspective materials in the field of laser technique, an optoelectronics, biology and medicine. Ensembles of semiconductor NC on substrate specially isolated from each other show an integrated size effect of energies quantization of the ground and the excited states of everyone NC separately, that is why they have interest in connection with an opportunity of making a new class of multifunctional materials for nano- and microelectronics.

In the present work nanocrystals PbS, CdS and ZnO the given size (2-10 nm) with a small dispersion in the sizes < 15 % has been grown up from water solutions by a method of the colloid synthesis and put on previously synthesized nanotemplates (the colloid particles SiO₂). The X-ray diffraction analysis has shown formation of NC PbS, CdS with a cubic structure and NC ZnO with wurtzite structure. The monodisperse silica nanoparticles of the spherical shape have been synthesized by the modified Stober method (diameter 120 and 350 nm with dispersion in the sizes < 10 %) and functionalized by organic molecules for maintenance of binding semiconductor NC on a nanotemplate surface (formation SiO₂/PbS, SiO₂/CdS, SiO₂/ZnO core-shell heteronanoparticles).

The technology of obtaining SiO₂/NC core-shell heteronanoparticles allows to control amount, diameter NC and their ordering on the spherical silica surface. Optical properties of received NC ensembles

have been investigated, quantum confinement effects in absorption spectra of nanocrystals PbS, CdS and ZnO ensembles have been shown. The optical band gap energy for each type of NC has been calculated from exciton peaks. It has been shown, that nanotemplate from the colloid silica particles does not influence on optical properties of obtained NC ensembles.

19:00 Poster P254

In situ investigation of growth kinetics of ammonium oxalate monohydrate single crystals in aqueous solutions containing metallic cation impurities

Keshra Sangwal¹, Kazimierz Wójcik, Jarosław Borec

Department of Applied Physics, Institute of Physics, Lublin University of Technology (LUT), Nadbystrzycka 38, Lublin 20-618, Poland

E-mail: k.sangwal@pollub.pl

During recent years the authors have investigated the kinetics of displacement rates of individual faces of ammonium oxalate monohydrate $[(\text{NH}_4)_2\text{C}_2\text{O}_4 \cdot \text{H}_2\text{O}]$ (AO) single crystals from aqueous solutions containing bi- and trivalent cationic impurities. However, displacement rates of different faces are a resultant of layer displacements on them, it is of interest to study the displacement rates of layers as a function of solution supersaturation and concentration of different impurities. The present work is addressed to this subject. Growth kinetics of growth layers was studied on the $\{110\}$ faces of specially prepared seeds of ammonium oxalate monohydrate (abbreviated as AO) crystals in a specially designed growth cell in which growth temperature was controlled to $\pm 0.05^\circ\text{C}$. Employing appropriate programmes and series of four photographs recorded by a digital camera in different growth experiments in a solution containing a known concentration c_i of a selected impurity at a constant growth temperature, the displacement rate in the $[00-1]$ direction of growth layers oriented along the $[-110]$ and $[-111]$ directions were determined. The experimental set up used earlier for growth kinetics was similar to that used for the study of the motion of steps on the $\{010\}$ faces of potassium acid phthalate single crystals. Using the values of the average displacement rate v of steps in the investigated supersaturation s interval, the kinetic coefficient β ($= dv/ds$) for step motion at different concentrations c_i of four impurities (i.e. Cu(II), Mn(II), Fe(III) and Cr(III)) was determined. The experimental data were analysed according to the theoretical dependence: $\beta/\beta_0 = 1 - \alpha K c_i / (1 + K c_i)$, where β_0 is the kinetic coefficient for impurity-free system ($\beta_0 = 2.55 \times 10^{-5}$ m/s), K is the Langmuir constant and α is the effectiveness parameter for an impurity. The values of constants α , K and differential heat of adsorption for different impurities are given in Table 1. As found from the data of impurity concentration dependence of face growth rates, Cu(II) and Fe(III) are practically ineffective in growth but Mn(II) and Cr(III) are effective growth inhibitors.

Table 1. Constants β_0 , α , K and Q_{diff}

Impurity	α (-)	K (-)	Q_{diff} (kJ/mol)
Cu(II)	1.0	5.8	4.4
Mn(II)	1.1	90	11.3

Impurity	α (-)	K (-)	Q_{diff} (kJ/mol)
Fe(III)	1.0	1.1	0.2
Cr(III)	0.95	1000	17.4

Acknowledgements. This work was financially supported by Ministry of Science and Higher Education under research project PB 1041/P03/2004/26. The authors also thank Dr E. Mielniczek-Brzóska for growing crystal seeds for this study.

19:00 Poster P260

Simulation of large sized silicon polycrystal growth by DS method added heat exchanger with the change of thermal parameter

Joong Won Shur¹, Jung Hoon Hwang², Youn Jea Kim², Dae Ho Yoon^{1,3}

1. Sungkyunkwan University, Department of Advanced Materials Engineering, 300 Cheoncheon-dong, Jangan-gu, Suwon 440-746, Korea, South 2. Sungkyunkwan University, School of Mechanical Engineering, 300 Cheoncheon-dong, Jangan-gu, Suwon 440-746, Korea, South 3. Sungkyunkwan University, Sungkyunkwan Advanced Institute of Nanotechnology, 300 Cheoncheon-dong, Jangan-gu, Suwon 440-746, Korea, South

E-mail: jwshur@skku.edu

The further development of the manufacturing processes of solar silicon ingot is one of the more important issues to guarantee the growth of the photovoltaic industry. The reason why is the saving of manufacturing costs of ingots, wafers, solar cells and of solar modules. Therefore, two of the main targets of the PV industry today are to increase the ingot weight and to accelerate the growing rate of polycrystalline solar ingots. One of the solutions to solve this issue is to make higher quality polycrystalline Si wafers capable of producing higher efficiency solar cells.

In this study, the directional solidification (DS) method added the heat exchanger was used to the growth of large sized polycrystalline Si ingot above 240°C . The use of heat exchanger has the advantages of the small heat loss, short cycle time and efficient directional solidification. The numerical simulation of the process is applied using a fluid dynamics model to simulate the temperature distribution. The changes of temperature in the DS equipment are simulated by variations of thermal parameters such as heating and cooling rate.

19:00 Poster P261

Preparation of the ZnO substrate surface

Paweł Skupiński¹, Krzysztof Graszka^{1,2}, Andrzej Mycielski¹, Elżbieta Łusakowska¹, Halina Sakowska²

1. Polish Academy of Sciences, Institute of Physics, al. Lotników 32/46, Warszawa 02-668, Poland 2. Institute of Electronic Materials Technology (ITME), Wólczyńska 133, Warszawa 01-919, Poland

E-mail: skupin@ifpan.edu.pl

ZnO is a material with a great potential for the applications in UV

light emitters, spin functional devices, gas sensors, transparent electronics and surface acoustic wave devices. Large bulk crystals are usually grown by the hydrothermal method. In our Institute we use a less expensive chemical vapor transport (CVT) method to grow ZnO crystals.

Very important factor, which drive the efforts to obtain large single crystals of zinc oxide is the possibility to use the ZnO wafers as substrates for homoepitaxy and epitaxial growth of GaN layers in MBE ammonia-free methods. ZnO is a good candidate because the lattice parameters for both materials are almost the same. The preparation of substrate surface plays a crucial role in epitaxial growth applications.

This work presents a method to obtain ZnO substrates with a very smooth surface. The surface of our samples was investigated using the atomic force microscopy (AFM). We present a series of experimental results and a method based on those results to obtain surfaces with RMS= 0.5 nm. Surface of such RMS was made by short mechanical polishing with two different powders having grain size of 20-30 μm and 5-6 μm and finally by two-phase mechano-chemical polishing in colloidal silica of various pH. The first phase of mechano-chemical polishing was made in aquatic colloid solution of SiO_2 nanoparticles reduced to pH=6 by hydrochloric acid. This part of polishing removes the layer degraded by mechanical polishing. The next step was polishing in colloidal solution reduced by nitric acid to pH=7. In this step we obtained very smooth surface. Short, low temperature annealing was a complementary procedure applied in order to remove the amorphous layer, keeping the roughness low.

19:00	Poster	P262
-------	--------	------

Luminescence characteristics of undoped and Eu-doped GdCOB single crystals and nanopowders

Piotr Solarz¹, Martin Nikl², Andrzej Kłos³, Radosław Lisiecki², Witold Ryba-Romanowski¹, Agnieszka Rzepka³, Anna Pajczkowska³

1. Polish Academy of Sciences, Institute of Low Temperature and Structure Research (INTiBS), Okólna 2, Wrocław 50-422, Poland
2. Czech Academy of Sciences, Institute of Physics, Cukrovarnická 10, Prague 16253, Czech Republic
3. Institute of Electronic Materials Technology (ITME), Wólczyńska 133, Warszawa 01-919, Poland

E-mail: solarz@int.pan.wroc.pl

Single crystals $\text{GdCa}_3\text{O}(\text{BO}_3)_3$ (GdCOB) pure and doped Eu with concentration of 1 at% and 4 at% were grown by Czochralski method. The distribution of Eu ions in GdCOB crystals was uniform. The substitution of Eu^{3+} in Gd, Ca(1) and Ca(2) cation sites and eventually formation Eu^{2+} have been investigated. The spectroscopic properties of crystals are compared with properties of nanopowders obtained by sol-gel method.

The excitation spectra recorded in the 125 - 330 nm spectral region consist of two broad bands with maxima at 182 and 250 nm and considerable less intense typical gadolinium narrow lines at about 312 nm. The broad bands can be assigned as $\text{Eu}^{3+} - \text{O}^{2-}$ (250 nm) and $\text{Gd}^{3+} - \text{O}^{2-}$ (182 nm). The origin of the $\text{Eu}^{3+} - \text{O}^{2-}$ band was confirmed by absorption spectrum of undoped GdCOB crystal.

Radioluminescence spectra of undoped GdCOB crystal show the characteristic emission of Gd at about 312 nm, whereas this emission dramatically decreases in Eu-doped crystals upon X-ray excitation, as well as in Eu-doped nanopowders excited in VUV region. The VUV excitation in the range from 125 to 333 nm (Eu-doped samples) leads to strong emission in red coming from the $^5\text{D}_0$ multiplet of Eu^{3+} , only. Even trace concentration of Eu^{2+} seems to be excluded due to complete absence of any emission within 360-500 nm [1]. It is interesting to note that absolute radioluminescence intensity in GdCOB:Eu 4at% crystal is somewhat weaker than in GdCOB:Eu 1 at% one. When the crystals were excited at 275 nm the emission of GdCOB:Eu 4 at% is stronger than GdCOB:Eu 1at% one (in opposite to X-ray excitation). Probably, GdCOB:Eu 4 at% crystal is of lower quality, which can induce higher nonradiative losses in radioluminescence processes, in which the energy of incoming X-rays is absorbed in the GdCOB host. In the photoluminescence decay kinetics of 312 nm emission it is clearly observed substantial shortening and departure for single exponential decay in Eu-doped samples. Higher Eu doping results in further acceleration of the decay. In undoped GdCOB crystal, the lifetime of $^6\text{P}_{7/2}$ is 3 ms. The $^5\text{D}_0$ decay kinetic monitored at 613 nm is rather constant. Numerical fitting, of fully exponential curves, returns 2.7 ms for nanopowder and 2.5 ms for single crystal. The presented data suggest this material maybe used as a phosphor in plasma display panels.

This work was supported by Ministry of Education and Science under the research project no. 3T11B00430.

[1] P. Dorenbos, J. Phys. Cond. Matter 15 (2003) 575

19:00	Poster	P263
-------	--------	------

Growth of $\text{K}_5\text{Li}_2\text{NdF}_{10}$ and $\text{K}_5\text{Li}_2\text{PrF}_{10}$ crystals by the Bridgman method

Piotr Solarz

Polish Academy of Sciences, Institute of Low Temperature and Structure Research (INTiBS), Okólna 2, Wrocław 50-422, Poland

E-mail: solarz@int.pan.wroc.pl

The growth of congruently melting $\text{K}_5\text{Li}_2\text{NdF}_{10}$ and $\text{K}_5\text{Li}_2\text{PrF}_{10}$ (KLLF) crystals by the Bridgman method is reported. The structure of these crystals are orthorhombic, with the space group $Pnma$. The unit-cell parameters are $a = 2.0775$ nm, $b = 0.7822$ nm and $c = 0.6963$ for the $\text{K}_5\text{Li}_2\text{LaF}_{10}$ crystal and they change a little upon substitutions of other lanthanide in the series from La to Gd [1]. The crystal structure is built from layers perpendicular to the a axis, formed by LnF_8 dodecahedra and LiF_4 tetrahedra. Lanthanide and lithium ions occupy sites with point symmetry C_2 whereas potassium and fluorine ions occupy sites with C_2 and C_1 symmetry. The polyhedra do not share fluorine ions and the closest lanthanide ion are separated by about 0.65 nm. Owing these features, exchange interactions between Ln ions maybe neglected. Based on the crystallographic structure, there is only one site for the lanthanide ions.

A stoichiometric mixture of appropriate LiF , KF , NdF_3 and PrF_3 was preliminary heated at about 500 K for 2 hours at vacuum conditions to remove traces of water. Then it was heated up to 1100 K for at least 2.5 hours, under Ar atmosphere, to accomplish the reaction. Finally the single crystal of KLLF were grown by the Bridgman one-zone method in the following conditions: the melt temperature 900

K, temperature gradient 120 K/cm, pulling rate 1 mm/h. For crystal growth the IG-110 graphite were used which gives also the possibility to remove traces of oxygen.

[1] P. Solarz and W. Ryba-Romanowski, Phys. Rev. B 72 (2005) 075105

19:00	Poster	P264
-------	--------	------

Transport properties on nitrogen at high pressure and temperature: viscosity – MD study.

Paweł Strak^{1,2}, Stanisław Krukowski²

1. Warsaw University of Technology, Faculty of Physics, Koszykowa 75, Warszawa 00-662, Poland 2. Polish Academy of Sciences, Institute of High Pressure Physics (UNIPRESS), Sokolowska 29/37, Warszawa 01-142, Poland

E-mail: strak@unipress.waw.pl

At present several methods are used to obtain GaN substrates for optoelectronic. The high nitrogen pressure solution growth (HNPSG) is characterized by its ability to provide very high crystallographic quality crystal substrates. The typical dislocation density is of order of 10^7 cm^{-2} , which fulfills industrial standards.

A considerable drawback of the method is the limited size of the GaN crystals. The routinely obtained GaN crystal are about 1 cm in linear dimensions and about 100-00 micron in thickness. Therefore further studies are necessary to develop the method to increase the size and also the efficiency of the HNPSG method.

The investigation of the method requires reliable knowledge of the equilibrium and transport properties of nitrogen at very high pressure and temperature. Recent works reported on ab initio and MD studies of nitrogen properties such as nitrogen intermolecular potential and equation of state [1,2]. In this paper we report on the preliminary results on nitrogen viscosity at the pressures up to 20 kbar and the temperatures up to 2000K.

[1] Krukowski S, Strak P, *Journal-of-Chemical-Physics*. 7 April 2006; 124(13): 134501-1-9

[2] Strak P, Krukowski S, *Journal-of-Chemical-Physics*. - accepted (2007)

19:00	Poster	P265
-------	--------	------

Measurement of Specific Surface Free Energy of Synthetic Quartz Crystal

Naoki Sugihara¹, Takaomi Suzuki¹, Katsuya Teshima¹, Shuji Oishi¹, Masayuki Kawasaki²

1. Shinshu University, 4-17-1 wakasato, Nagano 380-8553, Japan 2. Nihon Dempa Kogyo, Saitama 350-1321, Japan

E-mail: naokicola@yahoo.co.jp

We determined specific surface free energy of equilibrium form crystal such as chlorapatite or ruby using contact angles of liquid droplets. Because such specific surface free energies satisfies Wulff's relationship, the validity of experimentally determined specific surface free energy was certificated. This time we applied our experimental technique for determination of the specific surface free

energy even for growth from crystal. We used synthetic quartz crystal produced by Nihon Dempa Kogyo with rough and meta-stable faces (Z, S, +X, -X). Contact angles of water and formamide droplets on each meta-stable face were determined by sessile drop method with droplets in size of 0.1 micro liters. The specific surface free energy was calculated using Fowkes approximation and Wu's mean equation and compared with growth rate of the quartz crystal. The order of specific surface free energies were $-X < +X < Z < S$, and the growth rate had the same order. Therefore, we can say that the growth rate of each face of the crystal is determined by the specific surface free energy. Although our experimental measurement of the specific surface free energy was performed at room temperature, the quartz was synthesized at higher temperature. Because there is no phase transition between the synthesis and room temperature, the order of the specific surface free energy of each face might be kept even at room temperature.

19:00	Poster	P266
-------	--------	------

Electrical and optical studies of undoped GaP grown by LEC method

Stanisława Strzelecka, Hańcza Barbara Surma, Andrzej Hruban, Elżbieta Wegner, Mirosław Piersa, Artur Wnuk, Mariusz Grzegorz Pawłowski, Waław Orłowski

Institute of Electronic Materials Technology (ITME), Wólczyńska 133, Warszawa 01-919, Poland

E-mail: barbara.surma@itme.edu.pl

Gallium Phosphide (GaP) is known as one of the basic optoelectronic material since more than 30 years. Its light emitting features in a visible spectral range were intensively studied in the second half of the twentieth century. Lately GaP has been found to be also interesting material in dynamically developed infrared optic [1]. For this application undoped of high purity material is necessary. The growth of undoped GaP by liquid encapsulated method (LEC) showed that its electrical parameter can be changed not only by residual dopants distribution.

To understand the change of the electrical parameters along the length of GaP crystal or during its annealing one needs to assume the creation of electrically active native defect related centers. The purpose of this paper was to explain what kind of defects it can be.

Undoped GaP grown by LEC method was studied. The residual electrically active dopants in GaP grown by this method were silicon, carbon and oxygen. Carbon and oxygen amount was controlled by the intensity of low temperature local vibrational mode absorption (LVM) at 605.7 cm^{-1} and 569.7 cm^{-1} , respectively. Beside of this a residual amount of the nitrogen was also found (LVM at 496.3 cm^{-1}). Electrical parameters versus temperature were measured by Hall method. Optically active deep defects were measured by low temperature photoluminescence (PL) in the spectral range 2eV - 0.7eV. GaP samples of different thickness were also subjected to high temperature annealing from 4 to 88 hours under phosphorous overpressure. After annealing the electrical parameters and PL features were controlled. The results for the samples cut from 6 different GaP crystals were analysed.

The obtained results showed that modification of electrical paramet-

ers and luminescence feature can be partly understandable by assuming the creation of a native defect P_{Ga} (phosphorous atom occupying gallium site place) [2]. The presence of such defect has been confirmed by electron paramagnetic resonance (EPR) in our as grown GaP crystals. However, some of PL features still reminded unclear. During annealing at high temperature the creation of a new electrically active defect was stated. The model of a new defect that allowed us to explain all observed by us modification of electrical parameters has been proposed.

1. D. C. Harris, Infrared Physics and Technology 39, (1998), 185-201.
2. K. Chino, T. Kazuno, K. Satoh, M. Kubota, Semi-Insulating III-V Materials, (1988), 133p.

19:00 Poster P267

Experimental Study for Wulff's Relationship of Ruby Single Crystals Using Contact Angles of Liquid Droplets

Takaomi Suzuki, Eiichi Iguchi, Katsuya Teshima, Shuji Oishi

Shinshu University, 4-17-1 Wakasato, Nagano 380-8553, Japan

E-mail: takaomi@gipwc.shinshu-u.ac.jp

Wulff's relationship was proposed almost hundred years ago and this relationship is well accepted. This relationship was theoretically established, but no experimental evidence for this theory was demonstrated, because measurement of specific surface free energy of crystal surface was believed to be difficult. We have tried to measure the specific surface free energy of chlorapatite single crystal using contact angles of liquids and compared with its morphology. In that system, we could conform Wulff's relationship. This time we adopt this technique for ruby single crystal in order to prove the generality of our technique to determine the specific surface free energy using contact angle of liquid. The contact angles of water and formamide droplets on ruby single crystals were determined at room temperature by sessile drop method. Although the contact angles have wide distributions, the average of the contact angles was determined after more than hundred repetition of measurement. The specific surface free energy of each face of the ruby crystal was calculated by Fowkes approximation and Wu's mean equations. Wulff's point was postulated at the center of the crystal and the length of the normal line to each face of the crystal from Wulff's point was geometrically calculated and compared with the specific surface free energy. The ratio of specific surface free energy of the face and the normal length from center to the face of crystal was almost constant, which satisfies Wulff's relationship. We are going to discuss about the physical meaning of Wulff's constant from experimental viewpoint.

19:00 Poster P268

Initial Stage of SiC Crystal Growth by PVT Method

Emil A. Tymicki¹, Krzysztof Graszka^{1,2}, Ryszard Diduszko¹, Rafał Bożek³, Maciej Gała¹

1. Institute of Electronic Materials Technology (ITME), Wólczyńska 133, Warszawa 01-919, Poland 2. Polish Academy of Sciences, Institute of Physics, al. Lotników 32/46, Warszawa 02-668, Poland 3. Warsaw University, Faculty of Physics, Hoża 69, Warszawa 00-681, Poland

E-mail: Emil.Tymicki@itme.edu.pl

Silicon carbide is a promising material for high power devices application due to its wide gap, high thermal conductivity and high breakdown field. The reduction of structural defects, such as micropipes, dislocations and mosaic structure is the main challenge the crystal growers have to deal with.

The silicon carbide single crystals were grown by the seeded physical vapour transport method (PVT) using graphite resistance heater. The crystals were grown on c-face (0001) of 6H-SiC seeds. The temperature measured on the back side of the crystal holder was in the range 2000-2300°C. The growth atmosphere consisted of a mixture of argon and 5 vol. % of nitrogen. The total pressure was 100-300 mbar and was changed during the growth run. The SiC source was placed in a graphite crucible at temperature 50-200°C higher than temperature of the seed. The initial source to seed distance varied in the range 10-50 mm. The growth proceeded under quasi-equilibrium conditions. Defects in the crystallization fronts and wafers cut from the crystals were studied by optical microscopy, atomic force microscopy combined with KOH etching and X-Ray diffraction.

In this work we pay special attention to the initialization of crystal growth. We observed that many nucleation sites appeared on the seed surface during the initial stage of the growth. Shortly, at the same places many separated flat faces on the crystallization front were generated. Formation of facets depends on the growth conditions and crucible geometry [1]. The number of facets is dependent on the shape of the crystallization front. The formation of many facets leads to decrease of structural quality of crystals due to degradation of regions where crystallization steps from independent site meet [2,3]. As a result we observed mosaic structure and increased number of micropipes and dislocations. An increased level of boron and nitrogen was found in parts of the crystal grown with faceted morphology. Therefore, it can be concluded that the optimal crystallization front is a little convex one, which permits the growth of crystals with single nucleation site and evolution of single facet on the crystallization front.

[1] K.Graszka, E. Tymicki, J. Kisielewski, Materials Science Forum 527-529 (2006) pp 87-90

[2] Xianxiang Li, Shouzheng Jiang, Xiaobo Hu, Jie Dong, Juan Li, Xiufang Chen, Li Wang, Xiangang Xu, Minhua Jiang Materials Science Forum Vols. 527-529 (2006) pp 95-98

[3] C.Basceni, I.Khlebnikov, Y.Khlebnikov, P.Muzykov, M.Sharma, G.Stratiy, M.Silan, and C.Balkas, Materials Science Forum 527-529 (2006) 39

19:00 Poster P269

Longterm conductivity relaxation processes in CdTe

Igor Virt

Drohobych Ivan Franko state pedagogical university, 24, Ivan Franko Str., Drohobych 82100, Ukraine University of Rzeszow, Rejtana 16 A, Rzeszów 35-310, Poland

E-mail: isvirt@mail.ru

One of the main problems of CdTe material and sensors on its basis is instability of parameters which is mostly caused by a presence of various structural inhomogeneities. It results in deterioration of the detectors capabilities.

In this work we investigated the temporary evolution of samples dark conductivity after the electric field applying. It was examined both pure and chlorine doped CdTe with specific resistance in the range of 10^4 – 10^9 W×cm. All samples were in the form of rectangular parallelepipeds and $6'2'1$ mm³ in dimensions. Gold or indium contacts were deposited onto their opposite large grains. The value of external electric field was in the range of 0–100 V/cm. Samples resistance values measured in a time interval of 1 sec by means of digital multimeter connected to personal computer.

All studied samples can be divided into two groups. None non-equilibrium processes were revealed for the first one. The relaxation of specific resistance after dynamic excitation for the second type of samples in most cases is well described by empirical relation $r(t) = A \times t^{0.7} + r_{\infty}$ and saturates in a few minutes. Besides that, experimental $r(t)$ curves of some of these samples contain peaks – maxima as well as minima. The presence of instability does not depend on polarity of the applied field or type of contacts. It is worth also to note that the change of photoresistance is also expressed by power law dependence when the samples under investigations were illuminated by above bandgap light.

It is clear that observed spatial and time instability of electric characteristics in some CdTe samples relates to the structural inhomogeneities presented in these crystals. Modulation of the applied fields by extended defects (twins, low angle boundaries, stacking faults, etc.) and by non-uniformity of doping impurity distribution causes the polarization processes and substantially influences both the dark conductivity and photoconductivity.

19:00 Poster P270

Influence of number of quantum dot layers on possibility of achieving lasing threshold in vertical cavity surface emitting lasers

Lukasz Piskorski, Michał Wasiak, Robert P. Sarzała

Technical University of Łódź, Institute of Physics, Wólczńska 219, Łódź 93005, Poland

E-mail: mwasiak@p.lodz.pl

Arsenide quantum dots have attracted a lot of attention since late 1990s as potential light sources for the second telecommunication window (1310 nm). For this application the most suitable construction type is a Vertical Cavity Surface Emitting Laser (VCSEL). Unfortunately VCSELs require high material gain, but quantum dots

suffer from the gain saturation. Its level depends on the density of the dots and their uniformity, and is much lower than gain in quantum well structures. This is the reason why in a VCSEL one has to use many quantum-dot layers. Since such a layer should be placed at the anti-node of the standing wave, the number of the layers is limited by the resonator length. Usually at one anti-node a group of three layers is placed. The resonator length is a very important factor, because it has to be p-doped, so as to provide holes for the active layers. It obviously significantly increases the absorption. Despite all those drawbacks it is possible to fabricate a quantum-dot VCSEL, but only few groups make structures for InGaAs/GaAs VCSELs.

In this paper we want to analyse what is the minimal number of quantum-dot layers in a continuous-wave (CW) room-temperature (RT) VCSEL. In our simulations we model structures based on description presented in [1, 2]. We modify number of the active layers and the resonator length. The temperature distribution is determined by assumption that the applied voltage is 7 V, which is the threshold value in the actual laser. For each resonator and active region design we calculate the required material gain and compare it with the saturation level. Value of the latter parameter can be tuned by changing the density of the dots or their uniformity.

In the figure we present the required material gain versus number of 3-layer groups of quantum dots for different resonator lengths. Points which are over or near the saturation line represent structures which do not give enough gain for a VCSEL (unless the dot density or the uniformity are better than assumed by us). The figure suggests that the active region should contain at least 9 layers of dots (3 groups of 3 layers), which agrees with the fact that the actual devices contains usually 5 or 3 group, sometimes with additional two single layers.

The authors would like to acknowledge support from the Polish Ministry of Science and Higher Education (MNiSzW), grant No 85/SIN/2006/02.

References

- [1] H.C. Yu, J.S. Wang, Y.K. Su, S.J. Chang, F.I. Lai, Y.H. Chang, H.C. Kuo, C.P. Sung, H.P.D. Yang, K.F. Lin, J.M. Wang, J.Y. Chi, R.S. Hsiao, and S. Mikhlin, 1.3-um InAs-InGaAs quantum-dot vertical-cavity surface-emitting laser with fully doped DBRs grown by MBE, IEEE Photonics Technology Letters, vol. 18, p. 418, (2006)
- [2] Y.H. Chang, P.C. Peng, W.K. Tsai, Gray Lin, FangI Lai, R.S. Hsiao, H.P. Yang, H.C. Yu, K.F. Lin, J.Y. Chi, S.C. Wang, and H.C. Kuo, Single-mode monolithic quantum-dot VCSEL in 1.3 um with sidemode suppression ratio over 30 dB, IEEE Photonics Technology Letters, vol. 18, p. 847, (2006)

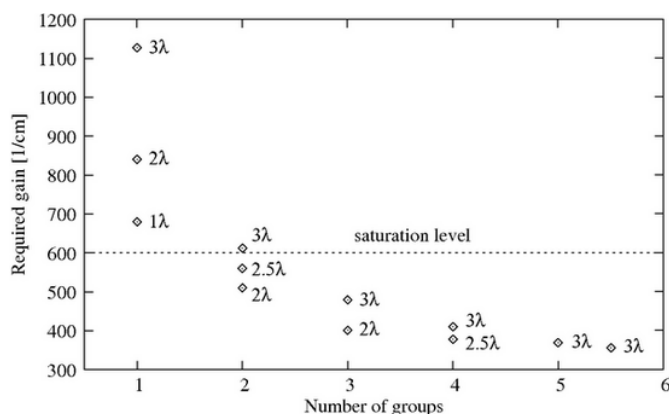


Figure 1. Relations between the number of 3-layers quantum-dot groups and material gain necessary for the lasing threshold. The non-integer value means that there are two additional layers near the DBRs.

19:00 Poster P271

Scaling Theory and Morphometrics of Coarsening Faceted Crystal Surfaces

Stephen J. Watson, Scott A. Norris

University of Glasgow, Department of Mathematics, University Gardens, Glasgow G12-8QW, United Kingdom

E-mail: s.watson@maths.gla.ac.uk

S. J. Watson & S. A. Norris, "Scaling theory and morphometrics for a coarsening multiscale surface, via a principle of maximal dissipation", *Physical Review Letters* vol. 96 (17), Art. No. 176103 (2006). We consider the coarsening dynamics of multiscale solutions to a dissipative singularly perturbed partial differential equation which models the evolution of a thermodynamically unstable crystalline surface. The late-time leading-order behavior of solutions is identified, through the asymptotic expansion of a maximal dissipation principle, with a completely faceted surface governed by an intrinsic dynamical system. The properties of the resulting Piecewise-Affine Dynamic Surface (PADS) predict the power-law scaling law $L \sim t^{1/3}$, for the growth in time t of a characteristic morphological length scale L . We also introduce a novel computational geometry tool which directly simulates a million-facet (PADS) by explicitly treating all the associated topological and critical events that arise as the surface coarsens. Our computed data is consistent with the dynamic scaling hypothesis and we report a variety of associated morphometric scaling-functions.

19:00 Poster P272

X-ray topography of $\text{GdCa}_4\text{O}(\text{BO}_3)_3$ doped of 4% Nd single crystal grown by Czochralski method

Edyta Wierzbicka^{1,2}, Maria Lefeld-Sosnowska¹, Andrzej Kłos², Anna Pajczkowska²

1. Warsaw University, Institute of Experimental Physics (IEP UW), Hoża 69, Warszawa 00-681, Poland 2. Institute of Electronic Materials Technology (ITME), Wólczyńska 133, Warszawa 01-919, Poland

E-mail: eolsz@fuw.edu.pl

$\text{GdCa}_4\text{O}(\text{BO}_3)_3$:Nd single crystals were grown by Czochralski method. The structure of GdCOB is monoclinic and non centrosymmetric with space group Cm. The lattice parameters are: $a = 0.80957$ nm, $b = 1.60186$ nm, $c = 0.35588$ nm, $\beta = 101.26^\circ$.

The unique combination of good mechanical properties, good non-linear and spectroscopic properties make this crystal an excellent candidate for solid state lasers. The Nd doped $\text{GdCa}_4\text{O}(\text{BO}_3)_3$ crystals give the possibility of realization of laser action and second harmonic generation in the same crystal. Crystal lattice defects introduce strains into the crystal lattice, which change its optical properties hence for optical applications the crystals of high structural quality are demanded.

The aim of our investigation was to detect and characterize defects in sample GdCOB doped of 4% neodymium (Nd), cut perpendicularly to the growth axis **b**. The crystal was investigated by means of conventional X-ray Lang projection topography in transmission and back reflection geometry.

With respect to the formerly studied undoped crystals the investigated crystal GdCOB: of 4% Nd showed more other defects. A set of dislocation loops generated around the precipitate particle by punching was observed. The short white or black contrasts of shape depending on the direction of the diffraction vector **g** were detected. The white or black contrasts in the form of concentric rings surrounding the core, are very well seen in all topographs of GdCOB:Nd crystal. These contrasts are probably due to the non uniform incorporation of dopant atoms, forming the striations. They depend on the diffraction vector **g** direction. The striations with small period were modulated by changes of the diffracted beam intensity with greater period. On the striations some precipitates or inclusions were observed. The central core region is free of any fringe contrasts.

The very long straight dislocations characteristic for undoped crystals are not observed but shorter dislocations inclined to the crystal surface were seen. They have the similar nature as the long dislocations: the Burgers vector is along **a** axis – [100]. The line directions are approximately along an intersection of the (100) plane with the crystal surface, so they exhibit strong edge component.

19:00 Poster P273

Flux growth and crystal structure determination of new $\text{M}^{1+}\text{-M}^{2+}\text{-M}^{3+}$ di-, tri- and tetrasilicates ($\text{M}^{1+} = \text{Na, K; M}^{2+} = \text{Sr, Ba; M}^{3+} = \text{Sc, Y, Gd, Er, Yb}$)

Maria Wierzbicka, Uwe Kolitsch, Ekkehart Tillmanns

Institute of Mineralogy and Crystallography, Althanstraße 14, Wien 1090, Austria

E-mail: maria.wierzbicka@univie.ac.at

Nanoporous mixed-framework silicates are of particular interest because they show promising physico-chemical properties similar to zeolites. In the course of an ongoing project on new micro- and nanoporous M^{3+} silicates new di-, tri- and tetrasilicate compounds were synthesised. All syntheses were carried out using the flux-growth technique (MoO_3 -based flux mixtures in Pt crucibles in air; $T_{\text{max}} = 1150^\circ\text{C}$, cooling rate 2°C/h , $T_{\text{min}} = 900^\circ\text{C}$). The crystal structures of all compounds have been determined from single-crystal X-ray in-

tensity data (Mo K α X-radiation, CCD area detector, 293 K).

The three isotopic compounds BaKYSi₂O₇ (Kolitsch *et al.*, 2007), BaKYbSi₂O₇ and BaKScSi₂O₇ crystallise as small colourless isometric crystals in space group $P2_1/n$. BaKREESi₂O₇ (REE = Y, Yb, Sc) represents a novel tetrahedral-octahedral framework structure type. The structure is based on isolated Si₂O₇ groups with octahedrally coordinated REE³⁺ cations and [9]-coordinated Ba atoms and [8]-coordinated K atoms. The isolated REEO₆ octahedra share each of their apices with oxygen atoms of the Si₂O₇ groups. The connectivity results in a three-dimensional framework with Ba²⁺ and K¹⁺ cations in channels running parallel to [10-1]. By comparison to other disilicates, the Si-O-Si angle in BaKREESi₂O₇ is unusually small (124.51(9), 124.9(2) and 128.2(1)°, respectively). No isoelectronic or other related silicates are known, although the monoclinic diphosphates M₂SrP₂O₇ (M = K, Rb, Cs) (Trunov *et al.*, 1991) have similar crystal structures.

A new dimorph of BaKYbSi₂O₇ crystallised together with $P2_1/n$ -type BaKYbSi₂O₇ (see above); it is also monoclinic (space group Cc). Its crystal structure is closely related to the BaKREESi₂O₇ (REE = Y, Yb, Sc) type; the Si-O-Si angle is alsosimilar, 126.0(7)°. The third new structure type based on disilicate groups is represented by BaNaScSi₂O₇ (Wierzbicka *et al.*, 2007). It is also topologically similar to BaKREESi₂O₇. BaNaScSi₂O₇ crystallises as small colourless isometric crystals in $P2_1/m$. Its structure consists of ScO₆ octahedra that share each of their apices with O atoms of the Si₂O₇ groups and [9]-coordinated Ba atoms and [4+4]-coordinated Na atoms (Na-O = 2.457 – 2.907 Å). The Si-O-Si angle in BaNaScSi₂O₇, 123.12(12)°, is the smallest of all the mentioned new disilicates. The three above structure types differ in localisation of Ba²⁺, K¹⁺, and Na¹⁺ atoms and direction of the linkages between REEO₆ (REE = Y, Yb, Sc) and Si₂O₇ units.

In the trisilicate family, a large number of new compounds was obtained: BaREE₂Si₃O₁₀ (REE = Gd, Y, Er, Yb, Sc) (Kolitsch *et al.*, 2006), SrY₂Si₃O₁₀ (Kolitsch *et al.*, 2006) and BaRbScSi₃O₉ (Wierzbicka *et al.*, 2007). All compounds formed small, colourless plates, with monoclinic or triclinic symmetry. BaREE₂Si₃O₁₀ crystallises in $P2_1/m$. Its crystal structure is based on zigzag chains parallel to [010] of edge-sharing distorted REEO₆-octahedra linked by horseshoe-shaped Si₃O₁₀ groups and [8]-coordinated Ba atoms, which occupy narrow channels extending parallel to [100]. The Si-Si-Si angle in Si₃O₁₀ units increase with decreasing REE³⁺ ionic radii (94.78(5), 96.12(4), 96.40(5), 97.09(5), 99.63(4)° for REE = Gd, Y, Er, Yb, Sc, respectively). The second trisilicate compound, SrY₂Si₃O₁₀, crystallises in $P-1$ (no. 2). The structure of SrY₂Si₃O₁₀ contains zigzag chains parallel to [100] of edge-sharing YO₇ polyhedra sharing further edges with YO₆ polyhedra. These decorated chains are linked by slightly curved Si₃O₁₀ groups (Si-Si-Si angle = 133.5°). It is noteworthy that one SiO₄ tetrahedron shares an edge with the YO₇ polyhedron. Voids in the resulting framework are occupied by Sr²⁺ cations in [8]-coordination (Kolitsch *et al.*, 2006). BaRbScSi₃O₉ crystallises as small pseudohexagonal plates (drillings) in $P-1/c$. The topology of BaRbScSi₃O₉ is based on Si₃O₉ rings connected to the isolated ScO₆ octahedra. The [6-7]-coordinated Ba and approximately [7-8]-coordinated Rb atoms are both arranged along rows parallel to [010].

The single new tetrasilicate obtained, Ba₂Gd₂Si₄O₁₃, crystallises as colourless pseudotetragonal prisms in $C2/c$. The structure consists of finite Si₄O₁₃ chains connected with GdO₇ polyhedra. Two such polyhedra share a common edge creating isolated Gd₂O₁₂ groups,

which form the basis of a heteropolyhedral slab in the *ab* plane. [8]-coordinated Ba atoms are located in channels running parallel to the *b*-axis. This compound shows structural similarities to Na₂Sc₂Si₄O₁₃ (Maksimov *et al.*, 1980) and Ba₂Nd₂Si₄O₁₃ (Tamazyán *et al.*, 1985).

Financial support by the Austrian Science Foundation (FWF) (Grant P17623-N10) and the ICDD (Grant 90-03ET) is gratefully acknowledged.

References

- U. Kolitsch, M. Wierzbicka, E. Tillmanns, Can. Mineral. (submitted) (2007).
- U. Kolitsch, M. Wierzbicka, E. Tillmanns, Acta Crystallogr, **C62**, 35 (2006).
- U. Kolitsch, M. Wierzbicka, E. Tillmanns, 15th Slovenian-Croatian Crystallographic Meeting, Jezersko, Slovenia, June 15-18, Book of Abstracts, 22 (2006).
- B. A. Maksimov, O. K. Mel'nikov, T. A. Zhdanova, V. V. Ilyukhin, N. V. Belov, Dokl. Akad. Nauk SSSR, **251**, 98 (1980).
- R. A. Tamazyán, Yu. A. Malinovskii, Dokl. Akad. Nauk SSR, **30**, 907 (1985).
- V. K. Trunov, Yu. V. Oboznenko, S. P. Sirotinkin, N. B. Tskhelashvili, Neorg. Mater., **27**, 1993 (1991).
- V. K. Trunov, Yu. V. Oboznenko, S. P. Sirotinkin, N. B. Tskhelashvili, Neorg. Mater., **27**, 2370 (1991).
- M. Wierzbicka, U. Kolitsch, E. Tillmanns, Z. Kristallogr. Suppl. (in press) (2007).

19:00	Poster	P274
-------	--------	------

Observation of defects in g - irradiated Cz-si annealed under high pressure

Krzysztof Wieteska¹, Wojciech Wierchowski², Andrzej Misiuk³, M. Prujarczyk³, Ivana Capan⁴, Deren Yang⁵, Walter Graeff⁶

1. Institute of Atomic Energy, Otwock-Świerk 05-400, Poland
2. Institute of Electronic Materials Technology (ITME), Wólczyńska 133, Warszawa 01-919, Poland
3. Institute of Electron Technology (ITE), al. Lotników 32/46, Warszawa 02-668, Poland
4. RUDJER BOSKOVIĆ INSTITUTE, BIJENIČKA C. 54, Zagreb 10 000, Croatia
5. Zhejiang University, State Key Lab of Silicon Materials (ZJU), Zhe Da Lu 38, Hangzhou 310027, China
6. Hamburger Synchrotronstrahlungslabor HASYLAB (HASYLAB), Notkestrasse 85, Hamburg D-22603, Germany

E-mail: wierzc_w@sp.itme.edu.pl

Samples cut out from Czochralski grown silicon crystals (Cz-Si) including those doped either with nitrogen to $1.2 \times 10^{15} \text{ cm}^{-3}$ or with germanium to $7 \times 10^{17} \text{ cm}^{-3}$, were subjected to different thermal and pressure treatments before and after irradiation with high intensity g - rays of ⁶⁰Co, up to 2350 Mrad. The pre-irradiation treatment was performed for 5 h at 800°C, 1000°C, or 1130°C under atmospheric or high argon pressure (HP, up to 11 kbar). The post implantation treatment was performed at room temperature or 1000°C under atmospheric pressure or HP. The reference, not irradiated Cz-Si crystals were also studied. It has been expected that the irradiation can

generate a nucleation centres for the formation of oxygen precipitates, while the presence of nitrogen or germanium usually moderates this process.

The creation of defects in the samples was investigated by means of various synchrotron X-ray diffraction methods including observation of the rocking curves, monochromatic beam topography and by several topographic methods using white synchrotron white beam. The experiments were performed at E2 and F1 experimental stations in HASYLAB. In the present case a very important method was the Bragg - case section topography, realised using 5 mm narrow slit, which allows to indicate the presence of small and not well resolved inclusions and to evaluate the perfection of the sample better than other X-Ray methods.

It was found that, in case when the initial treatment was performed at up to 1000°C, the effect of irradiation and of the treatments was not very distinct, and similar for different samples. In the case of the highest pre - irradiation treatment temperature applied (1130°C), we observed the formation of characteristic inclusions. These inclusions were usually of lower concentration and better resolved in the nitrogen - or germanium - doped samples.

The observed effects are related to enhanced radiation hardness of Cz-Si doped with germanium or nitrogen in comparison to that of non doped material (compare [1]).

[1] A. Misiuk, B. Surma, C.A. Londos, J. Bak-Misiuk, W. Wierzychowski, K. Wieteska, W. Graeff „Oxygen precipitation and creation of defects in neutron irradiated Cz-Si annealed under high pressure” *physica status solidi c* 2 (6) (2005) 1812-1816

19:00	Poster	P275
-------	--------	------

Observation of individual dislocations in 6h and 4h sic by means of back-reflection methods of x-ray diffraction topography

Wojciech Wierzychowski¹, Krzysztof Wieteska², Tomasz Balcer¹, Agnieszka Malinowska^{1,3}, Władysław Hofman¹, Walter Graeff⁴

1. *Institute of Electronic Materials Technology (ITME), Wólczyńska 133, Warszawa 01-919, Poland* **2.** *Institute of Atomic Energy, Otwock-Świerk 05-400, Poland* **3.** *Warsaw University of Technology, Faculty of Physics, Koszykowa 75, Warszawa 00-662, Poland* **4.** *Hamburger Synchrotronstrahlungslabor HASYLAB (HASYLAB), Notkestrasse 85, Hamburg D-22603, Germany*

E-mail: wierzc_w@sp.itme.edu.pl

The Bragg-case geometry is less popular in topographic experiments than the transmission geometry, because in some cases the visibility of individual dislocations can be lowered. Otherwise it can be often very useful, e.g. providing more transparent images at higher concentration of defects.

In the present work we investigated SiC crystals of high structural perfection with several methods of X-ray diffraction topography in Bragg-case geometry. The methods included section and projection ones as well as single crystal and double crystal methods exploring conventional and conventional sources of X-ray diffraction. The investigated 6H and 4H monotypic SiC wafers were manufactured by CREE and in large regions they contained the dislocation density

on the level not exceeding 10^3 cm^{-2} which cannot be interpreted as hollow core dislocations (micro- or nano-pipes). The concentration of the last ones was lower than 10^2 cm^{-2} .

The present investigation confirmed the possibility of revealing dislocations with all used methods, including most inconvenient case of single projection topography in Cu K_{a1} radiation. The character of the images was significantly different in case of different topographic methods. The images of dislocation in synchrotron and conventional multi-crystal arrangement consisted of characteristic rosettes with a “tail” coming from the dislocation core, while single crystal projection topographs provided the images of dislocation in form of characteristic dots or commas and section images reproduced the dislocations in form of black rosettes.

The quality of presently obtained Bragg-case multi-crystal and section images of dislocation enabled analysis based on comparison with numerically simulated images. The analysis confirmed the domination of screw-type dislocations in the investigated crystals.

19:00	Poster	P276
-------	--------	------

X-ray characterization of $\text{Sr}_{0.61}\text{Ba}_{0.39}\text{Nb}_2\text{O}_6$ single crystals

Paweł Pacek¹, Krystyna B. Wokulska¹, Jan Dec², Tadeusz Łukasiewicz³

1. *University of Silesia, Institute of Material Science, Bankowa 12, Katowice 40-007, Poland* **2.** *University of Silesia, Katowice, Poland* **3.** *Institute of Electronic Materials Technology (ITME), Wólczyńska 133, Warszawa 01-919, Poland*

E-mail: wokulska@us.edu.pl

The strontium barium niobate ($\text{Sr}_{1-x}\text{Ba}_x\text{Nb}_2\text{O}_6$ - SBN) with space group P4bm is relaxor ferroelectrics^x that have attracted considerable interest for its excellent optical, photorefractive and dielectric properties. Recently these materials are extensively studied because of its special smearing phase transitions. This broadened phase transition is probably caused by the wide variation of the non-equivalent crystallographic position in its structure. Our paper is devoted to studies of the SBN crystals with the congruently melting composition – $\text{Sr}_{0.61}\text{Ba}_{0.39}\text{Nb}_2\text{O}_6$. The single crystals were obtained by Czochralski method and they have extremely got perfect structure without any striations. Characterization of the investigated crystals was performed by X-ray powder diffraction and scanning electron microscopy with EDS techniques. The used methods confirmed high quality of the specimens and revealed of their anticipated compositions.

The Bond method of the precise lattice parameters measurements ($\text{dd}/d = 10^{-6}$) was used to study the structure changing of the crystals with a temperature. In this way we could measure lattice parameters of SBN, volume of unit cell and finally to calculate the thermal expansion coefficients. The temperature of the phase transition and its character is also determined.

19:00

Poster

P277

Direct melt crystal growth of isotactic polybutene-1 trigonal phase

Motoi Yamashita

Ritsumeikan University, Department of Applied Chemistry, Kato-laboratory, Noji-higashi 1-1-1, Kusatsu, Shiga 525-8577, Japan

E-mail: motoi-y@se.ritsumei.ac.jp

Introduction

Polybutene-1 (PB1) has outstanding mechanical properties. However, its applications are limited compared to those of the lighter olefin polymers such as polyethylene and polypropylene. One main reason is the complication introduced by crystal structure transformations. PB1 is polymorphous, with a trigonal form and a tetragonal form as the most common structures. Trigonal form is stable and tetragonal form is metastable, but despite the metastability it is always tetragonal form which is obtained when PB1 crystallizes from the melt. The transformation to trigonal form then takes place after cooling to room temperature, accompanied by strain of crystallized samples. Because of this transformation and strain, direct melt crystallization of PB1 trigonal form has long been a big issue.

In 1990's, Kopp *et al.* reported that the trigonal phase can crystallize in the melt via epitaxy on aromatic acids or salts [1]. At an elevated temperature of 110°C, Zhang *et al.* found that trigonal crystals can be obtained from molten ultrathin films under atmospheric pressure [2]. We present another solution to this issue. Using solution-grown trigonal crystals as nuclei, we observed that the trigonal phase can grow in the melt via self-seeding at atmospheric pressure. In this paper we present some experimental results regarding the *in-situ* observation of trigonal crystals growing from the melt at several different temperatures and a comparison between the crystal growths of the trigonal and tetragonal phases..

Experimental

The PB1 used in this study was purchased from Scientific Polymer Products (Mw=185,000; the melt index is 20 g/10 min). Thin PB1 films were prepared by casting a 0.1 wt% *p*-xylene solution onto carbon-coated mica kept at 60°C on a hot plate. The films were dried in air, an appropriate film thickness of ca. 80 nm being judged by a gold interference color.

Crystallization was carried out on a hot stage (Mettler FP82). The PB1 films were heated at 128-135°C for 2 min and cooled to a crystallization temperature between 65°C and 87.8°C at a rate of 15 K min⁻¹. *In-situ* observations of the crystallization process were performed using an optical microscope (OM; Nikon OPTIPHOT2); the growth rate was determined from the time dependence of the radius or the major axis of crystals observed by OM.

Transmission electron microscopy (TEM; JEOL JEM-1200EXII) was used to identify crystal structures. Samples were examined immediately after crystallization and quenching. The PB1-carbon films were floated on a water surface, picked up on electron microscope grids and used as samples.

Results and Discussions

A sequence of the isothermal crystallization process at 75°C after heat-treatment at 132°C for 2 min is shown by successive optical micrographs in Figure 1. Faint circular crystals emerge from the melt in Figure 1a. The crystals slowly increase in size (Figures 1b, c) and finally some of them impinge upon each other (Figure 1d).

Figure 2 shows a transmission electron micrograph of an PB1 film that was heat-treated at 132°C for 2 min and then isothermally crystallized at 75°C, and its corresponding electron diffraction pattern. A round crystal similar to those observed in the OM images can be seen. The electron diffraction pattern shows a net pattern with hexagonal symmetry, and all the Bragg reflections could be indexed with the trigonal form of PB1. The electron micrograph and diffraction pattern demonstrate that the round crystal grown from the melt is a single crystal in the trigonal form.

Trigonal crystals are known to be obtained in solutions. The PB1 films used in this study are prepared by casting an PB1 solution onto a carbon-coated mica, and therefore contain abundant trigonal crystals grown from the solution. When the films are heated up to a temperature near but below the equilibrium melting point of PB1, 136°C, melting of the trigonal crystals is incomplete, which eventually prepares numbers of trigonal nuclei; we can utilize the incompletely melted trigonal crystals for self-seeding. On cooling to a crystallization temperature, we can observe trigonal crystals growing in the melt. These facts are considered to enable the trigonal crystals to grow in the melt even at atmospheric pressure and lower crystallization temperatures.

The radius R of the circular crystals increased linearly with crystallization time t for all the crystallization temperatures investigated as shown in Figure 3. The linearity indicates that the crystal growth is controlled not by diffusion, but by kinetics at the interface. The growth rate G was determined from the slope of the time-radius curve. The logarithm of G is plotted against crystallization temperature in Figure 4. The values of the growth rate G of tetragonal crystals we observed in our previous work [3] are also included for comparison. It should be noted that the growth rate of trigonal crystals is one hundredth that of tetragonal crystals. In 1965, Powers *et al.* used trigonal crystals obtained by solid-state transformation from the tetragonal phase as nuclei and attempted to observe the growth of trigonal crystals in the melt. This was, unfortunately, not successful and they hypothesized that the growth rate of trigonal crystals is "exceedingly" slower than that of tetragonal crystals [4]. The result obtained in this work is consistent with the prediction made by Powers *et al.*

Summary

Crystal growth of the *it*-PB1 trigonal form was successfully observed in the melt at atmospheric pressure. The growth rate of trigonal crystals was obtained by *in-situ* optical microscopy. The growth rate G of trigonal crystals is one hundredth that of tetragonal crystals.

References

- [1] Kopp, S.; Wittmann, J. C.; Lotz, B. *Polymer* 1994, 35, 916.
- [2] Zhang, B.; Yang, D.; Yan, S. *J Polym Sci Part B: Polym Phys* 2002, 40, 2641.
- [3] Yamashita, M.; Miyaji, H.; Izumi, K.; Hoshino, A. *Polym J* 2004, 36, 226.

[4] Powers, J.; Hoffman, J. D.; Weeks, J. J.; Quinn Jr., F. A. J Res Nat Bur Std (U.S.) 1965, 69A, 335.

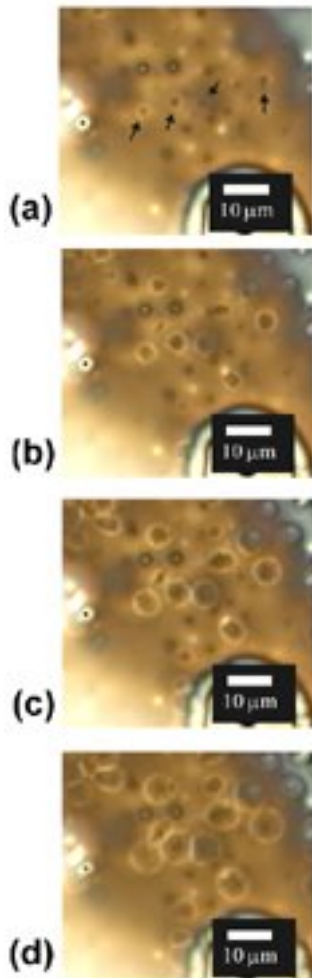


Fig1. In-situ optical micrographs of PB1 trigonal crystals taken at 75°C at intervals of 3 min.

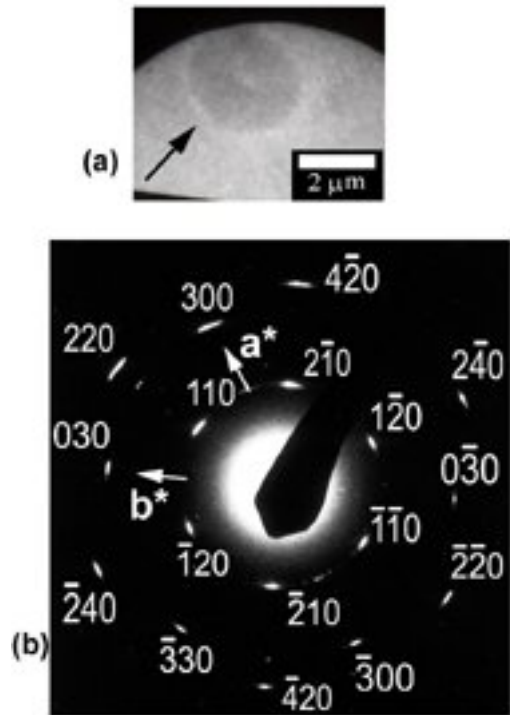


Fig 2. (a) Electron micrograph and (b) its corresponding selected area electron diffraction pattern of an PB1 single flat-on crystal in the trigonal form grown at 75 °C. A round PB1 crystal is indicated by an arrow. The arc in the upper part of (a) is an area-selecting aperture.

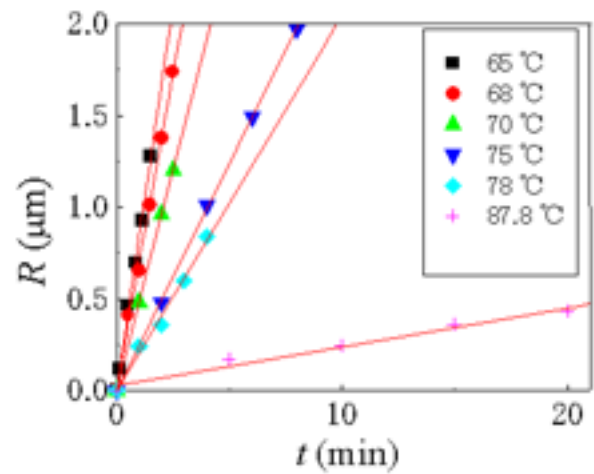


Fig 3. Time dependence of radius R of trigonal crystals at several crystallization temperatures.

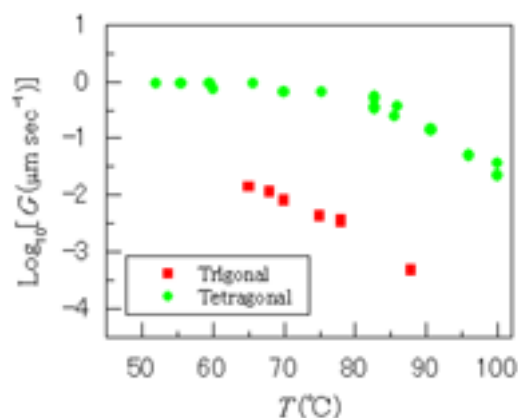


Fig 4. Growth rate G versus crystallization temperature T for the trigonal and tetragonal phases.

19:00 Poster P278

Characterization of in-plane structures of vapor deposited thin-films of distyryl-oligothiophenes by grazing incidence X-ray diffractometry

Noriyuki Yoshimoto¹, Keijyu Aosawa¹, Kazuhiko Omote², Jörg Ackermann³, Christine Vidélot-Ackermann³, Hugues Brisset³, Frédéric Fages³

1. Iwate University, Morioka 020-8551, Japan 2. Rigaku Co., Tokyo 196-8666, Japan 3. Université de la Méditerranée (GCOMM), UMR 6114 CNRS, Faculté des Sciences de Luminy, case 901, Marseille 13288, France

E-mail: yoshimoto@iwate-u.ac.jp

In recent years, organic thin-film transistors (OTFTs) have attracted great attention, and their performance has continually improved. OTFTs have many advantages in terms of a low-cost, low-temperature process, compatibility with flexible substrates, and a large variety of composite materials. In comparison to transistors made from conventional inorganic semiconductors such as amorphous silicon, the stability and uniformity of OTFTs require however improvements. The investigation of initial stages of crystal growth of organic semiconductors is important to solve the problems. Distyryl-oligothiophene, one of the representative organic semiconductors, has been used in OTFTs as a promising material. We have so far clarified that some kinds of distyryl-oligothiophenes show the marvelous stability in OTFT [1,2]. To reveal the cause of the stability in OTFTs based on distyryl-oligothiophene, investigation of in-plane structure of the thin films could be helpful. In this study, in-plane structures of thin films based of oligothiophenes on SiO₂ substrates were investigated by grazing incidence X-ray diffractometry (GIXD). The effects of film thickness and substrate temperatures on the in-plane structure were examined by GIXD. Distyryl-oligothiophene was vacuum deposited onto SiO₂ substrates under 1×10^{-4} Pa. The substrates were maintained at a temperature between 20°C and 100°C. The deposition rate was set at 0.1 Å/s. The mean film thicknesses were between 10 Å and 1000 Å. Characterization of the films were done by using x-ray diffractometers (Rigaku Co., ATX-G and synchrotron radiation at the BL13XU ATX-GSOR in

Spring-8) which were specially designed for characterization of thin films. Both in-plane and out-of-plane diffractions could be measured, because the goniometer has not only conventional $\theta/2\theta$ axes but also in-plane $\phi/2\theta$ axes. As the result, in-plane diffraction patterns were obtained from the ultra-thin films, and the lattice spacing obviously changed with increasing film thickness. Therefore, it was considered that the unique in-plane structures at the interface of the thin films could contribute to the remarkable stability in OTFT performance.

[1] C. Vidélot-Ackermann, J. Ackermann, H. Brisset, K. Kawamura, N. Yoshimoto, P. Raynal, A. El Kassmi, F. Fages, J. Am. Chem. Soc. 127 (2005) 16346.

[2] C. Vidélot-Ackermann, J. Ackermann, H. Brisset, K. Kawamura, N. Yoshimoto, P. Raynal, A. El Kassmi, and F. Fages, Organic Electronics, 7 (2006) 465.

Meeting of PSCG Council and Sections

Tuesday evening, 22 May, 20:30

Wednesday, 23 May

Session VIII: Bulk Oxides

Bożena Hilczer

Wednesday morning, 23 May, 8:30

Lecture of doctoral dissertation winner

Wednesday morning, 23 May, 8:31

8:45

Invited oral

On the solubility of Nd³⁺ in Y₃Al₅O₁₂

Detlef Klimm¹, Steffen Ganschow¹, Anna Pajaczowska², Ludwika Lipińska²

1. Institute for Crystal Growth (IKZ), Max-born Str. 2, Berlin 12489, Germany 2. Institute of Electronic Materials Technology (ITME), Wólczyńska 133, Warszawa 01-919, Poland

E-mail: klimm@ikz-berlin.de

Neodymium doped yttrium aluminum garnet (Nd:YAG or (Y_{1-x}Nd_x)Al₅O₁₂) is one of the most important laser materials. Crystals are available from different commercial suppliers with dopant concentrations up to 2.5 at% ($x \leq 0.025$). The crystals are grown from the melt usually by the Czochralski method. Besides, in the framework of this study Nd:YAG crystals with different doping levels are grown by the micro-pulling-down method. For both methods, the material has to be kept at the melting point that is for undoped ($x=0$) Y₃Al₅O₁₂ $T_f = 1940^\circ\text{C}$ and drops only slightly for $x>0$. Alternatively, single phase (Y_{1-x}Nd_x)Al₅O₁₂ powders with doping levels as high as $x = 0.275$ could be produced in a low-temperature sol-gel process. DTA measurements up to T_f showed that the highly doped Nd:YAG powders are in thermodynamic equilibrium only up to (depending on x) $T \leq 1650^\circ\text{C}$ and decompose irreversibly at higher T . These results can be understood if the crystals are considered as solid solutions within the concentration triangle Al₂O₃ –

$\text{Y}_2\text{O}_3 - \text{Nd}_2\text{O}_3$. Based such treatment a pseudo-binary "garnet" section of this concentration triangle will be proposed that explains the experimental findings known so far.

9:15 Invited oral

Prospects for the μ -PD method and solvothermal method in electrical and optical crystal growth

Tsuguo Fukuda

Tohoku University, Institute of Multidisciplinary Research for Advanced Materials, 2-1-1 Katahira, Aoba-ku, Sendai 980-8577, Japan
Fukuda X'tal Laboratory, c/o ICR 6-6-3, Minami Yoshinari, Aoba-ku, Sendai 981-3204, Japan

E-mail: fukuda@fxtal.co.jp

The melt growth by the Czochralski method was the major technology I have employed during my research career to fabricate a large variety of oxides, fluorides and semiconductors. Some of them could have been brought to production stage successfully like LiTaO_3 for SAW devices, GaAs for high-frequency devices or CaF_2 for UV lithography. More recently, Pr:LuAG as scintillator crystal and langasite-type crystals are being prototyped for industrial production. For future developments, I will give an outlook on present and future trends in crystal growth technology of tailor-made, long crystals of Pr:LuAG, sapphire, Nd:YAG, etc. by m-PD [1,2] and mass production of large-sized, wide band gap crystals ZnO [3] and GaN [4] by solvothermal growth techniques.

1. T. Fukuda, P. Rudolph, S. Uda (eds.): **Fiber Crystal Growth from the Melt**, Springer-Verlag Berlin Heidelberg New York, 2004.
2. T. Fukuda, V.I. Chani (eds.): **Micro-Pulling-Down Technique and Growth of Shaped Crystals**, Springer-Verlag Berlin Heidelberg New York, to appear in 2007.
3. D. Ehrentaut, Hideto Sato, Y. Kagamitani, Hiroki Sato, A. Yoshikawa, T. Fukuda, **Solvothermal Growth of ZnO**, *Prog. Cryst. Growth Ch.* **52** (2006) 280-335.
4. T. Fukuda and D. Ehrentaut, **Prospects for the Ammonothermal Growth of Large GaN Crystal**, *J. Cryst. Growth*, accepted.

9:45 Oral

Crystal growth and scintillating properties of (Ce, Sr)-doped PrAlO_3

Andrey Novoselov¹, Akira Yoshikawa¹, Jan Pejchal², Martin Nikl², Tsuguo Fukuda¹

1. Tohoku University, Institute of Multidisciplinary Research for Advanced Materials, Katahira 2-1-1, Aoba-ku, Sendai 980-8577, Japan **2.** Czech Academy of Sciences, Institute of Physics, Cukrovarnicka 10, Prague 16253, Czech Republic

E-mail: anvn@tagen.tohoku.ac.jp

Scintillator materials based on the Ce-doping are of persistent interest due to tens-of-nanoseconds range decay time depending on the crystal host. Doping PrF_3 with Ce^{3+} was shown to be a novel approach to obtain promising scintillators because of efficient energy transfer from the Pr^{3+} subsystem to Ce^{3+} -ions via the $^1\text{S}_0$ level of Pr^{3+} [1]. Successful crystal growth of PrAlO_3 and results of spectroscopic

properties characterization were reported recently [2]. Undoped PrAlO_3 hardly ever could be used as a scintillator because of strong concentration quenching of the Pr^{3+} 5d-4f emission. However, it also points to an enhanced energy migration over the Pr^{3+} -energy levels. On the other hand, a recent study has demonstrated facilitating energy transfer from the Gd^{3+} sublattice to Ce^{3+} emission centers by formation of the Ce^{3+} -distorted centers in YF_3 - GdF_3 solid solutions codoped with Me^{2+} ions such as Sr^{2+} [3].

To investigate this phenomenon, Ce (1, 2 and 5 mol%)-doped PrAlO_3 , and Ce (5 mol%), Sr (0.1, 0.5 and 1 mol%)-codoped PrAlO_3 single crystals were grown by the micro-pulling-down method. Using the UV and X-ray excitation their luminescence spectra and decay kinetics were investigated. Under X-ray excitation in the undoped PrAlO_3 a weak 5d-4f Pr^{3+} emission occurs within 250-300 nm at room temperature, which is well overlapped with the excitation spectra of Ce^{3+} emission in YAlO_3 host. In such circumstances an efficient energy transfer from the Pr-sublattice to the Ce^{3+} ions might occur in Ce-doped PrAlO_3 . Obtained results will be presented and discussed in the light of the $(\text{Pr}^{3+})_n \rightarrow \text{Ce}^{3+}$ energy transfer characteristics and potential of such a material to obtain a fast scintillator of elevated density.

[1] M. Nikl et al., *phys. stat. sol. (a)* 201 (2004) R108.

[2] D.A. Pawlak et al., *J. Cryst. Growth* 282 (2005) 260.

[3] M. Nikl et al., *J. Phys.: Condens. Matter* 18 (2006) 3069-3079.

Coffee Break

Wednesday morning, 23 May, 10:00

Session X: Fluorides & Oxides

Wednesday morning, 23 May, 10:30

Chair: Tsuguo Fukuda

10:30 Invited oral

Synthesis and growth of doped rare-earth BaY_2F_8 single crystals for laser applications.

Sonia L. Baldochi¹, Simone Ferreira de Almeida Cruz¹, Gerson Hiroshi de Godoy Nakamura¹, Laercio Gomes¹, Vera L. Mazzocchi¹, Carlos B R. Parente¹, Mario E G. Valerio², Detlef Klimm³

1. Instituto de Pesquisas Energéticas e Nucleares (IPEN-CNEN), Av. Prof. Lineu Prestes, 2242, USP, Sao Paulo 05508000, Brazil

2. Universidade Federal de Sergipe (UFS), Campus Universitário, São Cristovão, Sergipe 14000000, Brazil **3.** Institute for Crystal Growth (IKZ), Max-born Str. 2, Berlin 12489, Germany

E-mail: baldochi@ipen.br

The growth of single crystals has been developed over decades to meet the needs for basic research and applications in many different areas. On this aspect, fluorides materials have shown a continuous development on research and technological uses as dosimeters, x-ray monochromators and mainly as optical devices, such as optical windows and laser hosts. The BaY_2F_8 compound has recently been the subject of several studies, especially regarding the spectroscopy of rare earth (RE) doped crystals for determination of their potential for new compact diode pumped laser systems. Although numerous re-

ports in the literature deal with the laser properties of RE-doped BaY_2F_8 crystals, only a few of them study their preparation in details. In the present work we describe our results on the synthesis from constituent compounds, phase diagram study and growth process of pure and RE-doped BaY_2F_8 crystals. The basic constituents, BaF_2 and the YF_3 , and the rare earth dopants (REF₃) are available from different commercial suppliers with high purity. However, better results concerning the elimination of moisture and oxygen contamination can be obtained from fluorides prepared in laboratory from commercial Y_2O_3 (or RE₂O₃) and $BaCO_3$ by hydrofluorination [1]. In this work an open boat with the oxides (or carbonates) was placed inside a Pt chamber and heated up to the reaction temperature ($\sim 850^\circ\text{C}$). An HF/Ar flow was kept constant for 2-3 hours. The system was cooled to room temperature and before opening the chamber was rinsed with pure Ar to eliminate traces of HF.

The phase equilibrium relations for BaF_2 - YF_3 system were investigated with the particular intent of better understanding the growth process of BaY_2F_8 crystals. Samples of different compositions of BaF_2 and YF_3 previously synthesized were melted under HF atmosphere. The obtained samples were subjected to thermal analysis (differential thermal analysis, differential scanning calorimetry and thermogravimetry). The samples have also been subjected to analysis via X-ray powder diffraction and quantitative calculations of phase concentrations using the Rietveld method were performed. The obtained results were compared with the phase diagrams found in the literature [2,3].

DTA measurements were accomplished in a simultaneous TG/DTA system from TA Instruments, model SDT 2960. As the fluorides are known to be highly sensitive to moisture, fast heating rates ($40^\circ\text{C}/\text{min}$) were used to minimize contamination together with a constant flow of high purity inert gas during measurements. DSC/TG measurements were performed with a Netzsch STA 449C-Jupiter model using heating/cooling rates of 10 K/min. In this case the sample powders were evacuated prior to heating to remove adsorbed water. During the measurements a flow of Ar was maintained. Usually DSC curves from the second heating run were used for analysis.

Different compositions were observed to the right and to the left of the 1:2 composition (BaY_2F_8 phase), respectively. Figure 1 shows DSC curve obtained for 1:2 composition showing the melting peak in detail. More than one thermal effect seems to occur in a very short temperature range. Tkachenko *et al* [3] proposed that a polymorphous transition from a β - BaY_2F_8 to an α - BaY_2F_8 structure associated with small atomic displacements occurs. A phase transformation may occur some degrees below the BaY_2F_8 melting point, nevertheless, as it occurs at sufficiently high temperature defect healing can occur and single crystals of good quality can be grown from the melt. The second curve also showed in Figure 1, corresponds to one of the eutectic compositions at the phase diagram.

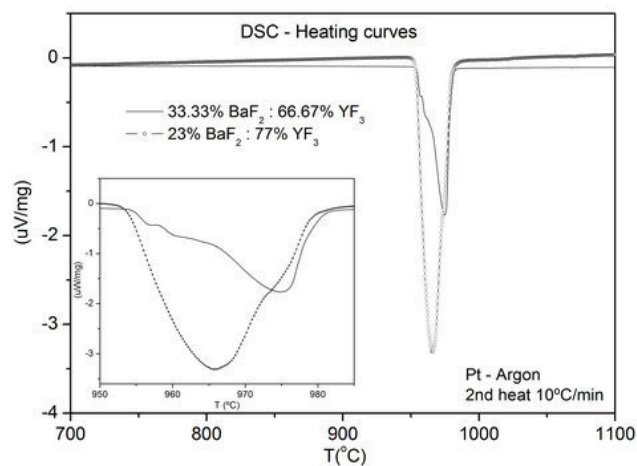


Figure 1. DSC heating curves obtained from second heating of two different compositions of YF_3 and BaF_2 .

Rietveld quantitative phase analyses were done using experimental CuK _{α} X-ray powder patterns obtained with the same samples prepared to thermal analyses. Rietveld analyses were performed by using the program DBWS-9807a [4]. The results are listed in Table 1. Pure and Nd, Er, Tb single doped and Nd:Dy co-doped crystals were obtained by zone melting (ZM) under fluorinating atmosphere. The choice of ZM was done taking into account the simplicity of the process when compared to other growth methods from the melt used in the production of small and high purity crystals as those required by diode pumping laser systems. ZM experiments were carried out in vitreous-carbon crucibles inserted in a platinum tubular reactor under HF flow. The total length of the ingots was about 290 mm and the length of the liquid zone was 26 mm. Experiments were performed using a zone speed rate of 2mm/h. The resulting crystals were characterized by spectroscopy and x-ray diffraction. The absorption spectra showed no evidence of incorporation of optically active impurities (except dopants) that could compromise their optical performance. The concentration of rare earth ions along the obtained zone melted ingots was measured by EDX showing uniform distribution.

(This work was supported by CNPq and CAPES).

References

- [1] S.L. Baldochi, S.P. Morato, Fluoride bulk crystals growth. In: K.H.J. Buschow, R.W. Cahn, M.C. Flemings, B. Ilshner, E.J. Kramer, S. Mahajan (eds.), *Encyclopedia of Materials: Science and Technology* (Elsevier Science Amsterdam, 2001) pp. 3200-3205.
- [2] E. G. Ippolitov, A.G. Maklachko, Inorg. Mater. (USSR) (Engl. Tranl.), 6 (1), (1970) 124.
- [3] N.L. Tkachenko, M. Svantner, B.P. Sobolev, Inorg. Mater. (USSR) (Engl. Tranl.), 13 (5), (1977) 693.
- [4] R.A. Young, A.C. Larson and C.O. Paiva-Santos., User's Guide to Program DBWS-9807a for Rietveld Analysis of X-ray and Neutron Powder Diffraction Patterns (Georgia Institute of Technology, Atlanta., 1999).

11:00

Invited oral

Large Fluoride Single Crystals by CZ method for the Next Generation Lithography

Eiichi Nishijima

Tokuyama Corporation, Shibuya Konno Bldg.3-1, Shibuya 3-chome, Shibuya-ku, Tokyo 150-8383, Japan

E-mail: e-nishijima@tokuyama.co.jp

In 2001, under the technical support by Prof. Fukuda from Tohoku University,

Tokuyama Corporation started to develop the large diameter Calcium Fluoride (CaF_2) single crystal by using Czochralski (CZ) method. The goal of this development is to get in operation of Fluoride Single Crystal Business. 'Large diameter', 'CZ method' and 'Fluoride materials' are 3 key words of our project. We have been established 4 core technologies, 'Large diameter single crystal growth', 'CZ method furnace', 'Mass production', 'Optical evaluation for Lithography', and also have been acquired 'processing' and 'annealing' technologies.

In 2004, we have become the first in the world to successfully grow ultra-large diameter (300mm) CaF_2 single crystals by the CZ technique. We made efforts to improve the crystal qualities in order to satisfy the requirements for optical material of next generation lithography.

A transmittance, a laser durability, a homogeneity of refractive index and a stress birefringence are the four major optical properties. Because of growth conditions have significant influence for the quality of single crystals, we have to carefully control the growth conditions such as temperature gradient, growth rate and melt convection. Also we need to optimize the annealing process to reduce the internal stress. As a consequence of our research, we find out the CZ method has some advantages and good properties in compare to another method. Last year, Tokuyama CaF_2 single crystals have been adopted by 193 nm lithography system. Now we have to establish mass production technology with a high productivity and stability. And also, we have been developed other fluoride materials such as MgF_2 and BaLiF_3 . The mission of this development is not only to market entry but also to suggest Tokuyama Research & Development capability.

11:30

Oral

Spiral growth of high melting point oxide crystals

Nebojša Crnogorac¹, Hermann Wilke¹, Andrew K. Cliffe²

1. Institute for Crystal Growth (IKZ), Max-born Str. 2, Berlin 12489, Germany 2. University of Nottingham, Nottingham, United Kingdom

E-mail: nesoc@ikz-berlin.de

The current importance of rare-earth scandate crystals (ReScO_3 ; $\text{Re}=\text{Y, La, Pr, Nd, Sm, Gd, Tb, Dy, Ho, Er, Tm and Lu}$) is initiated by commercial interest. For this reason a deeper investigation of Czochralski crystal growth from the melt at the Institute for Crystal Growth in Berlin (IKZ) is promoted. Rare-earth scandate crystals show good chemical and physical properties to be used as substrates of ferroelectric materials (e.g. non-volatile FeRAMs). Unfortunately

most scandate crystals tend to undesired spiral growth, i.e. symmetry breaking of an initially axisymmetric behaviour.

The melting point of scandate crystals is about 2000°C. Therefore internal measurements are hard to do and a numerical approach is mandatory. Nevertheless, we can monitor the temperature during the growth (Czochralski method) in a complicated setup at specific locations very close to the crucible. We use this data for comparison with numerical results.

Our objective is to figure out the reasons of spiral growth using a hydrodynamic approach. The hypothesis is that this undesired spiral instabilities are being initiated by heat and momentum disturbances in the melt [1]. The crystal grower is interested in getting stable parameters which do not lead to spiral instabilities.

To get such stable parameters the theoretical approach will lead to a full 3D model, while currently a 2D axisymmetric solution is superposed with a 3D disturbance. And this leads to a large scale eigenvalue problem which has to be solved efficiently. For this reason we are improving permanently our simulation tools (solver, eigensolver) in order to be efficient(time/cost).

Experiments have shown that some scandate crystals (e.g. GdScO_3) which are transparent with respect to thermal radiation do not tend to spiral growth. Therefore the numerical model must be extended to take into account the internal thermal radiation.

Using effective branch following techniques (bifurcation problem) it is possible to detect oscillatory behaviour, ambiguity of solutions and the general solution behaviour of our strongly non-linear system. This helps us to decide where an extended eigenvalue analysis should be performed in order to well characterize the solution type.

Further experiments have shown, that a change of crystal growth rotation direction implies a change of the direction of grown spiral. This behaviour is confirmed by numerical results also.

We are collaborating with our partners in Israel [2] in order to compare numerical results.

Our future work will focus on doing a full 3D approach using a more accurate model. This will require more computational performance and therefore we have to work out further improvements in our software.

References:

- [1] Numerical study of hydrodynamic instabilities during growth of dielectric crystals from the melt, H. Wilke, N. Crnogorac, K. A. Cliffe, Journal of Crystal Growth (2006), In press
- [2] A. Yu Gelfgat, School of Mechanical Engineering, Tel-Aviv University, Israel

11:45

Oral

Growth and characterization of dye doped KH_2PO_4 crystals for nonlinear optical applications

Ihor M. Prytula¹, Vladimir Y. Gayvoronsky², Yuri Gromov², Vyacheslav M. Puzikov¹, Alexandr N. Levchenko³, Marina I. Kolybaeva¹, Stanislav Bondarenko¹

1. Institute for Single Crystals NAS of Ukraine (ISC), 60 Lenin Ave., Kharkov 61001, Ukraine 2. Institute of Physics National Academy of Sciences of Ukraine, prosp. Nauki, 46, Kiev 0365, Ukraine 3. Kharkov National University, 4 Svoboda Sq., Kharkov 61077, Ukraine

E-mail: pritula@isc.kharkov.ua

As it is known, potassium dihydrogen phosphate KH_2PO_4 (KDP) crystal is a unique material, which attracts attention of specialists in various fields of science such as non-linear optics, quantum electronics, solid state physics. It is one of the best materials for transformation of laser radiation frequency (due to its high non-linear susceptibility). Moreover, KDP is widely used in electrooptics and is promising for bulk record of information as well as for other applications.

Recently it has been shown [1] that KDP is a remarkable general host for a wide variety of organic dyes. Therefore investigation of physical processes in dye inclusion crystals (DIC) with potassium dihydrogen phosphate as a host is a necessary step for creating DIC solid-state dye lasers on the base of nonlinear optical (NLO) media and thus is of considerable scientific and practical interest.

The aim of this work is to describe and discuss the experimental results concerning the influence of organic dye such as xlenol orange (XO) on the linear and nonlinear optical properties of the KDP crystals.

KDP single crystals were grown in the supersaturated solution containing an organic dye (xlenol orange). The potassium dihydrogen phosphate reagents were used as solutes, the concentration of impurities (Fe, Cr, Al, Sb, Bi, Cu, Hg, Ag, Pb) did not exceed $5 \cdot 10^{-5}$ wt. %. The content of XO dye in the crystals was determined by comparing the absorption spectra of the samples and the solutions with known dye contents. The absorption spectra were measured by UV-V-NIR spectrophotometer SF-56 (LOMO) and the luminescence spectra anisotropy was studied on "Hitachi F4010" fluorimeter with two linear polarizers.

It was shown that the triphenylmethane compound xlenol orange dyes the prism {100}, the pyramid {110} of the crystal remaining practically colorless. The performed study of anisotropy of the optical absorption and luminescence spectra shows that KDP/XO single crystals are intrasectoral zoned. In the prismatic part of the crystals the dye is distributed more uniformly in the crystal bulk in comparison with the pyramidal part. The dependences of the transmission coefficient on the angle between the direction of the electric vector of the incident light wave \mathbf{E} and the directions of the crystallographic axes were measured for determination the spatial orientation of the transition dipole moment. The angle value was varied in the interval from 0° to 360° with a step of 10° . The angular dependences were measured along all the crystal axes. It was shown that the dipole transition moments of the dye in the neighboring growth sectors of the prismatic (and pyramidal) crystal parts are oriented in two mutually perpendicular directions.

The NLO experiments were performed with the picosecond (~ 40 ps FWHM) mode-locked Nd:YAG laser at 1064 nm with far field spatial profile analysis technique. It was found that dye doping caused the photoinduced absorption of the crystals with saturation threshold at about 1 MW/cm^2 . The darkening of the samples is accompanied with selffocusing phenomenon of the laser beam. The highest nonlinear refractive index response was achieved for the annealed KDP:XO crystal (up to 150°C). The effective cubic nonlinear susceptibility $\chi^{(3)}_{\text{eff}} \sim 2.7 \cdot 10^{-8}$ esu was 1.7 times higher in comparison with a pure KDP crystal.

1. M. Kurimoto, L.D.Bastin, D.Fredrickson, P.N.Gustavson, S.-H.Jang, W.Kaminsky, S.Lovel, C.A.Mitchell, J. Chmielewski,

B.Kahr, Mat. Res. Soc. Symp. **620**, M9.8.1- M9.8.10 (2000).

2. Borshch A.A., Brodyn M.S., Gayvoronsky V.Ya. "Diagnostics of Optical Nonlinearities: Spatial Beam Distortion Technique and Its Application to Semiconductors and Novel Materials", Proc. SPIE **5024**, 128-136 (2003).

Coffee Break

Wednesday afternoon, 23 May, 12:00

Session IX: Nanostructures

Wednesday afternoon, 23 May, 12:30

Chair: Włodzimierz Nakwaski

12:30

Invited oral

Optical and Morphological Properties of Self-Assembled Quantum Dots Grown on Novel Index Surfaces

Mohamed Henini

University of Nottingham, Nottingham, United Kingdom

E-mail: mohamed.henini@nottingham.ac.uk

The study of strained heterostructures based on III-V semiconductors has attracted much interest due to the possibility of obtaining defect-free quantum dots (QD) by spontaneous self-assembling [1,2]. In particular, $\text{In}_{1-x}\text{Ga}_x\text{As}/\text{GaAs}$ QDs have good optical properties [3-5]. Recently, it has been shown that the photoluminescence (PL) properties of $\text{In}_{1-x}\text{Ga}_x\text{As}$ QDs on GaAs can be improved by growing the dots on high index (n11) substrates [6-9]. Also a clear morphological ordering of (311)B (InGa)As QDs has been observed [10,11].

In this talk I will report a study of the optical and microscopic properties of $\text{In}_{1-x}\text{Ga}_x\text{As}/\text{GaAs}$ heterostructures grown on various high index GaAs surfaces. The substrate orientation strongly affects the two-dimensional to three-dimensional growth mode transition.

References

- [1] L. Goldstein et al, Appl. Phys. Lett., 47, No.10, 1985, pp.1099-1101.
- [2] C. W. Snyder et, Phys. Rev. Lett., 66, No.23, 1991, pp.3032-3035
- [3] J. Oshinowo et al, Appl. Phys. Lett. 65, No. 11, 1994, pp.1421-1423.
- [4] K. Kamath et al, Appl. Phys Lett. 71, No. 7, 1997, pp. 927-929.
- [5] S. Raymond et al, Phys. Rev. B 54, No. 16, 1996, pp. 11548-11554.
- [6] K. Nishi et alJ. Appl. Phys. 80, No. 6, 1996, pp. 3466-3470.
- [7] D. I. Lubyshev et alJ. Vac. Sci. Technol. B 14, No. 3, 1996, pp. 2212-2215.
- [8] P. O. Vaccaro et al, J. Phys. D: Appl. Phys. 29, No. 9, 1996, 2221-2228.
- [9] R. Nötzel, Semicond. Sci. Technol. 11, No. 10, 1996, pp.1365-1379.

[10] K. Nishi et al, Appl. Phys. Lett. 70, No. 26, 1997, pp. 3579-3581.

[11] M. Kawabe et al, Jpn. J. Appl. Phys. 36, No. 6B, 1997, pp. 4078-4083

13:00

Oral

Self-organized eutectic microstructures for photonic crystals and metamaterials

Dorota A. Pawlak¹, Katarzyna B. Kołodziejak¹, Sebastian Turczynski¹, Krzysztof Rozniatowski², Ryszard Diduszko¹, Jarosław Kisielewski¹, Marcin Kaczkan³, Michał Malinowski³, Tadeusz Łukasiewicz¹

1. Institute of Electronic Materials Technology (ITME), Wólczyńska 133, Warszawa 01-919, Poland **2.** Warsaw University of Technology, Faculty of Materials Science and Engineering (InMat), Wołoska 141, Warszawa 02-507, Poland **3.** Warsaw University of Technology, Institute of Microelectronics & Optoelectronics (imio), Koszykowa 75, Warszawa 00-662, Poland

E-mail: Dorota.Pawlak@itme.edu.pl

There are already many sophisticated methods for obtaining photonic crystals and metamaterials. A simple way could be to obtain a material by self-organization. A very promising method for growth of self-organized micro- and nanostructures is based on directional solidification of eutectics. Eutectics are special materials which are both a MONOLITH and a MULTIPHASE MATERIAL.[1] Eutectics have two kinds of properties: additive and product properties. The additive properties depend on spatial distribution and volume fraction of the phases. The product properties depend on such structural factors as phase size or periodicity. Product properties can exist in the eutectic but not in the particular phases of the eutectic.[1] The product properties may define metamaterials, since “metamaterials are engineered composites that exhibit superior properties that are not found in nature and not observed in the constituent materials”. The eutectic microstructure can exhibit many geometrical forms. It can be regular-lamellar, regular-rod-like, irregular, complex regular, quasi-regular, broken-lamellar, spiral and globular. The most interesting from the point of view of photonic crystals would be the microstructures with regular shapes, i.e. lamellar and rod-like. For metamaterials applications the other shapes could be also of interest - for example the percolated structures (for giant dielectric constant); or the spiral one for chiral metamaterials. The general overview of the road of eutectics towards photonics as well as new experimental data will be presented.[2]

[1] J. Llorca, and V.M. Orera, *Progress in Mat. Sci.*, 51, 711 (2006).

[2] D. A. Pawlak, K. Kołodziejak, S. Turczynski, J. Kisielewski, K. Rozniatowski, R. Diduszko, M. Kaczkan, M. Malinowski, *Chem. Mat.*, 18, 2450, (2006).

Lunch

Wednesday afternoon, 23 May, 13:15

Session XI: Magnetic properties and superconductivity

Wednesday afternoon, 23 May, 15:00

Chair: Anna Pajaczkowska

15:00

Invited oral

Crystal growth and physical properties of the ternary Uranium compound $U_3M_3Bi_4$

Tomasz Klimczuk^{1,2}, Han-oh Lee¹, Filip Ronning¹, Eric Bauer¹, Michael F. Hundley¹, Joe D. Thompson¹

1. Los Alamos National Laboratory (LANL), Los Alamos, NM 87545, United States **2.** Gdansk University of Technology, Narutowicza 11/12, Gdańsk 80-952, Poland

E-mail: klimczuk@lanl.gov

Kondo insulator is one of the systems which got particular interest, but

not yet understood well. Metal-insulator (MI) transition by doping in these systems is one of the examples poorly understood. $U_3M_3Bi_4$ forms in

the same crystal structure with $Ce_3Pt_3Bi_4$, which is well known Kondo

insulator. We have succeeded in synthesizing new single crystals of $U_3M_3Bi_4$, where $M = Rh, Ni$, with metallic Kondo lattice and semiconducting behaviors, respectively. It provides the opportunity to

investigate metal-insulator transition in Kondo insulating system without affecting the crystal structure.

15:30

Invited oral

Kinetically trenches on bcc(110) for the formation of versatile magnetic nanowires

Olivier Fruchart, Bogdana Borca, Anthony Rousseau, Claire Meyer

CNRS, Institut Néel (NEEL), 25 rue des Martyrs, Grenoble 38042, France

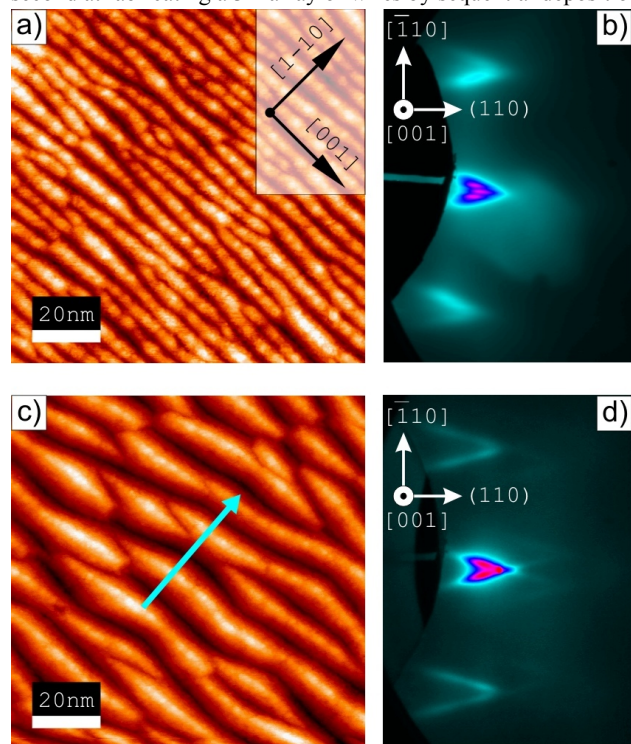
E-mail: Olivier.Fruchart@grenoble.cnrs.fr

We first optimized the fabrication of self-organized templates consisting of arrays of trenches aligned along [001] on cc(110) (cc=Mo,W). These are formed upon deposition of body-centered cubic elements (bcc) at moderate temperature (~300-550K depending on bcc), taking advantage of the anisotropy of atomic diffusion at the steps and/or of the Ehrlich-Schwoebel barrier. The kinetic building of roughness is self-limited owing to the relative stability of {210} facets, not noticed previously. Each atomic terrace of this vicinal facet is three atoms wide. Starting from a liquid-type order, this favors the ordering of the array of grooves. The order was evidenced by satellites on RHEED patterns, whose spacing is in agreement with STM. The lateral period is influenced by the nucleation temperature, while growth proceeds at 150°C. Periods in the range 4-12nm were already demonstrated, with a depth of grooves 0.8-2.5nm, respectively.

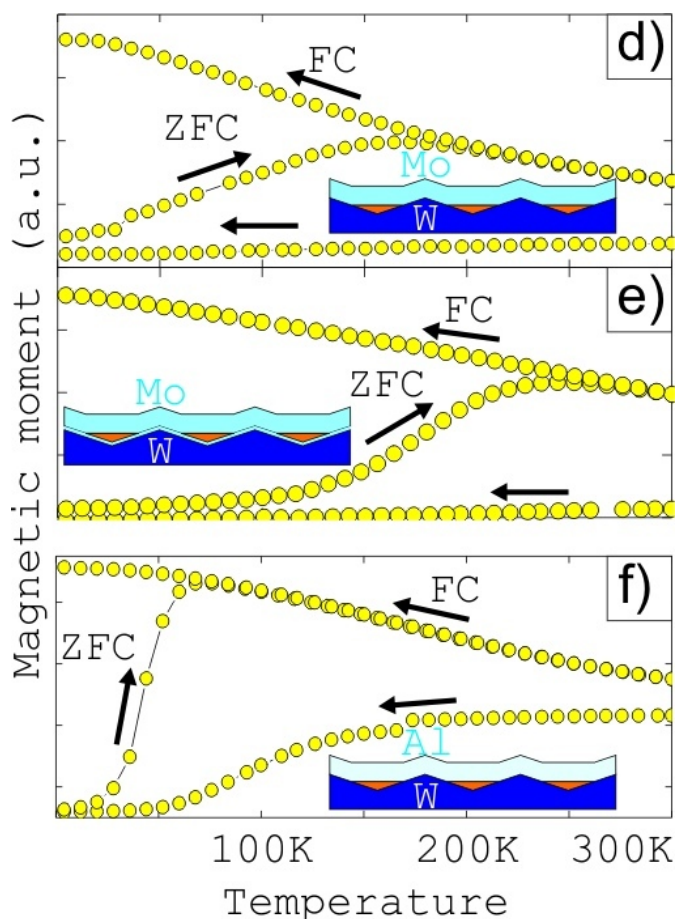
Then, upon deposition at 150°C Fe(110) grows layer-by-layer, progressively filling the grooves and thus forming magnetic wires. Auger-Electron Spectroscopy suggests that only partial wetting of the terraces of the microfacets occurs before Fe wires are formed.

We will report the magnetic properties of Fe wires with a period 10nm, width=7nm and height=1.5nm, deposited on W grooves. The surface was capped with Mo for ex situ measurement with Squid. For W\Fe\Mo the easy axis of magnetization lies along [001], and the mean blocking temperature is 100K. We have started to engineer the anisotropy of the wires using interfacial magnetic anisotropy. When the capping of Mo is replaced with Al the magnetic anisotropy is reduced as expected from this films studies, and so does the superparamagnetic temperature. On the reverse when a Mo bi-layer is inserted between W and Fe the magnetic anisotropy of the wires along [001] is increased. This again is expected from thin films data, as W/Fe interfaces weaken the anisotropy along [001], while Mo/Fe interfaces reinforce it. The mean blocking temperature could thus be raised to 200K.

Current efforts target first at raising the average blocking temperature above 300K by further engineering the magnetic anisotropy, and second at fabricating a 3D array of wires by sequential deposition.



STM view of W(110) trenches with (a) small and (c) large period, and associated RHEED patterns with the beam azimuth along the trenches. The half-angle of the arrows (approx. 18°) reveals the tilt of the facets of the trenches, of type {210}.



Zero-field-cooled/Field-cooled magnetization curves, revealing the blocking temperature for three samples with different cappings or underlayers, as sketched in the insets.

References:

1. Kinetic self-organization of trench templates for the fabrication of versatile ferromagnetic nanowires, B. Borca, O. Fruchart, Ph. David, A. Rousseau, C. Meyer, **cond-mat/0701304**
2. Growth modes of Fe(110) revisited: a contribution of self-assembly to magnetic materials, O. Fruchart, M. Eleoui, P.-O. Jubert, Ph. David, V. Santonacci, A. Liénard, F. Cheynis, B. Borca, M. Hasegawa, C. Meyer, **J. Phys. : Cond. Mat.** **19** (5), 053001 (2007). (topical review)

16:00

Oral

Single crystals of MgB_2 : synthesis, substitutions and properties

Janusz Karpinski¹, Nikolai D. Zhigadlo¹, Sergiy Katrych¹, Roman Puzniak², A. Wisniewski², K. Rogacki³

1. Laboratory for Solid State Physics ETH (ETH), Schafmatstr. 16, Zürich 8093, Switzerland
2. Polish Academy of Sciences, Institute of Physics, al. Lotników 32/46, Warszawa 02-668, Poland
3. Polish Academy of Sciences, Institute of Low Temperature and Structure Research (INTiBS), Okólna 2, Wrocław 50-422, Poland

E-mail: karpinski@phys.ethz.ch

Structural and superconducting properties of MgB_2 are strongly anisotropic. Therefore investigations of its intrinsic properties should

be performed on single crystals rather than on polycrystalline samples with randomly oriented grains. Unfortunately, conventional methods of crystal growth did not work for MgB_2 . High temperature solution growth in metals (Mg, Al, Cu, etc.) at normal pressure used for other borides is not possible due to very low solubility of MgB_2 in these metals or formation of other compounds. The solubility of MgB_2 in Mg is extremely low up to the boiling temperature of Mg (1107°C) at ambient pressure. At higher temperature solubility increases, but partial pressure of Mg vapor above molten Mg increases with temperature, at temperature of crystal growth ($1800\text{--}2200^\circ\text{C}$) is very high and using of high pressure methods is necessary. Single crystals of MgB_2 have been grown from flux with a high-pressure cubic anvil technique. Investigations of the P – T phase diagram prove that the MgB_2 phase is stable up to 2200°C at high hydrostatic pressure. Superconducting and normal state properties of pure MgB_2 are now well evidenced by experiments and explained by theory. However, modification of properties through chemical substitutions is still not well understood. Specific band structure of MgB_2 with two bands, π and σ , involved in superconductivity is strongly influenced by chemical substitutions. Substitutions of Al for Mg and C for B dope MgB_2 with electrons and lead to increase of scattering within both π and σ bands, however, with different rates for both elements. Therefore, different changes of the upper critical field, H_{c2} , and its anisotropy, γ_{Hc2} , for $\text{Mg}_{1-x}\text{Al}_x\text{B}_2$ and $\text{MgB}_{2-x}\text{C}_x$ are observed. By introduction of C, Al, Li, Mn, Fe in the melt we were able to substitute partially Mg or B in MgB_2 crystals and to dope the crystals with electrons or holes. Hole doping with Li decreases superconducting transition temperature, T_c , but in much slower rate, than electron doping with C and Al. In the crystals co-doped simultaneously with both Li and C or Li and Al one can expect compensation of electron doping with C or Al by holes from Li and increase of T_c . In this presentation the review of the results of crystal growth of pure and substituted MgB_2 crystals as well as investigations of the structure and superconducting properties is given.

16:15 Oral

Ferroelectric and relaxor properties of strontium-barium niobate

Jan Dec^{1,2}, Wolfgang Kleemann², Seweryn Miga¹, Vladimir Shvartsman², Tadeusz Łukasiewicz³, Marek A. Swirkowicz³

1. University of Silesia, Institute of Physics, Uniwersytecka 4, Katowice 40-007, Poland 2. Angewandte Physik, University Duisburg-Essen, Lotharstr. 1-21, Duisburg 47048, Germany 3. Institute of Electronic Materials Technology (ITME), Wólczyńska 133, Warszawa 01-919, Poland

E-mail: dec@us.edu.pl

Strontium-barium niobates $\text{Sr}_x\text{Ba}_{1-x}\text{Nb}_2\text{O}_6$ (SBN) are environmental friendly (lead free) polar materials. Their potential applications are based on very attractive pyroelectric, electromechanical, electro-optic, photorefractive, and nonlinear optical properties. By changing the ratio between strontium and barium components one may tune the system from a conventional ferroelectric ($x < 0.5$) to an extreme relaxor ($x > 0.6$) behaviour while maintaining the structure unchanged.

In this contribution we present results of systematic investigations of

the dielectric response measured along the polar c -axis of the four single crystalline compounds with nominal $x = 0.40, 0.50, 0.61$ and 0.75 , designated hereafter as SBN40, SBN50, SBN61, and SBN75, respectively. Temperature dependences of the linear dielectric susceptibility reveal a gradual crossover from the conventional ferroelectric (SBN40) to extreme relaxor (SBN75) behaviour. Analysis of the data within the framework of the Fisher law shows that the Curie point of ferroelectric SBN40 is a linear extrapolation of the transition temperatures determined for the other SBN crystals. Correspondingly, a change from the "normal" compact domains to the smaller ones with jagged (fractal-like) boundaries was revealed by piezoresponse force microscopy (PFM).

The dielectric spectra of SBN61 and SBN75 disclose two distinct slow dynamics modes. They refer to the borders of mesoscopic polar nanoregions (PNRs) embedded in the neutral paraelectric environment. Due to their very broad size distribution the largest PNRs become visible by PFM.

From the nonlinear dielectric response the nonlinearity coefficient B appearing in the equation of state is determined. It is found to decrease when approaching the phase transition point even in the extreme relaxor crystal. This kind of behaviour shows that the uniaxial SBN relaxor cannot be considered as a dipole glass system.

Financial support by KBN (under grant 4 T08A 007 25) and DFG (SPP "Strukturgradienten in Kristallen") is gratefully acknowledged.

Coffee Break

Wednesday afternoon, 23 May, 16:30

Session XII: Theory and kinetics

Wednesday afternoon, 23 May, 17:00

Chair: Ewa Talik

17:00 Invited oral

Growth morphology of crystals from kinetic and geometric perspective

Jolanta Prywer

Technical University of Łódź, Institute of Physics, Wólczańska 219, Łódź 93005, Poland

E-mail: jolanta.prywer@p.lodz.pl

During the growth process crystals take a variety of habits. The question why and how do crystals form such a wide variety of habits was posted in the seventeenth century [1] and is still of vital importance. The question is important not only for modern technology but also to understand the formation of minerals and crystals in living organisms. For crystals whose growth cannot be observed in situ, e.g. rock-crystals, crystals formed in living bodies or crystals synthesized by high temperature solution or hydrothermal solution methods the crystal morphology is a very important source of information [2]. The morphologies that crystals take result from the internal and external factors. To external factors we may include, for example, supersaturation or temperature, while to internal, for example specific symmetry of crystal.

In this paper we focus on the correlation between the crystal geo-

metry, the evolution of individual surfaces, their morphological importance and stability. The presented analytical view pays attention to the big role, not appreciated enough so far, of crystal geometry in the formation of the final crystal morphology. In particular we show that for specific geometry characterized by interfacial angles the given face can increase in size for a very wide range of relative growth rates and need not be the slow-growing face [3]. Even growing faster than the neighbouring faces, such a face increases its size. On the other hand, there are other faces with other specific geometry which can decrease the size growing more slowly than one of the neighbouring faces. If the growth time is long enough, such a face may disappear and not be represented in the final crystal morphology. We show also that the seed-faces may influence crystal morphology modifying the evolution of directly neighbouring faces. The scale of such an influence depends, among other factors, on the geometry of a given crystal. This influence of seed-faces is the most significant for short growth time, however, seed-faces may also modify crystal morphology after a very long growth time. All these theoretical predictions are verified by computer experiments performed for various faces of different crystals or by real experiments performed for potassium dichromate (KBC) crystals grown by the method of decreasing temperature.

The presented geometric point of view in connection with the standard crystal growth models, as Burton-Cabrera-Frank (BCF) model [4], may give more comprehensive understanding of the crystal morphology formation and of interconnection between the external and internal factors, which determined the morphology of crystals.

1. N. Steno, *De solido intra solidum naturaliter contento dissertationis prodromus*, Florence (1669); English translation by J. G. Winter: *The Prodromus of Nicolaus Steno's Dissertation Concerning a Solid Body Enclosed by Process of Nature Within a Solid*, Hofner, New York, (1968).
2. I. Sunagawa, *Crystals, growth, morphology and perfection*, Cambridge University Press, Cambridge 2005
3. J. Prywer, *Prog. Cryst. Growth Charact.* 50 (2005) 1.
4. W.K. Burton, N. Cabrera, F. Frank, *C. Philos. Trans. Roy. Soc. Lond. Ser. A* 244 (1951) 299.

17:30 Oral

Modelling of the growth of nitrides in ammonia rich environment

Stanisław Krukowski^{1,3}, Paweł Kempisty^{1,2}, Paweł Strąk²

1. *Polish Academy of Sciences, Institute of High Pressure Physics (UNIPRESS), Sokolowska 29/37, Warszawa 01-142, Poland*
2. *Warsaw University of Technology, Faculty of Physics, Koszykowa 75, Warszawa 00-662, Poland*
3. *Warsaw University, Interdisciplinary Centre for Materials Modelling (ICMM), Pawin-skiego 5a, Warszawa 02-106, Poland*

E-mail: stach@unipress.waw.pl

Nitride epitaxy methods can be divided into two categories: plasma-activated and ammonia sources of active nitrogen. The first is essentially limited to PA-MBE, which has relatively limited use at present. The method was analyzed using ab-initio approach by Neugebauer et al [1]. It was shown that the growth occurs in Ga-rich

environment, allowing effective surface diffusion of nitrogen ad-atoms.

Ammonia-based variants of nitride growth include: ammonia-MBE, MOVPE, HVPE and also ammonothermal methods. They constitute dominant portion of nitride epitaxy and considerable portion of the growth of bulk nitrides. In all these methods growth occurs in highly dominant nitrogen-rich environment.

Ammonia based methods have not been analyzed using ab initio methods in much detail. Recently it was shown however, that the state GaN(0001) surface is opposite to PA MBE method [2] -the GaN(0001) surface remains in nitrogen rich state.

The results of the ab initio calculations and their consequences to the basic growth processes: adsorption, desorption and surface diffusion of the growth controlling species: Ga, Al and In will be discussed. Their influence on the Al and In segregation related to surface morphology and growth mechanism will be analyzed.

[1] Neugebauer J., Zywiets-TK, Scheffler-M, Northrup-JE, Huajie-Chen, Feenstra-RM, *Physical-Review-Letters*. 7 Feb. 2003; 90(5): 056101/1-4

[2] Kempisty P. Krukowski S. *Journal ofCrystalGrowth* 2007, doi:10.11016/j.jcrystgro.2006. 12057

Banquet - Doctoral dissertation - PTWK prize

Wednesday evening, 23 May, 20:00

Thursday, 24 May

Session XIII:Organic and soft crystals

Thursday morning, 24 May, 8:30

Chair: Keshra Sangwal

8:30 Invited oral

Crystallization, Crystal Growth and Characterization of Biological Macromolecules by X-ray Diffraction and Atomic Force Microscopy

Abel Moreno

National University Autonomous of Mexico (UNAM), Circuito Ext. S/N Cd. Universitaria, México 04510, Mexico

E-mail: carcamo@servidor.unam.mx

Most of the scientific contributions in biological chemistry have been devoted to the knowledge of the 3D structure of specific biomolecules for different applications in biomedical sciences. However, few scientific contributions have been focused on investigating the physical and chemical parameters of these biological molecules to be applied in crystal growth, and the enhancement of crystal quality for 2D and 3D structural characterization. In this work, it is presented in the first part of the talk a short review of methods of crystal growth of a variety of biological macromolecules. In the second part, as a case study it is presented the purification, crystallization, and high resolution X-ray crystallographic structure of cytochrome c (an electron-transfer protein isolated and purified from the

mitochondria of bovine's heart). Additionally, a new approach to the design of a novel electron-transfer biosensor using cytochrome c films coupled with Indium Tin Oxide electrodes for 2D structural characterization is presented. This investigation was performed by using an Atomic Force Microscope (EC-AFM) coupled to electrochemical analysis (Digital Co Santa Barbara). Finally, as a second case study this methodology allowed us also to develop a novel selective biosensor of alkaline cations, and carbonates by means of using proteins involved in biomineralization processes.

Acknowledgements: The author gives thanks for the financial support from the DGAPA-UNAM project number IN214506

9:00

Invited oral

Synchrotron Radiation X-ray Diffraction Study for Observation of the Crystallization through Interfacial Heterogeneous Nucleation of Oil-in-Water Emulsion

Satoru Ueno

Hiroshima University, Graduate School of Biosphere Sciences, Kagamiyama 1-4-4, Higashi-Hiroshima 739-8528, Japan

E-mail: sueno@hiroshima-u.ac.jp

Crystallization on encapsulated systems such as micelles, vesicles, emulsions, cubic phases etc, are highlighted recently because it will be potentially able to control nucleation and crystal growth rate, and to select the crystallization of the special polymorphs. In this presentation, crystallization of oil droplet in oil-in-water emulsion system are focused on the following two results: (i) crystallization of new polymorph appeared in oil phase of n-hexadecane-in-water emulsion measured by time-resolved synchrotron radiation small- and wide-angle X-ray scattering (SAXS/WAXS) and differential scanning calorimetry (DSC) simultaneous method. In more detail, n-hexadecane-water emulsion system was prepared by high-pressure homogenization techniques. The average droplet size was ~1 micro meter. Tween 20 was put as an emulsifier. When the high-melting hydrophobic emulsifiers was added to n-hexadecane, the model of oil phase in O/W emulsion, the hexagonal and orthorhombic type polymorphs appeared as new polymorphic forms in O/W emulsion together with triclinic type polymorph which was observed only in bulk system. These new polymorphs would be crystallized on the oil-water interface of oil droplets after the added high-melting hydrophobic emulsifiers crystallized. In other words, the high melting emulsifier plays a role of the template for heterogeneous nucleation and following crystal growth of the new polymorphs. These new polymorphs were observed more than 0.1 wt% concentration of the high-melting emulsifiers. On the other hand, no new polymorph was observed without high-melting hydrophobic emulsifiers added in the oil phase of O/W emulsion. However, when we prepared the larger droplet size, such as 30 or 40 micro meter, of n-hexadecane droplet in O/W emulsion system, the transient rotator phase, meaning hexagonal phase, was observed without any high-melting emulsifiers in oil droplet of O/W emulsion. (ii) Clarifying the template effect occurred on the oil-water interface described above, synchrotron radiation micro-beam analysis has been done. The 5 x 5 micro meter-sized micro-beam is hit a specific area in an oil droplet and the diffraction from the area is detected. The 30 ~ 50 micro meter droplet samples were prepared. Imaging plate and image intensifier connec-

ted with CCD camera type two dimensional detector were employed. When the micro-beam was hit the center of a droplet, a circle-like diffraction peaks appeared, meaning a lot of small single crystals existed. On the other hand, when the micro-beam was hit the edge of a droplet, i.e. the oil-water interface, arc-like diffraction peak appeared. In addition, the micro-beam was hit the edge rotated the right angle from the previous edge of the same droplet, arc-like diffraction peak rotated the right angle appeared, meaning the existence of the lamellar structure along the oil-water interface. The same kind of result has been obtained in the triacylglycerol-in-water emulsions. From above results, it is clear that the heterogeneous nucleation occurred on the oil-water interface of oil droplet of oil-in-water emulsion.

9:30

Oral

Growth of Unidirectional Semi-organic and Inorganic single crystals from solution by Sankaranarayanan-Ramasamy (SR) method and their characterization

Gopalakrishnan Rengasamy¹, Ramesh babu Ramraj¹, Sethuraman Kunjidapadham¹, Ramasamy Perumalsamy²

1. AnnaUniversity (AU), Sardar Patel Road, Guindy, Chennai 600025, India **2.** Centre for crystal growth, SSN college of engineering, kalavakkam, Chennai 603110, India

E-mail: krgrkrishnan@annauniv.edu

Defect free bulk single crystals are needed for electronic industries because of their usage in the field of semiconductor, nonlinear optical, piezoelectric devices and so on. The research on organic crystals in application point of view was started during 1980's. For practical applications, we need good optical transparency and also crystal should withstand high optical powers, and should have chemical stability. It is difficult to find a material that satisfies most of the above said requirements, however, amino acid crystals are good candidates for NLO applications. Especially, the complex of amino acid and strong inorganic acid plays a vital role in SHG applications. Several authors grew a number of organic-inorganic complex based crystals. Most of these complexes are exhibiting SHG.

There are different techniques to grow bulk crystals in which melt and solution growth techniques are mostly used. The main advantages of solution growth method are convenience, simplicity and the possible avoidance of complex growth apparatus. The use of high purity solvent and solute and low viscosity of solution can give controlled supersaturation in growth. In conventional solution growth technique, there are different methods (viz. slow evaporation, slow cooling and temperature gradient methods) employed to grow bulk single crystals, however, a newly discovered novel method called "Sankaranarayanan-Ramasamy (SR) method" [1-2] gives bulk unidirectional crystals with good quality from solution.

We have employed this technique to grow the technologically important Ammonium Dihydrogen Orthophosphate (ADP) and unidirectional <110> ammonium dihydrogen orthophosphate (ADP) single crystal was grown by Sankaranarayanan-Ramasamy (SR) method. <110> orientational seed was mounted at the bottom of the glass crucible and the crystal of diameter 20 mm and length of 60 mm was successfully grown by this novel SR method [3]. Almost hundred percent solute-crystal conversion efficiency was achieved.

Also, 70mm length and 18mm dia. uni-directional bulk semi organic nonlinear optical single crystal of L-Lysine monohydrochloride dihydrate (L- LMHCl) has been grown by Sankaranarayanan-Ramasamy (SR) method for the first time in the literature [4]. The growth rate was 5mm/day. The optical transparency of the grown crystal was measured. The results will be presented in detail.

References

- [1] K.Sankaranarayanan and P. Ramasamy, J. Crystal Growth 280 (2005) 467.
- [2] K. Sankaranarayanan, J. Crystal Growth, 284 (2005) 203.
- [3] K.Sethuraman, R.Ramesh babu, R.Gopalakrishnan and P.Ramasamy J. Crystal Growth 294 (2006) 349
- [4] R.Ramesh Babu, K.Sethuraman, R.Gopalakrishnan and P.Ramasamy J. Crystal Growth 297(2) (2006) 356-360

Coffee Break

Thursday morning, 24 May, 9:45

Session XIV:Optical and other crystals

Thursday morning, 24 May, 10:15

Chair: Miroslaw Drozdowski

10:15

Invited oral

Crystal growth of oxides by Optical Floating Zone techniques

Antoni Dabkowski

Brockhouse Institute for Materials Research, McMaster University, 1280 Main Street West, Hamilton L8S4MI, Canada

E-mail: dabko@mcmaster.ca

ABSTRACT

The crystal growth using Optical Floating Zone (OFZ) technique (employing halogen lamps and ellipsoidal mirrors for heating) is gaining importance since the first systems were introduced into the market in the '80. The growing number of OFZ apparatus used, proves the usefulness of this method in the growth of various complex oxides including high temperature superconductors, new magnetic materials and complex oxides with "exotic" oxidation states of some cations. Wide range of materials including metals, intermetallic compounds and semiconductors have been grown by this method. Crystals grown by the OFZ technique are of high quality but relatively small (usually not bigger than few mm in diameter and few cm long) so the majority of the work concentrates on exploratory growth of new materials - mainly for research purposes. There is limited industrial application of this method ($Y_3Fe_5O_{12}$, TiO_2 and $\beta-Ga_2O_3$). The Laser Heated Pedestal Growth (LHPD) technique used for growth of oxide fibres for optical applications is an important variation of the FZ technique.

OFZ requires the starting material to be prepared in the form of high density, uniform ceramic rods ("feed rods") and the quality of these rods is very important for the stability of the crystal growth process. Limited number of growth parameters (power, translations and rota-

tions of crystal and feed rod) are accessible during the growth process and they can vary over a wide range depending on the material grown. The growth of incongruently melting oxides is possible using a variation of this technique called Travelling Solvent Floating Zone (TSFZ). This is interesting for exploration of new materials. In such a case a high temperature solution (flux) can be used or a "practical" steady state can be achieved in the self-flux approach. In all cases, some information about the phase diagram of materials to be grown is very important. OFZ method is also very well suited for producing crystals of solid solutions. The pressure and composition of growth atmosphere are both important to stabilize a phase with appropriate oxidation states of cations. Additionally, high pressure capabilities of some systems can help to grow volatile materials.

In this presentation the advantages and disadvantages of the FZ technique for growth of crystals of congruently and incongruently melting oxides and their solid solutions will be discussed. Additionally, important problems of crystal characterization and assessment of micro and macro defects will be presented.

10:45

Oral

Growth and investigation of optical properties of YAG:Co,Si single crystals.

Andrzej L. Bajor¹, Jarosław Kisielewski¹, Krzysztof Kopczynski², Tadeusz Łukasiewicz¹, Jadwiga Mierczyk², Dorota A. Pawlak¹, Marek A. Swirkowicz¹

1. *Institute of Electronic Materials Technology (ITME), Warszawa 01919, Poland* **2.** *Military University of Technology, Institute of Optoelectronics (IOE), Kaliskiego 2, Warszawa 00-908, Poland*

E-mail: Andrzej.Bajor@itme.edu.pl

Since our primary attempts to use Czochralski-grown YAP:Co,Si as Q-switching elements have failed, we also developed new technology of growth and thermal reduction of yttrium aluminium garnet (YAG) crystals doped with Co and Si. The crystals were found to be a promising material for optical applications, and especially useful as non-linear absorber (Q-switches) working in a broad spectral range of approx. 1150 to 1700 nm. Besides, it has a considerable absorption band around 600 nm which makes it useful in diode pumped lasers.

YAG:Co,Si single crystals were grown by the Czochralski method using Cyberstar Oxypuller. Thermal system consisted of iridium crucible of 50 mm diameter and a passive iridium afterheater of 60 mm diameter. Inductive heating with Hüttinger generator was used. It was very important that the cobalt ions were incorporated in specific locations in the crystalline lattice. To obtain this, we grew our crystals in nitrogen atmosphere with admixture of oxygen (1 vol. %), and the as-grown boules were next annealed in reducing atmospheres. As a result, good quality single crystals, [111]-oriented, with cobalt content of 0.4 at.% to 1.6 at.% and silicon content of 0.2 at.% to 0.6 at.% were obtained. They were up to 25 mm in diameter and up to 80 mm in length.

By spectroscopic and polariscopic investigations we have also found that the crystals were optically homogeneous. The absorption coefficient was exceeding 8 cm^{-1} in the best crystals doped with largest concentration of Co, and this makes our crystals magnificent material for Q-switching device.

Coffee Break

Thursday morning, 24 May, 11:00

Session XV: Optical characterization

Thursday morning, 24 May, 11:30

Chair: Wojciech Sadowski

11:30

Invited oral

Phonons and local modes around paramagnetic defect centers in solids studied by electron spin relaxation

Stanisław K. Hoffmann

Institute of Molecular Physics, Polish Academy of Sciences, Smoluchowskiego 17, Poznań 60-179, Poland

E-mail: skh@ifmpan.poznan.pl

Defects can appear accidentally or intentionally in crystalline solids. Question is if a defect participates in phonon motions of a host lattice or it has its own dynamics. If so, what is a coupling between defect motions and collective motions of the crystal lattice? These questions are important in doped semiconductors, and in solids where defects are generated for modification of physical properties.

Phonons spectra are available for rather simple inorganic solids and can be theoretically calculated or measured by neutron scattering technique. The phonon spectra usually deviate significantly from Debye-type phonon spectra presented in most of textbooks of solid-state physics. Vibrations of a simple defect appear in a narrow frequency range are called local mode. Because of a low defect concentration the local modes can be not detected by neutron scattering, but can be detected by classical spectroscopy methods. Local modes can be identified by Raman and IR spectroscopy when appear in an optical phonon region. Local modes appearing in acoustic phonon region are difficult to observation. They can be detected in studies of electron spin relaxation measured by pulsed electron paramagnetic resonance methods. Electron spin system of paramagnetic defects after a pulse excitation relaxes (in time order of micro- to milliseconds) to initial equilibrium transmitting the excitation energy to phonons and/or to local mode of the defect. A method of local mode detection with electron-spin echo will be described and results will be presented for paramagnetic ions doped into inorganic and organic solids and for free radicals generated by ionizing radiation in crystals.

[1] J. Murphy, Spin-lattice relaxation due to local vibrations with temperature independent amplitudes, *Phys. Rev.* 145, 241-247 (1966)

[2] J. Goslar, S. K. Hoffmann, W. Hilczner, Local vibration mode mechanism of electron spin-lattice relaxation of PO_3^{2-} -radicals in g-irradiated (glycine) H_3PO_3 crystal, *Sol. State Comm.* **121**, 423-427 (2002).

[3] S. K. Hoffmann, W. Hilczner, T. Radczyk, Electron spin-lattice relaxation in polymers and crystals related to disorder and structure defects. *Acta Phys. Pol. A* **103**, 373-385 (2003).

12:00

Invited oral

Spectroscopic methods in characterization of crystals and nanopowders

Witold Ryba-Romanowski

Polish Academy of Sciences, Institute of Low Temperature and Structure Research (INTiBS), Okólna 2, Wrocław 50-422, Poland

E-mail: ryba@int.pan.wroc.pl

The purpose of this presentation is to outline spectroscopic methods that proved to be useful in characterization of crystalline materials. In general understanding the notion "spectroscopic" encompasses a wide variety of methods, e.g.: NMR, EPR, Mossbauer spectroscopy, optical spectroscopy etc. They differ in basic concepts and methodology. For the sake of clarity and conciseness the topic of presentation is restricted to spectroscopic methods that make use of optical frequencies and rely on acquisition and analysis of optical absorption and emission spectra and emission kinetics. They can be applied to crystals showing inherent ability to absorb and/or emit radiation as well as to crystals endowed with this ability by intentional doping with "probe" ions such as Eu, Cr. Principles of methods and also various kinds of information that can be extracted from analysis of spectral line positions, line-shapes and luminescence decay curves are considered. Examples of typical applications and results from our work are included.

12:30

Oral

The effect of thermal treatment on the photorefractive properties of Ru-doped lithium niobate

Chang-Hung Chiang¹, Jyh-Chen Chen¹, Chung-wei Lu²

1. National Central University, Department of Mechanical Engineering, Chung-Li 32001, Taiwan **2.** Department of Information Management, Jen-Teh Junior College, Hou- Lung,, Miao-Li 35664, Taiwan

E-mail: s9323061@cc.ncu.edu.tw

The effect of thermal treatment on the photorefractive properties of Ru-doped lithium niobate was studied. First, lithium niobate (LiNbO_3) single crystals doped with Ruthenium (Ru) were grown by the Czochralski method. In this study, the six samples of $\text{Ru}:\text{LiNbO}_3$ crystals, two as-grown (with 0.01mol% and 0.065 mol% RuO_2 , respectively), two oxidized ones (with 0.01mol% and 0.065 mol% RuO_2 , respectively), and two reduced ones (with 0.01mol% and 0.065 mol% RuO_2 , respectively), were prepared. Ru ions have three valences Ru^{3+} , Ru^{4+} , and Ru^{5+} . The concentrations of each Ru ions valence in lithium niobate would be altered with different conditions of thermal treatment. To get the oxidized crystal, the as-grown crystals were placed under the O_2 atmosphere at the 1000°C for 12h. The oxidized treatment was changed the Ru valences in the as-grown crystal from Ru^{4+} to Ru^{5+} and increased the ratio of $\text{Ru}^{5+}/\text{Ru}^{4+}$. To get the reduced crystal, the as-grown crystals were placed under the 100ppm CO/CO_2 mixture atmosphere at the 1000°C for 12h. The reduced treatment was changed the Ru valences in the as-grown crystal from Ru^{4+} to Ru^{3+} and increased the ratio of $\text{Ru}^{3+}/\text{Ru}^{4+}$. Fig. 1 shows the 0.01mol% $\text{Ru}:\text{LiNbO}_3$ crystals with as-grown, oxidization, and reduction respectively. Fig. 2 shows the

0.065mol% Ru:LiNbO₃ crystals with as-grown, oxidization, and reduction respectively. We can see that the color of the as-grown Ru:LiNbO₃ crystal is orange and darkened as the Ru concentration increased. In addition, the color of oxidized crystals are lighter slightly, the color of oxidized crystals are darkened and had a little puce. Fig. 3 and 4 show the absorption spectra of as-grown, oxidized, and reduced Ru-doped LiNbO₃ crystals with different Ru concentrations. We can observe that there is a absorption peak centered around on 530nm in the Ru:LiNbO₃ crystals, and the absorption coefficient increase as the RuO₂ dopant concentration increases. Furthermore, the absorption coefficients at 530nm decrease after the oxidized treatment and increase after the reduced treatment.

In addition, the photorefractive properties of the Ru: LiNbO₃ crystals will be changed by different valences of Ru dopant. They were investigated with the two-beam coupling method. The diffraction efficiency, holographic writing time constant, erasing time constant, the sensitivity, and the dynamic range of Ru-doped LiNbO₃ crystals after different thermal treatment conditions would also be discuss in this study.

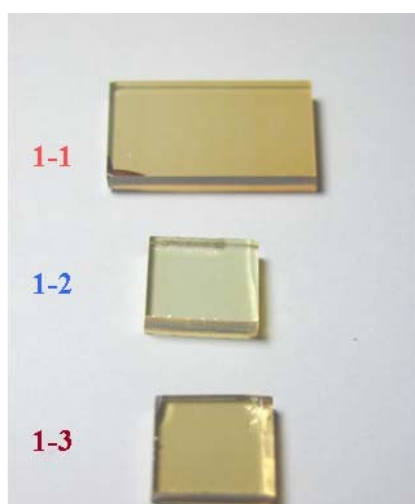


Fig. 1 Photography of 0.01mol%Ru:LiNbO₃ crystals with different thermal treatment conditions; 1-1:As-grown; 1-2: Oxidization; 1-3: Reduction.

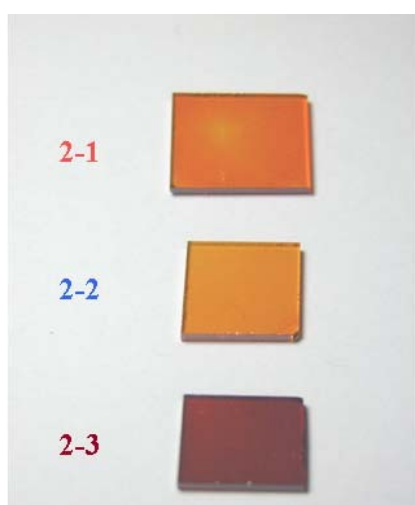


Fig. 2 Photography of 0.065mol%Ru:LiNbO₃ crystals with different thermal treatment conditions; 2-1:As-grown; 2-2: Oxidization; 2-3: Reduction.

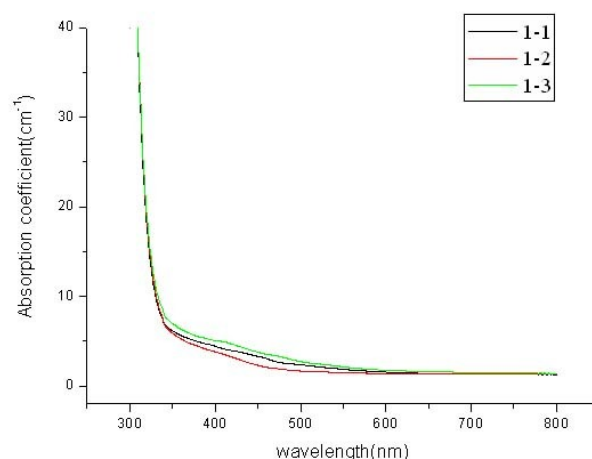


Fig. 3 Absorption spectra of 0.01mol%Ru:LiNbO₃ crystals with different thermal treatment conditions.

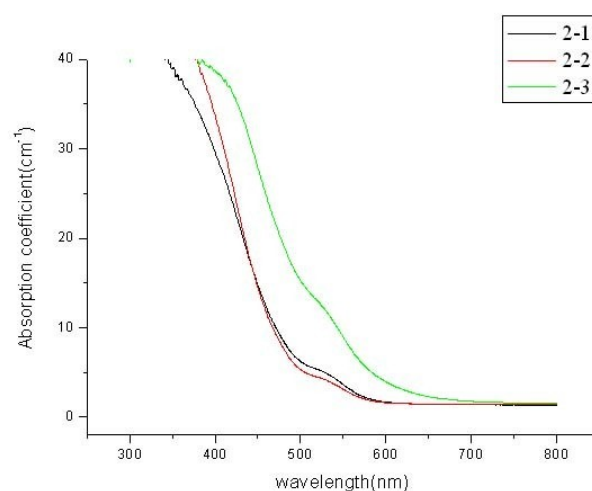


Fig. 4 Absorption spectra of 0.065mol%Ru:LiNbO₃ crystals with different thermal treatment conditions.

Closing

Wojciech Sadowski

Thursday afternoon, 24 May, 12:45

Lunch

Thursday afternoon, 24 May, 13:00

Abstracts

Unscheduled abstracts

Author alphabetical order

Oral

**High Light Extraction and Far-field Pattern Modulation
by GaN-based Gradient Microstructures on Blue LEDs**

Sheng Han Tu, Yeeu Chang Lee, Yun Chih Lee, Che Lung Hsu,
Jenq Yang Chang

*National Central University, Department of Optics and Photonics,
Chung-Li 32001, Taiwan*

E-mail: shdo@ios.ncu.edu.tw

Periodical microstructures fabricated on p-GaN to enhance light extraction are generally attributed to two categories, the micro structure generates band gaps to prevent emission in the guided mode, or the micro structure is used to couple the guided modes to the radiation mode. In the previous researches the microstructures mentioned above are constructed as a periodical 1-D or 2-D binary texture on GaN surface. In this study a concept of periodical gradient structure is introduced to reduce the loss caused by large refractive index difference between air and GaN. Meanwhile, this periodical microstructure is also applied to modulate the far field light pattern. The microstructures are fabricated by EBL (E-beam lithography) and dry etching techniques, and angular-resolved micro-PL (photo luminescence) is used to measure the far field pattern.

Satellite events

The 2nd Polish - Japanese - German Crystal Growth Meeting

The 2nd Polish - Japanese - German Crystal Growth Meeting

Programme

Thursday, 24 May

Opening

Thursday afternoon, 24 May, 15:00

Chair: Stanisław Krukowski

Session I: Bulk GaN crystals

Thursday afternoon, 24 May, 15:15

Chair: Tsuguo Fukuda

15:15

Invited oral

Growth anisotropy of GaN single crystals by high pressure and HVPE methods

Izabella Grzegory

Polish Academy of Sciences, Institute of High Pressure Physics (UNIPRESS), Sokolowska 29/37, Warszawa 01-142, Poland

E-mail: izabella@unipress.waw.pl

Orientation of the growing crystal surface is determined by orientation of the seed and by growth conditions influencing rates and mechanisms of the crystallization process. Physical properties of crystals are dependent on growth direction (growth surface) due to differences in microscopic growth mechanisms determining point and structural defects in the crystal. For quantum structures the crystallographic orientation can decide about their fundamental properties, which follows from symmetry of a particular crystal lattice.

In this presentation, crystallization of GaN by High Pressure Solution (HPS) and by HVPE on HPS grown seeds of different shapes and on large, flat seeds (substrates) will be considered. Also the differences in physical properties of GaN-AlGaIn quantum structures grown on GaN bulk substrates of different orientations by PA MBE will be discussed.

The ~10 h HVPE growth on near dislocation free seeds in the form of (0001) oriented relatively small (~1cm) and thin (~0.1mm) platelets, leads to the formation of a few mm thick bulk crystals bonded by {0001} polar and {1-101} semi-polar side faces. The crystals are result of simultaneous growth in directions both lateral and normal to the (0001) plane of the initial seed. These different growth directions are reflected in large differences in physical properties of corresponding sectors of bulk crystals. As follows from PL, photo etch-

ing and micro-Raman measurements, the free electron concentration can vary by more than two orders of magnitude between the material grown on (0001) surface of the seed (electron concentration $< 10^{17} \text{ cm}^{-3}$) and the one grown laterally on semi-polar side faces of the crystal (electron concentration $> 10^{19} \text{ cm}^{-3}$). Crystal sectors grown on the semi-polar faces are always near dislocation free whereas sectors grown on (0001) face can be both almost defect free (like the seeds) or containing dislocations, depending on the applied growth conditions (growth rate and carrier gas were varied).

As follows from micro-Raman characterization, much more uniform crystals in terms of their physical properties can be grown on the seeds in the form of hexagonal needles where the HVPE growth occurs mainly in non-polar {10-10} directions. The crystals of free electron concentration of about $5 \times 10^{18} \text{ cm}^{-3}$ were grown in this way.

The change of orientation of the crystallization front can be induced also on the large flat substrates by their patterning and the use of growth conditions allowing formation of the required crystal facets. Such crystals are non-uniform in distribution of both point defects which results in non-uniform electrical and optical properties and structural defects (dislocations). Such crystal often contain large almost dislocation free areas being result of lateral growth. These features of the crystals grown by HVPE on the patterned (0001) substrates will be shown with the use of photo-etching and defect selective etching methods.

The substrates of both (0001) polar and (11-20) non-polar orientations (5 x 10mm) were cut from the bulk crystals grown by HVPE and used for growth of GaN-AlGaIn quantum structures by PA MBE. Optical properties of these structures will be compared.

15:45

Invited oral

Solvothermal Growth of Gallium Nitride Crystals

Fumio Orito, Shigeru Terada

MC Research and Innovation Center (MC-RIC), 601 Pine Avenue Suite C, Goleta, CA 93117, United States

E-mail: fumio_orito@m-chem.com

The ammonothermal growth of GaN basically is a process where a precursor and mineralizer is being combined in supercritical ammonia as solvent to achieve considerable solubility of GaN. Due to the high reactivity of acidic mineralizer such as ammonium chloride, platinum inner container was applied in an autoclave with the dimension of 100 mm in diameter and 1000 mm in height which is capable of growing 3-inch-diameter crystal. The purpose of this study is to investigate the industrialization of the ammonothermal technology of GaN with the diameter of 3 inch.

Computer aided simulation was utilized for designing the inner structure of the autoclave such as diameter/height aspect ratio and baffle position. The growth conditions were selected intending to be as closer to those of quartz crystal. The temperature range up to about 500 °C and the pressure up to 130 MPa were applied.

Self-standing substrates grown by H-VPE (Halide Vapour Phase Epitaxy) up to 2-inch-diameter were used as the seed crystals. Epitaxial Lateral Overgrowth was not applied for H-VPE for the seed crystals, therefore, uniform distribution of dislocation density in the

range of 10 to the power of 6 was achieved. Quasi-transparent 2-inch-diameter crystal was grown.

16:15

Invited oral

Growth of Large High-Quality GaN Crystals by Na Liquid Phase Epitaxy Method.

Fumio Kawamura, Mamoru Imade, Masashi Yoshimura, Yasuo Kitaoka, Yusuke Mori, Takatomo Sasaki

Graduated School of Engineering, Osaka University (OSAKAUNIV), Osaka, Japan

E-mail: fkawamura@cryst.eei.eng.osaka-u.ac.jp

GaN-based semiconductors have already begun to be used even for power devices or electronic devices including high frequency devices. In order to apply the GaN based semiconductors to these applications, high quality GaN single crystal substrates has been needed more than ever before. Although the crystals with the dislocation density of about 10^6 cm^{-2} and the size of 2 inch has been required so far, the size of more than 3 inch and dislocation density of less than 10^5 cm^{-2} begun to be needed. The hydride vapor phase epitaxy (HVPE) method has a lead in the growth of GaN single crystal substrate because of an advantage of high growth rate of GaN single crystals. However, further decrease in the dislocation density is difficult in the HVPE method. Although the Na flux method enables us to grow low dislocation density GaN single crystals [1-3] (shown in Figure1), low growth rate has been pointed out as a problem to be solved.



Figure 1. 2 inch GaN single crystal substrate grown by the Na flux-LPE method.

We tried to increase the growth rate by applying the thermal convection to the Na flux method. The setup for applying the thermal con-

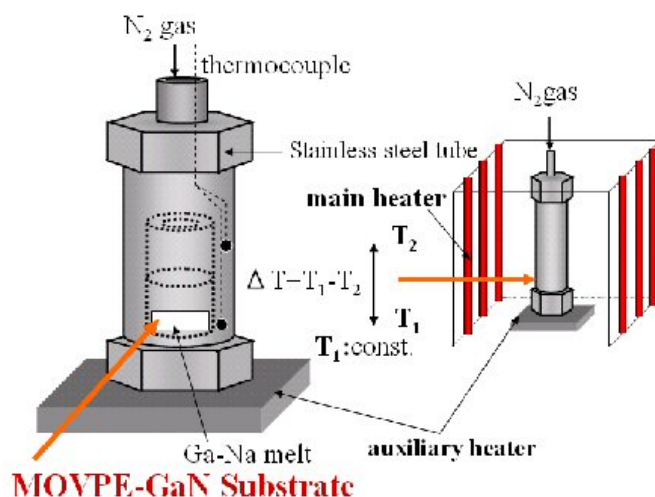


Figure 2. Experimenta setup for the LPE growth under the thermal convection.

As a result, growth rate could be increased nearly three-fold as compared to the case without thermal convection as shown in Figure 3. In the Na flux method, supersaturation is generated by dissolution of pressurized nitrogen gas. By this effort, growth rate of about 30 $\mu\text{m/h}$ could be achieved in the Na flux method for the first time. The result mentioned above indicates that dissolution of the nitrogen gas is limited by the diffusion.

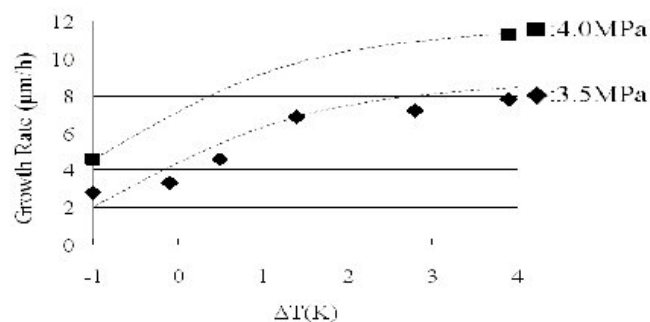


Figure 3. The effect of thermal convection on the growth rate of Na flux-LPE method.

Another advantage of the convection is that the high nitrogen concentration in the solution can be easily attained, which can suppress the nucleation of GaN on the crucible near gas-liquid interface. High rate growth without heterogeneous nucleation was used to obtain the 2 inch GaN single crystal with the thickness of over 3 mm. Current message is that the Na flux method is also effective for the growth of non-polar GaN substrate. Although non-polar GaN thin film could already be grown by the metal organic chemical vapor deposition (MOCVD) method, crystallinity was poor. We tried the LPE growth on the non-polar thin film with poor crystallinity [4,5]. As a result, crystalline quality could be drastically improved from several thousands arcsec to about 200 arcsec in both m- and a-face GaN substrate.

References

- [1] H.Yamane, M.Shimada et.al., Chem.Mater., 9 (1997) 413.
- [2] F. Kawamura, M. Morishita, K. Omae, M. Yoshimura, Y. Mori, and T. Sasaki, J. Mater. Sci.: Mater. Electron, 16 (2005) 29-34.
- [3] F. Kawamura, H. Umeda, M. Morishita, M. Kawahara, M.

Yoshimura, Y. Mori, T. Sasaki and Y. Kitaoka, Jpn. J. Appl. Phys., 45, 43 (2006) L1136

[4] T. Iwahashi, Y. Kitaoka, M. Kawahara, F. Kawamura, M. Yoshimura, Y. Mori, T. Sasaki, R. Armitage and H. Hirayama, Jpn. J. Appl. Phys., 46, 4 (2007) L103

[5] T. Iwahashi, Y. Kitaoka, F. Kawamura, M. Yoshimura, Y. Mori, T. Sasaki, R. Armitage and H. Hirayama, Jpn. J. Appl. Phys., 46, 10 (2007) L227

Coffee Break

Thursday afternoon, 24 May, 16:45

Session II: Templates and other substrates

Thursday afternoon, 24 May, 17:00

Chair: Izabella Grzegory

17:00

Invited oral

Low dislocation density GaN-templates grown by the Low Pressure Solution Growth technique

Stephan Hussy, Isabel Knoke, Patrick Berwian, Elke Meissner, Jochen Friedrich, Georg Mueller

Fraunhofer Institut IISB, Schottkystr. 10, Erlangen 91058, Germany

E-mail: Stephan.Hussy@iisb.fraunhofer.de

Gallium nitride (GaN) is a wide-band-gap semiconductor material, which is used for the production of light emitting devices and LASER diodes. Presently, nearly all GaN devices are manufactured on so-called GaN-templates. These templates are made e.g. by MOCVD deposition of GaN onto a sapphire or SiC substrate. In order to obtain a superior quality and performance of the device, substrates with lower defect density are required.

One way to produce such low-defect substrates is the Liquid Phase Epitaxy (LPE). Our LPE process is performed at ambient pressure and differs from classical LPE by the fact that one component of the grown material, i.e. the nitrogen, is not included in the solution itself from the beginning, but supplied during the process via the gas atmosphere in form of ammonia. To distinguish our process from the classical LPE technique we call it Low Pressure Solution Growth (LPSG) technique.

Details of the LPSG process will be presented. Especially the influence of the ammonia partial pressure and the temperature on the formation of epitaxially and parasitically grown GaN will be addressed, leading to the determination of a kind of Ostwald-Miers region. The growth of parasitical GaN is considered to be the limiting factor for the maximum achievable process time as well as for the growth rate of the epitaxial GaN, which is a main drawback of the method. However the quality of the epitaxial layer as well as the total process time is enhanced by applying process parameters suppressing parasitical GaN growth.

Additionally the growth mechanism of the epitaxial layer is a great benefit of the method. During heating of the solution the GaN seeding layer is etched back due to the lack of dissolved nitrogen. After saturation of the solution, growth process starts by the formation of

oriented islands. During this initial growth state a considerable reduction of the dislocation density takes place. By TEM observations it was proven that the typical dislocation density of the MOCVD seeding layer was reduced by at least one order of magnitude to about 10^8 cm^{-2} within 1 μm of LPSG layer thickness. Within this first micrometer the coalescence of the LPSG islands is completed and a continuous GaN layer is formed across the whole wafer diameter.

With the LPSG technique it is possible to produce GaN templates with 3 inch diameter and various layer thicknesses (e.g. from 1 to 40 μm). The growth process can easily be applied for larger diameter templates as well as for multi-wafer-processes, mainly determined by the dimensions of the reactor.

17:30

Invited oral

Solubility of GaN in Acidic Supercritical Ammonia

Chiaki Yokoyama

Tohoku University, Institute of Multidisciplinary Research for Advanced Materials, 2-1-1 Katahira, Aoba-ku, Sendai 980-8577, Japan

E-mail: chiaki@tagen.tohoku.ac.jp

Ammonothermal crystal growth processes appear as the most feasible method for producing GaN bulk crystals of sufficient size and quality for commercial applications. Various kinds of mineralizers have been applied for the ammonothermal processes for solubility enhancement. For process design purpose, accurate knowledge of the GaN solubility in supercritical ammonia is essential. While few experimental solubility data have been reported for the basic ammonothermal systems, the data for the acidic ammonothermal systems have never been reported. In this study, we present our experimental study for the GaN solubility in acidic supercritical ammonia. We show firstly our experimental apparatus and procedures in details. The experimental method was based on a weight loss method. The mineralizer used was mainly ammonium chloride and the GaN sample used is the GaN crystals grown by H-VPE (Halide Vapor Phase Epitaxy). Experimental conditions were in the temperature range from 450 K to 770 K and at pressure about 100 MPa. The weight ratios of the ammonium chloride to ammonia were 5 to 20 wt%. It was found that the solubility increases with increasing temperature in the present experimental conditions. This type of temperature dependence of the GaN solubility has never been observed in the basic ammonothermal systems. This result suggests that we can assume same solubilization phenomena in the present experimental conditions. Also more importantly this result indicates that the acidic ammonothermal process can be designed with the similar principles developed by the hydrothermal crystal growth processes for quartz and zinc oxide.

By combining with the present solubility data and simulation results for ammonothermal autoclaves, spatial distributions of the GaN supersaturation degree in the autoclave can be determined. The ideal crystal growth rate in the whole region in the autoclave can be estimated. From these results, we will discuss configuration of the autoclave to provide good productivity of the GaN bulk crystals.

Coffee Break

Thursday evening, 24 May, 18:00

Session III: InN, AlN & AlGaIn single crystals

Thursday evening, 24 May, 18:30

Chair: Jochen Friedrich

18:30

Oral

Flat lattice of truly bulk ammonothermal GaN

Robert Dwilinski¹, Roman Doradziński¹, Jerzy Garczyński¹, Leszek P. Sierzputowski¹, Arkadiusz Puchalski¹, Kentaro Yagi², Yasuo Kanbara²

1. AMMONO Sp. z o.o., Czerwonego Krzyża 2/31, Warszawa 00-377, Poland **2.** Nichia Corporation (NICHIA), 491 Oka, Anan 774-0044, Japan

E-mail: dwilinski@ammono.com

Bulk gallium nitride, demanded as a substrate for high power lasers and other devices, typically reveals high dislocation density, incorporated stress and substantial lattice curvature due to involvement of non-native seeds applied in its production process. Resulting bow limits both enlargement of substrates diameter and yield in laser manufacturing. Within approaching limits of methods resulting in such quasi bulk material, increase of interest in truly bulk material is observed.

In this work results of structural characterization of high quality ammonothermal GaN are presented. Besides expected low dislocation density (being of the order of 10^3 cm^{-2}) the most interesting feature seems perfect flatness of the crystal lattice of studied crystals. Regardless the size of crystals, lattice curvature radius exceeds 100 m, whereas better crystals reveal radius of several hundred meters and the best above 1000 m. Excellent crystallinity manifests in very narrow X-ray diffraction peaks of FWHM values about 17 arc sec.

High quality and homogeneity of ammonothermal GaN crystals proves that hopes put in such truly bulk material are justified and that it can be a breakthrough in mass implementation of high-power GaN-based devices.

18:45

Invited oral

Physical Vapor Transport Growth of Bulk AlN Crystals

Boris Epelbaum

University Erlangen-Nürnberg, Inst. for Material Science, Martensstr. 7, Erlangen 91058, Germany

E-mail: boris.epelbaum@ww.uni-erlangen.de

At present physical vapor transport (PVT) growth method has been recognized as the only reasonable approach to produce true bulk crystals of aluminum nitride.

(i) *Sublimation conditions and growth rate.* In the course of dissociative evaporation AlN is completely transformed into gas. Vapor pressure over solid AlN at temperatures ensuring sufficient surface diffusion is rather high in the order of 10^2 mbar. AlN demonstrates

technologically favorable evaporation behavior, as completely reversible transformation of AlN virtually allows effective growth process with continuous supply of raw material. The growth rate of AlN in sublimation process remains the subject of wide disagreement. In some publications the growth rate of AlN is treated as completely dependent on vapor transport, i.e. the temperature difference between the crystal and the powder source is considered as the only parameter relevant for growth rate. In some other publications, contrary, the surface kinetics (and also very little investigated surface chemistry of condensation process) are predicted accountable for growth rate limitations. Additional complications are arising from the wide range of processing parameters used in the growth process of AlN: for example the crystal temperature reported in the available literature varies for bulk AlN from 1800 to 2250°C. In this presentation we compare our experimental data on PVT growth of single crystals of AlN grown at different temperatures with the maximum condensation rate calculated according Hertz-Knudsen equation. It is concluded that the growth rate is determined mainly by the surface kinetics as it is very sensitive to crystal temperature and little dependent on temperature difference in sublimation system. (ii) *Self-nucleation and formation of freestanding crystals.* Self-nucleation and subsequent growth of cm-sized freestanding crystals known as Lely procedure for SiC has been established by our group for AlN also. The presentation will explain the habit and zonal structures in freestanding AlN. (iii) *Directional crystallization and seeded growth.* Unidirectional crystallization of AlN is possible with growth rates in the range of 0.1-1.0 mm/h. Seeded growth of AlN still remains a challenge, but successful seeding has been already demonstrated. In the presentation our recent results on growth of large nominally pure single crystals of AlN up to 1.5 inch in diameter will be presented (iv) *Specific defects.* Open core screw dislocations (micropipes), of particular concern in SiC, are not observed in AlN. Dislocation density in freestanding and seeded crystals of AlN revealed by wet chemical etching in our recent studies was in the range of 10^4 - 10^5 cm^{-2} . The lowest defect density and best optical properties are observed in crystal zones grown on basal Al-terminated (0001) and adjacent pyramidal faces.

19:15

Invited oral

Mysterious material InN in nitride semiconductors - what's bandgap energy and its applications?

Takashi Matsuoka, Masashi Nakao

Institute for Materials Research, Tohoku University (IMR), Sendai 980-8577, Japan

E-mail: matsuoka@imr.tohoku.ac.jp

The progress in nitride semiconductors is reviewed. The current status in the growth and characteristics of InN, which remains the most mysterious compound, is reviewed. The phase diagram for InN growth, the optical absorption characteristic, polarity, temperature dependence of photoluminescence, future prospects are described. The application of InN for light emitting devices is discussed.

Friday, 25 May

Session IV: SiC single crystals

Friday morning, 25 May, 8:30

Chair: Boris Epelbaum

8:30

Invited oral

Defect Control for Electric Property of SiC CrystalsToshihiko Hayashi¹, Tomoaki Furusho¹, Taro Nishiguchi¹, Keiichi Ikeda¹, Hiroyuki Kinoshita¹, Hiromu Shiomi¹, Michio Tajima²

1. SiXON Ltd. (SiXON), 47, Umezaki-Takasecho, Ukyo-ku, Kyoto 615-8686, Japan 2. Institute of Space and Astronautical Science (JAXA), 3-1-1 Yoshinodai, Sagami-hara, Kanagawa 229-8510, Japan

E-mail: toshihiko_hayashi@sixon.com

Today Silicon Carbide (SiC) is recognized as an appropriate semiconductor for high power, high frequency and low loss devices application owing to its wide bandgap, high thermal conductivity and high breakdown field. However it was difficult to get the single crystal of a high quality until recently, because the properties of SiC, which has no liquid phase at practical pressure, obstruct an application of conventional semiconductor crystal growth experience.

Recently, the development of SiC crystal growth technology has brought about a large progress in the techniques of growing high-quality SiC boule crystal. And wafer size becomes large year by year too. Especially the density of micropipes, which are defects peculiar to SiC crystal, has been considerably decreased in these past several years. While huge crystal defect such as micropipes and small grain boundaries are decreased, small defects such as dislocations and point defect are outstanding. And these defects have bad influence on an electric property of semiconductor devices. But the correlation with some kinds of defects and electrical properties is not known clearly yet and the methods of detection and evaluation of defects are also important. It is desirable to analyze the whole wafer region, by non-destructively, for a short time.

In this presentation, a typical defect of SiC crystal is discussed with the detection and evaluation method, and is also discussed with the influence to electric property of electronic devices.

9:00

Invited oral

Recent Progress in the Growth of 4H-SiC Bulk Crystals

Thomas Straubinger, Erwin Schmitt, Michael Rasp, Michael Vogel

SiCrystal AG, Günther-Scharowsky-Str.1, Erlangen 91058, Germany

E-mail: thomas.straubinger@sicrystal.de

Although significant improvements in material quality of 4H-SiC substrates have been achieved, and wafers nearly free of Micropipes were demonstrated by several groups the specified Micropipe density of commercial available substrates is still non-zero.

In this work we will discuss the influence of thermal field, doping and C/Si-ratio on the formation of modification changes and their secondary defect micropipes. Since it is clear that dislocations are

the main reason for degradation in power devices prevailing attention has shifted to that field of material research. Therefore intense studies were also utilized on dislocation formation during growth.

We found out that for the improvement of substrate quality emphasis has to be laid on the C/Si-ratio and reduction of thermo-elastic stress in the growing crystal. From results of numerical calculations we were able to derive moderate growth conditions with reduced temperature gradients and correspondingly low defect concentration.

Finally we achieved reproducible low Micropipe densities (MPD) $< 1 \text{ cm}^{-2}$ in our 4H-3" growth process. Additionally we were able to demonstrate a new substrate quality with MPD $< 0.1 \text{ cm}^{-2}$, without low angle grain boundary contrasts in stress birefringence and correspondingly uniform dislocation density $< 1 \cdot 10^4 \text{ cm}^{-2}$.

Coffee Break

Friday morning, 25 May, 9:30

Session V: ZnO crystals

Friday morning, 25 May, 10:00

Chair: Takashi Matsuoka

10:00

Invited oral

Melt Growth of Bulk Zinc Oxide

Detlef Klimm, Detlev Schulz, Steffen Ganschow, Roberto Fornari
Institute for Crystal Growth (IKZ), Max-born Str. 2, Berlin 12489, Germany

E-mail: klimm@ikz-berlin.de

Whenever possible, bulk single crystals of any substance are grown from the melt. If no suitable crucible material can be found, alternative methods like cold crucible (*skull melting*), sublimation, chemical transport or solution growth can be applied. Problems arise for ZnO, as the substance has a high melting point $T_f = 1975^\circ\text{C}$ combined with a high vapor pressure at T_f of $p_{\text{ZnO}} = 1.06 \text{ bar}$. The dissociation $2 \text{ ZnO} \rightarrow 2 \text{ Zn} + \text{O}_2$ upon evaporation makes a partial pressure $p_{\text{O}_2} = 0.35 \text{ bar}$ necessary in order to stabilize the ZnO bath. In case of dissociation the metallic Zn excess would destructively attack any metallic crucible. Thermodynamic equilibrium calculations allow to predict and experiments showed that ZnO can be molten in iridium crucibles under suitable conditions (T , p , atmosphere). This invention offers the chance to grow ZnO by conventional melt growth techniques (Bridgman, Czochralski, gradient freeze) and to avoid some technical problems like the extremely high T gradients inherent to skull melting and the contamination problems inherent to hydrothermal growth. Up to now crystal slices with diameter of $> 30 \text{ mm}$ and X-ray rocking curve widths better 1 arc min could be produced.

10:30

Invited oral

Room temperature epitaxial growth of group III nitridesHiroshi Fujioka

Institute of Industrial Science, The University of Tokyo, 4-6-1 Komaba, Meguro-ku, Tokyo, Tokyo 153-8505, Japan Kanagawa Academy of Science and Technology (KAST), KSP E301 3-2-1, Sakado, Takatsu-ku, Kanagawa 213-00112, Japan

E-mail: hfujioka@iis.u-tokyo.ac.jp

For the last two decades, group III nitrides have attracted much attention because of their excellent optical and electrical properties. These materials have been successfully utilized for fabrication of efficient blue LEDs, lasers, and FETs. So far, growth of thin film III nitrides has been performed by MOCVD or MBE at high temperatures, above 700°C. This high growth temperature limits the growth substrates to thermally stable materials such as sapphire. However, sapphire has large mismatch in both lattice constants and thermal expansion coefficients with the group III nitrides and it is well known that these both mismatch types cause degradation in crystalline quality. We have recently found that the use of pulsed laser deposition (PLD) allows us to improve surface migration of the film precursors and to reduce the growth temperature down to room temperature (RT). [1-9] Hence, we can expect that the use of PLD makes it possible to use various chemically vulnerable substrates with small mismatches such as ZnO and Hf. In this presentation, we will discuss advantages of RT epitaxial growth of group III nitrides on the substrates with small mismatches by PLD.

Growth of group III nitrides was performed using an rf-plasma-assisted UHV-PLD apparatus. Various materials which include ZnO, MnZn ferrite, LiGaO₂, and Hf, were used as substrates for RT growth. Group III metals such as In, Al, and Ga were irradiated with a KrF excimer laser light at an energy density of about 3.0 J/cm² and reacted with active nitrogen generated by rf-plasma. After the film growth, we characterized the structural properties of the RT grown nitride films by EBSD, RHEED, HRXRD, AFM, photoluminescence, and GIXR.

We have observed clear streaky RHEED patterns and their intensity oscillation during the RT growth, which indicates that the RT growth proceeds epitaxially in the layer-by-layer mode. HRXRD measurements have revealed that reduction in growth temperature leads to improvement in crystalline quality of nitrides probably due to the suppression in the interfacial reactions between the nitrides and the substrates. This improvement of crystalline quality is particularly important when it is used for the growth of non-polar nitrides because the film quality of nonpolar nitrides achieved by conventional high temperature growth techniques is quite poor. We have also found that the reduction in growth temperature suppresses the phase separation of InGa₂N. The InGa₂N films grown at RT exhibited a sharp X-ray peak with single component and a strong photoluminescence at long wavelengths. We have found that reduction in growth temperature also suppresses the introduction of misfit dislocations at the heterointerfaces between the nitrides and the substrates. These results indicate that the RT growth technique is quite promising for fabrication of nitride optical and electron devices with high performance.

References

- [1] K. Ueno, A. Kobayashi, J. Ohta, and H. Fujioka, Appl. Phys. Lett., (in press).
- [2] A. Kobayashi, S. Kawano, Y. Kawaguchi, J. Ohta, and H. Fujioka, Appl. Phys. Lett., **90**, 041908 (2007).
- [3] G. Li, T.-W. Kim, S. Inoue, K. Okamoto, and H. Fujioka, Appl. Phys. Lett., **89**, 241905 (2006).
- [4] T.-W. Kim, N. Matsuki, J. Ohta, and H. Fujioka, Appl. Phys. Lett., **88**, 121916 (2006).
- [5] A. Kobayashi, J. Ohta, H. Fujioka, K. Fujiwara, and A. Ishii, Appl. Phys. Lett., **88**, 181907 (2006).
- [6] S. Inoue, K. Okamoto, N. Matsuki, T. W. Kim, and H. Fujioka, Appl. Phys. Lett., **88**, 261910 (2006).
- [7] M.-H. Kim, M. Oshima, H. Kinoshita, Y. Shirakura, K. Miyayama, J. Ohta, A. Kobayashi, and H. Fujioka, Appl. Phys. Lett., **89**, 031916 (2006).
- [8] A. Kobayashi, Y. Kawaguchi, J. Ohta, and H. Fujioka, Appl. Phys. Lett., **89**, 111918 (2006).
- [9] G. Li, J. Ohta, K. Okamoto, A. Kobayashi, and H. Fujioka, Appl. Phys. Lett., **89**, 182104 (2006).

11:00

Invited oral

Nanotechnology in GaN and ZnO growths for Novel Device ApplicationsTakafumi Yao^{1,2}, Meoungwhan Cho²

1. Tohoku University, Center for Interdisciplinary Research, Aramaki-Aoba, Aoba-ku, Sendai 980-8578, Japan **2.** Institute for Materials Research, Tohoku University (IMR), Sendai 980-8577, Japan

E-mail: yao@cir.tohoku.ac.jp

Both GaN and ZnO are widegap semiconductors and have similar properties in terms of crystal structure, optical and electrical properties. The conductivity control of GaN has been established, so that p-n junction devices such as light emitting devices (LEDs) and laser diodes (LDs) have been already commercially available. However, it is still difficult to grow ZnO with optical and electrical properties sufficient for light-emitting devices. One of the big emerging markets for GaN-based LEDs is general lighting, in which high-brightness white LEDs are strongly required. Although various high-brightness LED structures have been proposed, the best solution would be vertical LEDs. Vertical LEDs have been fabricated either by lift-off of substrates on which LED structures are fabricated or by growing LED structures on conductive substrates. Although the lift-off technique is considered to offer superior characteristics to the other methods in terms of process and cost, the inferior reliability of the laser-lift-off technique hampers form high-yield fabrication of the devices. We have most recently developed a chemical lift-off technique, in which chemicals are used to detach device layers from substrates. This process offers a reliable method for fabricating LED structures with high reproducibility. We would like to demonstrate the fabrication of vertical LEDs using this process in this presentation.

On the other hand, the most unique feature of ZnO lies in its high exciton binding energy (60 meV). Since excitons still survive even at room temperature, this material should show nonlinear optical phenomena even at low excitation level, if excitonic processes participate in the nonlinear optical phenomena. In order to exhibit nonlinear optical effects at low excitation level, phase matching conditions should be satisfied. For this purpose, quasi-phasing matching structures are very favorable, which can be realized by the fabrication of periodically polarity inverted (PPI) structures. We have developed the fabrication processes of ZnO-based PPI structures based on interface engineering. Second-harmonic generation of light from the fabricated PPIs will be demonstrated.

Coffee Break

Friday morning, 25 May, 11:30

Session VI: Epitaxy and Characterization

Friday afternoon, 25 May, 12:00

Chair: Stanisław Krukowski

12:00

Invited oral

Synchrotron topographic investigation of SiC bulk crystals and epitaxial layers

Wojciech Wierzchowski¹, Krzysztof Wieteska², Walter Graeff³

1. Institute of Electronic Materials Technology (ITME), Wólczyńska 133, Warszawa 01-919, Poland **2.** Institute of Atomic Energy (IEA), Otwock-Świerk 05-400, Poland **3.** Hamburger Synchrotronstrahlungslabor HASYLAB (HASYLAB), Notkestrasse 85, Hamburg D-22603, Germany

E-mail: wierzc_w@sp.itme.edu.pl

X-Ray diffraction topographic methods exploring synchrotron source of X-Ray were applied for studying different monotypic 6H and 4H SiC crystals and SiC homoepitaxial layers. A set of investigated samples included the crystals and epitaxial layers of a very good crystallographic perfection, with reduced number of micro-pipes and with low concentration of dislocations. Some of the samples were cut out along the $[00\times 1]$ growth axis of a 6H SiC boule.

The synchrotron topographic methods included both those exploring white and monochromatic beam of 0.111 nm wavelength. The monochromatic beam topographs were completed by recording of local diffraction curves using the 50mm \times 50 mm spot beam.

The synchrotron topographic methods provided valuable information both in the case of higher and low density of defects in crystals. In the first case particularly useful results were obtained using back-reflection white beam synchrotron section topography, which reproduced the images from a large thickness of the samples intersected by the beam. The section topographs revealed a great part of macro and micro-pipes present in the samples, reproduced as white areas, similarly as hexagonal voids formed in some crystals.

The additional possibility offered exposing the white beam topographs through a fine mesh with the distance between the wires equal to 0.7mm, which was very useful in revealing and evaluation

of the lattice deformation. Thanks to low attenuation of radiation in SiC crystals very good results were obtained using a mesh also in case of Bragg-case section topography.

It was possible to reveal some interesting cases of lattice deformation in the investigated crystals. In particular a structure of oval grains with the disorientation of some minutes was observed in some samples cut out perpendicular to $[00\times 1]$ growth axis, while in samples cut out along growth axis the characteristic misoriented stripes were revealed.

It was possible to obtain well resolved dislocations images in crystals of good quality with the use of all considered synchrotron topographic methods. The Bragg-case monochromatic beam topographs and white beam section topographs provided the images of dislocation enabling the numerical simulation of the images. It was possible to confirm the dominant screw-type character of observed dislocations.

12:30

Invited oral

Low Dislocation density GaN Crystals by Advanced-DEEP

Koji Uematsu, Kensaku Motoki, Takuji Okahisa, Ryu Hirota, Seiji Nakahata, Naoki Matsumoto

Sumitomo Electric Industries (SEI), 1-1-1, Koyakita, Itami, Hyogo, Hyogo 664-0016, Japan

E-mail: k-uematsu@sei.co.jp

GaN substrates with low dislocation density are key material for the commercial production of violet lasers. Hydride vapor phase epitaxy (HVPE) is a practical growth method for the production of GaN substrates. In this report a newly-improved method for the reduction of dislocations in GaN crystals by HVPE is described.

In the past, we developed a method for the dislocation reduction named dislocation elimination by the epitaxial-growth with inverse-pyramidal pits (DEEP) [1]. The typical process of the DEEP is as follows. Using HVPE a GaN layer starts to be grown epitaxially on a foreign substrate with a high dislocation density generated at the interface. The thick GaN layer grows with numerous large hexagonal inverse-pyramidal pits maintained on the surface. The pit is constructed by facet planes such as $\{11\bar{2}2\}$. As the growth proceeds, dislocations in the GaN crystal are concentrated to the center of the pit through $\{11\bar{2}2\}$ facet plane. As a result a wide area with low dislocation density is formed within the pit except the center area with high dislocation density. These pits are randomly positioned.

By the DEEP process a GaN crystal with pits about 100 μm in diameter was obtained and then flattened. The dislocation density of this substrate was in the range of 10^5cm^{-2} or lower at a low density area and in the range of 10^8cm^{-2} at a high density area. A GaN crystal with pits about 500 μm in diameter was also obtained and examined. Although the dislocation density was in the range of 10^5cm^{-2} or lower at the low density area, the area with the dislocation density over $1\times 10^7\text{cm}^{-2}$ was extended around the center. These pits positioned randomly. They are considered barriers for the device manufacturing process.

In order to improve this issue we made a new approach. A initial substrate having a layer of round shape patterns with the spacing of

400 μ m on the surface was used as a starting substrate. The GaN was grown on that by HVPE, then, a thick GaN epitaxial layer was obtained, on which all the pits arranged orderly. The spacing of the center of the pits was 400 μ m, which was determined by the patterned layer. After flattend this new type substrate was examined. The distribution of dislocations was examined by cathodoluminescence (CL). The CL image showed that in each pit area at the center a core (We named this area a core) was observed. Each core was clearly distinguished by a boundary from the other area in the CL image. These cores and pit areas were positioned regularly. The dislocation density near the core was as high as 10^7 cm^{-2} . It decreased as low as the order of 10^4 cm^{-2} at a distance from the core. Total amount of dislocation is greatly reduced. We named this new method for the reduction of dislocations as advanced-DEEP (A-DEEP). The A-DEEP can have other type of facet structure, which will be introduced at the oral presentation.

[1] K. Motoki et al.: Journal of Crystal Growth 237-239 (2002) 912-921.

13:00

Invited oral

Solid-state, ultraviolet, high-power laser system using a Ce: LiCAF gain medium

Nobuhiko Sarukura¹, Tsuguo Fukuda^{2,3}

1. Institute of Laser Engineering (ILE), Yamada-oka 2-6, Suita, Osaka, Japan, Osaka 565-0871, Japan **2.** Tohoku University, Institute of Multidisciplinary Research for Advanced Materials, 2-1-1 Katahira, Aoba-ku, Sendai 980-8577, Japan **3.** Fukuda X'tal Laboratory, c/o ICR 6-6-3, Minami Yoshinari, Aoba-ku, Sendai 981-3204, Japan

E-mail: sarukura-n@ile.osaka-u.ac.jp

High peak-power, femtosecond (fs), ultraviolet (UV) lasers have recently attracted new interest. Chirped pulse amplification (CPA) in the UV region has been previously demonstrated using Ce:LiCaAlF₆ (Ce:LiCAF) crystal as the gain medium. The peak power of the amplified and compressed pulse (115 fs) reached 30 GW at 290 nm. To increase the peak power to the terrawatt (TW) level, further pulse compression is desired. Since Ce:LiCAF has a tunability of 281 nm to 315 nm, it holds promise for 3-fs pulse generation which is required for seeding TW-class Ce:LiCAF lasers. The pulse width of the frequency-tripled Ti-sapphire regenerative amplifier was measured to be 210 fs. The seed pulses were then focused unto a hollow fiber filled with argon to spectrally broaden the pulses due to self phase-modulation. The pulses were then compressed to 25 fs by dispersion-compensation. The fourth harmonics of a Nd:YAG laser (266 nm) is an ideal pump source as it falls within the absorption band of Ce:LiCAF. We have previously generated 430 mJ of fourth harmonics with a total conversion efficiency of 30.5% using Li₂B₄O₇ (LB4) crystals. A Ce:LiCAF double-pass power amplifier was then designed with a peak energy of 98 mJ for a 13 mJ seed pulse and an extraction efficiency of 25%.

Closing

Friday afternoon, 25 May, 13:30

Chair: Jochen Friedrich, Stanisław Krukowski, Tsuguo Fukuda

Lunch

Friday afternoon, 25 May, 13:45

Posters

Index

A

Abolhasani, MohamadReza, 62
Ackermann, Jörg, 75
Addou, Marid, 10
Albrecht, Martin, 45
Aleszkiewicz, Marta, 8
Ali, Saif, 31, 63
Anandha babu, Govindan, 9
Antic, Bratislav, 26
Aosawa, Keijyu, 75
Artel, Darek, 21
Ashraf, Hina, 51

B

Babayevskaya, Nataliya V., 10
Baczewski, Lech T., 8
Bajor, Andrzej L., 10, 20, 36, 85
Bak-Misiuk, Jadwiga, 42, 59
Bala, Wacław, 10
Balcer, Tomasz, 72
Baldochi, Sonia L., 76
Baranowski, Jacek, 6
Barański, Marek, 14
Barcz, Adam, 13, 42, 53, 59
Batlogg, Bertram, 26
Bauer, Eric, 80
Baumer, Vyacheslav N., 14
Bażela, Wiesława, 11
Belka, Radosław, 11
Berezovskaya, Liudmila Y., 18, 35
Berkowski, Marek, 14, 30, 33
Berwian, Patrick, 93
Beskrovniy, Anatoliy I., 39
Bisen, Durga P., 12
Boćkowski, Michał, 5
Bodzenta, Jerzy, 54
Bogdanowicz, Włodzimierz, 25, 25
Bogodaev, Nikolai V., 18, 35
Bondarczuk, Krzysztof, 17
Bondarenko, Stanislav, 78
Borc, Jarosław, 65
Borca, Bogdana, 80
Borowiec, Mieczysław T., 14
Borysiuk, Jolanta, 12, 43, 43
Bove, Philippe, 45, 54
Bożek, Rafał, 68
Brahme, Nameeta, 12
Brisset, Hugues, 75
Brushko, Benjamin, 22
Buzanov, Oleg A., 23
Bystrzejewski, Michał, 9, 12, 55

C

Caban, Piotr, 43, 43

Caliebe, Wolfgang, 8
Capan, Ivana, 71
Chai, Guangyu, 13, 53
Chang, Jenq Yang, 47, 88
Chang, Penhsiu, 7
Chellamuthu, Muthamizhchelvan C., 36
Chen, Jyh-Chen, 47, 51, 86
Chen, Naichuan, 7
Chi, Pei-Hung, 48
Chiang, Chang-Hung, 86
Cho, Meoungwhan, 96
Choi, Eun S., 13, 53
Chow, Lee, 13, 53
Cieślak, Krystian, 60
Cliffe, Andrew K., 78
Conder, Kazimierz, 14
Crnogorac, Nebojša, 78
Cruz, Simone Ferreira de Almeida, 76
Cudziło, Stanisław, 9
Cvejic, Zeljka, 26
Czapkiewicz, Magdalena, 54
Czernecki, Robert, 41
Czyzak, Aleksandra, 44, 54

D

Dabkowski, Antoni, 85
Dd, Kanjilal, 31, 63
Dec, Jan, 72, 82
Derkowska, Beata, 10, 16
Didusko, Ryszard, 21, 26, 34, 68, 80
Dobosz, Danuta, 54
Dolzhenkova, Elena, 14, 30
Domagala, Jarosław, 8, 20, 41, 42, 44, 45, 54
Domańska, Marta, 55
Dominiak-Dzik, Grażyna, 13
Domuchowski, Wiktor, 14
Doradziński, Roman, 94
Doroshenko, Andrey G., 13
Drozdowski, Mirosław, 19, 33
Dubovik, Mikhail F., 39
Dumiszewska, Ewa, 43, 47
Dwilinski, Robert, 94
Dyakonov, Vladimir P., 14
Dynowska, Elzbieta, 8, 53
Dłużewski, Piotr, 8

E

Efros, Boris M., 62
Ehrentraut, Dirk, 44, 46
Epelbaum, Boris, 94

F

Fages, Frédéric, 75
Faiez, Reza, 15
Fink-Finowicki, Jan, 15
Firszt, Franciszek S., 16, 16
Foldvari, Istvan, 13
Fornari, Roberto, 45, 95

Friedrich, Jochen, 93
Fruchart, Olivier, 80
Fujioka, Hiroshi, 96
Fujito, Kenji, 6
Fukuda, Tsuguo, 29, 44, 46, 76, 76, 98
Furusho, Tomoaki, 95

G

Gąbka, Oliwia M., 57
Gaca, Jarosław A., 45, 52
Galas, Jacek, 58
Ganschow, Steffen, 17, 75, 95
Garczyński, Jerzy, 94
Gayvoronsky, Vladimir Y., 78
Gała, Maciej, 68
Gebicki, Wojciech, 26
Gg, Bhagavannarayana, 31, 63
Gholampoor, Mahdi, 62
Gierlotka, Stanisław, 43
Godavarthi, Bhagavannarayana, 28
Godlewski, Marek, 22, 22
Golaszewska, Krystyna, 18, 45, 52, 53, 54, 54
Golnik, Andrzej, 8
Gomes, Laercio, 76
Gorski, Piotr T., 17
Grabias, Agnieszka, 12
Graeff, Walter, 21, 27, 71, 72, 97
Grasza, Krzysztof, 8, 65, 68
Gromov, Yuri, 78
Grym, Jan, 17
Grzegory, Izabella, 51, 91
Gurdziel, Wojciech, 25, 37
Gutowska, Maria, 14
Guziewicz, Elżbieta, 22, 22
Guziewicz, Marek, 18, 22, 45
Gułkowski, Sławomir, 60

H

Hageman, P.R., 51
Hartmann, Carsten, 45
Hashimoto, Tadao, 6
Hayashi, Toshihiko, 95
Hemmingsson, Carl, 51
Henini, Mohamed, 79
Hirota, Ryu, 97
Hoffmann, Stanisław K., 86
Hofman, Władysław, 72
Hoshino, Naruhiro, 44, 46
Hruban, Andrzej, 48, 55, 67
Hsu, Che Lung, 88
Huczko, Andrzej, 9, 55
Hundley, Michael F., 80
Hussy, Stephan, 93
Hwang, Jung Hoon, 65
Hwu, Farn-Shiun, 51

I

Iguchi, Eiichi, 68

Ikeda, Keiichi, 95
Imade, Mamoru, 92
Itoh, Hirohisa, 44, 46
Ivleva, Liudmila I., 18, 35
Izdebski, Marek, 18

J

Jakiela, Rafał, 22
Janik, Elżbieta, 8
Janik, Jerzy F., 43
Jasik, Agata, 45
Jovalekic, Cedomir, 26
Jóźwik, Iwona, 60

K

Kaczkan, Marcin, 21, 26, 80
Kaczmarek, Barbara, 20, 21
Kaczmarek, Sławomir, 30
Kagamitani, Yuji, 44, 46
Kakimoto, Koichi, 4
Kaliamoorthy, Rajarajan, 19
Kaminska, Eliana, 18, 45, 49, 54
Kamiński, Paweł, 46, 56, 57
Kanbara, Yasuo, 94
Karbownik, Piotr, 50
Karczewski, Grzegorz, 8
Karpinski, Janusz, 26, 81
Kasprowicz, Dobrosława, 19
Katrych, Sergiy, 26, 81
Kawamura, Fumio, 92
Kawasaki, Masayuki, 67
Kazmierczak-Balata, Anna, 54
Kempisty, Paweł, 46, 83
Kher, Rajeev S., 12
Kim, Sang Woo, 62
Kim, Youn Jea, 65
Kinoshita, Hiroyuki, 95
Kirmse, Holm, 8
Kisielewski, Jarosław, 10, 80, 85
Kitaoka, Yasuo, 92
Kleemann, Wolfgang, 82
Klimczak, Monika, 38
Klimczuk, Tomasz, 80
Klimm, Detlef, 17, 75, 76, 95
Knoke, Isabel, 93
Kokh, Konstantin A., 57
Kolitsch, Uwe, 70
Kolybaeva, Marina I., 78
Komorowski, Krzysztof, 28
Kopalko, Krzysztof, 22, 22
Kopczynski, Krzysztof, 10, 36, 85
Korbutowicz, Ryszard, 47, 53
Korshikova, Tatyana, 30
Kosmala, Michał, 45
Kossacki, Piotr, 8
Kotlyarchuk, Bohdan K., 59
Kowalczyk, Andrzej, 38
Kowalik, Iwona A., 22

Kowalski, Wojciech, 22
Kozlova, Nina S., 23
Kozubal, Michał, 46, 56
Kozłowski, Roman, 46, 56
Kołodziejak, Katarzyna B., 21, 21, 21, 26, 80
Krajewski, Tomasz, 22
Kraśńska, Krystyna R., 23
Kraśński, Mariusz J., 23, 24
Krawczyk, Jacek, 25, 25, 25
Kremenovic, Aleksandar, 26
Kret, Sławomir, 8
Kruczek, Magdalena M., 37
Krukowski, Stanisław, 46, 67, 83
Kruszka, Renata, 49, 52, 53
Krysko, Marcin, 41
Kryzhanovskaya, Alexandra S., 10
Kucharczyk, Włodzimierz W., 17, 18
Kujawa, Magdalena, 16
Kulriya, Pawankumar, 31, 63
Kumar, Krishna, 27, 32
Kunjidapadham, Sethuraman, 84
Kuświk, Piotr, 34
Kwietniewski, Norbert, 18, 49
Kłos, Andrzej, 20, 20, 66, 70

L

Lahreche, Hacene, 45, 54
Lange, Hubert, 9, 12, 55
Langer, Robert, 45, 54
Ledzion, Rafał, 17
Lee, Han-oh, 80
Lee, Ho Jun, 51, 57, 62
Lee, Ko-Tao, 47
Lee, Tsung-Xian, 47
Lee, Yeeu Chang, 88
Lee, Yeeu-Chang, 47
Lee, Yun Chih, 88
Lefeld-Sosnowska, Maria, 27, 70
Lesyuk, Rostyslav I., 59
Leszczynski, Mike, 41
Levchenko, Alexandr N., 78
Lewandowska, Renata, 51
Lipińska, Ludwika, 34, 75
Lisiecki, Radosław, 13, 66
Litwin, Dariusz, 58
Litwin-Staszewska, Elżbieta, 46
Lorenc, Michał, 58
Lörinčík, Jan, 17
Lu, Chung-wei, 48, 86
Lucznik, Bolesław L., 51
Lykov, Pavel A., 18, 35
Lysacek, David, 58
Łęgowski, Stanisław, 16
Łukasiewicz, Tadeusz, 10, 21, 21, 26, 72, 80, 82, 85
Łusakowska, Elżbieta, 65

M

Maier, Dirk, 17

Majchrowski, Andrzej, 19
Malinowska, Agnieszka, 27, 72
Malinowski, Michał, 21, 21, 26, 80
Marasek, Agnieszka, 16, 16
Mares, Jiri A., 29
Maruthamuthu, Anbuezhhiyan M., 36
Materna, Andrzej, 48, 55, 58
Matsumoto, Naoki, 97
Matsuoka, Takashi, 94
Matveevskaya, Neonila A., 64
Mazzocchi, Vera L., 76
Męczyńska, Hanna, 16
Meissner, Elke, 93
Meyer, Claire, 80
Michalski, Edward, 19
Miczuga, Marcin, 46, 56
Mielcarek, Sławomir, 19, 28
Mierczyk, Jadwiga, 10, 36, 85
Miga, Seweryn, 82
Miros, Artur, 58
Mirowska, Aleksandra, 48
Misiuk, Andrzej, 13, 42, 53, 59, 62, 71
Mlynczak, Jarosław, 36
Moreno, Abel, 83
Morhange, Jean F., 8
Mori, Yusuke, 92
Motoki, Kensaku, 97
Mroz, Bogusław, 28
Mueller, Georg, 3, 93
Mycielski, Andrzej, 65

N

Nakahata, Seiji, 97
Nakamura, Gerson Hiroshi de Godoy, 76
Nakamura, Shuji, 6
Nakao, Masashi, 94
Nakwaski, Włodzimierz, 42, 49
Narayanasamy, Vijayan, 28
Neugebauer, Joerg, 3
Nicoara, Irina, 29
Niinisto, Lauri, 22
Nikl, Martin, 29, 66, 76
Nishiguchi, Taro, 95
Nishijima, Eiichi, 78
Nn, Vijayan, 63
Norris, Scott A., 70
Norton, Paul, 40
Novoselov, Andrey, 29, 76

O

Oishi, Shuji, 67, 68
Okahisa, Takuji, 97
Olchowik, Jan M., 60
Omote, Kazuhiko, 75
Orito, Fumio, 91
Orlińska, Natalia, 30
Orzyłowski, Marek, 58
Orłowski, Wacław, 48, 55, 67

Osica, Magdalena, 9
Osiko, Vjatcheslav V., 18, 35
Osinniy, Victor, 22
Ostapska, Anna, 60
Oszwaldowski, Maciej, 34, 59

P

Pacek, Paweł, 72
Pacuski, Wojciech, 8
Padmanabhan, Srinivasan, 32, 38, 63
Pagowska, Karolina, 43
Pajaczkowska, Anna, 27, 34, 66, 70, 75
Pakuła, Krzysztof, 6
Papis, Ewa, 49, 52, 53
Parente, Carlos B R., 76
Parkhomenko, Sergey, 30
Paszkiewicz, Bogdan, 53
Paszkiewicz, R., 53
Paszula, Józef, 30
Pavlyuchkov, Dmytro, 22
Pawlak, Dorota A., 10, 21, 21, 26, 80, 85
Pawłowska, Joanna, 60
Pawłowska, Marta, 55
Pawłowski, Mariusz Grzegorz, 67
Pawłowski, Michał, 56
Pejchal, Jan, 29, 76
Perera, Unil, 41
Perumalsamy, Ramasamy, 84
Petrouchik, Alexei, 8
Piątkowski, Bronisław, 58
Piersa, Mirosław, 67
Pierściński, Kamil, 45
Piotrowska, Anna, 18, 45, 49, 52, 53, 54
Piotrowski, Józef, 40
Piotrowski, Tadeusz T., 52, 53, 54
Piskorski, Łukasz, 49, 69
Piwowarska, Danuta, 30
Podlesnyak, Andrew, 14
Poisson, Marie-Antoinette, 45
Polak, Wiesław, 4
Politov, Anatoly A., 57
Poloczek, Przemysław, 50
Pomjakushina, Ekaterina, 14
Popu, Sagayaraj, 19
Potheher, Vetha, 19
Prakasam, Mythili, 31, 31, 38, 63
Prażmowska, Joanna, 47, 53
Presz, Adam, 8
Procházková, Olga, 17
Prudnikov, Anatoly, 62
Prujszczyk, M., 13, 62, 71
Prystawko, Paweł, 41, 46
Prytula, Ihor M., 78
Prywer, Jolanta, 24, 82
Puchalski, Arkadiusz, 94
Pucicki, Damian, 50
Putkonen, Matti, 22
Puzikov, Vyacheslav M., 78
Puzniak, Roman, 26, 81

Pyka, Monika, 54

R

Ra, Sankar, 19
Radziewicz, Damian, 50
Rakic, Srdan, 26
Ramamoorthy, Nagalakshmi, 27, 32
Ramasamy, Perumalsamy, 9
Ramraj, Ramesh babu, 84
Rasp, Michael, 95
Ratajczak, Jacek, 53
Rębarz, Mateusz, 10
Rengasamy, Gopalakrishnan, 31, 31, 32, 38, 63, 84
Rogacki, K., 26, 81
Romanowski, Przemysław, 42
Ronning, Filip, 80
Rousseau, Anthony, 80
Rozniatowski, Krzysztof, 21, 21, 26, 80
Rudolf, Zbigniew, 58
Runka, Tomasz, 33
Rutkowski, Jarosław, 52, 53
Ryba-Romanowski, Witold, 13, 34, 66, 86
Rzepka, Agnieszka, 34, 66
Rzeszutek, Janusz, 34
Rzodkiewicz, Witold, 49

S

Sadowski, Janusz, 8, 42
Sahraoui, Bouchta, 10, 16
Sahu, Vidya, 12
Saievar iranizad, Esmail, 62
Saito, Makoto, 6
Sakowska, Halina, 37, 65
Samavat, Feridoun, 35, 35
Sangwal, Keshra, 65
Sarukura, Nobuhiko, 98
Sarzała, Robert P., 49, 50, 69
Sasaki, Takatomo, 92
Savchuk, Viktor K., 34, 59
Savin, Yuriy N., 10, 13
Schmitt, Erwin, 95
Schulz, Detlev, 95
Ściana, Beata, 50, 53
Seitz, Christoph, 45
Sęk, Grzegorz, 50
Semikina, Tetyana V., 61, 61
Serafińczuk, Jarosław, 50
Sethu, Gunasekaran S., 36
Shailesh, Sharma, 31, 63
Shalayev, Rostyslav V., 62
Shekari, Leila, 62
Shemchenko, Evgeny, 62
Sheu, Gwo-Jiun, 51
Shin, Tongik, 51, 57, 62
Shiomi, Hiromu, 95
Shkir, Mohd, 63
Shunmugavelu, Arun, 13
Shur, Joong Won, 57, 65

Shvartsman, Vladimir, 82
Siennicki, Antoni, 57
Sierzputowski, Leszek P., 94
Sinyakova, Elena F., 57
Sitarek, Stefan, 58
Skierbiszewski, Czeslaw, 7
Skupiński, Paweł, 65
Sofiani, Zouhair, 10
Solarz, Piotr, 66, 66
Song, Won young, 51, 57, 62
Speck, J. S., 6
Starnawska, Ewa, 21, 21
Stefaniuk, Ireneusz, 30
Stelmakh, Svetlana, 43
Stingaciu, Marian, 14
Story, Tomasz, 22
Strąk, Paweł, 46, 67, 83
Straubinger, Thomas, 95
Strupinski, Wlodek, 43, 43, 52
Strzałkowski, Karol, 16
Strzelecka, Stanisława, 48, 55, 67
Sugihara, Naoki, 67
Sun, Ching-Cherng, 47
Surma, Barbara, 58
Surma, Hańcza Barbara, 36, 67
Surowiec, Marian, 22
Suruttaiya Udaiyar, Ponnusamy S., 36
Suzuki, Takaomi, 67, 68
Swirkowicz, Marek A., 10, 36, 82, 85
Szade, Jacek, 52
Szczytko, Jacek, 12
Szewczyk, Andrzej, 14
Szostek, Krzysztof, 37
Szuszkiewicz, Wojciech, 8
Szymczak, Henryk, 14, 39
Szyrski, Włodzimierz, 21, 36, 37

T

Tajima, Michio, 95
Talik, Ewa, 37, 38
Targowski, Grzegorz, 41
Tavakoli, Mohammad Hossein, 63
Terada, Shigeru, 91
Teshima, Katsuya, 67, 68
Thangavel, Kanagasakaran, 31, 31, 32, 38, 63
Thompson, Joe D., 80
Tillmanns, Ekkehart, 70
Tlaczala, M., 50
Toliński, Tomasz, 38
Tolmachev, Alexander, 30, 39
Tolmachev, Alexander V., 10, 13, 14, 64
Tortello, Mauro, 26
Trukhanov, Aleksey, 39
Trukhanov, Sergei, 39
Trzaskowska, Aleksandra, 19, 28
Tsai, Chenwen, 7
Tu, Sheng Han, 88
Turczynski, Sebastian, 80
Turowski, Andrzej, 43, 45, 52

Twardowski, Andrzej, 12
Tymicki, Emil A., 68

U

Uematsu, Koji, 97
Ueno, Satoru, 84
Ulanowski, Zbigniew, 23

V

Valek, Lukas, 58
Valerio, Mario E G., 76
Vanfleet, Richard, 13, 53
Varyukhin, Victor M., 62
Vedda, Anna, 29
Videlot-Ackermann, Christine, 75
Virt, Igor, 69
Vogel, Michael, 95
Voronina, Irina S., 18, 35

W

Wagner, Joachim, 41
Wasiak, Michał, 69
Watson, Stephen J., 70
Wawro, Andrzej, 49
Wegner, Elżbieta, 67
Weyher, Janusz, 51
Wierzbička, Edyta, 20, 70
Wierzbička, Maria, 70
Wierzchowski, Wojciech, 21, 27, 71, 72, 97
Wieteska, Krzysztof, 21, 27, 71, 72, 97
Wilke, Hermann, 63, 78
Winiarski, Antoni, 52
Wisniewski, A., 81
Wnuk, Artur, 59, 67
Wójcik, Aleksandra, 22, 22
Wójcik, Kazimierz, 65
Wojcik, Marek, 45, 52
Wojdyła, Michał, 10
Wojtowicz, Tomasz, 8
Wokulska, Krystyna B., 72
Wokulski, Zygmunt, 25, 30, 37
Wollweber, Jürgen, 45
Wu, Chenyen, 39
Wu, Feng, 6
Wu, Gwomei, 7, 39

Y

Yagi, Kentaro, 94
Yakovec, Alexander, 62
Yamashita, Motoi, 73
Yang, Deren, 71
Yao, Takafumi, 96
Yavetskiy, Roman P., 30, 39
Yermolayeva, Yulia V., 64
Yokoyama, Chiaki, 93
Yoon, Dae Ho, 51, 57, 62, 65
Yoshikawa, Akira, 29, 46, 76
Yoshimoto, Noriyuki, 75

Yoshimura, Masashi, 92

Z

Zabelina, Evgeniya V., 23

Zakrzewski, Jacek, 16

Zaleski, Andrzej, 30

Zaleszczyk, Wojciech, 8

Zavadil, Jiří, 17

Zayarnyuk, Tetyana, 14

Zborowska-Lindert, Iwona, 50

Žďánský, Karel, 17

Żelazko, Jarosław, 46, 56

Zemskova, Svetlana, 39

Zhigadlo, Nikolai D., 26, 81

Zhuravleva, Mariya, 29

Zubov, Eduard E., 14

Zybert, Paweł, 26

Zytkiewicz, Zbigniew R., 44, 54